The morphology and development of normal and abnormal spermatozoa in the emu, *Dromaius novaehollandiae*

by

Lizette du Plessis

Submitted in partial fulfillment of the requirements for the degree
Doctor of Philosophy

Faculty of Veterinary Science
University of Pretoria
Pretoria

October 2012

My journey the last few years was adventurous
At times it has been dark
the road steep and fraught with dangers for me
At times joyous
filled with sunshine, fun and laughter
even a bit of magic
Sometimes I have been foolish
sometimes wise
Often I have despaired
but continued in blind belief
I gave my everything, my heart, my soul
My journey continues

CONTENTS

DECLARATION

I, Lizette du Plessis, declare that the thesis which I hereby submit for the degree Doctor of Philosophy in Anatomy at the University of Pretoria, is my own work, with the exception of the electron tomography which was done at The University of Cape Town. I have not submitted the contents of this thesis for a degree at this or any other tertiary institution.

October 2012

ACKNOWLEDGEMENTS

I am grateful for the support that I received from family and friends, with special thanks to the following people:

My supervisor, mentor and friend, Prof. John Soley, for introducing me to the vast and wonderful world of sperm. Through our many talks and discussions, sharing your knowledge and guiding me, you gave me confidence, motivated and inspired me to do the best I can;

My support team - my husband Dion du Plessis, my sister Anne-Marié Rogers and my friend Gerda McDonald - without your constant encouragement this would never have happened. Dion, the last two years were filled with hardship and heartache for us, thank you for your patience and loving support;

Mrs. Erna van Wilpe, Manager of the Electron Microscope Unit at the Faculty of Veterinary Science, Onderstepoort, always willing to help in whichever way possible, give advice (and a shoulder to cry on) and allowing me freedom and time to work on my 'spermpies';

The Unit for Microscopy and Microanalysis, Main Campus, University of Pretoria for use of their facilities;

Prof. Trevor Sewell, Electron Microscope Unit, University of Cape Town, for help with the electron tomography;

The Eastern Cape Emu Breeders Association, in particular Mr Peter Bezuidenhout and The Grahamstown Ostrich Abattoir, as well as Mrs Petra Rough from The Emu Ranch, Rustenburg for making material and facilities available;

Prof. John Soley and Dr. David Phillips for supplying ostrich and rhea testicular blocks from their personal collections;

The Jotello F. Soga library staff for friendly service and going the extra mile to help me find articles;

Ms. Estelle Mayhew, Department for Education Innovation,Onderstepoort, for the schematic illustrations in Chapters 2 and 3**;**

The University of Pretoria for financial support.

PUBLICATIONS

Du Plessis, L. & Soley, J.T. (2011) Incidence, structure and morphological classification of abnormal spermatozoa in the emu (*Dromaius novaehollandiae*). *Theriogenology* **75,** 589–601.

Du Plessis, L. & Soley, J.T. (2011) Head-base bending and disjointed spermatozoa in the emu (*Dromaius novaehollandiae*): a morphological comparison of two closely related defects. *Theriogenology* **76**. 1275–1283.

Du Plessis, L. & Soley, J.T. (2012) Abaxial tail implantation in the emu, *Dromaius novaehollandiae*: morphological characteristics and origin of a rare avian sperm defect. *Theriogenology* **77**, 1137–1143.

Du Plessis, L. & Soley, J.T. (2012) Structural peculiarities associated with multiflagellate sperm in the emu, *Dromaius novaehollandiae. Theriogenology* **78**, 1094–1101.

SUMMARY

The morphology and development of normal and abnormal spermatozoa in the emu, *Dromaius novaehollandiae*

by

Lizette du Plessis

Supervisor: Prof. J.T. Soley

Department: Department of Anatomy & Physiology, Faculty of Veterinary Science,
University of Pretoria, Private Bag X04, Onderstepoort, 0110,
Republic of South Africa

Degree: Ph.D.

The morphological features and development of normal and abnormal sperm were studied in the emu, *Dromaius novaehollandiae*, using both light and electron microscopy. Detailed descriptions of normal as well as abnormal forms were documented. Where possible, the origin and development of the defects were examined and interpreted. Based on these observations, a system for the morphological classification of ratite sperm abnormalities was proposed.

Emu sperm typically revealed the basic filiform morphology which is common in other ratites and non-passerine birds in general. At the ultrastructural level, emu sperm displayed a conical acrosome covering the tip of the nucleus and a long distal centriole running the entire length of the midpiece. Mitochondria of the *pars spiralis* were more numerous than in other ratites, but no intermitochondrial cement was present in the mitochondrial sheath. Although sharing basic ultrastructural features, a distinct difference between sperm of the emu and other ratites was the complete absence of a perforatorium and endonuclear canal. Another distinctive feature revealed by all forms of microscopy was the presence of a cytoplasmic appendage located at the base of the nucleus and which

appeared to represent the point of cytoplasmic release during spermiation.

Based on the examination of a total of 15 semen samples collected during the middle of the breeding season from the distal deferent ducts of commercially slaughtered adult emus, a total of 14% morphologically abnormal cells were identified. Head defects were represented by bent, microcephalic, macrocephalic or round heads. Acephalic sperm were also present in all samples. Zones of incomplete chromatin condensation and retained cytoplasmic droplets appeared to be implicated in head bending, while giant heads were often associated with multiple tails. In acephalic sperm the tail was complete, but the head was absent, often being replaced by a small spherical structure. Tail defects were subdivided into defects of the neck/midpiece and those of the principal piece. In the neck/midpiece region two anomalies were noted, namely abaxial tail implantation and disjointed sperm. Abaxial tail implantation involved the eccentric positioning of the centriolar complex relative to the head base while disjointed sperm were characterized by the complete separation of the head and midpiece in the neck region, but within the confines of the plasmalemma. Defects observed in the principal piece were subdivided into short, coiled and multiple tails. Cytoplasmic droplets were classified as a separate defect. A small percentage of sperm displayed multiple abnormalities. Defective alignment and/or migration of the centriolar complex (diplosome) was implicated in a number of the defects observed, including head-base bending, disjointed sperm, acephalic sperm and abaxial sperm.

Spermiogenesis in the emu broadly paralleled the development of spermatids reported in other non-passerine birds. However, a previously undescribed morphological feature of avian sperm development was observed. During the circular manchette stage of spermatid development, a unique transient structure appeared. It was associated with the outer nuclear membrane and formed regular finger-like projections into the cytoplasm. This structure was present during both the circular and longitudinal manchette stages of development and was particularly obvious towards the apical aspect of the nucleus where it abutted the cone-shaped acrosome. There were no obvious connections between the structure and the microtubules of the manchette. During the final stages of spermatid development the structure abruptly disappeared. Despite employing immunogold labelling techniques and electron tomography, the nature and function of this structure remained unresolved. Descriptions of a similar structure in various lizard species and the Caiman crocodile, although restricted in its location to the nuclear membrane immediately beneath the acrosome, would appear to reinforce the phylogenetic link previously identified between birds and crocodiles.

Chapter 1 General introduction and basic architecture of the male reproductive tract

General background

Emus are the second largest living birds after the ostrich. Both belong to the flightless group of birds called the ratites (order Struthioniformes, families Dromaiidae and Struthionidae, respectively). They are native to Australia and are found predominantly in the state of Western Australia (Davies, 1963; Serventy & Whittell, 1976). The first written description of the emu can be found under the common name of "New Holland cassowary" in Arthur Phillip's "*Voyage to Botany Bay"* which was published in 1789 (Gould, 1865). The ornithologist, John Latham, who contributed towards Phillip's book, first named and described the species *Dromaius novaehollandiae,* which means 'fast footed New Hollander'. The origin of the common name, emu, dates back to the 17th century and originates from an Arabic word for large bird, which the Portuguese explorers used to describe the related cassowary in New Guinea (Anonymous, 2001). There were originally four different emu species, three of which are now extinct. Apparently there was also one prehistoric species that is only known from fossils. The extinction of the birds is ascribed to hunting, fires and change of habitat. Three subspecies have been recognised within the remaining genus, *D. novaehollandiae,* namely, *D. novaehollandiae novaehollandiae, D. novaehollandiae woodwardi* and *D. novaehollandaie rothschildi* (Sales, 2007).

Commercial value

In Australia wild emus are considered a pest since the birds compete with other livestock for food and water and trample and destroy crops when migrating (Minnaar & Minnaar, 1994; Thompson, 1997). During the early 1900's the Australian government set a bounty on emus and in 1932 even attempted to exterminate the bird. Fences were put up to protect crops and livestock from migrating emus and commercial farming of the birds was prohibited. Despite their status as pests, the economic value of the birds has long been recognized. The meat was a source of food for the Aboriginal people who also used the fat for medicinal purposes such as healing wounds (Whitehouse *et al*., 1998; Sales, 2007) and to oil their wooden tools. The early European settlers used the fat as fuel for their lamps. In 1987 the first permits were issued to a few farmers in Western Australia which

made it possible to initiate the commercial farming of the birds, and the first farmed emus were slaughtered three years later.

Today, the main commercial products are oil, meat and leather. Emu oil is harvested from the subcutaneous and retroperitoneal fat of the bird (Sales, 2007) and has several pharmaceutical and cosmetic applications (Zemtov *et al*., 1996; López *et al*., 1999; Yoganathan *et al*., 2003). It is particularly valued for its anti-inflammatory properties (Thompson, 1997; Bennett *et al*., 2008; Howarth *et al*., 2008). As in the ostrich, the meat is low in cholesterol and fat. The leather has a distinctive pattern and is used for making shoes, wallets and other leather products, while the eggs and feathers are used in the decorative arts and crafts.

In common with other niche industries world-wide such as ostrich and crocodile farming, the commercial raising of emus is a relatively small enterprise and is severely hampered by high production costs. One suggestion to overcome these inherent constraints is to educate the public about emu products and to aim at exclusive, higher value markets (Sales, 2007). Despite these drawbacks, the commercial farming of emus is now a world-wide enterprise. The first emus were exported to the USA between 1930 and 1950 as exotic zoo animals. It has since become a viable industry in many countries, including North America, China, Peru and South Africa (Wikipedia, 2012; personal communication with farmers). Emu farmers, particularly the fledgling South African operation, appear to be suffering the same teething problems as those experienced by the now well-established ostrich industry regarding reproductive performance.

Breeding of emus

The ratite industry currently relies on natural reproduction which is not always cost effective, partly due to the monogamous nature of ratites (Malecki *et al*., 1998a; 2000). This means that a large number of males must be kept for the sole purpose of breeding, which adds an unnecessary financial burden to farming operations. The emu is a seasonal breeder and breeding, in the southern hemisphere, is restricted to autumn and winter (Malecki, *et al*., 1998a; personal communication with farmers). Mating usually starts towards the end of summer, with eggs being laid from autumn through to the spring months. The peak season is in winter (O'Malley, 1994). Males often become quite aggressive during the breeding season and can cause serious injuries to each other which leads to additional veterinary expenses. In order to address these problems, it has been suggested that the ratite industry should employ advanced reproductive technologies such as artificial insemination (AI), which has been successfully employed in commercial poultry enterprises (King *et al*., 2000; Foote,

2002; Łukaszewicz, 2010). AI represented the first meaningful application of biotechnology aimed at improving reproduction and genetics of farm animals and has had an enormous influence on reproduction worldwide. It has been used successfully in birds since 1913 when Ivanov produced fertile chicken eggs using sperm harvested from the *ductus deferens* (Quinn & Burrows, 1936; Smyth, 1968; Gee *et al*., 2004). Since then AI has become an important production tool in the poultry industry, as well as in the conservation of endangered birds (Gee, 1995). For instance, in turkey farming AI has increased fertility by up to 50% (Minnaar & Minnaar, 1994). The success of this technique is directly dependent on the quality of the collected semen. The evaluation of semen prior to applying AI is thus of the utmost importance and sperm morphology has been identified as one of its most important qualitative characteristics. Although most AI efforts in non-domestic birds have been research orientated (Blanco *et al*., 2009), the practical and financial benefits of this technique can clearly be applied in niche industries such as emu farming. Whereas a great deal of information is available on the reproductive system of the male ostrich, particularly in respect of sperm morphology (Soley, 1992, 1993, 1996; Soley & Roberts, 1994; Irons *et al*., 1996; Hemberger *et al*., 2001; Rozenboim *et al*., 2003), relatively little data have been presented on these aspects of the male reproductive tract in the emu (Malecki *et al*., 1997,1998a,b, 2000; 2008; Malecki & Martin, 2002; Ozegbe *et al*., 2008, 2010; Sood *et al*., 2011). Apart from the brief description provided by Baccetti *et al*. (1991), little or no work has been published on the actual process of spermiogenesis or even normal sperm structure (Baccetti *et al*., 1991), and no pictorial information on normal and abnormal sperm morphology at the light microscopical level has been presented. A detailed description of normal and aberrant sperm structure and the attendant process of spermiogenesis is thus urgently required to address this problem.

Basic architecture of the male emu reproductive tract

This section is intended to briefly describe the topography and basic anatomical features of the male reproductive tract of the emu and is not a definitive anatomical study. The information presented is based on personal observations made on 15 birds used in this study, supported by the limited data reflected in the literature. The anatomy of the reproductive tract of the male ratite, and in particular that of the ostrich, is well documented (Fowler, 1991; Bezuidenhout, 1986; Soley & Groenewald, 1999). Descriptions, albeit less detailed, are also available for the emu (Cho *et al.*, 1984; Fowler, 1991; Malecki *et al*.,1998a, 2000; Sales, 2007).

Emu testes are intra-abdominal and are located on either side of the midline, ventral to both the vertebral column and the kidneys and caudal to the adrenal glands (Cho *et al*., 1984). Incidental

observations on the size, shape and colour of the emu testes examined in this study were consistent with the information presented by Malecki *et al.* (1998a). During the non-breeding season, and in sexually immature birds, the testes are small, but increase dramatically in size when the birds are sexually active during the breeding season. In the emu this increase may be as much as two fold (Malecki *et al*., 1998a). The testes are asymmetrical, with the left testis always being larger than the right. The left testis is mainly bean-shaped to elongated, while the smaller right testis is round to oval-shaped (Figs. 1 & 2). Contrary to the situation in most other birds where the testes are white in colour, the testes of ratites display colouration. In the ostrich, rhea and cassowary the testis are tan-coloured, (Fowler, 1991; Soley, 1992) while in the emu they are black, presumably due to the presence of melanin pigment in the capsule (personal observations) and interstitial tissue (Cho *et al*., 1984; Fowler, 1991; Malecki *et al*., 1998a). The reason for the presence of the pigment is not clear.

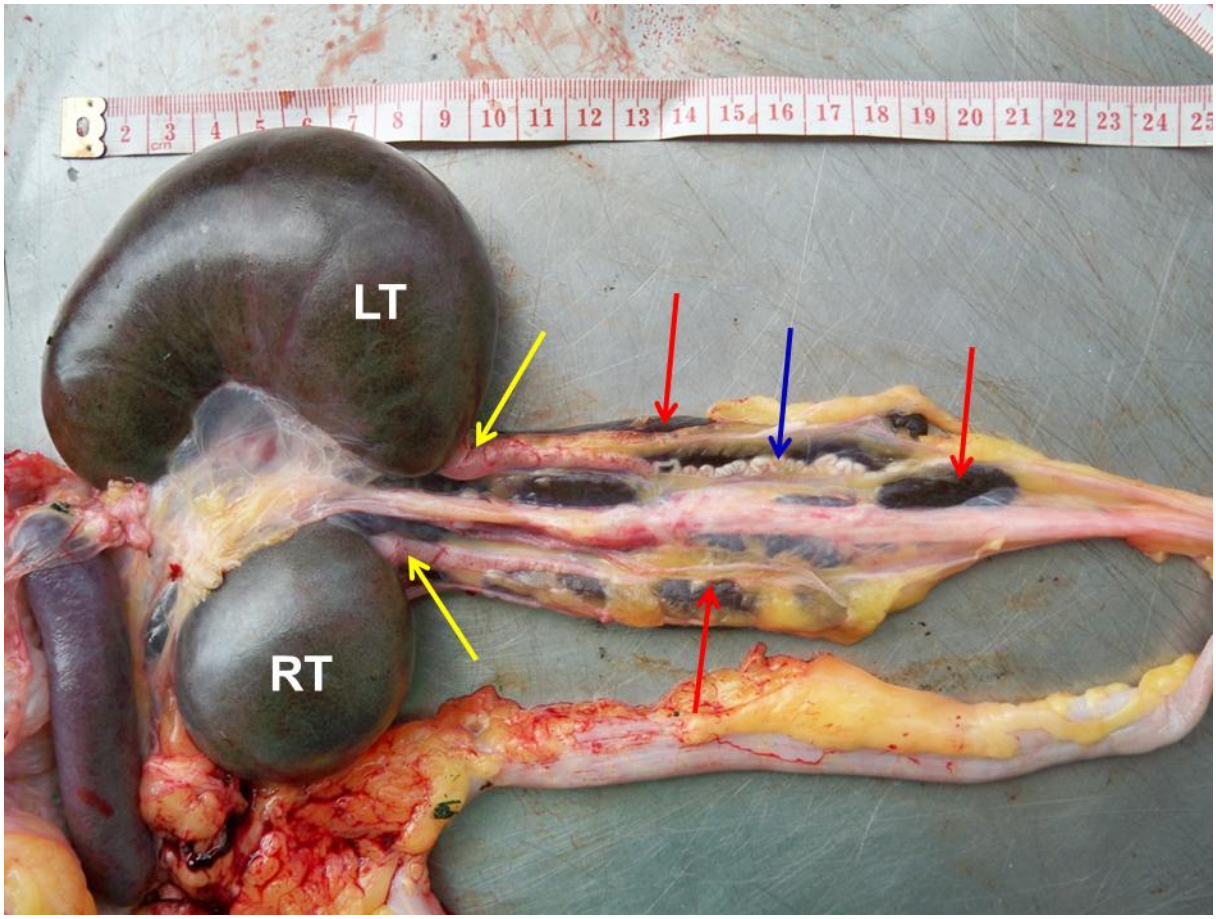

Figure 1. Ventral view of the excised reproductive tract of a sexually mature emu. Note the difference in size and shape between the left (LT) and right (RT) testis, and the convoluted nature of the *ductus deferens* (blue arrow). The body of the epididymis is partially obscured due to its dorso-medial positioning but the wide caudal termination (yellow arrows) is obvious. The various divisions of the kidneys (red arrows) lie dorsal to the testes and deferent ducts.

According to Budras and Meier (1981) the epididymis of ratites can be divided into two regions, the main part and an *appendix epididymidis*. In the ostrich the appendix is a considerable structure, extending appreciably beyond the cranial pole of the testis and closely associated with the adrenal gland (Budras & Meier, 1981; Soley, 1992). In the emu the epididymis is pink to cream coloured. The main part or body lies on the dorso-medial aspect of the testis and stretches from just beneath the cranial pole to the caudal pole, following the concave curve of the testis. Although the study of Budras and Meier (1981) would suggest that the *appendix epididymidis* in the emu is a substantial structure, the present study revealed only a small, sometimes insignificant (Fig. 2b) cranial extension of the epididymis. The body of the epididymis was a flat, elongated structure situated predominantly on the dorsomedial aspect of the testis and surrounded by peritoneal fat. It was intimately attached to the testis. Transverse sections through the epididymis revealed a flattened triangular profile. The epididymis widened caudally and extended an appreciable distance beyond the caudal pole of the testis (Figs. 1 & 2a) before narrowing to form the *ductus deferens* (Fig. 3). This duct lay suspended in a peritoneal fold ventro-lateral to the ureters. The initial (proximal) portion was highly convoluted but straightened distally towards the cloaca (Fig. 3) into which it opened via the urodeum.

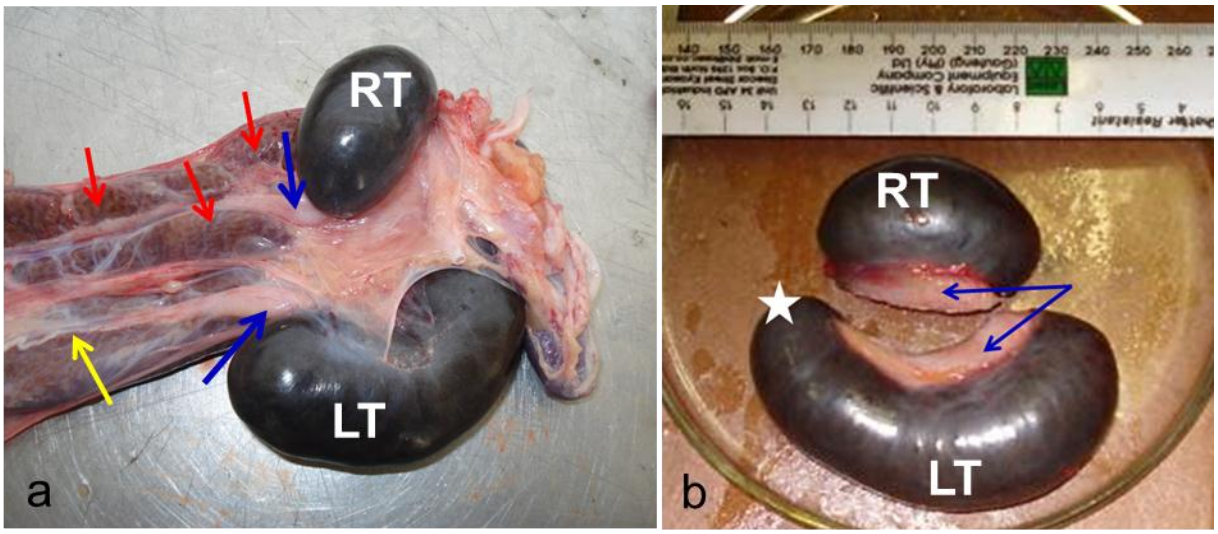

Figure 2. (a) Ventral view of the excised reproductive tract of a sexually mature emu. The larger left testis (LT) is more evenly bean-shaped than the example in Fig. 1. The broad terminal portion of the epididymis (blue arrows) is shown leaving both the left and right (RT) testes before continuing as the *ductus deferens* (yellow arrow). Note the peritoneal lining covering the various divisions of the kidneys (red arrows). In (b) the main part of the epididymis is indicated by the blue arrows which in the left testis (LT) ends just beneath the cranial pole (star). The *appendix epididymidis* is not obvious on either testis. Right testis (RT).

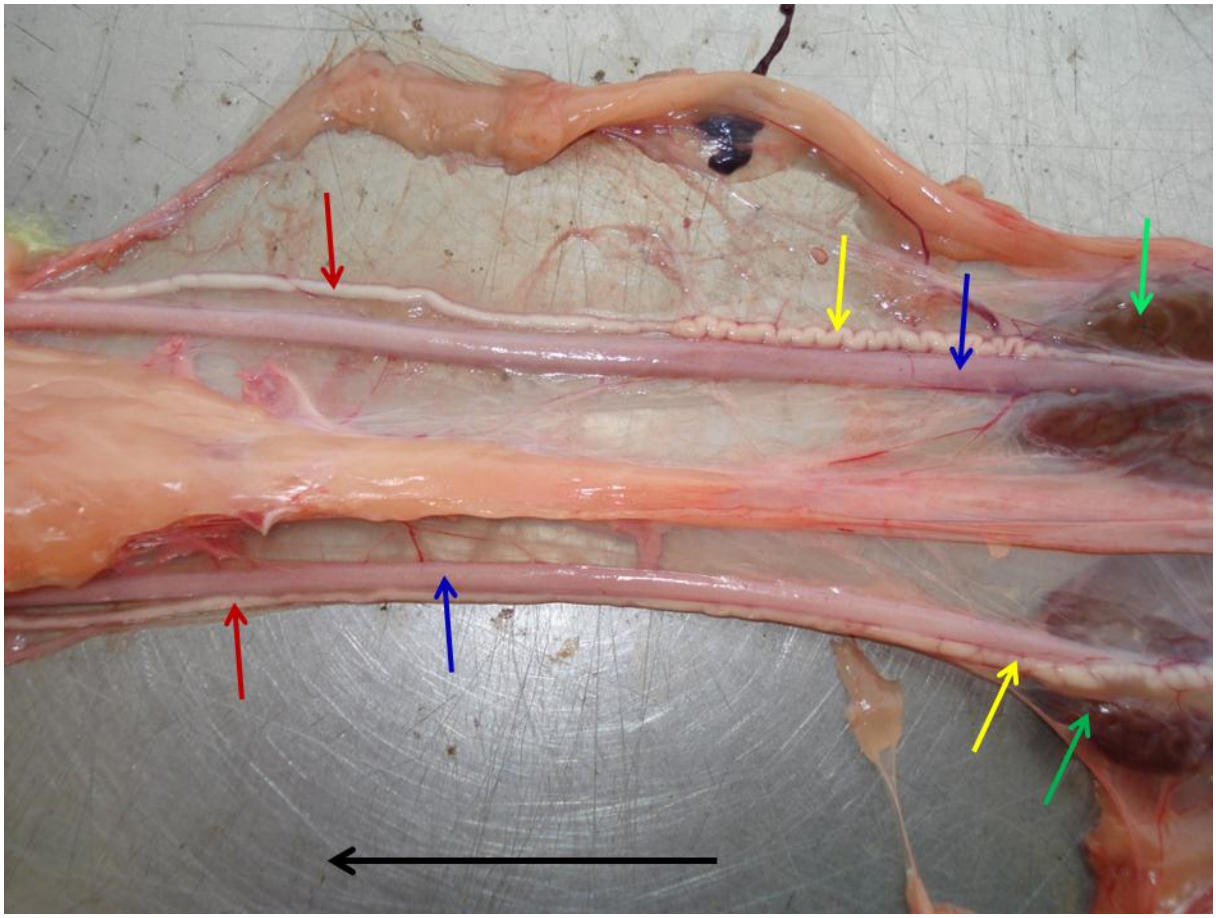

Figure 3. Ventral view of the excised *ductus deferens* and ureters (blue arrows) caudal to the caudal division of the kidneys (green arrows). Note the convoluted nature of the *ductus deferens* (yellow arrows) which straightens (red arrows) before terminating at the cloaca. The horizontal arrow indicates cranio-caudal direction.

The testes were enclosed by a well-developed layer of fibrous connective tissue. The testicular capsule was intimately associated with the walls of adjacent seminiferous tubules and was continuous with the boundary tissue enclosing each tubule (Fig. 4). As in the ostrich (Ozegbe *et al*., 2008) very few interlobular septa were observed. Whereas the testicular capsule appears to vary in thickness from one testicular region to another in mammals, it is reportedly relatively thin in birds (Lake, 1971; Aire & Ozegbe, 2007). However, compared to other birds, in particular galliform species (Lake, 1971; Hodges 1974; Aire, 2007; Aire & Ozegbe, 2007), the testicular capsule of ratites is remarkably thick (Ozegbe *et al.,* 2008). In a comparative study of the emu and ostrich (Ozegbe *et al.,* 2008) the testicular capsule of emus measured 176 ± 57.5µm, and that of the ostrich three times thicker (578.1 ± 73.4µm), compared to only 81.5µm in the rooster and 91.8µm in the drake (Aire &

Ozegbe, 2007). This observation was confirmed in the present study where the testicular capsule measured approximately 200µm in thickness (Fig. 4).

The seminiferous tubules formed the bulk of the testicular parenchyma (Fig. 4) and were tightly packed. The tubules were surrounded by a thin layer of boundary (peritubular) tissue composed of regularly arranged collagen fibres and interposed blood vessels and melanocytes. Wedges of interstitial tissue, which contained deposits of pigment, blood vessels, Leydig cells, fibroblasts and macrophages (Aire, 2007, present study) were present at the interstice between groups of seminiferous tubules (Fig. 4). The seminiferous tubules presented mainly elongated to angular profiles and were lined by a thick germinal epithelium composed of Sertoli cells and developing spermatogenic cells. The various cell stages typical of spermatogenesis could be identified, namely, spermatogonia, primary and secondary spermatocytes, round spermatids and elongated spermatids (Fig. 5). The flagellum of developing spermatids was typically oriented towards the tubular lumen and spermiation could be observed at the germinal epithelium/lumen interface. Free residual bodies were also characteristic of this region (Fig. 5b).

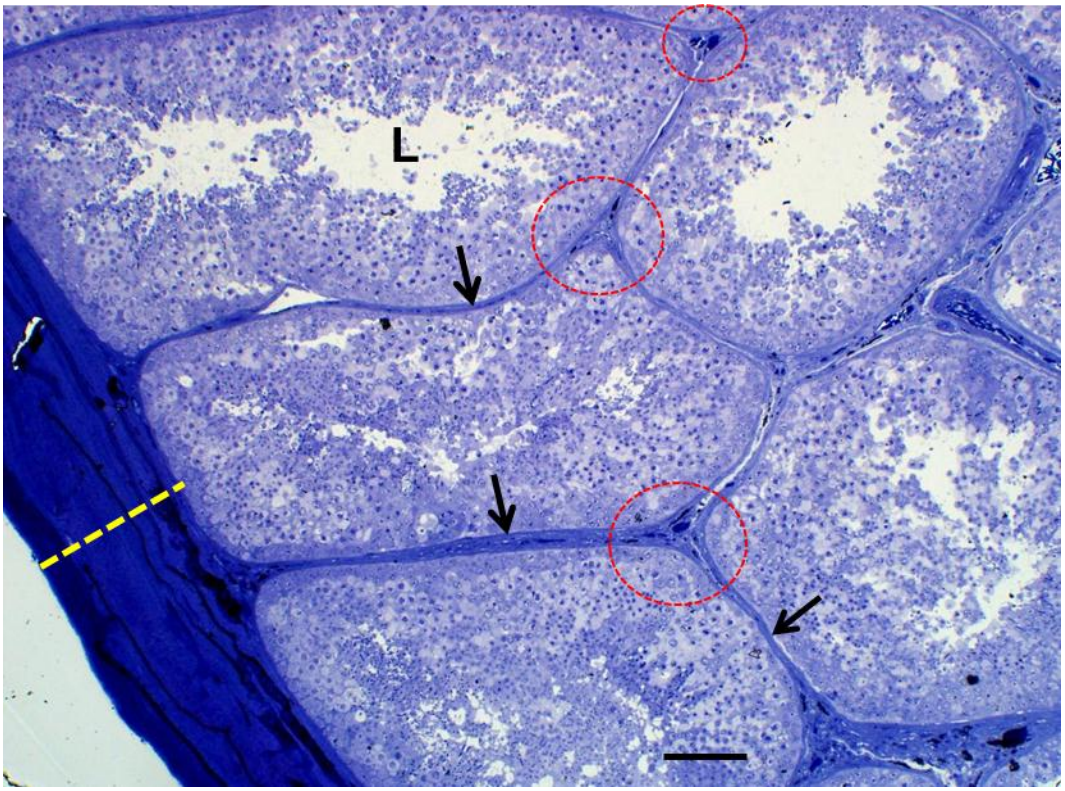

Figure 4. Low-power micrograph of the emu testis demonstrating the closely packed seminiferous tubules separated by thin strips of boundary tissue (arrows). Note the thick testicular capsule (dotted yellow line) and the interstices between groups of three seminiferous tubules (red circles). Lumen of seminiferous tubule (L). Toluidine blue. Bar = 100µm.

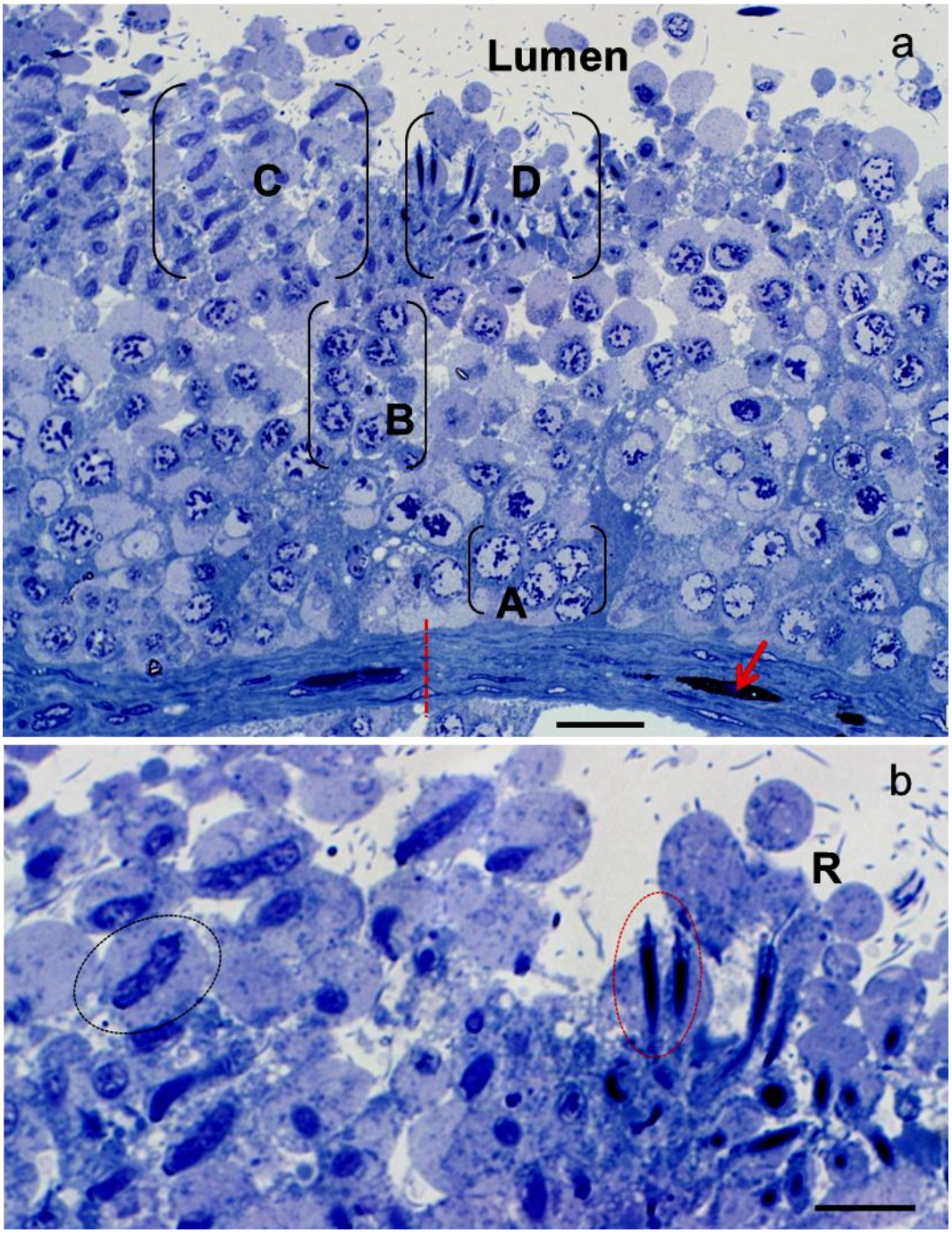

Figure 5. Light micrographs of the germinal epithelium lining a seminiferous tubule. In (a) the brackets [A] and [B] indicate different stages in the development of primary spermatocytes, whereas [C] and [D] show early and late stage elongating spermatids, respectively. No secondary spermatocytes/round spermatids appear in this image. The red dotted line indicates the boundary tissue separating adjacent seminiferous tubules. A pigmented cell, presumably a melanocyte, is apparent (red arrow). Figure 5 (b) is a higher magnification of the areas marked C and D in Fig. 5 (a). The specific orientation of the elongating spermatids can clearly be seen with their flagella oriented towards the lumen, and the dark-staining acrosome situated at the opposite pole of the cell. An early elongating spermatid is indicated in the black circle, while two late elongating spermatids are encircled in red. Residual bodies (R) are also present. Toluidine blue. Bar (a) = 20µm; Bar (b) = 10µm.

Aims of the study

Although there have been a number of studies on the collection of spermatozoa and on aspects of the application of AI techniques in the emu (Malecki *et al*., 1997; 2008; Sood *et al*., 2011, 2012), it is clear from the available literature that there is a paucity of basic information regarding sperm development, sperm morphology and the classification of defective sperm in the emu. For AI to be consistently successful, it is important to establish the normal parameters for emu semen and spermatozoa. Detailed descriptions of abnormal forms of spermatozoa in the emu are an essential prerequisite for accurate semen evaluation. This information is currently limited to a brief and superficial report by Malecki *et al*. (1998b) and the cursory description of the ultrastructure of normal emu sperm by Baccetti *et al*. (1991). Accordingly, the present study aims to document in detail the process of spermiogenesis in the emu and in particular those aspects which have not previously been addressed in the literature. It further aims to provide detailed descriptions on the morphology of normal as well as abnormal spermatozoa. This approach will potentially provide baseline data of value for the application of AI in the industry and for other farming practices such as the selection of male birds with good semen parameters. The incidence of sperm defects will be determined and, where possible, the origin and formation of the defective sperm will be described. The apparent confusion regarding the terminology currently in use to describe sperm abnormalities in birds will be addressed.

References

Aire, T.A. (2007) Anatomy of the testis and male reproductive tract. In: Jamieson, B.G.M. (ed.) Reproductive Biology and Phylogeny of Birds Part A. Science Publishers, Jersey, pp. 37-113.

Aire, T.A. & Ozegbe, P.C. (2007) The testicular capsule and peritubular tissue of birds: morphometry, histology, ultrastructure and immunohistochemistry. *Journal of Anatomy* **210,** 731-740.

Anonymous. (2001) Emu *Dromaius novaehollandiae*. Australian Museum, Sydney.

Baccetti, B., Burrini, A.G. & Falchetti, E. (1991) Spermatozoa and relationships in Palaeognath birds. *Biology of the Cell* **71,** 209-216.

Bennett, D.C., Code, W.E., Godin, D.V. & Cheng, K.M. (2008) Comparison of the antioxidant properties of emu oil with other avian oils.*Australian Journal of Experimental Agriculture* **48,** 1345-1350.

Bezuidenhout, A.L. (1986) The topography of the thoro-abdominal viscera in the ostrich (*Struthio camelus*). *Onderstepoort Journal of Veterinary Research* **53,** 111-117.

Blanco, J.M., Wildt, D.E., Höfle, U., Voelker, W. & Donoghue, A.M. (2009) Implementing artificial insemination as an effective tool for *ex situ* conservation of endangered avian species. *Theriogenology* **71,** 200–213.

Budras, K. & Meier, U. (1981) The epididymis and its development in ratite birds (ostrich, emus, rhea). *Anatomy and Embryology* **162**, 281-299.

Cho, P., Brown, R. & Anderson, M. (1984) Comparative gross anatomy of ratites. *Zoo Biology* **3,** 133-144.

Davies, S.J.J.F. (1963) Emus. Australian Natural History pp. 225-229.

Foote, R.H. (2002) The history of artificial insemination: Selected notes and notables. *Journal of Animal Science* **80**, 1-10.

Fowler, M.E. (1991) Comparative clinical anatomy of ratites.*Journal of Zoo and Wildlife Medicine* **22,** 204-227.

Gee, G.F. (1995) Artificial insemination and cryopreservation of semen from non-domestic birds. In: Bakst, M.R. & Wishart, G.J. (eds.) First international symposium on the artificial insemination of poultry. Poultry Science Association, pp. 262-279

Gee, G.F., Bertschinger, H., Donoghue, A.M., Blanco, J. & Soley, J.T. (2004) Reproduction in nondomestic birds: Physiology, semen collection, artificial insemination and cryopreservation. *Avian and Poultry Biology Reviews* **15,** 47-101.

Gould, J. 1865. Handbook to the birds of Australia, volume 2. Landsdowne Press.

Hemberger, M.Y., Hospes, R. & Bostedt, H. (2001) Semen collection, examination and spermiogram in ostriches. *Reproduction in Domestic Animals* **36,** 241-243.

Hodges, R.D. (1974) The histology of the fowl. Academic Press, London.

Howarth, G.S., Lindsay, R.J., Butler, R.N. & Geier, M.S. (2008) Can emu oil ameliorate inflammatory disorders affecting the gastrointestinal system? *Australian Journal of Experimental Agriculture* **48,** 1276-1279.

Irons, P.C., Berthschinger, H.J., Soley, J.T. & Burger, W.P. (1996) Semen collection and evaluation in the ostrich. In: Deeming, D.C. (ed.) Improving our understanding of ratites in a farming environment. Ratite Conference, Oxford, pp.157-199.

King, L.M., Holsberger, D.R. & Donoghue, A.M. (2000) Correlation of CASA velocity and linearity parameters with sperm mobility phenotype in turkeys. *Journal of Andrology* **21,** 65-71.

Lake, P.E. (1971) The male in reproduction. In: Bell, D.J. & Freeman, B.M (eds.) Physiology and biochemistry of the domestic fowl volume 3, Academic Press, London, pp. 1411-1447.

López, A., Sims, D.E., Ablett R.F., Skinner, R.E., Léger, L.W., Lariviere, C.M., Jamieson, L.A., Martinez-Burnes, J. & Zawadzka, G.G. (1999) Effect of emu oil on auricular inflammation induced with croton oil in mice. *American Journal of Veterinary Research* **60,** 1158-1561.

Łukaszewicz, E. (2010) Artificial insemination in geese. *World's Poultry Science Journal* **66,** 647-658.

Malecki, I.A., Martin, G.B. & Lindsay, D.R. (1997) Semen production by the emu (*Dromaius novaehollandiae*). 1. Methods for collection of semen. *Poultry Science* **76,** 615-621.

Malecki, I.A., Martin, G.B., O'Malley, P.J., Meyer, G.T., Talbot, R.T. & Sharp, P.J. (1998a) Endocrine and testicular changes in a short-day seasonally breeding bird, the emu (*Dromaius novaehollandiae*), in southwestern Australia. *Animal Reproduction Science* **53,** 143-155.

Malecki, I.A. Cummins, J.M., Martin, G.B. & Lindsay, D.R. (1998b) Effect of collection frequency on semen quality and the frequency of abnormal forms of spermatozoa in the emu. *Animal Production in Australia* **22,** 406.

Malecki, I.A., Beesley, J. & Martin, G.B. (2000) Changes in the characteristics of emu sperm with season. *British Poultry Science Supplement* **41,** S18.

Malecki, I.A. & Martin, G.B. (2002) Fertility of male and female emus (*Dromaius novaehollandiae*) as determined by spermatozoa trapped in eggs. *Reproduction, Fertility and Development* **14,** 495-502.

Malecki, I.A., Rybnik, P.K. & Martin, G.B. (2008) Artificial insemination technology for ratites: a review. *Australian Journal of Experimental Agriculture* **48,** 1284-1292.

Minnaar, P. & Minnaar, M. (1994) The Emu farmer's handbook 5th edition. Induna Company, Texas.

O'Malley, P. (1994) Artificial hatching and rearing. In*:* Smetana,P*.* (ed.) Emu Farming—Background Information. Department of Agriculture, South Perth, Western Australia, pp. 90–98*.*

Ozegbe, P.C., Aire, T.A., Madekurozwa, M-C. & Soley, J.T. (2008) Morphological and immunohistochemical study of testicular capsule and peritubular tissue of emu (*Dromaius novaehollandiae*) and ostrich (*Struthio camelus*). *Cell and Tissue Research* **332,** 151-158.

Ozegbe, P.C., Kimaro, W., Madekurozwa, M-C., Soley, J.T. & Aire, T.A. (2010) The excurrent ducts of the testis of the emu (*Dromaius novaehollandiae*) and ostrich (*Struthio camelus*): Microstereology of the epididymis and immunohistochemistry of its cytoskeletal systems. *Anatomia, Histologia, Embryologia* **39,** 7-16.

Quinn, J.P. & Burrows, W.H. (1936) Artificial insemination in fowls. *Journal of Hereditary* **27,** 31-37.

Rozenboim, I., Navot, A., Snapir, N., Rosenstrauch, A., El Halawani, M.E., Gvaryahu, G. & Degen, A. (2003) Method for collecting semen from the ostrich (*Struthio camelus*) and some of its quantitative and qualitative characteristics. *British Poultry Science* **44,** 607-611.

Sales, J. (2007) The emu (*Dromaius novaehollandiae*): a review of its biology and commercial products. *Avian and Poultry Reviews* **18,** 1-20.

Serventy, D.L. & Whittell, H.M. (1976) Birds of Western Australia. University of Western Australia Press, Perth, pp. 65-71.

Smyth, J.R. (1968) Poultry. In: Perry, E.J. (ed.) Artificial insemination of farm animals. Rutgers University Press, New Brunswick, pp. 258.

Soley, J.T. (1992) A histological study of spermatogenesis in the ostrich (*Struthio camelus*). Ph.D. Thesis. University of Pretoria.

Soley, J.T. (1993) Ultrastructure of ostrich (*Struthio camelus*) spermatozoa: 1. Transmission electron microscopy. *Onderstepoort Journal of Veterinary Research* **60,** 119-130.

Soley, J.T. (1996) Differentiation of the acrosomal complex in ostrich (*Struthio camelus*) spermatids. *Journal of Morphology* **227,** 101-111.

Soley, J.T. & Roberts, D.C. (1994) Ultrastructure of ostrich (*Struthio camelus*) spermatozoa: 2. Scanning electron microscopy. *Onderstepoort Journal of Veterinary Research* **61,** 239-246.

Soley, J.T. & Groenewald, H.B. (1999) Reproduction. In: Deeming, D.C. (ed.) The Ostrich: Biology, Production and Health. CABI Publishing, Oxon, pp. 129-158.

Sood, S., Malecki, I.A., Tawang, A. & Martin, G.B. (2011) Response of spermatozoa from the emu (*Dromaius novaehollandiae*) to rapid cooling, hyperosmotic conditions and dimethylacetamide (DMA). *Animal Reproduction Science***129,** 89-95.

Sood, S., Malecki, I.A., Tawang, A. & Martin, G.B. (2012) Survival of emu (*Dromaius novaehollandiae*) sperm preserved at subzero temperatures and different cryoprotectant concentrations. *Theriogenology* **78**, 1557-1569.

Thompson, R.S. (1997) Raising emus and ostriches. USDA, National Agricultural Library, Beltsville Maryland.

Whitehouse, M.W., Turner, A.G., Davis, C.K.C. & Roberts, M.S. (1998). Emu oil(s): a source of non-toxic transdermal anti-inflammatory agents in Aboriginal medicine. *Inflammopharmacology* **6,** 1-8.

Wikipedia. Viewed on 10 October 2012. http://en.wikipedia.org/wiki/Emu.

Yoganathan, S., Nicolosi, R., Wilson, T., Handelman, G., Scollin, P., Tao, R., Binford, P. & Orthoefer, F. (2003) Antagonism of croton oil inflammation by topical emu oil in CD-1 mice. *Lipids* **38,** 603-607.

Zemtov, A., Gaddis, M. & Montalvo-Lugo, V. (1996) Moisturizing and cosmetic properties of emu oil: A pilot double blind study. *Australasian Journal of Dermatology* **37,** 159-162.

Chapter 2 Morphology of normal sperm

Introduction

Sperm morphology, sperm motility and sperm concentration are viewed as the three most important parameters to consider when assessing semen quality (MacLeod & Gold, 1951; Barth & Oko, 1989; Zamboni 1992; Malmgren, 1997). The morphological features of sperm serve as a reliable indicator for predicting the fertilizing capacity of spermatozoa and also reflect some disorders in spermatogenesis. In humans treated by assisted reproductive technologies, the accurate assessment of morphological abnormalities is of prognostic value in predicting the results of assisted reproduction and fertilization when male infertility is compromised. Likewise, artificial insemination (AI) is an important and widely used technique in ensuring and maintaining genetic traits in domestic animals such as the bull and stallion and relies on a clear understanding of normal sperm structure. The value of sperm morphology in determining reproductive success is reflected in the numerous studies carried out, for example, on man (Holstein & Roosen-Runge, 1981; Zamboni, 1987, 1992; Menkveld *et al.*, 1991; Afzelius, 1996) and domesticated animals such as the bull (Blom, 1972; Barth & Oko, 1989; Specher & Coe, 1996; Nöthling & Irons, 2008; Freneau *et al.*, 2010), stallion (Dowsett *et al.*, 1984; Jasko *et al.*, 1990; Kavak *et al.*, 2004; Card, 2005; Brito, 2007), boar (Briz *et al.*, 1996) and dog (Oettlé & Soley, 1988; Stockner & Bardwick, 1991; Oettlé, 1993; Martínez, 2004).

Avian sperm structure, in particular that of non-passerine birds of economic importance, has likewise received considerable attention. Numerous studies have detailed the morphological features of both normal and defective sperm in the chicken (Grigg & Hodge, 1949; Lake *et al.*, 1968; Tingari, 1973; Bakst & Howarth, 1975; Nwakalor *et al.*, 1988; Łukaszewicz *et al.*, 2008; Tabatabaei *et al.*, 2009), turkey (Wakely & Kosin, 1951; Kamar & Rizik, 1972; Marquez & Ogasawara, 1975; Alkan *et al.*, 2002), duck (Maretta 1975a,b), goose (Marvan *et al.*, 1981; Ferdinand, 1992), Japanese quail (Wooley, 1995; Chelmońska *et al.*, 2008), pintailed duck (Penfold *et al.*, 2000) and guinea fowl (Thurston *et al.*, 1982; Thurston & Hess, 1987). The commercial exploitation of ratite species such as the ostrich, rhea and emu, has prompted a renewed interest in ratite sperm structure. Since artificial insemination has been suggested as a means of improving the economic viability of these niche industries (Malecki *et al.*, 2008), a thorough knowledge of normal sperm structure in these birds is of paramount importance. This view was further emphasised by Bertschinger *et al*. (1992) who considered sperm morphology to be one of the most important factors in predicting fertility in the ostrich. The morphology of normal

sperm has been well documented for the ostrich by both light and electron microscopy (Soley, 1989, 1993; Baccetti *et al.*, 1991; Bertschinger *et al.*, 1992; Soley & Roberts, 1994; Irons *et al.*, 1996; Gee *et al.*, 2004; Jamieson, 2007), while the ultrastructure of rhea sperm and aspects of their development were reported by Phillips and Asa (1989). Apart from a brief ultrastructural description of the development and morphology of emu sperm (Baccetti *et al.*, 1991), little definitive information has been published on the structure of normal emu sperm.

Recent detailed publications on the classification and description of defective sperm in the emu (Du Plessis & Soley, 2011a,b, 2012a,b) have focused attention on the need to re-evaluate the dearth of published information on normal emu sperm, particularly at the LM level. This information is required in order to provide comparative data for a meaningful description of abnormal forms. This chapter provides a detailed account of the normal morphology of emu, *Dromaius novaehollandiae*, sperm as observed by light and electron microscopy.

Materials & Methods

Light microscopy

Semen samples were collected during mid-breeding season from 15 healthy (animals approved for slaughter) and sexually active emus following slaughter at commercial abattoirs. Two groups of birds were sampled. One group (n=5) was sourced from the Rustenburg district in the North West Province, South Africa and slaughtered at The Emu Ranch Abattoir. The second group of birds was from the Grahamstown district, Eastern Cape Province, South Africa (n=10), and slaughtered at The Grahamstown Ostrich Abattoir. The birds ranged in age from 22 months to five years. Samples were collected approximately 60 minutes after the birds had been slaughtered. Drops of semen were gently squeezed from the distal *ductus deferens* into test tubes containing 2.5% glutaraldehyde in 0.13M Millonig's phosphate-buffer. Smears for light microscopy (LM) were prepared from the fixed cell suspensions, air-dried and stained with Wrights' stain (Rapidiff®, Clinical Sciences Diagnostics, Johannesburg, South Africa). The dried smears were fixed in methanol for 20 seconds, stained with eosin for 30 seconds, blotted and then stained with methylene blue solution for 60 seconds. The smears were then gently rinsed with distilled water and allowed to dry before mounting with Entellan® and a coverslip. Smears from each bird were examined with an Olympus BX63 light microscope (Olympus Corporation, Tokyo, Japan) using a 100x oil immersion objective (bright field as well as phase contrast microscopy) to evaluate sperm morphology and determine the incidence of sperm defects by counting the number of normal/abnormal sperm present in a total of 300 cells. Images of sperm cells were digitally recorded.

The linear dimensions of the various segments of the sperm (acrosome, nucleus, midpiece, principal piece and end piece), as well as the total length of the cells, were determined using phase contrast light microscopy. A minimum of 20 cells from each of the ten Grahamstown birds and the five Rustenburg birds were measured. The measurements were processed using the Soft Imaging System iTEM software (Olympus, Műnster, Germany) and expressed as the average ± SD. Statistical analysis of the different parameters assessed was performed using a computer package (Microsoft Office Excel 2010) and descriptive statistics for each of the sperm segments as well as the total sperm length were generated. The two groups of birds (Grahamstown and Rustenburg) were further compared using the Student's two-tailed unpaired t-test with a 95% probability to determine if there were any statistical differences between the two groups.

Electron microscopy

Samples for transmission (TEM) and scanning electron microscopy (SEM) were fixed overnight at 4ºC in 2.5% glutaraldehyde in 0.13M Millonig's buffer, pH7.4. Using gentle centrifugation and re-suspension throughout, the samples were washed in Millonig's phosphate buffer, pH 7.4, before post-fixation in similarly buffered 1% osmium tetroxide for one hour. After two subsequent washes in buffer, the samples were dehydrated through a graded ethanol series (50%, 70%, 90%, 96%, 3x 100% for 20 minutes each) and cleared with propylene oxide for 20 minutes before embedding in epoxy resin (TAAB 812 resin; TAAB Laboratories, England). Thin sections were cut with a Reichert-Jung Ultracut (C. Reichart AG., Vienna, Austria) ultramicrotome using a diamond knife and stained with lead citrate and uranyl acetate before being viewed in a Philips CM10 transmission electron microscope (Philips Electron Optical Division, Eindhoven, The Netherlands) operated at 80kV.

After the dehydration steps indicated above, the samples for SEM were incubated in hexamethyldisilazane (HMDS) for 30 min after which they were centrifuged, the supernatant discarded and the pellets re-suspended in HMDS. A drop of this suspension was placed on a cover slip and allowed to air dry, after which it was sputter-coated with gold and viewed in a JEOL 840 scanning electron microscope (JEOL Electron Optics Instrumentation, Tokyo, Japan) operated at 8kV. Additionally, for each sample a drop of the re-suspended pellet in HMDS was placed on a carbon stub and allowed to air dry. These samples were viewed uncoated at 0.5kV in a Zeiss Ultra Plus 55 High Resolution FEG scanning electron microscope (Carl Zeiss International, Oberkochen, Germany).

Results

Light microscopy

When viewed by LM, spermatozoa were typically filiform-shaped, consisting of a head and tail (Fig. 1). The relatively straight or gently convoluted head tapered anteriorly and consisted of a clearly defined nucleus capped by a small conical acrosome. In some instances, a thin, thread-like appendage could be discerned at the base of the nucleus (Fig. 1c). The tail was composed of three distinct segments, namely, the midpiece, principal piece and endpiece. The base of the nucleus was continuous with the midpiece, the first segment of the tail. The nuclear base and the proximal end of the midpiece were of similar diameter. The midpiece revealed no special features on LM and was often difficult to distinguish from the rest of the tail on the Rapidiff® smears using bright field microscopy (Fig. 1a). However, the various components of the sperm could clearly be distinguished from each other using phase contrast microscopy (Fig. 1b,c). After termination of the midpiece, the tail continued as the long undulating principal piece. The principal piece was thinner than the midpiece and terminated in a short, visibly thinner and non-conspicuous endpiece of variable length (Fig. 1). In the 15 birds studied, 86.4% of the sperm displayed normal morphological features.

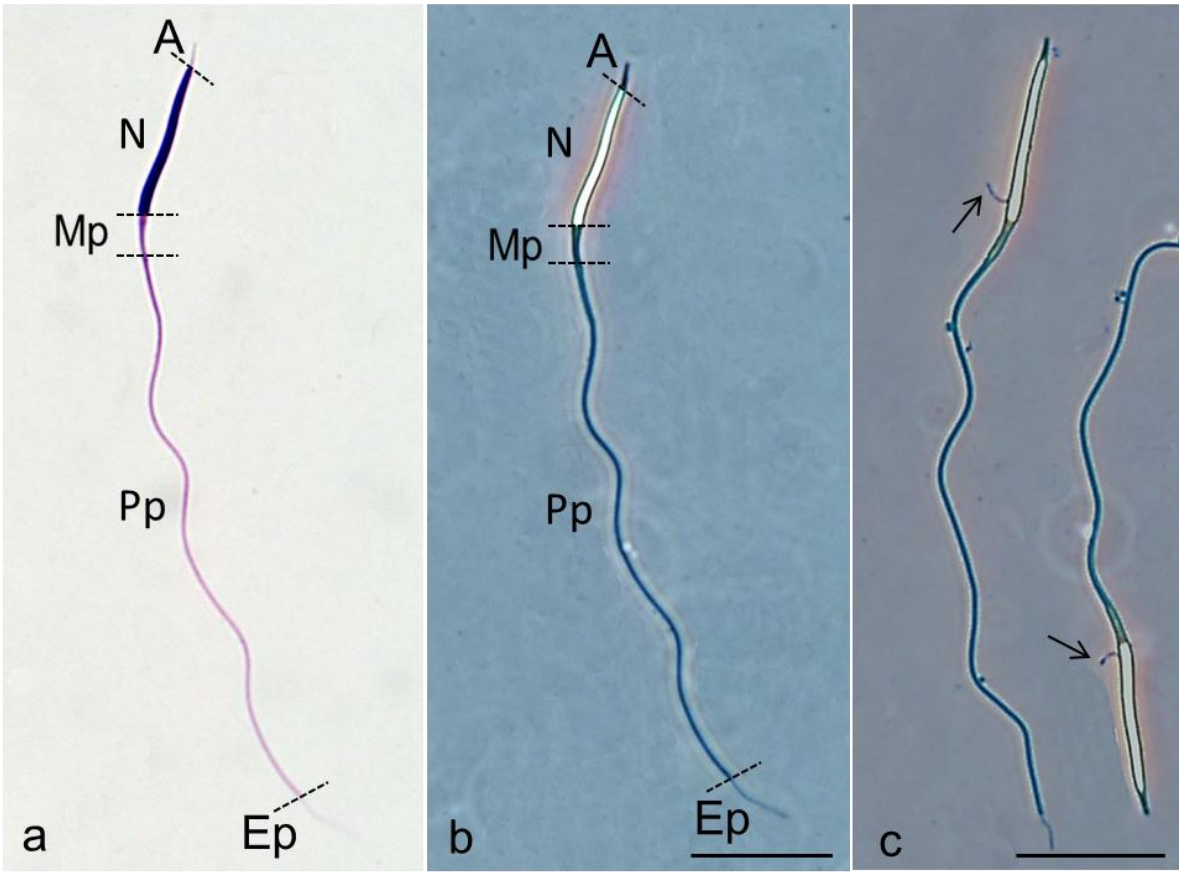

Figure 1. Light microscopy, Wright's stain. The various components of the sperm, namely, the acrosome (A), nuclear region of the head (N), midpiece (Mp), principal piece (Pp) and endpiece (Ep) are more clearly resolved using phase contrast microscopy (b,c) than normal bright field illumination (a). In (c) the thread-like appendage situated near the nuclear base can be seen (arrows). Bar = 10µm.

Cell dimensions:

The dimensions of the various segments of the sperm are presented in Figures 2-7 which reflect the measurements for each individual bird (see Materials & Methods) as well as the pooled values for the Rustenburg and Grahamstown birds and for all birds combined. The acrosome was short, measuring on average 1.84 ± 0.31µm (range 0.94 - 3.01µm) (Fig. 2), while the nucleus measured 11.77 ± 0.93µm in length (range 9.09 - 14.49µm) (Fig. 3). The average lengths of the segments of the flagellum were 2.91 ± 0.4µm (range 1.27 - 4.16µm) for the midpiece (Fig. 4), 47.45 ± 2.8µm (range 41.04 - 59.25µm) for the principal piece (Fig. 5), and 3.69 ± 0.82µm (range 1.38 - 6.33µm) for the endpiece (Fig. 6). The average total sperm length was 67.64 ± 3.13µm (range 60.14 - 79.49µm) (Fig. 7). Based on the above measurements, total head length was determined to be 13.61µm, and the total tail length 54.05µm, giving a head:tail ratio of 1:4. There were no statistically significant differences (P >0.05) observed between any of the measurements when comparing the Rustenburg and Grahamstown birds.

Legend for Figures 2-7: Grey vertical line = observed range; blue block = mean value; black dumbbell line = standard deviation on either side of the mean; G = Grahamstown birds (Eastern Cape); R = Rustenburg birds (North West Province).

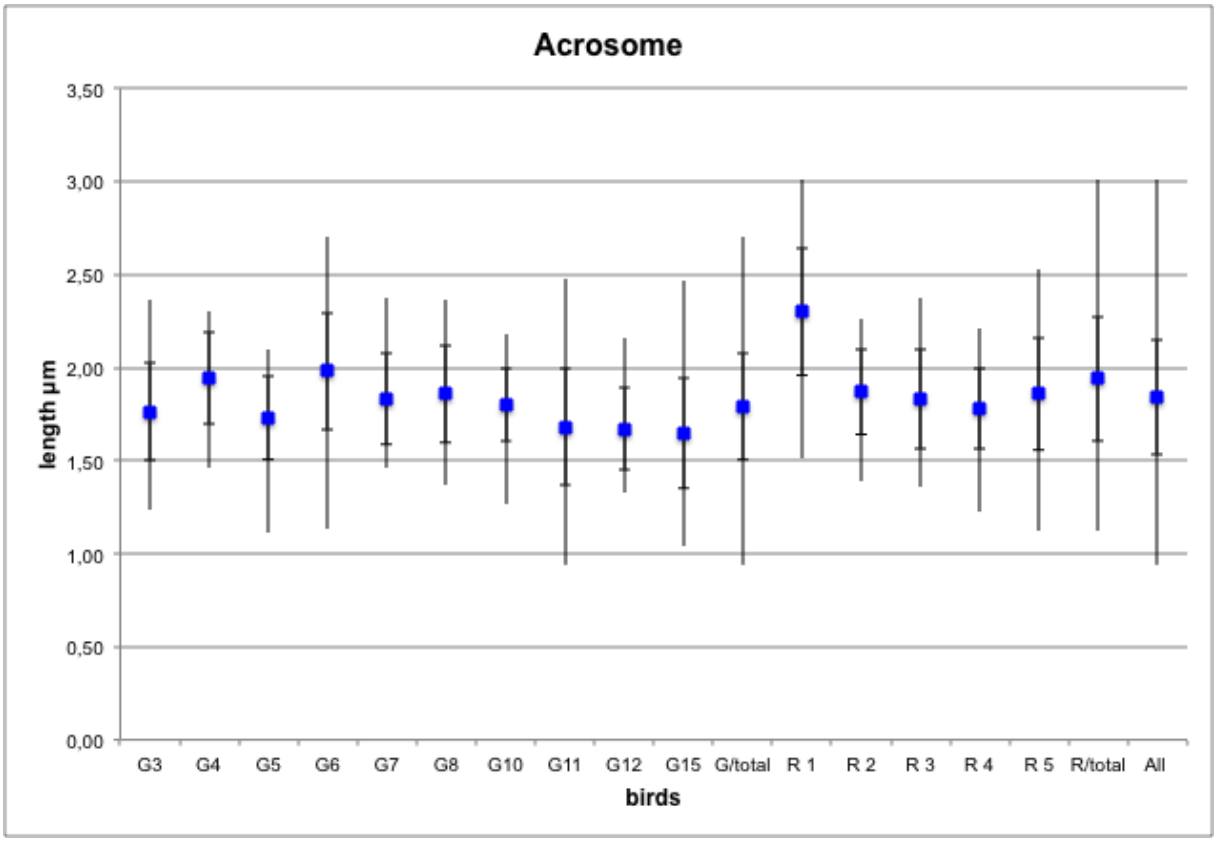

Figure 2. Length of the acrosome.

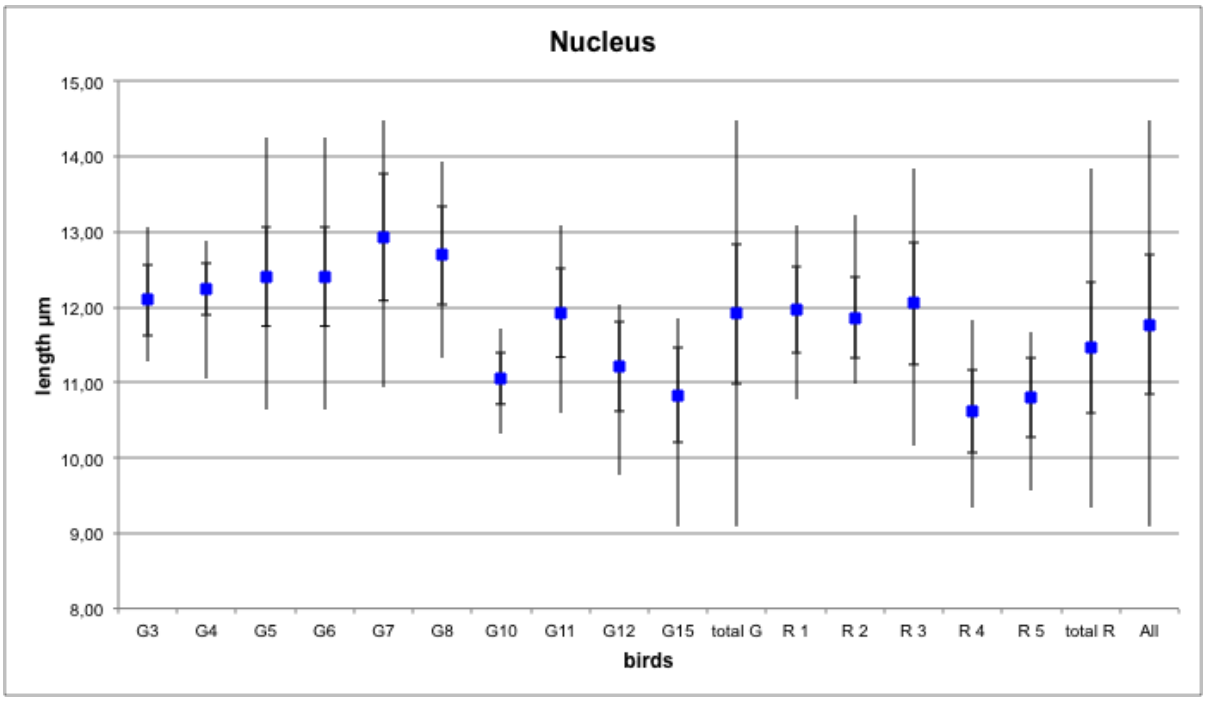

Figure 3. Length of the nucleus.

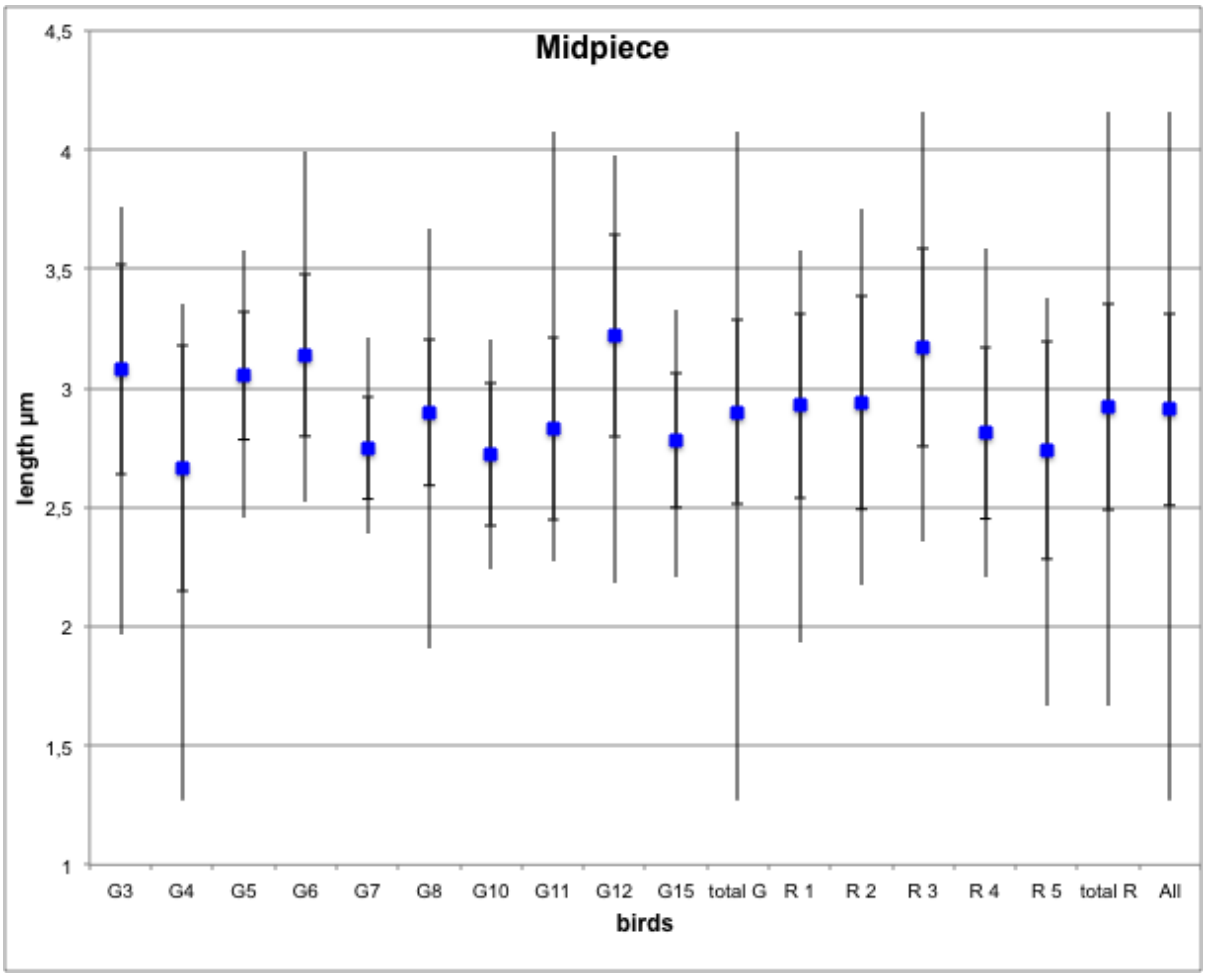

Figure 4. Length of the midpiece.

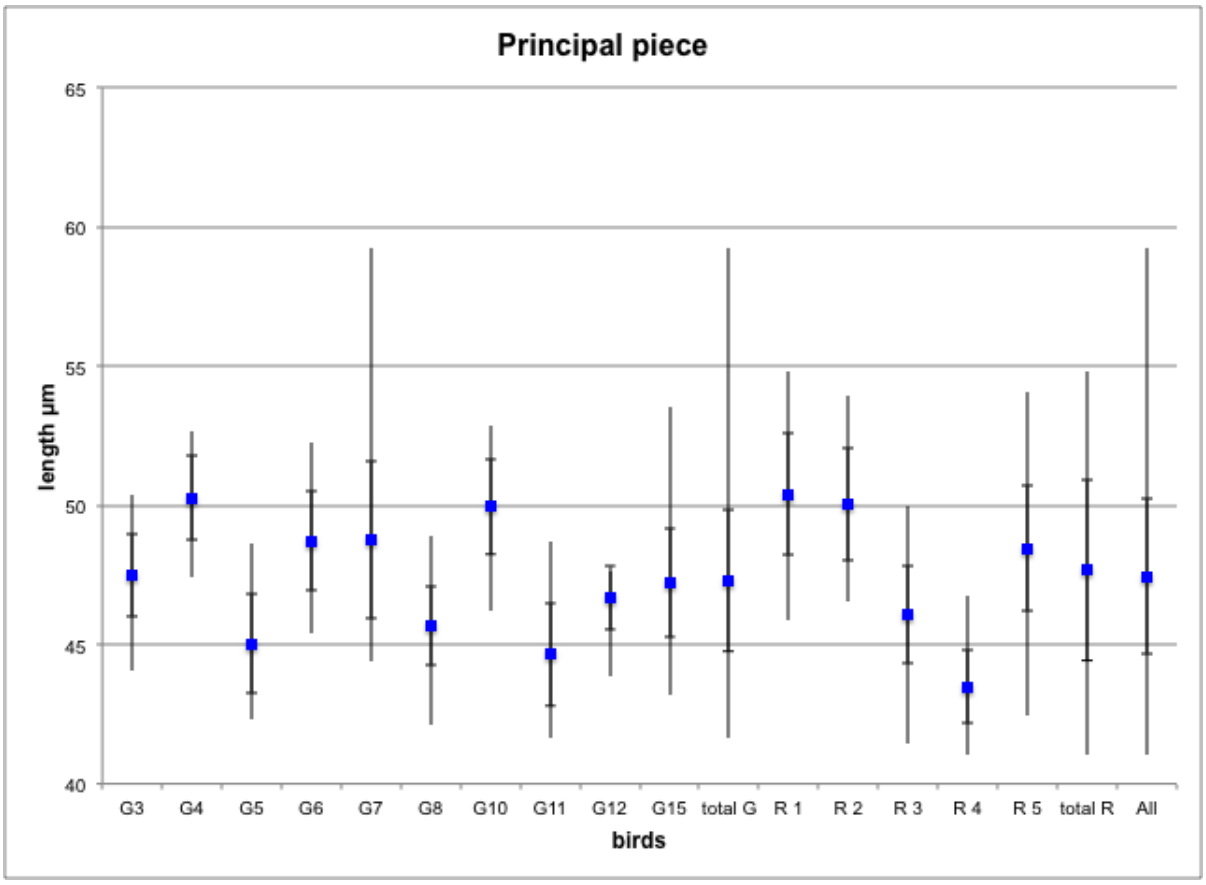

Figure 5. Length of the principal piece.

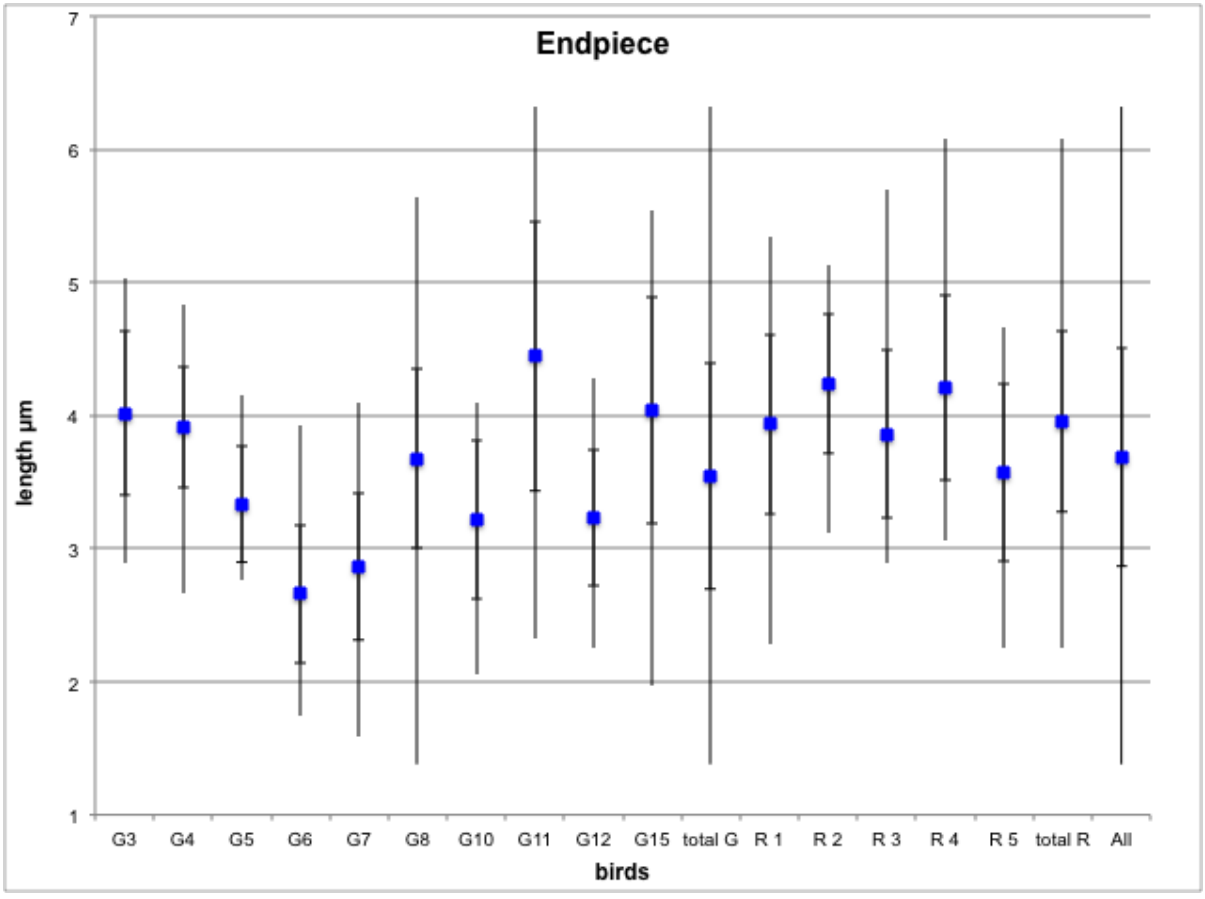

Figure 6. Length of the endpiece.

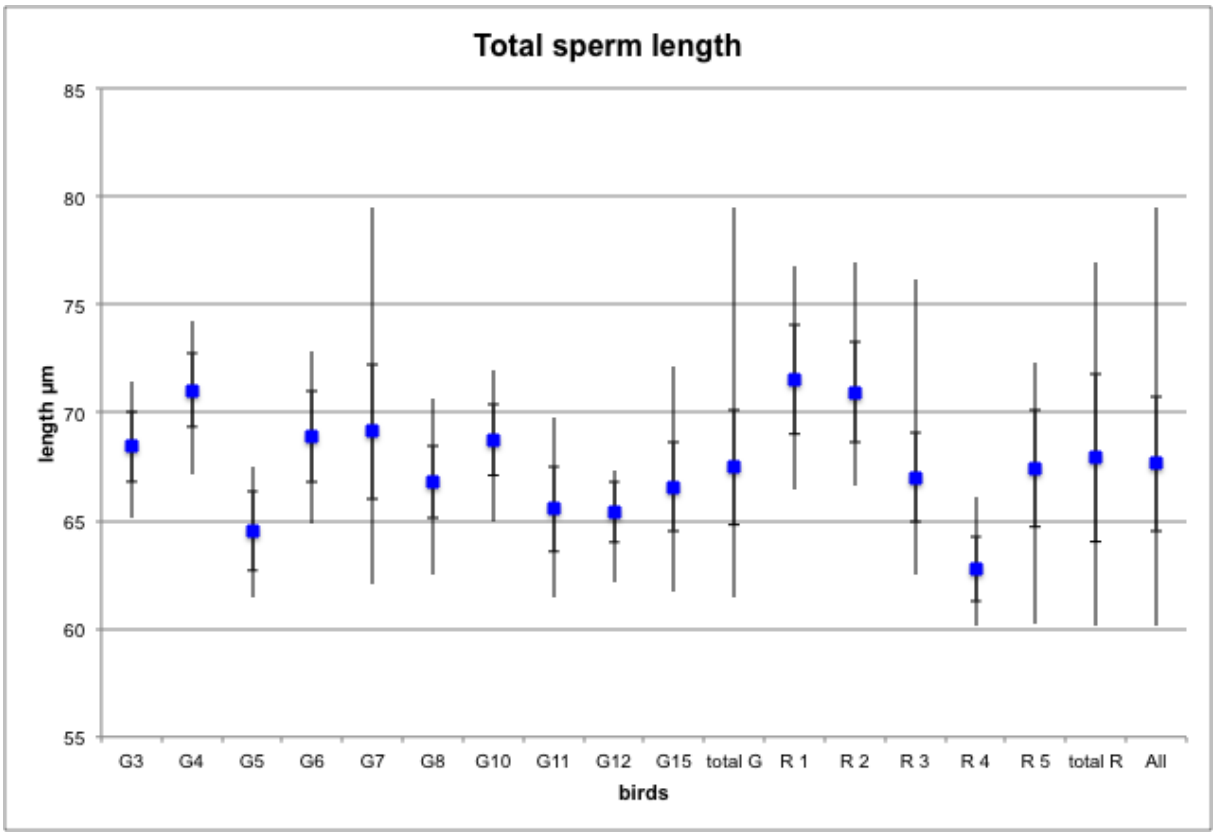

Figure 7. Total sperm length.

Scanning electron microscopy

Conventional SEM confirmed the basic morphological features of emu sperm observed by LM. The cells were long and narrow and the various segments, namely, the acrosome, nucleus, midpiece, principal piece and endpiece, could clearly be distinguished (Fig. 8). The acrosome formed the anterior tip of the sperm head with the nucleus constituting the longest segment of the head. The base of the acrosome was clearly demarcated from the nucleus. The surface of the head, in particular that of the acrosome, was smooth when viewed by SEM (Fig. 8 inset a). The head was often gently curved with the nucleus widening slightly towards its base. In most of the sperm a thin thread-like or wedge-shaped appendage could be seen to extend at right angles from the cell surface in the vicinity of the head base (Fig. 9). However, in some cells the appendage emerged from the proximal aspect of the midpiece. In some instances the appendage lay stretched along the nucleus or midpiece (Fig. 8 inset b).

There was a clear demarcation between the head and midpiece. Mitochondrial profiles could often be seen beneath the plasmalemma in this region, giving the surface of the midpiece a rough/cobbled appearance (Fig. 8 inset b). The midpiece tapered gradually towards the noticeably thinner principal piece. The principal piece formed the longest segment of the sperm

and ended abruptly in a thin, short endpiece. Unlike the midpiece, the principal piece and endpiece displayed smooth surface profiles with no distinct surface characteristics (Fig. 8 inset c).

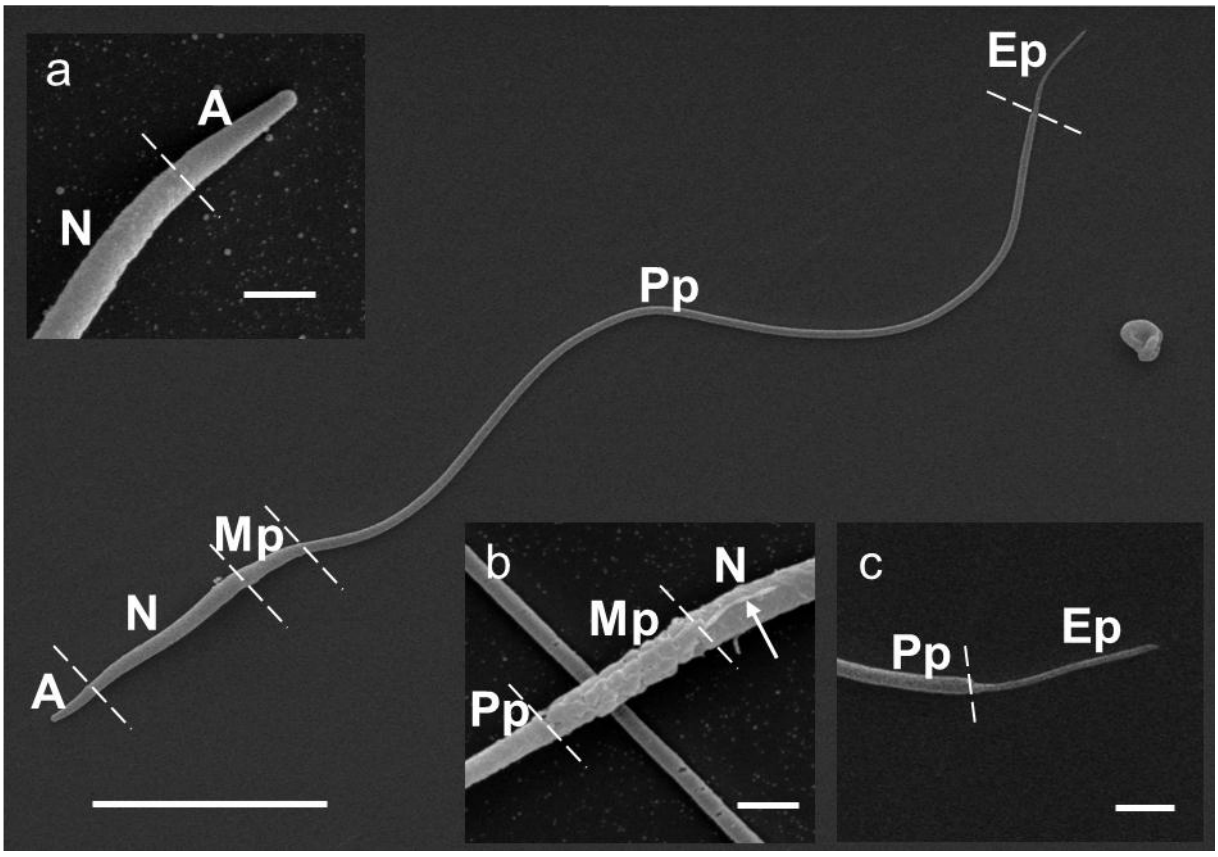

Figure 8. Scanning electron micrograph of a typical emu sperm. Inset (a) shows the proximal tip of the sperm head capped by the acrosome, while inset (b) demonstrates the midpiece with its mitochondrial profiles. The thread-like appendage (arrow) at the base of the nucleus is clearly visible. Inset (c) shows the endpiece of the flagellum. Acrosome (A), nuclear region of the head (N), midpiece (Mp), principal piece (Pp), endpiece (Ep). Bar = 10µm; insets, Bar = 1µm.

When viewed uncoated and at low kV using high resolution SEM, the various segments of the sperm could more accurately be discerned than by standard SEM. The acrosome displayed a much smoother surface than the rest of the head (Fig. 10a), with a clear junction between the two segments being visible (Fig. 10a). The transition between the sperm head and midpiece was abrupt with the surface features of the two segments appearing markedly different. The midpiece tapered slightly towards its distal end with mitochondrial profiles again being obvious (Fig. 10b). The annulus, which demarcated the transition between the midpiece and principal piece, was particularly obvious using this technique, appearing as a prominent circular band or ring between the two segments (Figs. 10b,c). The ribs of the fibrous sheath were visible throughout the length of the principal piece, and ended abruptly at the transition to the endpiece which displayed smooth contours with a hint of the underlying microtubules of the axoneme (Fig. 10d).

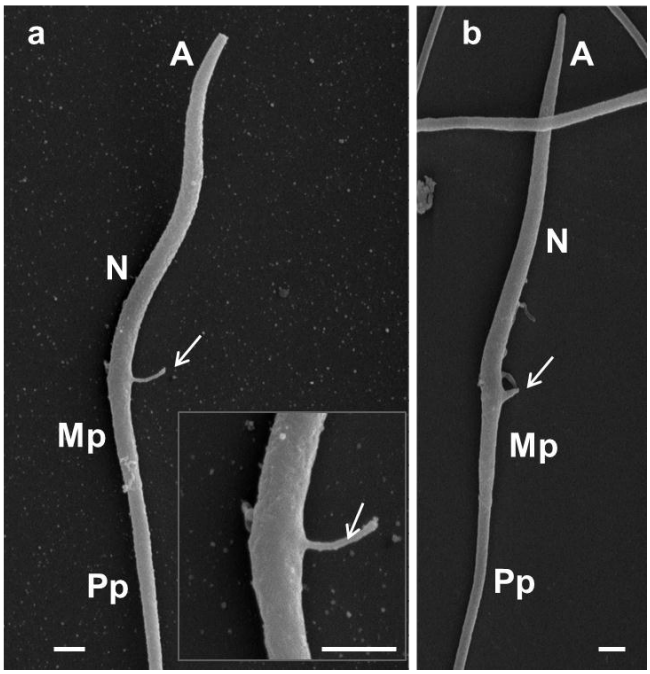

Figure 9. The typical single appendage observed by SEM. In (a) and in the inset, the appendage is thread-like, while in (b) it appears as a short, stubby projection. Acrosome (A), nuclear region of the head (N), midpiece (Mp), principal piece (Pp). Bar = 1µm; inset, Bar = 1µm.

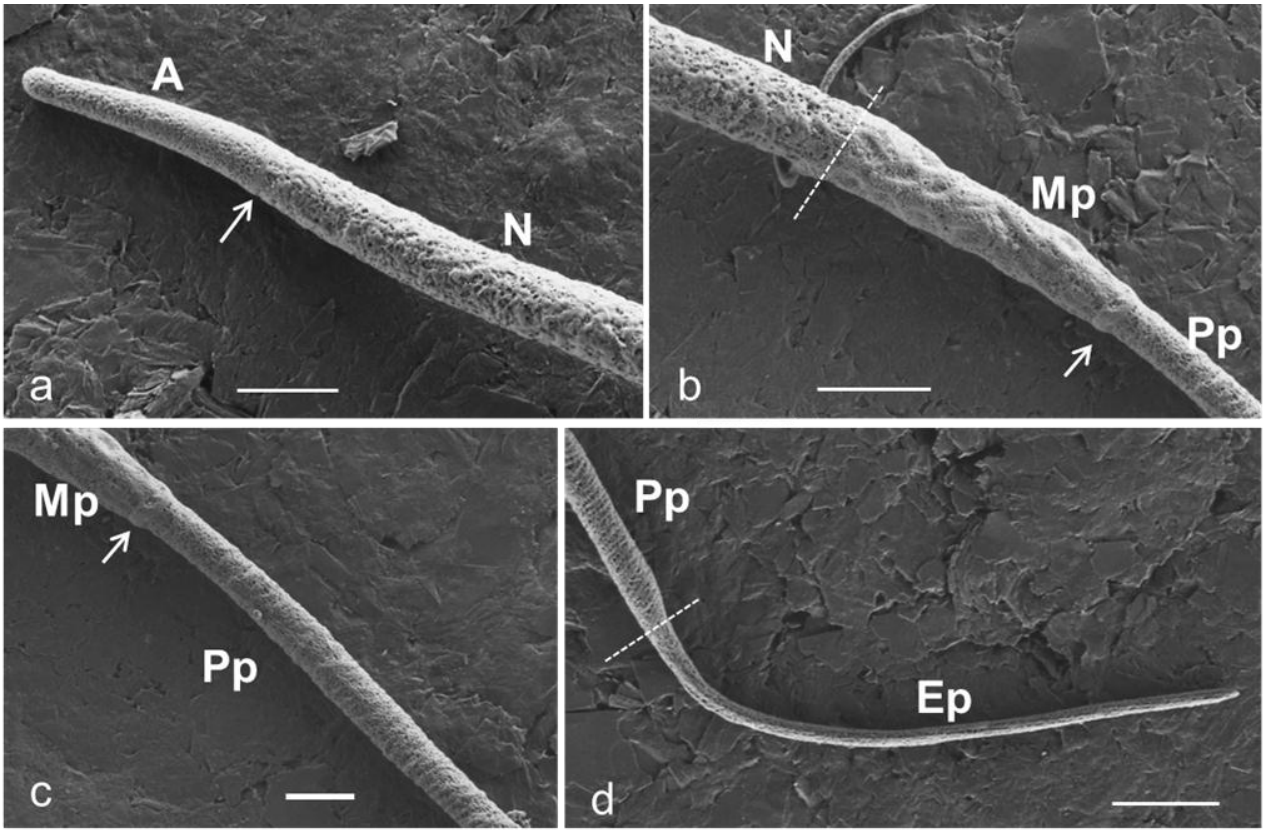

Figure 10. Low kV scanning electron micrographs of the various sperm segments. (a) Note the smooth surface of the acrosome when compared to the rest of the head. An arrow indicates the demarcation between the acrosome and nucleus. (b) The midpiece demonstrating profiles of the mitochondria. The annulus appears as a ring-like structure (arrow), indicating the termination of the midpiece. (c) A section of the principal piece clearly demonstrating the ribs of the fibrous sheath.The annulus is again prominent (arrow). (d) The endpiece is smooth and devoid of a fibrous sheath although the underlying microtubules of the axoneme appear to be displayed. Acrosome (A), nuclear region of the head (N), midpiece (Mp), principal piece (Pp), endpiece (Ep). Bar = 1µm.

Transmission electron microscopy

The head:

Longitudinal sections of sperm examined by TEM confirmed that the apical tip of the highly condensed nucleus extended a variable distance beneath the acrosome, depending on the plane of section (Fig. 11). The acrosome formed a cone-like structure covering the tip of the nucleus and was composed of a homogeneous, moderately electron-dense substance. The narrow sub-acrosomal space between the acrosome and nucleus was often occupied by flocculant, moderately electron-dense material. In some instances this space appeared empty. The nuclear rostrum beneath the acrosome was bluntly tapered while the body of the nucleus was cylindrical, widening slightly towards the base. The plasmalemma was tightly attached to the entire head (acrosome and nucleus), with a thin intervening layer of cytoplasm which was often present towards the nuclear base. The chromatin of the nucleus generally appeared extremely electron dense and tightly compacted, although in some cells there were localized areas that appeared granular or filamentous in nature, presumably representing regions of incomplete or decondensed chromatin. The base of the nucleus terminated in a shallow implantation fossa. No perforatorium or endonuclear canal was present in the emu sperm head.

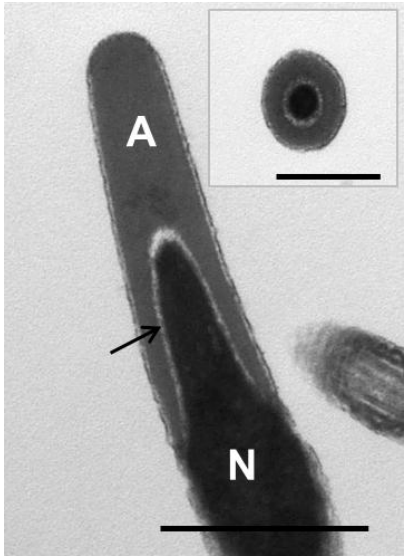

Figure 11. Longitudinal section through the apex of the sperm head showing the conical acrosome (A) covering the tip of the nucleus (N). Inset: Transverse section through the base of the acrosome illustrating the central core of nuclear material surrounded by the acrosome. Bar = 1µm; inset Bar = 0.5µm.

The thread-like appendage observed on LM and SEM was also noted on TEM in both longitudinal and transverse sections of the head base (Fig. 12). In transverse section the appendage generally appeared as a thin finger-like protrusion at the base of the nucleus, but sometimes formed a small stubby triangle. It was always covered by the plasmalemma and was composed of pale, homogenous material (presumably representing a remnant of the residual cytoplasm) devoid of cytoplasmic organelles.

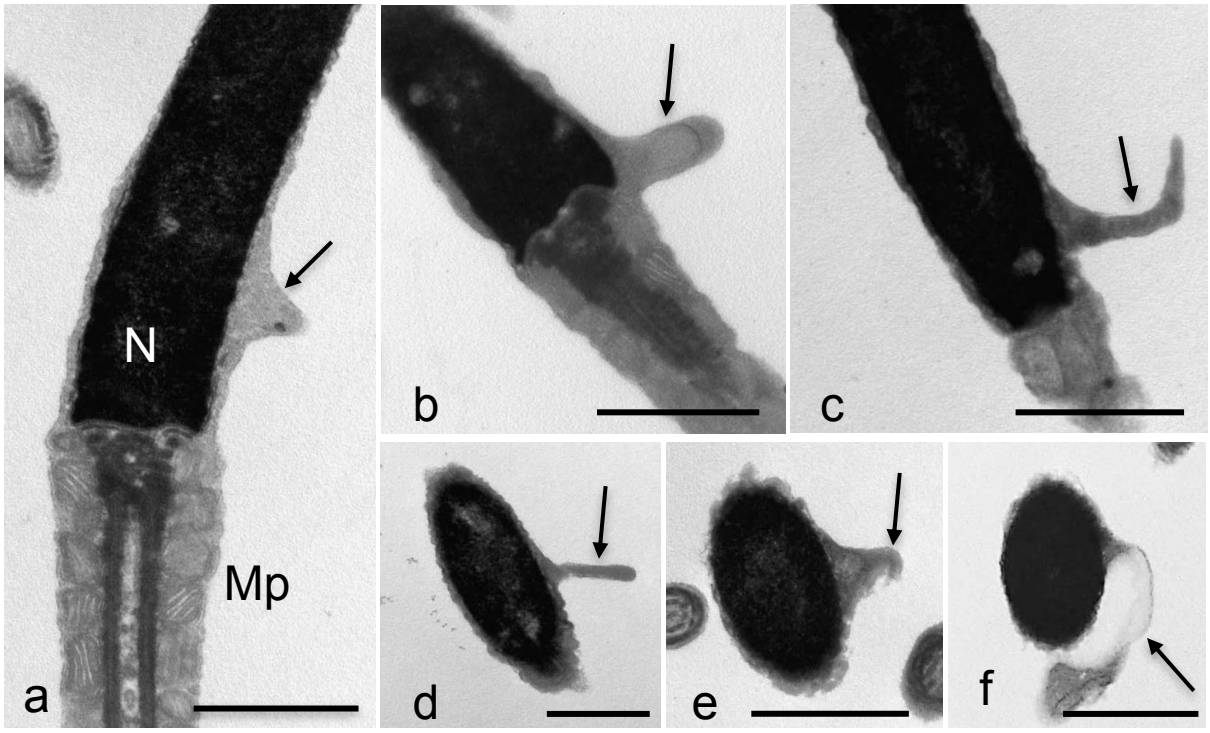

Figure 12. Longitudinal (a-c) and transverse (d-e) sections of sperm demonstrating the cytoplasmic appendage situated at the head base – midpiece region. The appendage varies in shape from short, stubby finger-like (b); slender finger-like (d); bent (c); club-shaped (f); and triangular (a,e). Bar = 1µm.

The neck:

The neck region (forming the connection between the head and the midpiece) (Fig. 13) displayed a shallow concave implantation fossa at the base of the nucleus lined by a thin layer of moderately electron-dense material, the basal plate. The fossa appeared in the form of individual impressions each housing one of the poorly defined segmented columns that, together with the capitulum, formed the connecting piece. Depending on the plane of section, two shallow impressions were generally observed at the nuclear base (Fig. 13a,b), suggesting that the implantation fossa consisted of a series of depressions running along the perimeter of the nuclear base. The tips of the segmented columns merged to form the capitulum, which was separated from the basal plate by an intervening layer of clear material. The short proximal centriole lay below the base of the nucleus, was enclosed by the connecting piece and lay on top of, and at right angles to, the long distal centriole. In transverse section, the proximal centriole displayed nine sets of triplet microtubules embedded in a ring of moderately electron dense material (Fig. 13b). In longitudinal section it appeared as a hollow, cup-shaped structure with thick walls in which the triplet microtubules were embedded (Fig. 13c). The central cavity of the centriole appeared empty although in some instances it contained fine flocculant material. Mitochondria of

the *pars spiralis* extended into the neck region, lying sandwiched between the plasmalemma and the segmented columns (Fig. 13a).

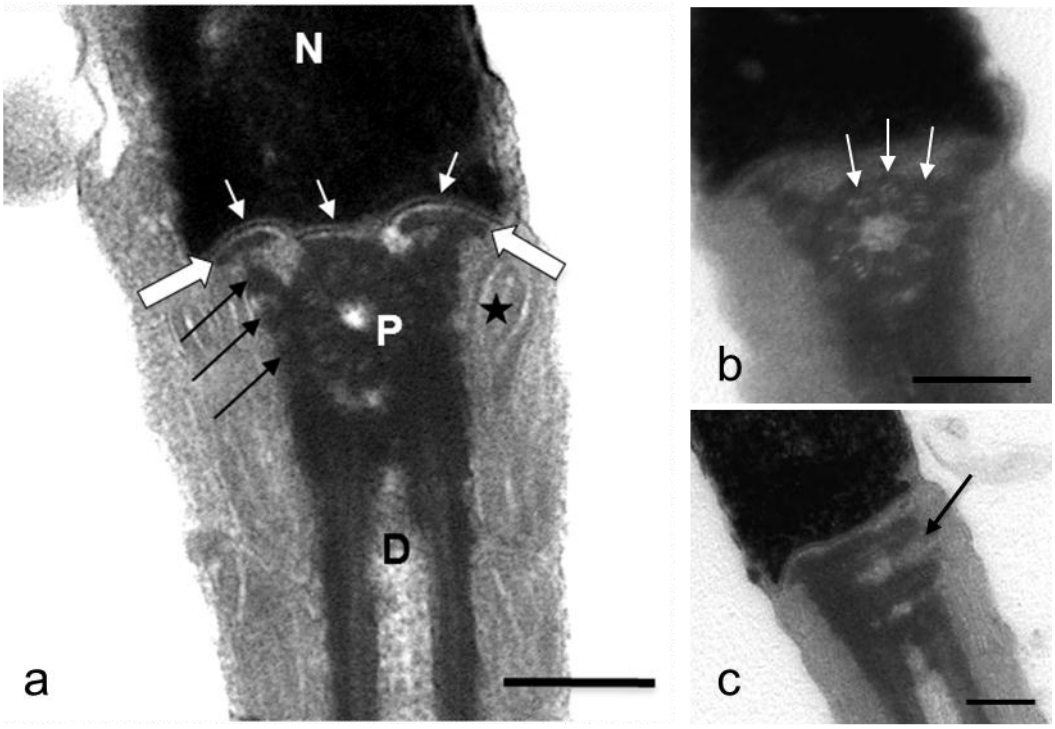

Figure 13. (a) Neck region of a normal emu sperm. Nucleus (N), basal plate (white arrows), capitulum (block arrows), segmented columns of connecting piece (black arrows), proximal centriole (P), distal centriole (D), mitochondria (star). Note the two shallow impressions representing the implantation fossa and which house elements of the connecting piece. In (b) the triplets of the nine microtubules (arrows) can clearly be distinguished, while in (c) the proximal centriole appears cup-shaped (arrow) due to the plane of section. Bar = 0.25µm.

The midpiece:

The distal centriole lay immediately below and at right angles to the proximal centriole and extended the full length of the midpiece (Figs. 14a, 15a-c). Transverse sections through the anterior segment of the distal centriole revealed a thick electron-dense wall containing nine sets of triplet microtubules (Fig. 14c). The centriolar lumen generally appeared empty in this part of the midpiece, although in some instances granular/flocculant material, similar to that seen in the proximal centriole, was observed (Fig. 14a). In transverse sections through the posterior segment of the distal centriole, a rod of dense material containing two free microtubules was evident. This rod was generally centrally placed within the centriolar lumen (Fig. 14d) although in some cells it adopted an eccentric position. The eccentric positioning would explain why in some longitudinal sections the lumen of the distal centriole appeared empty (Fig. 15c). In a few instances the rod appeared to extend the full length of the distal centriole (Fig. 15a). From its point of origin, which was variable within the distal centriolar lumen, the rod extended the full length of the midpiece to

terminate just above the annulus. The two free microtubules, however, continued caudally as the central pair of microtubules of the axoneme (Figs. 14a, 15b).

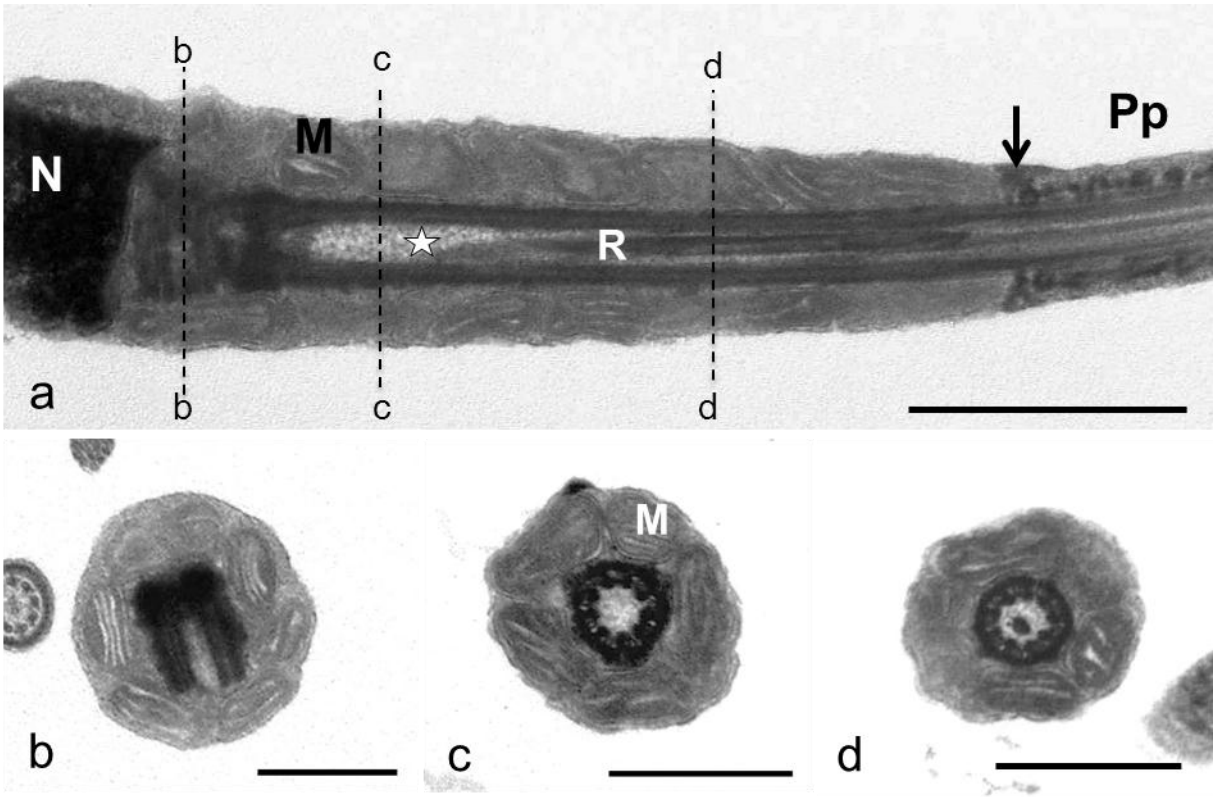

Figure 14. (a) Longitudinal section through the neck and midpiece. Note the long distal centriole which is filled with flocculant material in the anterior region (star), and the rod (R) containing the central pair of microtubules in the posterior segment of the centriole. The annulus (arrow) demarcates the boundary between the midpiece and principal piece. Figs. (b-d) represent equivalent cross-sections of the regions marked b – d in Fig. 14(a). Fig. (b) illustrates a section through the proximal centriole, (c) a section through the anterior aspect of the distal centriole showing the lumen filled with flocculant material and (d) a section through the posterior region of the distal centriole with the centrally positioned rod of dense material. Nucleus (N), mitochondria (M), principal piece (Pp). Bar (a) =1µm; Bar (b-d) = 0.5µm.

The distal centriole was bordered peripherally by the mitochondria of the *pars spiralis*. In longitudinal sections seven to eight mitochondrial profiles could be seen running the entire length of the midpiece and into the neck region (Fig. 14a), while in most transverse sections of the midpiece five to six mitochondria could be discerned (Figs. 14 b-d). This gave an approximate number of 40 mitochondria forming the mitochondrial sheath. The mitochondria were closely packed and mostly rectangular in form with parallel cristae, although some round forms were observed. There appeared to be no inter-mitochondrial cement present.

The midpiece terminated at the poorly-developed annulus. This structure formed an indistinct band or ring of moderately electron-dense material that demarcated the boundary between the midpiece and the principal piece of the flagellum (Fig. 16). The annulus abutted the last row of

mitochondria and extended roughly halfway between the plasmalemma and the outer microtubular doublets of the axoneme. In some instances elements of the fibrous sheath of the principal piece were observed interposed between the annulus and the axoneme (Fig. 16b) or even between the mitochondria of the *pars spiralis* and the axoneme (Fig. 16c). However, in a small number of sperm, the annulus was relatively well-developed and filled the space between the plasmalemma and the axoneme. No retro-annular recess was observed in the mature sperm.

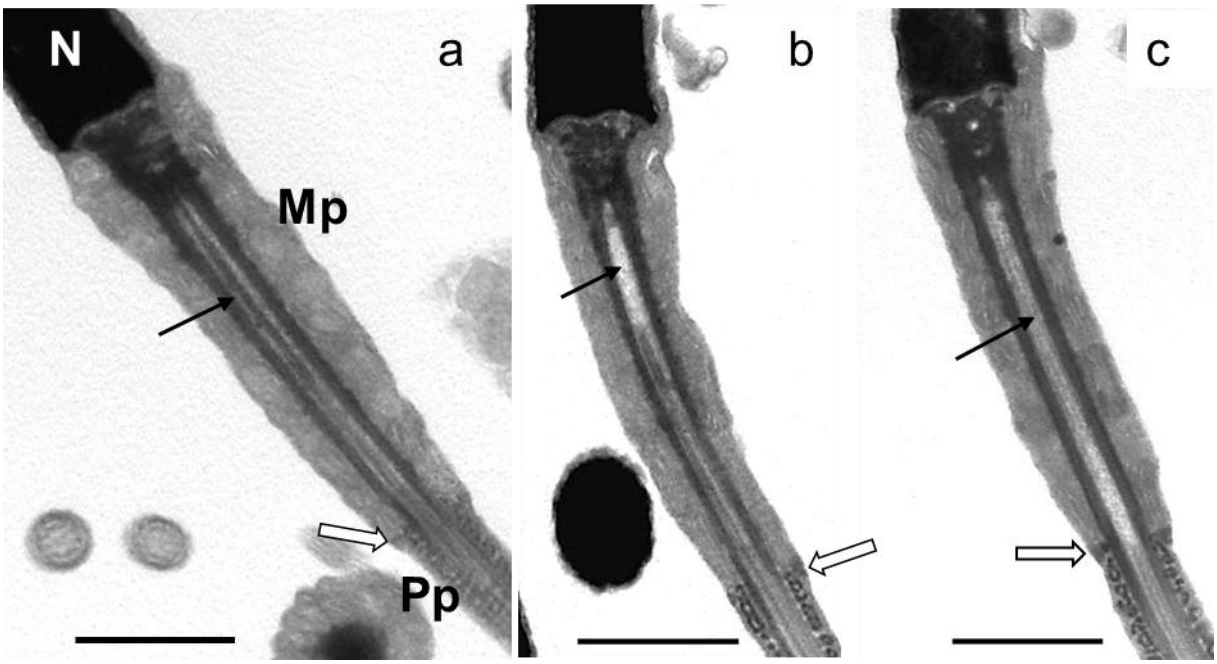

Figure 15. Longitudinal sections through the neck and midpiece. Note in (a) the rod of dense material (arrow) running the complete length of the midpiece. In (b) the lumen of the anterior part of the distal centriole appears empty (arrow) with the rod of dense material only occupying the posterior two thirds of the centriolar lumen. In (c) the lumen of the entire centriole appears empty (arrow). The annulus (open arrows) in (a) and (b) is indistinct, while in (c) it is slightly more pronounced. Nucleus (N), midpiece (Mp), principal piece (Pp). Bar = 1µm.

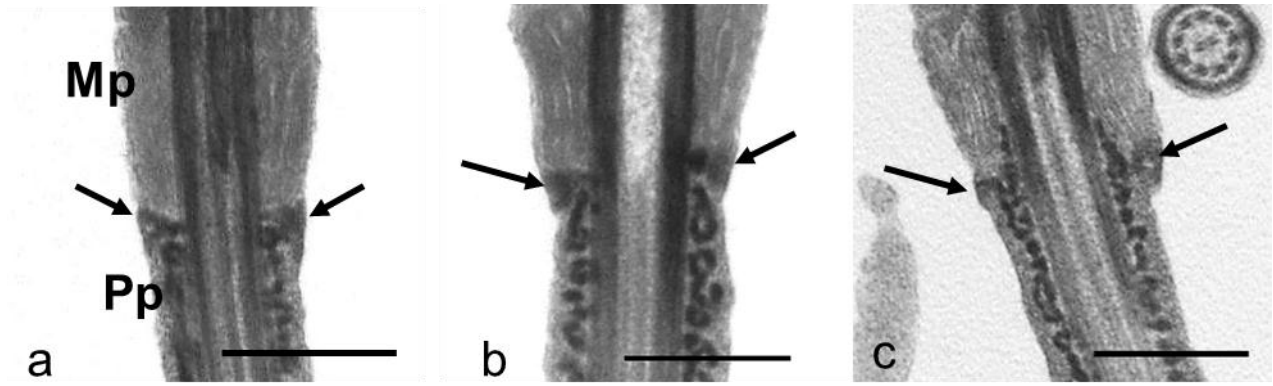

Figure 16. Transition between the midpiece (Mp) and the principal piece (Pp). Note the annulus (arrows) and (a) the positioning of elements of the fibrous sheath beneath the annulus, (b) between the annulus and axoneme and (c) between the mitochondria of the midpiece and the axoneme. Bar = 0.5µm.

The principal piece:

The long principal piece (average length 47.45 ± 2.8µm) consisted of the axoneme surrounded by an electron-dense, ribbed fibrous sheath. The axoneme displayed the typical structural features previously recorded for the ostrich (Soley, 1992, 1993) and was composed of nine regularly spaced outer doublet microtubules surrounding a central pair of single microtubules. In transverse section the A subunit of each doublet exhibited a circular profile and was filled with dense material, whereas the B subunit formed an incomplete lucent cylinder attached to subunit A (Fig. 17). Dynein arms were seen projecting in a clockwise direction from the A microtubule towards subunit B of the neighbouring doublet. Radial spokes connected the peripheral doublets to the central pair of microtubules and could be clearly discerned in both transverse (Figs. 17, 18) and longitudinal (Fig. 19a) sections of the principal piece.

The principal piece could be divided into two regions based on structural peculiarities and differences in diameter. The first (proximal) region lay immediately beneath the annulus, was relatively short and was approximately 0.5µm in diameter. The fibrous sheath consisted of two poorly defined longitudinal columns lying in line with the central pair of axonemal microtubules, although this arrangement was not obvious in all the cells studied. The columns, when present, manifested as discrete, broad thickenings of the fibrous sheath which gave the principal piece in transverse sections a laminated appearance (Figs. 17, 18). Although the columns themselves were not always obvious, their position could be determined by the presence of a small septum-like extension of the columns linking them to the adjacent microtubular doublets (doublets 3 and 8) (Fig. 17). The columns were connected by flimsy rib-like structures which in some transverse sections also appeared laminated. Due to the relatively loose arrangement of the fibrous sheath in this region, it sometimes appeared as a multi-layered structure in longitudinal sections of the tail (Fig. 19a). A layer of cytoplasm, composed of fine flocculant material, was present between the fibrous sheath and plasmalemma (Fig. 18a). Another notable feature of this region was the presence of nine small outer dense fibres positioned between the fibrous sheath and the axonemal doublets. Each dense fibre was closely associated with its corresponding doublet (Figs. 17, 18). Dense fibres 3 and 8 were lost a short distance beneath the annulus and replaced by a discrete projection of material emanating from the longitudinal columns. It was clear from the relative scarcity of transverse sections of the principal piece demonstrating the dense fibres that they only occupied a short segment of the anterior region of this part of the tail.

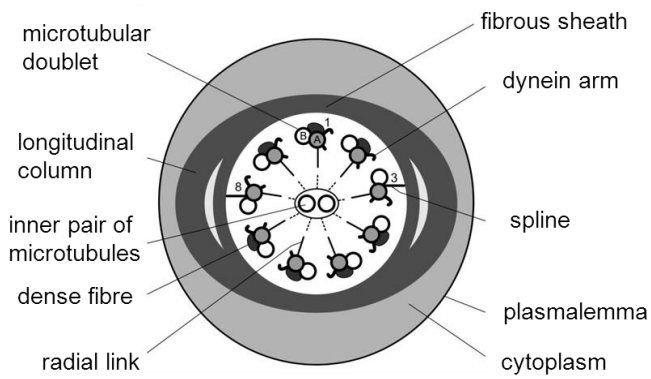

Figure 17. Schematic diagram showing the various structures of the proximal part of the principal piece.

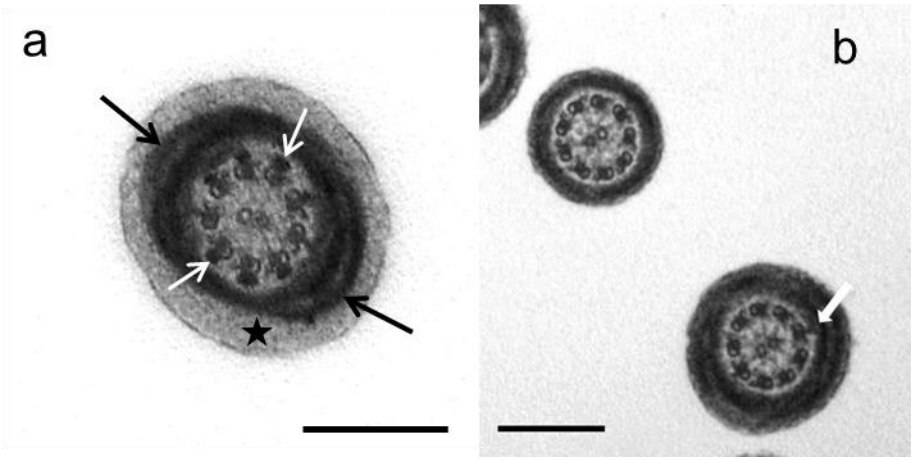

Figure 18. Transverse sections through the proximal (a) and distal (b) segments of the principal piece. Note the difference in diameter [particularly of the distal segment shown in (b)], the laminated longitudinal columns (black arrows) joined by ribs, the various components of the axoneme and in (a) the small dense fibres (white arrows) associated with the doublet microtubules as well as the layer of cytoplasm (star) present between the plasmalemma and fibrous sheath. In (b) the spline connecting one of the doublets to the fibrous sheath is indicated (white arrow). Bar = 0.25µm.

The second (distal) and longest region of the principal piece was markedly thinner in diameter (approximately 0.3µm) and tapered gradually towards the endpiece. The fibrous sheath was thinner and more compact, the longitudinal columns were no longer present or were poorly developed and the plasmalemma lay closely apposed to the fibrous sheath (Figs. 18b, 19c). The axoneme displayed the characteristic structure although the spline of dense material linking doublets 3 and 8 to the fibrous sheath was often poorly developed or absent.

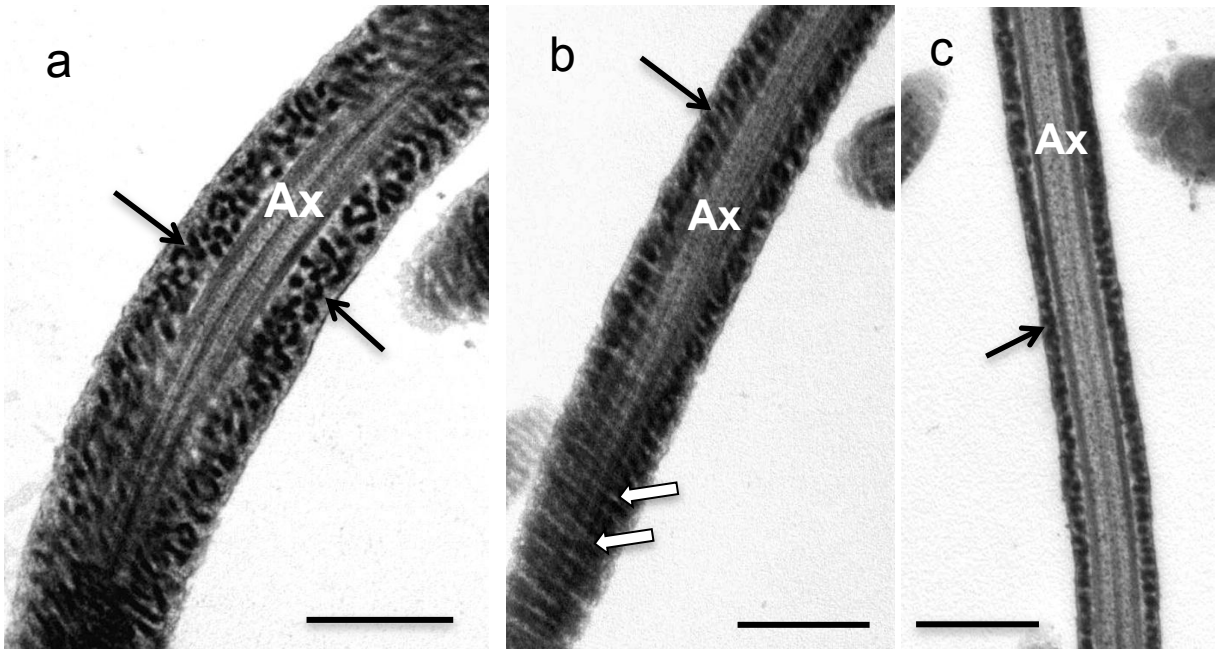

Figure 19. Longitudinal sections of the proximal (a and b) principal piece. In (a) the fibrous sheath appears multi-layered (arrows) and the outer and central microtubules of the axoneme (Ax) are connected by evenly-spaced radial spokes. In (b) the connecting ribs are illustrated in transverse (black arrow) and longitudinal (white arrows) section. In (c) the fibrous sheath of the distal principal piece (arrow) is markedly thinner and tightly covered by the plasmalemma. Bar = 0.5µm.

The endpiece:

The flagellum terminated in a short endpiece essentially composed of the axoneme covered by the plasmalemma. The fibrous sheath sometimes terminated evenly at the transition between the principal piece and endpiece (Fig. 20a), but generally ended in a staggered fashion (Fig. 20b). The organized arrangement of the axoneme was disrupted along the length of the endpiece with separation of the microtubular doublets being observed as well as loss of the dynein arms and radial spokes. A random decrease in the number of microtubules, most of which were electron-lucent, was obvious towards the termination of the endpiece (Fig. 20 inset).

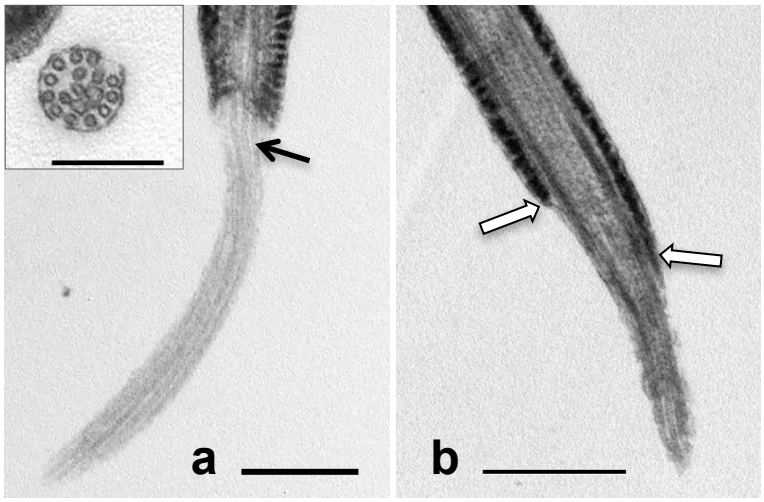

Figure 20. Longitudinal sections through the endpiece of the flagellum. Note the continuation of the axonemal microtubules (arrows) from the principal piece into the endpiece. The inset in (a) demonstrates a transverse section of the endpiece containing 15 electron lucent microtubules. In (b) the staggered arrangement of the fibrous sheath can clearly be seen (white arrows). Bar = 0.5µm; inset Bar = 0.25µm.

Discussion

Avian sperm can be divided into two basic types according to their structure, namely, the more "primitive" filiform sperm typical of non-passerine birds and the complex helical sperm of passerine species (Asa & Phillips, 1987). A degree of overlap between the two basic morphological sperm types has been observed, based mainly on the tendency towards spiralization seen in some non-passerine birds (McFarlane, 1963). Sub-oscine species are also reported to display morphological features of both passerine and non-passerine bird sperm (Asa & Phillips, 1987). The primitive filiform sperm is 'worm-like' in appearance and is also referred to as 'sauropsid' since it resembles reptilian sperm (Jamieson, 2007). Emu sperm are typically filiform in appearance and on LM closely resemble those of other ratites such as the ostrich (Soley, 1992) as well as galliform birds, notably the chicken (Grigg, 1951), goose (Ferdinand, 1992) and turkey (Wakely & Kosin, 1951).

Various methods have been used to prepare and examine avian sperm at the light microscope level. Despite the use of these techniques, however, published light micrographs on avian sperm morphology are not always convincing. In a light microscopic study of chicken sperm, Lake *et al*. (1968) reported that it was difficult to discern the different segments of the cell with the limited magnification and resolution of the light microscope while Soley (1992) reported that the endpiece in ostrich sperm was difficult to resolve by light microscopy irrespective of which imaging technique was used. The use of wet mount protocols, although necessary for motility studies, is limited in scope for the morphological examination of sperm (Mocé & Graham, 2008) and fewer normal sperm are identified using this method than with stained smears (Meschede *et al.*, 1993). While some studies on avian sperm have used air-dried fresh semen smears (Humphreys, 1972; Hemberger *et al.*, 2001; Łukaszewicz *et al.*, 2008; Tabatabaei *et al.*, 2009), the use of fixed avian semen samples for light microscopic evaluation has been found to be advantageous. Various fixatives have been employed, for example, formaldehyde (Ferdinand, 1992) and Hancock's solution (Alkan *et al.*, 2002). The current study used 2.5% glutaraldehyde in 0.13M Millonig's phosphate-buffer as this was also the fixative of choice for ultrastructural studies. This fixative, in combination with the specific stain used, gave excellent results (see below). Fixing semen immediately after collection preserves the overall sperm morphology and the specimens can then be stained and examined at the investigator's convenience. It also has the added benefit of reducing cell shrinkage that results from air-drying fresh semen smears. In respect of ostrich sperm, Gee and co-workers (2004) compared non-fixed eosin-nigrosin stained semen smears and unstained glutaraldehyde fixed semen smears and found that fixing with glutaraldehyde gave the best structural detail. This was also the method of choice of Bertschinger *et al*. (1992) in an earlier study of ostrich sperm morphology.

Mammalian sperm studies have also largely relied on the use of stains, particularly the Romanowsky type stains, to reveal structural detail. Mota and Ramalho-Santos (2006) found the Diff-Quick® stain useful in revealing head abnormalities in cat sperm. This stain is similar to Wright's stain used in the present study and is employed routinely in human reproduction laboratories, usually in conjunction with bright field microscopy. Similarly, the SpermBlue® stain, developed by Van der Horst and Maree (2009) and tested on a number of mammalian and non-mammalian species, also differentially stains the various sperm components with the added benefit that the stained smears are suitable for automated analysis. In their study on bull sperm, Specher and Coe (1996) found that phase contrast microscopy of unstained smears was a more accurate method of studying sperm morphology as it revealed a greater number of cytoplasmic droplets and head abnormalities than standard bright field microscopy of eosin-nigrosin stained semen smears. This study demonstrated that the characteristic filiform shape of emu sperm was particularly amenable to the use of phase contrast microscopy with glutaraldehyde-fixed and Wright's-stained smears. Examining stained smears with phase contrast microscopy proved to be a rapid and convenient method for clearly distinguishing the various components of emu sperm.

Morphometry

Although based on a limited number of species, the length of non-passerine bird sperm appears to be highly variable (McFarlane, 1963, Humphreys, 1972; Briskie *et al*., 1997; Briskie & Montgomery, 2007). However, a comparison of the dimensions of sperm from three ratite species (Table 1) demonstrates a remarkable uniformity. The average length of emu sperm (67µm) was similar to that (65µm) previously reported by Baccetti *et al*. (1991). It is noteworthy that Baccetti and co-workers (1991) based their measurements on SEM images whereas the present study used light micrographs. As the semen samples in both studies were fixed with glutaraldehyde, it would therefore appear that there was little additional shrinkage as a result of the samples being dehydrated for SEM. No obvious difference in total sperm length or head length was observed between the birds from the Eastern Cape and North-West Province. In contrast, Soley and Roberts (1994) distinguished two subgroups of domesticated South African ostriches based on total sperm length, suggesting that "the two different ranges of sperm size observed may reflect persistent genetic (subspecies) variations in the domestic ostrich population". Farmed South African ostriches are known to be hybrids resulting from the crossing of local *S.camelus australis* stock with North African (*S.camelus camelus*) and Syrian (*S.camelus syriacus*) birds for the improvement of feather quality (Smit 1964). Emus on the other hand have only recently been introduced into South Africa and the provenance of these birds is unknown. If sperm head length and total length are indicators of genetic origin, as appears to be the case with South African ostriches, the emus investigated in the present study could conceivably be of the same genetic stock. It is interesting to note that three subspecies of emu have been recognised in Australia,

namely, *Dromaius navaehollandiae novaehollandiae, D. novaehollandiae woodwardi* and *D. novaehollandaie rothschildi* (Sales, 2007). Whether differences in head length would reflect the identity of these subspecies as reported in sandhill cranes (Sharlin *et al*., 1979) remains speculative.

With a total length of approximately 66µm, ratite sperm are appreciably shorter (see Table 1) than sperm from a number of other non-passerine birds. Chicken sperm, for example, range in total length from 90µm (Thurston & Hess, 1987) to 109µm (Lake *et al.* 1968) while turkey sperm measure from 75 - 80µm (Marquez and Ogasawara, 1975; Thurston & Hess, 1987). Sperm of another galliform bird, the guinea fowl, also display similar dimensions, varying in length between 75-87 µm (Thurston *et al.,* 1982; Thurston & Hess, 1987). On the other hand, pigeon (Szumowski *et al.*, 1976) and quail (Woolley, 1995) sperm are appreciably longer with lengths of approximately 165µm and greater than 227µm, respectively. There are also non-passerine birds with sperm that fall within the range of ratite sperm. For instance, Ferdinand (1992) reported an average sperm length of 67µm in geese. Budgerigar sperm, which have features of both passerine and non-passerine birds, are slightly shorter with a total average length in the region of 62µm (Samour *et al.*, 1986).

Table 1: Comparison of ratite sperm length (µm).

	Acrosome	*Nucleus*	*Head*	*Midpiece*	*Principal piece*	*Endpiece*	*Total length*	*Technique*	*Reference*
Ostrich	2.0	(14)	16.0	3.0	40.0	1.0	60.0	SEM	Baccetti *et al.*, 1991
	1.91	10.95	12.86	3.16	51.18	2.39	69.58	SEM	Soley, 1992; Soley & Roberts, 1994
Rhea				3.0				SEM	Phillips & Asa, 1989
Emu	1.5	(10.5)	12.0	3.0	47.0	3.0	65.0	SEM	Baccetti *et al.*, 1991
	1.8 ± 0.3	11.8 ± 0.9	(13.6)	2.9 ± 0.4	47.5 ± 2.8	3.7 ± 0.8	67.64 ± 3.1	LM	Present study

Values in brackets are extrapolated.

The avian acrosome differs markedly from that of mammals in respect of its size relative to the rest of the head. In the emu it is a relatively short structure (1.8µm present study; 1.5µm reported by Baccetti *et al.*, 1991) being similar in length to that of the ostrich (maximum length of 2 µm) (Baccetti *et al.*, 1991; Soley, 1993). The acrosome of other non-passerine birds such as the chicken (Lake *et al.*, 1968; Thurston & Hess, 1987) and duck (Maretta, 1975a) are marginally longer. Nuclear length in the emu (11.8 ± 0.9µm) corresponds closely to that reported for other non-passerine birds, such as the ostrich (Soley & Roberts, 1994), chicken (Lake *et al*., 1968),

duck (Maretta, 1975a) and guinea fowl (Thurston *et al*., 1982). It should be noted, however, that nuclear length as measured in ratites and tinamous is not an accurate representation of this segment of the head due to the nuclear rostrum in these species extending deep within the acrosome.

The midpiece of emu sperm and other ratites (Phillips & Asa 1989; Baccetti *et al.*, 1991; Soley, 1993), measures approximately 3µm in length. Similar values have been presented for the chicken (Grigg & Hodge, 1949; Lake *et al.*, 1968), pigeon (Szumowski *et al.,* 1976) and turkey (Marquez & Ogasawara, 1975). However, the midpiece of non-passerine sperm can vary from very short (as in the trogon) to very long (in doves) as illustrated by McFarlane (1963) and Jamieson (2007). Some extremely long midpiece lengths have also been reported, for example, that of the domestic pigeon (98µm) (Vernon & Woolley, 1999) and Japanese quail (161µm) (Woolley 1995). To what extent midpiece length in non-passerine birds reflects the number of mitochondria required to provide the necessary energy for forward motility remains unknown, although studies in passerine birds and mammals have shown that essential biological functions, such as the provision of energy, determine gross sperm morphology (Cardullo & Baltz, 1991; Immler & Birkhead, 2007) (see also discussion on midpiece morphology and numbers of mitochondria below).

The only comparative data available on the length of the principal piece and endpiece in ratites is that for the ostrich and emu (Baccetti *et al*., 1991; Soley, 1992; Soley & Roberts, 1994). The present study revealed that the dimensions of these two regions are comparable to those reported by Baccetti *et al*. (1991). Moreover, the values are similar to those found in the ostrich (Soley 1992, Soley & Roberts, 1994). The head:tail ratio of 1:4 for emu sperm calculated in the present study is similar to the deduced value of 1:4.4 for the emu (Baccetti *et al*., 1991) and the reported value of 1:4.4 for the ostrich (Soley, 1992; Soley & Roberts, 1994). This ratio further indicates the uniformity of both head and tail lengths in ratite sperm. It remains unclear why a discrepancy exists regarding the head:tail ratio of 1:2.7 (extrapolated from data reported by Baccetti *et al*., 1991) for the ostrich as opposed to 1:4.4 (Soley, 1992; Soley & Roberts, 1994). Of the non-passerine birds, the head:tail ratio of the guinea fowl (1:4.3, extrapolated from data given by Thurston *et al*., 1982) is similar to that of the ratites (Thurston *et al*., 1982; Thurston & Hess, 1987). However, the head:tail ratio in most other non-passerines is much higher (Soley & Roberts, 1994), due to the greater length of the principal piece in these birds. Sperm tail lengths in the chicken exceed 70µm (Lake *et al*., 1968; Szumowski *et al*., 1976; Thurston & Hess, 1987) while pigeon sperm tails are reportedly longer than140µm (Szumowski *et al*., 1976), resulting in head:tail ratios of 1:6 (or higher) for the chicken and 1:9.4 for the pigeon. Studies on sperm size have mainly focussed on the benefits of increased length as a way of adapting to variations in the

female reproductive tract; for instance, longer heads have been proven to positively influence fertility (Sharlin *et al*., 1979) while the general assumption is that longer sperm tails will increase the swimming potential of sperm (Humphries *et al*., 2008; Calhim *et al*., 2011). Humphries *et al*. (2008), working on various animal species, came to the conclusion that, although there are a number of factors which may influence the swimming speed of sperm, the head:tail ratio provides a simple measurement to assess potential speed. Kleven and co-workers (2009) came to a similar conclusion in their study on passerine birds stating that swimming speed and sperm length develop independently as a result of sperm competition in birds. Reportedly polygamous species (primates and rodents) have longer and therefore faster swimming sperm than monogamous species (Gomendio & Roldan, 1991). A similar situation, due to the influence of sperm competition, is reported in promiscuous birds (Briskie & Montgomerie, 2007). Ratites, including the emu, are considered to be monogamous species (Malecki *et al*., 1998, 2000). It is therefore tempting to suggest that ratites (with relatively short sperm and a low head:tail ratio) do not require fast-swimming sperm to compete with those of other males, unlike in the shorebirds (Johnson & Briskie, 1999) that are considered to be promiscuous. This question can probably be resolved by the application of computer-aided sperm analysis (CASA).

Morphology

Whereas sophisticated and presumably more 'objective' methods such as CASA and flow cytometry are used by larger laboratories for sperm analysis, these techniques are costly and not always economically feasible for application in smaller laboratories. Conventional light microscopy is a relatively cheap, accessible option and will remain the most practical and cost effective manner of evaluating sperm morphology, particularly when used in conjunction with different staining and illumination techniques. Although there are limitations in the use of electron microscopy for determining the frequency of defective sperm, the higher resolution of this imaging technique allows for a more accurate appraisal of sperm morphology. The value of SEM to form a three dimensional image and of TEM to identify specific structural features, have been recognized in the evaluation of sperm morphology, with the three methods of microscopy complementing and supporting each other. This was clearly demonstrated in the present study.

During the past 25 years a number of papers have presented information on the structure of ratite and tinamou sperm (Asa *et al*., 1986; Phillips & Asa, 1989; Baccetti *et al*., 1991; Soley 1992, 1993; Soley & Roberts, 1994; Jamieson, 2007). Morphologically, ratite sperm display certain common features such as a conical acrosome capping the apex of the nucleus, a long distal centriole occupying the entire length of the midpiece and a ribbed fibrous sheath surrounding the axoneme along the length of the principal piece. However, distinct species differences within this group of birds have also been noted.

The acrosome is a small conical structure at the tip of the emu sperm head, similar to that described in the ostrich (Baccetti *et al*., 1991; Soley, 1993) and rhea (Phillips & Asa, 1989). However, when viewed in sagittal section, the apical tip of the acrosome in the emu displayed a more rounded profile than the sharper tip described for the ostrich and rhea. The nuclear rostrum extends deep within the acrosome in ratite sperm, resulting in the lateral profiles of the acrosome thinning towards the acrosome-nuclear shoulder. The acrosome of the budgerigar, parrots and cockatiel, although also conical in form, does not form a cap over the tip of the nucleus as described in ratites, but ends adjacent to the nucleus without overlapping it (Samour *et al*., 1986; Jamieson *et al*., 1995; Lovas *et al*., 2012). Not all non-passerines have a cap-like acrosome (Jamieson *et al*., 1995), for example, in the white-naped crane (Phillips *et al*., 1987), jacana (Saita *et al*., 1983) and woodpecker (Henley *et al*., 1978), a small spherical, button-like acrosome has been described which nestles at the blunt apex of the nucleus. These species are considered to be advanced non-passerines on the basis of DNA studies (Sibley *et al*., 1988). It is also noteworthy that they do not possess a perforatorium or endonuclear canal, as in the emu (see below). The sub-acrosomal space in ratites and the tinamou is limited due to the intrusion of the nuclear rostrum beneath the acrosome. A similar situation is also apparent in members of the Columbiformes (Jamieson, 2007). However, in most other non-passerine birds, for example, the chicken (Lake *et al*., 1968; Bakst & Howarth, 1975), goose (Ferdinand, 1992), turkey (Thurston & Hess, 1987) and duck (Maretta, 1975a), the sub-acrosomal space present between the acrosome and the perforatorium, is much wider. Whether this phenomenon represents a true morphological feature or a preparation artefact remains unknown.

The sperm of most non-passerine birds display a prominent fibrous structure, the perforatorium, which is partially lodged within a shallow invagination (the endonuclear canal) of the apical nuclear membrane and partially covered anteriorly by the acrosome (Nagano, 1962; Lake *et al.*, 1968; Humphreys, 1972; Baccetti *et al*., 1980; Saita *et al*., 1983, Thurston *et al*., 1982; Samour *et al*., 1986; Jamieson, 2007). The extent to which the perforatorium lies beneath the acrosome differs between species. In some galliform birds, such as the chicken, it extends approximately halfway beneath the acrosome, whereas in the turkey (Thurston & Hess, 1987), duck (Maretta, 1975a) and white-necked crane (Phillips *et al*., 1987) the perforatorium is comparatively short and limited to the posterior aspect of the acrosome. In the budgerigar (Samour *et al*., 1986) and parrots (Jamieson *et al*., 1995), it is an extremely long structure, extending almost the full length of the sub-acrosomal region. The situation in palaeognaths is strikingly different. In the tinamou the endonuclear canal is a slim, centrally positioned, tube-like structure that extends the complete length of the nucleus (Asa *et al*., 1986), whereas in the ostrich (Baccetti *et al*., 1991; Soley, 1993) and rhea (Phillips & Asa, 1989) it is shorter and only extends part of the way into the nucleus.

The endonuclear canal is filled with moderately electron dense material analogous to the perforatorium of neognaths. In these birds the flimsy perforatorium does not extend beyond the confines of the nucleus and is not found in the sub-acrosomal space. The present study confirmed that neither an endonuclear canal nor perforatorium is present in emu sperm (Baccetti *et al*., 1991). Although this situation is unique amongst the ratites (and tinamou) examined thus far, there are some non-passerine species that do not possess a perforatorium, for example, the woodpecker (Henley *et al*., 1978) and jacana, (Saita *et al*., 1983; Jamieson, 2007). These species characteristically display a button-like acrosome and not the conical acrosome associated with a nuclear rostrum typical of the palaeognaths.

An endonuclear canal and perforatorium have also been described in reptiles (Jamieson & Scheltinga, 1993; Jamieson *et al.*, 1997) and amphibians (Scheltinga *et al.*, 2003), whereas in mammals only a poorly developed perforatorium has been identified (Olsen *et al*., 1976a; Baccetti *et al*., 1980) According to some authors (Thurston & Hess, 1987; Jamieson *et al*., 2006), the diminishing length and ultimate disappearance of the perforatorium may be indicative of an advancing evolutionary trend whereas Soley (1993) suggested that the perforatorium may represent a residual structure. Within the context of the ratites and tinamous it is tempting to ascribe phylogenetic significance to the degree of development of the perforatorium. This argument would place the tinamou in a basal position followed by the ostrich and rhea and culminating in the emu which lacks a perforatorium. It is tempting to suggest that the various ratite clades (African, South American and Australasian) originated from a common ancestor and reflect their current historical distribution due to the breakup of the palaeocontinent of Gondwana (Sibley & Ahlquist, 1995; Van Tuinen & Hedges, 2001; Johnston, 2011). However, recent evidence linking the ratites and tinamous as a polyphyletic group suggests that the various ratite clades may have developed independently, and that certain common features within this grouping may simply reflect convergent or parallel evolution (Harshman *et al*., 2008). An investigation as to the absence or presence of a perforatorium in cassowary and kiwi sperm would provide interesting supplementary information relevant to this question. The actual function of the perforatorium remains unclear (Baccetti *et al*., 1980; Thurston & Hess, 1987). Baccetti *et al*. (1980) suggest that it may act as a scaffold for the acrosome, although this clearly would not be the case in ratites where the perforatorium is entirely enclosed within the nucleus. The identification of actin filaments within the perforatorium (Baccetti, 1979; Campanella *et al*., 1979) would hint a role in sperm penetration of the ovum although Baccetti *et al*. (1980) are of the opinion that the perforatorium in birds is not involved in the acrosome reaction.

The presence of a thread-like appendage near the base of the nucleus confirmed by all three modes of microscopy (LM, SEM and TEM) employed in this study has not previously been

described in any other bird sperm. The cytoplasmic features of the appendage would suggest that it represents a remnant of residual cytoplasm resulting from the release of the mature sperm from the surrounding Sertoli cells during spermiation. The close positioning of cytoplasmic bridges to the location of the thread-like appendage during spermatogenesis is also suggestive of their involvement in the origin of the appendage (see Chapter 3, Spermiogenesis).

The neck and midpiece of ratite sperm, in common with that of non-passerine birds, extends from the base of the head to the annulus. In the emu this region displays mitochondria of the *pars spiralis* and the proximal centriole surrounded by the components of the connecting piece (segmented columns and capitulum) as in the ostrich (Soley, 1993) and rhea (Phillips & Asa, 1989). The segmented appearance of the columns is more pronounced in the emu than in the other two species. A common feature of ratite sperm is the presence of shallow, twin implantation fossae separated by a nuclear projection (Phillips & Asa, 1989 [Fig. 1a]; Soley, 1993; present study). The implantation fossa of other non-passerine birds is also described as being shallow (Jamieson, 2007) but is formed by a single concave depression of the nuclear base, as seen for example in the domestic chicken (Lake *et al*., 1968; Thurston & Hess, 1987) and duck (Maretta, 1975b).

A characteristic feature of ratite sperm is the presence of a long distal centriole which runs almost the entire length of the midpiece. It has been described in the ostrich (Baccetti *et al.*, 1991; Soley, 1993), rhea (Phillips & Asa, 1989) tinamou (Asa *et al.*, 1986) and emu (Baccetti *et al*., 1991; present study) and lies perpendicular to the proximal centriole. In other non-passerines such as the chicken (Bakst & Howarth, 1975), duck (Maretta, 1975b), turkey (Thurston & Hess, 1987), mallard (Humphreys, 1972), and budgerigar (Samour *et al*., 1986), the distal centriole is restricted to the anterior region of the midpiece. In contrast to the situation in the ratites, the axoneme in those species with a shorter distal centriole is already present in the posterior part of the midpiece, together with the nine outer dense fibres (see below). According to Thurston *et al.* (1982) guinea fowl sperm possess only a distal centriole. However, it has been demonstrated that both proximal and distal centrioles are present in this species but unusually arranged in-line, creating the impression that only a single organelle is present (Aire & Soley, 2003). The reason for this alternate arrangement of the centrioles is unknown. In the emu, as in the ostrich (Soley, 1993), the lumen of the initial (anterior) part of the distal centriole, just beneath the proximal centriole, generally appeared empty or contained flocculant material. The posterior centriolar lumen was occupied by a rod of moderately electron-dense material which contained two longitudinally disposed microtubules. The microtubules were continuous, in the vicinity of the annulus, with the central pair of axonemal microtubules as also described for the ostrich (Soley, 1993), rhea (Phillips & Asa, 1989) and tinamou (Asa *et al*., 1986). In the rhea the central

microtubules do not appear to be embedded in a rod of dense material (Phillips and Asa, 1989 [Fig. 1e]).

The present study confirmed the previous observation (Baccetti *et al.,* 1991) regarding the high number (40 or more) of tightly compacted mitochondria present in the emu sperm midpiece. The ostrich and rhea, as well as the tinamou, both have fewer mitochondria (20 and 30 respectively) (Phillips & Asa, 1989; Baccetti *et al.*, 1991; Soley, 1993) despite the midpiece lengths being similar for all the ratites. This variation in number can be attributed to either the mitochondria in the emu being smaller than those of other ratites, or to the absence of inter-mitochondrial cement in the emu, which is present in both the ostrich (Soley, 1993) and rhea (Phillips & Asa, 1989). Similarly, the tinamou also has fewer mitochondria in the midpiece as well as inter-mitochondrial cement (Asa *et al*., 1986). Other non-passerines such as the chicken (Thurston & Hess, 1987), turkey (Bakst, 1980; Thurston & Hess, 1987), duck (Maretta, 1975b) and guinea fowl (Thurston & Hess, 1987) all have fewer mitochondria (25-30) in the midpiece when compared to the emu, despite the midpiece length being similar. However, intermitochondrial cement appears to be absent in the midpiece of these birds. It has been reported that in promiscuous birds the midpiece contains many more mitochondria than the same region in monogamous birds (Johnson & Briskie, 1999), purportedly to propel the longer tail in these species. As tail lengths in the emu, ostrich and rhea are similar (see Table1), and these species are described as monogamous (Malecki *et al*., 1998, 2000), this link would appear tenuous for the emu.

The annulus, demarcating the boundary between the midpiece and principal piece, appears to be present in most non-passerine birds, including the ratites, although it is reportedly absent in the tragopan (Jamieson, 2007). In contrast to the well-developed structure described by Baccetti *et al*. (1991) and Soley (1993) in the ostrich, the annulus was not prominent in TEM sections of emu sperm. However, with the use of low voltage high resolution SEM, the ring-like nature of the annulus was well defined in uncoated emu sperm samples. An appreciation of the morphology of the annulus may be important considering the reported observation of changes in the structure of the annulus during the formation of biflagellate sperm in the drake (Maretta, 1979).

The small, dense fibres seen in emu sperm associated with the doublets in the proximal region of the principal piece, are also present as rudimentary dense fibres in the ostrich (Soley, 1993) and rhea (Phillips & Asa, 1989). It was originally reported (Asa *et al*., 1986) that dense fibres were absent in tinamou sperm, but later confirmed that they were present in the proximal region of the principal piece (Asa & Phillips, 1987). In other non-passerines such as the chicken (Lake *et al*., 1968; Bakst & Howarth, 1975), duck (Maretta, 1975b), turkey (Thurston & Hess, 1987) and guinea fowl (Thurston *et al*., 1982), similar dense fibres have been observed. In these birds the

dense fibres are more conspicuous and are detected in the distal part of the midpiece at the point caudal to the termination of the distal centriole. In the phylogenetically more advanced passerine birds the fibres are large and uniform in shape (Asa & Phillips, 1987) and present throughout the flagellum. They also appear in reptiles (Jamieson, 2007) as poorly developed fibres, whereas in mammals they are pronounced with each fibre displaying a distinctive form and extending the entire length of the principal piece (Fawcett & Phillips, 1970; Phillips, 1974; Fawcett, 1975). The outer dense fibres of ratite sperm thus appear to be rudimentary when compared to the sperm of other vertebrates and of little functional significance. To what extent these fibres may be involved in supporting the short segment of the principal piece immediately beneath the annulus, remains open to conjecture. Again, it is tempting to speculate that the evolutionary trend favours the development of larger outer dense fibres in vertebrate sperm, although Jamieson (2007) dismisses the use of this feature for the determination of phylogeny.

As is the case with mammalian sperm (Fawcett, 1975; Olsen *et al*., 1976b), the fibrous sheath of the ratite principal piece begins immediately caudal to the annulus and extends posteriorly for most of the length of the flagellum, terminating just proximal to the endpiece. In both the mammalian and the ratite flagellum, the sheath consists of two sets of circumferentially orientated ribs linked by two longitudinal columns running the length of, and on opposite sides (in line with doublets 3 and 8) of the principal piece. These longitudinal columns are prominent structures and run for most of the length of the principal piece in mammals (Fawcett, 1975; Olsen *et al*., 1976b). In contrast, in ratites the columns appear to be rudimentary as indicated by their relatively flimsy nature and laminated appearance (Asa *et al.*, 1986; Phillips & Asa, 1989; Baccetti *et al*., 1991; Soley, 1993; present study). The ribbed fibrous sheath was particularly obvious with high resolution SEM as well as in longitudinal and transverse sections of the principal piece examined by TEM. A typical ribbed fibrous sheath is absent in other non-passerine birds (Lake *et al.*, 1968; Tingani, 1973; Maretta, 1975b; Thurston & Hess, 1987), and is replaced by an amorphous sheath of moderate electron-density with no specific structural detail. The termination of the axoneme at the endpiece of the flagellum in the emu followed the general vertebrate pattern with a random decrease in the number of axonemal microtubules as previously described in the ostrich (Soley, 1993).

In conclusion, although typically filiform in general appearance, a number of common morphological features link ratite and tinamou sperm, setting them apart from other non-passerine bird sperm. These include a long distal centriole occupying almost the full length of the midpiece, extension of the two central microtubules of the axoneme deep within the lumen of the distal centriole, the presence of rudimentary outer dense fibres, a deep endonuclear canal housing a poorly developed rod-like perforatorium, and a characteristic fibrous sheath

surrounding the axoneme in the principal piece of the tail (Asa *et al*., 1986; Asa & Phillips, 1987; Phillips & Asa, 1989; Baccetti *et al*., 1991; Soley 1992, 1993; Soley & Roberts, 1994; Jamieson, 2007). Although displaying similar basic morphological features, there were nevertheless clear and marked differences between the sperm of the emu and other ratites, notably the lack of an endonuclear canal and a perforatorium in emu sperm. The tip of the acrosome is also more rounded in emu sperm than that of the other ratites and the tinamou. Moreover, there were significantly more mitochondria present in the midpiece of emu sperm coupled with an absence of inter-mitochondrial cement. Whereas the broad morphological features outlined above would appear to add credence to the general view that the ratites, together with the tinamou, form a monophyletic group at the base of the avian phylogenetic tree (Stapel *et al*., 1984; Cracraft, 2001; Johnston, 2011), it is also clear that emu sperm are distinctly different from those of the ostrich, rhea and tinamou which together share morphological affinities. This observation may lend some support to the alternate view

(Harshman *et al*., 2008) that the Australasian ratites represent a separate clade that developed independently from flightless ancestors. The close structural similarity between sperm of the ostrich, rhea and tinamou would seem to favour grouping these birds as a distinct entity. Based solely on the development and morphology of the perforatorium and endonuclear canal, and assuming that the ratites and tinamous form a monophyletic group, the tinamou appears to be the most “primitive”, followed by the ostrich and rhea, with the emu possibly representing the most advanced genus within the palaeognaths.

References

Aire, T.A. & Soley, J.T. (2003) The guinea fowl spermatozoon centriolar complex: a morphological deviation for a non-passerine bird. *Proceedings of the Microscopy Society of Southern Africa* **33**, 75.

Afzelius, B.A. (1996) The sperm cytoskeleton and its defects. *The Cytoskeleton* **3**, 325-357.

Alkan, S., Baran, A,, Özdaş, Ő,B, & Evecen, M. (2002) Morphological defects in turkey semen. *Turkish Journal of Veterinary and Animal Sciences* **26**, 1087-1092.

Asa, C., Phillips, D.M. & Stover, J. (1986) Ultrastructure of spermatozoa of the crested tinamou. Journal of Ultrastructure and Molecular Structure Research **94**, 170-175.

Asa, C.S. & Phillips, D.M. (1987) Ultrastructure of avian spermatozoa: A short review. In: Mohri, H (ed.) New Horizons in Sperm Cell Research. Gordon and Breach Science Publishers, New York, pp. 365-373.

Baccetti, B., Bigliardi, E. & Burrini, A.G. (1980) The morphogenesis of vertebrate perforatorium. *Journal of Ultrastructure Research* **71**, 272-287.

Baccetti, B., Burrini, A.G. & Falchetti, E. (1991) Spermatozoa and relationships in Paleognath birds. *Biology of the Cell* **71**, 209-216.

Bakst, M.R. (1980) Ultrastructure of chicken and turkey gametes, fertilization and oviductal sperm transport: a review. 9th International Congress of Animal Reproduction and Artificial Insemination. Madrid. Volume II: 511-517.

Bakst, M.R. & Howarth, B. (1975) The head and midpiece of cock spermatozoa examined with the transmission electron microscope. *Biology of Reproduction* **12**, 632-640.

Barth, A.D. & Oko, R.J. (1989) Abnormal morphology of bovine spermatozoa. Iowa State University Press, Ames.

Bertschinger, H.J., Burger, W.P., Soley, J.T. & de Lange, J.H. (1992) Semen collection and evaluation of the male ostrich. *Proceedings of the Biennial Congress of the South African Veterinary Association*, Grahamstown, pp.154-158.

Blom, E. (1972) The ultrastructure of some characteristic sperm defects and a proposal for a new classification of the bull spermiogram. Atti del VII Simposia Internationale de Zootechnia., Milano, pp.125-139.

Briskie,J.V., Montgomerie, R. & Birkhead, T.R. (1997) The Evolution of Sperm Size in Birds. *Evolution* **51**, 937-945.

Briskie, J.V. & Montgomerie, R. (2007) Testis size, sperm size and sperm competition. In: Jamieson BGM (ed.) Reproductive Biology and Phylogeny of Birds Part A. Science Publishers, Jersey, pp. 513-551.

Brito, L.F.C. (2007) Evaluation of stallion sperm morphology. *Clinical Techniques in Equine Practice* **6**, 249-264.

Briz, M.D., Bonet, S., Pinart, B. & Camps, R. (1996) Sperm malformations throughout the boar epididymal duct. *Animal Reproduction Science* **43**, 221-239.

Calhim, S., Double, M.C., Margraf, N., Birkead, T.R. & Cockburn, A. (2011) Maintenance of sperm variation in a highly promiscuous wild bird. *PLoS One* **6**, e28809.

Campanella, C., Gabbiani, G., Baccetti, B., Burrini, A.G. & Pallini, V. (1979) Actin and myosin in the vertebrate acrosomal region. *Journal of Submicroscopic Cytology* **11**, 53-71.

Card, C. (2005) Cellular associations and the differential spermiogram: Making sense of stallion spermatozoal morphology. *Theriogenology* **64**, 558-67.

Cardullo, R.A. & Baltz, J.M. (1991) Metabolic regulation in mammalian sperm: mitochondrial volume determines sperm length and flagellar beat frequency. *Cell Motility and the Cytoskeleton* **19**, 180-188.

Chelmońska, B., Jerysz, A., Łukaszewicz, E., Kowalczyk, A. & Malecki, I. (2008) Semen collection from Japanese Quail (*Coturnix japonica*) using a teaser female. *Turkish Journal of Veterinary and Animal Sciences* **32**, 19-24.

Cracraft, J. (2001) Avian evolution, Gondwana biogeography and the Cretaceous-Tertiary mass extinction event. *Proceedings of the Royal Society of London, Series B* **268**, 459-469.

Dowsett, K.F., Osborne, H.G. & Pattie, W.A. (1984) Morphological characteristics of stallion spermatozoa. *Theriogenology* **22**, 463-472.

Du Plessis, L. & Soley, J.T. (2011a) Incidence, structure and morphological classification of abnormal spermatozoa in the emu (*Dromaius novaehollandiae*). *Theriogenology* **75**, 589-601.

Du Plessis, L. & Soley, J.T. (2011b) Head-base bending and disjointed spermatozoa in the emu (*Dromaius novaehollandiae*): a morphological comparison of two closely related defects. *Theriogenology* **76,**1275-1283.

Du Plessis, L. & Soley, J.T. (2012a) Abaxial tail implantation in the emu, *Dromaius novaehollandiae*: morphological characteristics and origin of a rare avian sperm defect. *Theriogenology* **77**, 1137-1143.

Du Plessis, L. & Soley, J.T. (2012b). Structural peculiarities associated with multiflagellate sperm in the emu, *Dromaius novaehollandiae. Theriogenology* **78**, 1094-1101.

Fawcett, D.W. (1975) The mammalian spermatozoon. *Developmental Biology* **44**, 394-436.

Fawcett, D.M. & Phillips, D.W. (1970) Recent observations on the ultrastructure and development of the mammalian spermatozoon. In: Baccetti, B. (ed.) Comparative Spermatology, Academic press, New York, pp.13-28.

Ferdinand, A. (1992) Licht- und elektronenmikroskopische Untersuchungen zur Morphologie von Ganterspermatozoen. Ph.D Thesis, University of Veterinary Medicine, Hannover.

Freneau, G.E., Chenoweth, P.J., Ellis, R. & Rupp, G. (2010) Sperm morphology of beef bulls evaluated by two different methods. *Animal Reproduction Science* **118**, 176-181.

Gee, G.F., Bertschinger, H., Donoghue, A.M., Blanco, J. & Soley, J.T. (2004) Reproduction in nondomestic birds: Physiology, semen collection, artificial insemination and cryopreservation. *Avian and Poultry Biology Reviews* **15**, 47-101.

Gomendio, M. & Roldan, E.R.S. (1991) Sperm size and sperm competition in mammals. *Proceedings of the Royal Society of London B* **243**, 181-185

Grigg, G.W. & Hodge, A.J. (1949) Electron microscopic studies of spermatozoa. I. The morphology of the spermatozoon of the common domestic fowl (*Gallus domesticus*). *Australian Journal of Scientific Research, Series B* **2**, 271-286.

Grigg, G.W. (1951) The morphology of fowl spermatozoa. 9th World's Poultry Congress, Paris. Volume 1 pp.142-145.

Harshman, J., Braun, E.L., Braun, M.J., Huddleston, C.J., Bowie, R.C.K., Chojnowski, J.L., Hackett, S.J., Han, K-L., Kimball, R.T., Marsk, B.D., Miglia, K.J., Moore, W.S., Reddy, S., Sheldon, F.H., Steadman, D.W., Steppan, S.J., Witt, C.C. & Yuri, T. (2008) Phylogenetic evidence for multiple losses of flight in ratite birds. *Proceedings of the National Academy of Sciences of the United States of America (PNAS)* **105**, 13462-13467.

Hemberger, M.Y., Hospes, R. & Bostedt, H. (2001) Semen collection, examination and spermiogram in ostriches. Reproduction in Domestic Animals **36**, 241-243.

Henley, C., Feduccia, A. & Costello, D. P. (1978) Oscine spermatozoa: A light and electron-microscopy study. *The Condor* **80**, 41-48.

Holstein, A.F. & Roosen-Runge, E.C. (1981) Atlas of human spermatogenesis. Grosse Verlag, Berlin.

Humphreys, P.N. (1972) Brief observations on the semen and spermatozoa of certain passerine and non-passerine birds. *Journal of Reproduction and Fertility* **29**, 327-336.

Humphries, S., Evans, J.P. & Simmons, L.W. (2008) Sperm competition: linking form to function. *BMC Evolutionary Biology* **8,** 319.

Immler, S. & Birkhead, T.M. (2007) Sperm competition and sperm midpiece size: no consistent pattern in passerine birds. *Proceedings of the Royal Society B* **274**, 561-568.

Irons, P.C., Bertschinger, H.J., Soley, J.T. & Burger, W.P. (1996) Semen collection and evaluation in the ostrich. In: D.C. Deeming (ed.) Improving our understanding of ratites in a farming environment. Ratite Conference, Manchester, pp. 157-199.

Jamieson, B.G.M. (2007) Avian spermatozoa: Structure and Phylogeny. In: Jamieson, B.G.M. (ed.) Reproductive Biology and Phylogeny of Birds Part A. Science Publishers, Jersey, pp. 349–511.

Jamieson, B.G.M. & Scheltinga, D.M. (1993) The ultrastructure of the spermatozoa of *Nangura spinosa* (Scincidae, Reptilia). *Memoirs of the Queensland Museum* **34**, 169-179.

Jamieson, B.G.M., Koehler, L. & Todd, B.J. (1995) Spermatozoal ultrastructure in three species of parrots (Aves, Psittaciformes) and its phylogenetic implications. *The Anatomical Record* **241**, 461-468.

Jamieson, B.G.M., Scheltinga, D.M. & Tucker, A.D. (1997) The ultrastructure of spermatozoa of the Australian freshwater crocodile, *Crocodylus johnstoni* Krefft, 1873 (Crocodylidae, Reptilia). *Journal of Submicroscopic Cytology and Pathology* **29**, 265-274.

Jamieson, B.M.G., Hodgson, A. & Spottiswood, C.N. (2006) Ultrastructure of the spermatozoon of *Myrmecocichla formicivora* (Vieillot, 1881) and *Philetairus socius* (Latham, 1790) (Aves; Passeriformes), with a new interpretation of the passeridan acrosome. *Acta Zoologica* **87**, 297-304.

Jasko, D.L., Lein, D.H. & Foote, R.H. (1990) Determination of the relationship between sperm morphologic classifications and fertility in stallions: 66 cases (1987-1988). *Journal of the American Veterinary Medicine Association* **197**, 389-394.

Johnson, D.D.P. & Briskie, J.V. (1999) Sperm competition and sperm length in shorebirds. *Condor* **101**, 848-854.

Johnston, P. (2011) New morphological evidence supports congruent phylogenies and Gondwana vicariance for palaeognathous birds. *Zoological Journal of the Linnean Society* **163**, 959-982.

Kamar, G.A.R. & Rizik, M.A.A. (1972) Semen characteristics of two breeds of turkeys. *Journal of Reproduction and Fertility* **29**, 317-325.

Kavak, A., Lundeheim, N., Aidnik, M. & Einarsson, S. (2004) Sperm morphology in Estonian and Tori breed stallions. *Acta Veterinaria Scandinavica* **45**, 11-18.

Kleven, O., Fossøy, Laskemoen, T., Robertson, R.J., Rudolfsen, G. & Lifjeld, J.T. (2009). Comparative evidence for the swimming speed by sperm competition and female sperm storage duration in passerine birds. *Evolution* **63**, 2466-2473.

Lake, P.E., Smith, W. & Young, D. (1968) The ultrastructure of the ejaculated fowl spermatozoan. *Quaterly Journal of Experimental Physiology* **53**, 356-366.

Lovas, E.M., Filippich, L.J. & Johnston, S.D. (2012) Spermiogenesis in the Australian cockatiel *Nymphicus hollandicus. Journal of Morphology in press.*

Łukaszewicz, E., Jerysz, A., Partyka, A. & Siudzińska, A. (2008) Efficacy of evaluation of rooster sperm morphology using different staining methods. *Research in Veterinary Science* **85**, 583-588.

MacLeod, J. & Gold, R.Z. (1951) The male factor in fertility and infertility, IV: sperm morphology in fertile and infertile marriage. *Fertility and Sterility* **2**, 394-414.

Malecki, I.A., Cummins, J.M., Martin, G.B. & Lindsay, D.R. (1998) Effect of collection frequency on semen quality and the frequency of abnormal forms of spermatozoa in the emu. *Animal Production in Australia* **22**, 406.

Malecki, I.A., Beesley J.R. & Martin, G.B. (2000) Changes in the characteristics of emu semen with season. *British Poultry Science* **41**, Supplement S18.

Malecki, I.A., Rybnick, P.K. & Martin, G.B. (2008) Artificial insemination technology for ratites: a review. *Australian Journal of Experimental Agriculture* **48**, 1284-1292.

Malmgren, L. (1997) Assessing the quality of raw semen: a review. *Theriogenology* **48**, 523-530.

Maretta, M. (1975a) The ultrastructure of the spermatozoon of the drake. I. Head. *Acta Veterinaria Academiae Scientiarum Hungaricae* **25**, 47-52.

Maretta, M. (1975b) The ultrastructure of the spermatozoon of the drake. II. Tail. *Acta Veterinaria Academiae Scientiarum Hungaricae* **25**, 53-60.

Maretta, M. (1979) Ultrastructure of double and multiple sperm tails in drakes. *Veterinarni Medicina* **24**, 679-689.

Marquez, B.J. & Ogasawara, F.X. (1975) Scanning electron microscope studies of turkey semen. *Poultry Science* **54**, 1139-1143.

Martínez, AI Peña. (2004) Canine fresh and cryopreserved semen evaluation. *Animal Reproduction Science* **82**, 209-224.

Marvan, F., Rob, O. & Janeckova, E. (1981) Classification of morphological abnormalities of gander sperm. *Zuchthygiene* **16**, 176-183.

McFarlane, R. W. 1963. The taxonomic significance of avian sperm. In: Sibley, G.C. (ed.) *Proceedings of the XIII International Ornithological Congress.* American Ornithologists' Union: Ithaca, New York, pp. 91-102.

Menkveld, R., Oettlé, E.E., Kruger, T.F., Swanson, R.J., Acosta, A.A. & Oehninger, S. (1991) Atlas of human sperm morphology. Williams & Wilkins, Baltimore.

Meschede, D., Keck, C., Zander, M., Cooper, T.G., Yeung, C,-H. & Nieschlag, E. (1993) Influence of three different preparation techniques on the results of human sperm morphology analysis. *International Journal of Andrology* **16**, 362-369.

Mocé, E. & Graham, J.K. (2008) In vitro evaluation of sperm quality. *Animal Reproduction Science* **105**, 104-118.

Mota, P.C. & Ramalho-Santos, J. (2006) Comparison between different markers for sperm quality in the cat: Diff-Quick as a simple optical technique to assess changes in the DNA of feline epididymal sperm. *Theriogenology* **65**, 1360-1375.

Nagano, T. (1962) Observations on the fine structure of the developing spermatid in the domestic chicken. *Journal of Cell Biology* **14**, 193-205.

Nöthling, J.O. & Irons, P.C. (2008) A simple multidimensional system for the recording and interpretation of sperm morphology in bulls. *Theriogenology* **69**, 603-611.

Nwakalor, L.N., Okeke, G.C. & Njoku, D.C. (1988) Semen characteristics of the guinea fowl *Numida meleagris meleagris*. *Theriogenology* **29**, 545-554.

Oettlé, E.E. (1993) Sperm morphology and fertility in the dog. *Journal of Reproduction and Fertility Supplement* **47**, 257-260.

Oettlé, E.E. & Soley, J.T. (1988) Sperm abnormalities in the dog: a light and electron microscopic study. *Veterinary Medicine Review* **59**, 28-70.

Olsen, G.E., Hamilton, D.W., Fawcett D.W. (1976a) Isolation and characterization of the perforatorium of rat spermatozoa. *Journal of Reproduction and Fertility* **47**, 293-297.

Olsen, G.E., Hamilton, D.W., Fawcett D.W. (1976b) Isolation and characterization of the fibrous sheath of rat epididymal spermatozoa. *Biology of Reproduction* **14**, 517-530.

Penfold, L.M., Wildt, D.E., Herzog, T.L., Lynch, W., Ware, L., Derrickson, S.E. & Monfort, S.L. (2000) Seasonal patterns of LH, testosterone and semen quality in the Northern pintail duck (*Anas acuta*). *Reproduction, Fertility and Development* **12**, 229-235.

Phillips, D.M. (1974) Spermiogenesis. Academic Press, London.

Phillips, D.M., Asa, C.S. & Stover, J. (1987) Ultrastructure of spermatozoa of the white-naped crane. *Journal of Submicroscopic Cytology* **19**, 489-494.

Phillips, D.M. & Asa, C.S. (1989) Development of spermatozoa in the rhea. *Anatomical Record* **223**, 276–282.

Saita, A., Longo, O.M., & Tripepe, S. (1983) Osservazioni comparative sulla spermiogenesi. III. Aspetti ultrastrutturali della spermiogenesis di *Jacana jacana* (Charariformes). *AccademiaNazionale Dei Lincei. (Rendiconti Della Classe Di Scienze Fisiche,Matematiche E Naturali)* **74,** 417-430.

Sales, J. (2007) The emu (*Dromaius novaehollandiae*): a review of its biology and commercial products. *Avian and Poultry Reviews* **18,** 1-20.

Samour. J.H., Smith, C.A., Moore, H.D. & Markham, J.A. (1986) Semen collection and spermatozoa characteristics in budgerigars (*Melopsittacus undulates*). *The Veterinary Record* **118**, 397-399.

Scheltinga, D.M., Wilkinson, M., Jamieson, B.G.M. & Oommem, V.O. (2003) Ultrastructure of the mature spermatozoa of caecilians (Amphibia: Gymnophiona). *Journal of Morphology* **258**, 179-192.

Sharlin, J.S., Shaffner, C.S. & Gee, G.F. (1979) Sperm head length as a predictor of fecundity in the sandhill crane, *Grus canadensis*. *Journal of Reproduction and Fertility* **55**, 411-413.

Sibley, C.G., Ahlquist, J.E. & Monroe, B.L. (1988) A classification of the living birds of the world based on DNA-DNA hybridization studies. *The Auk* **105**, 409-423.

Sibley, C.G. & Ahlquist, J.E. (1995) Phylogeny and classification of birds: a study in molecular evolution. Yale University Press, New Haven.

Smit, D.J. van Z. (1964) Ostrich farming in the Little Karoo. Bulletin No. 358, Department of Agricultural Technical Services, V & R Printers, Pretoria.

Soley, J.T. (1989) Transmission electron microscopy of ostrich (*Struthio camelus*) sperm. *Proceedings of the Electron Microscopy Society of Southern Africa* **19**, 145-146.

Soley, J.T. (1992) A histological study of spermatogenesis in the ostrich (*Struthio camelus*). Ph.D. Thesis, University of Pretoria, Pretoria.

Soley, J.T. (1993) Ultrastructure of ostrich (*Struthio camelus*) spermatozoa: I. Transmission electron microscopy. *Onderstepoort Journal of Veterinary Research* **60**, 119-130.

Soley, J.T. & Roberts, D.C. (1994) Ultrastructure of ostrich (*Struthio camelus*) spermatozoa: II. Scanning electron microscopy. *Onderstepoort Journal of Veterinary Research* **61**, 239-246.

Specher, D.J. & Coe, P.H. (1996) Differences in bull spermiograms using eosin-nigrosin stain, Feulgen stain and phase contrast microscopy methods. *Theriogenology* **45**, 757-764.

Stapel, S.O., Leunissen, J.A.M., Versteeg, M., Wattel, J. & De Jong, W.W. (1984) Ratites as oldest offshoot of avian stem – evidence from α-crystallin sequences. *Nature* **311**, 257-259.

Stockner, P.K. & Bardwick, C. (1991) The relationship of semen parameters to fertility in the dog. *Canine Practice* **16**, 15-23.

Szumowski, P., Theret, M. & Denis, B. (1976) Semen and artificial insemination of pigeons. VIIIth International Congress on Animal Reproduction and Artificial Insemination, Cracow, pp.1086-1089.

Tabatabaei, S., Batavani, R.A. & Talebi, A.R. (2009) Comparison of semen quality in indigenous and Ross broiler breeder roosters. *Journal of Animal and Veterinary Advances* **8**, 90-93.

Thurston, R.J., Hess, R.A., Hughes, B.L. & Froman, D.P. (1982) Ultrastructure of the guinea fowl (*Numidia meleagris*) spermatozoan. *Poultry Science* **61**, 1738-1743.

Thurston, R.J. & Hess, R.A. (1987) Ultrastructure of spermatozoa from domesticated birds: Comparative study of turkey, chicken and guinea fowl. *Scanning Microscopy* **1**, 1829-1838.

Tingari, M.D. (1973) Observations on the fine structure of spermatozoa in the testis and excurrent ducts of the male fowl, *Gallus domesticus*. *Journal of Reproduction and Fertility* **34**, 255-265.

Van der Horst, G. & Maree, L. (2009) SpermBlue®: A new universal stain for human and animal sperm which is also amenable to automated sperm morphology analysis. *Biotechnic and Histochemistry* **84**, 299-308.

Van Tuinen, M. & Hedges, S.B. (2001) Calibration of avian molecular clocks. Molecular Biology and Evolution **18**, 206-213.

Vernon, G.G. & Woolley, D.M. (1999) Three-dimensional motion of avian spermatozoa. *Cell Motility and the Cytoskeleton* **42**, 149-161.

Wakely, W.J. & Kosin, I.L. (1951) A study of the morphology of the turkey spermatozoa with special reference to the seasonal prevalence of abnormal types. *American Journal of Veterinary Research* **12**, 240-245.

Wooley, D.M. (1995) The structure of the spermatozoon of the Japanese quail, *Coturnix coturnix* L. var. *japonica*. *Acta Zoologica* (Copenhagen) **76**, 45-50.

Zamboni, Z. (1987) The ultrastructural pathology of the spermatozoon as a cause of infertility: the role of the electron microscope in the evaluation of semen quality. *Fertility and Sterility* **48**, 711-734.

Zamboni, Z. (1992) Sperm structure and its relevance to infertility: an electron microscopic study. *Archives of Pathology and Laboratory Medicine* **116**, 325-344.

Chapter 3 Spermiogenesis

Introduction

The complex process of sperm development that changes an undifferentiated haploid cell into the highly specialized mature spermatozoon capable of fertilizing an egg is termed spermiogenesis, or spermateliosis (Aire, 2007) and is the final stage of spermatogenesis. It was first established that sperm develop from cells in the testis in 1841 (Holstein & Roosen-Runge, 1981) but it was only with the advent of the electron microscope and other sophisticated instruments and techniques that the details of sperm development could be fully explored. The process has since been extensively studied in vertebrates, especially mammals (Leblond & Clermont, 1952a,b; Fawcett & Phillips, 1969; Yasuzumi *et al*., 1972; Phillips, 1974; Holstein, 1976; Barth & Oko, 1989; Lin *et al*., 1997, Lin & Jones, 2000; Lloyd *et al*., 2008; Sharma *et al*., 2009).

Despite the fact that there are more than 10 000 avian species (Donoghue *et al*., 2003), only a few studies on avian sperm development have been reported (Aire, 2007). For obvious reasons most investigations have been carried out on birds of economic importance such as the chicken (Nagano, 1962; McIntosh & Porter, 1967, Tingari, 1973, Gunawardana & Scott, 1977; Xia *et al*., 1986; Sprando & Russell, 1988), turkey (Aire, 2003), duck (Maretta, 1995; Simões *et al*., 2005) and quail (Lin & Jones, 1993), although a number of other bird species have also been studied. These include, for example, the house sparrow (Góes & Dolder, 2002), European nightjar (Tripepi *et al*., 2006) and Australian cockatiel (Lovas *et al*., 2012). Most of these reports are fragmentary and only a few cover the complete process of spermiogenesis at the ultrastructural level (Aire, 2007).

Based on ultrastructural observations, various stages of spermatid differentiation can be identified and different ways of classifying these stages have been proposed. Based on acrosome development, Leblond and Clemont (1952a) sub-divided spermiogenesis into four phases, namely the Golgi phase, cap phase, acrosome phase and maturation phase. Gunawardana and Scott (1977) identified four different phases of spermatid development in the fowl based on the appearance of the nucleus, namely, spermatids with round nuclei, spermatids with irregular nuclei, spermatids with elongating nuclei containing coarse granular chromatin and spermatids with long, homogeneously condensed nuclei. Concurrently, three different specializations occur which transform the undifferentiated round spermatid into the mature spermatozoon: A. acrosome

development, B. centriole development and formation of the flagellum, and C. development of the manchette microtubules and nuclear condensation.

A number of descriptions of sperm development in ratites are available. The various aspects of sperm development, as well as the complete process of spermiogenesis, have been documented for the ostrich (Baccetti *et al*., 1991; Soley, 1992, 1994, 1996, 1997), while Phillips and Asa (1989) provided an account of spermiogenesis in the rhea. A brief report on spermiogenesis in the emu chiefly comparing it to the process in the ostrich, was presented by Baccetti *et al*. (1991). However, to fully appreciate the formation and development of normal and abnormal sperm in the emu, a thorough knowledge of the process of spermiogenesis is essential. This information will form the basis for the classification of normal as well as abnormal sperm and by providing new information on morphological peculiarities may assist in solving certain phylogenetic questions regarding ratite affinities and the position of this group of non-passerine birds within the avian phylogenetic tree.

Materials & Methods

Transmission electron microscopy

The testes of 15 sexually mature emus were collected during the breeding season following slaughter at commercial abattoirs (see Chapter 2). Small blocks of testicular tissue were immediately fixed for 24 hours at 4°C in 4% glutaraldehyde, buffered with 0.13M Millonig's phosphate buffer, pH 7.4. Samples were post-fixed for 1hour in 1% similarly buffered osmium tetroxide, dehydrated through a graded ethanol series (50%, 70%, 90%, 96%, 2x100% for 20 minutes each) and cleared with propylene oxide for 20 minutes. Thereafter the samples were incubated in a 2:1 propylene oxide:resin mix for 2 hours and 1:2 propylene oxide:resin mix overnight before embedding in TAAB 812 epoxy resin (see Chapter 2 for resin details). Ultrathin sections were collected on copper grids and contrasted with uranyl acetate and lead citrate before being viewed in a Philips CM10 transmission electron microscope (Philips Electron Optical Division, Eindhoven, The Netherlands) operated at 80kV.

Results

Phases of spermiogenesis

To establish the sequence of cellular events resulting in the differentiation of the spermatid into the mature sperm, the spermatids were categorized into four developmental stages according to their nuclear structure (shape and degree of chromatin condensation) as proposed by Gunawardana and Scott (1977) and applied to spermiogenesis in the ostrich (Soley, 1992, 1994,

1996, 1997). Phase 1 spermatids presented with round nuclei, phase 2 spermatids with irregularly shaped nuclei, phase 3 spermatids displayed elongating nuclei containing coarse granular chromatin and phase 4 spermatids elongated nuclei with dense, homogeneous chromatin (Fig. 1).

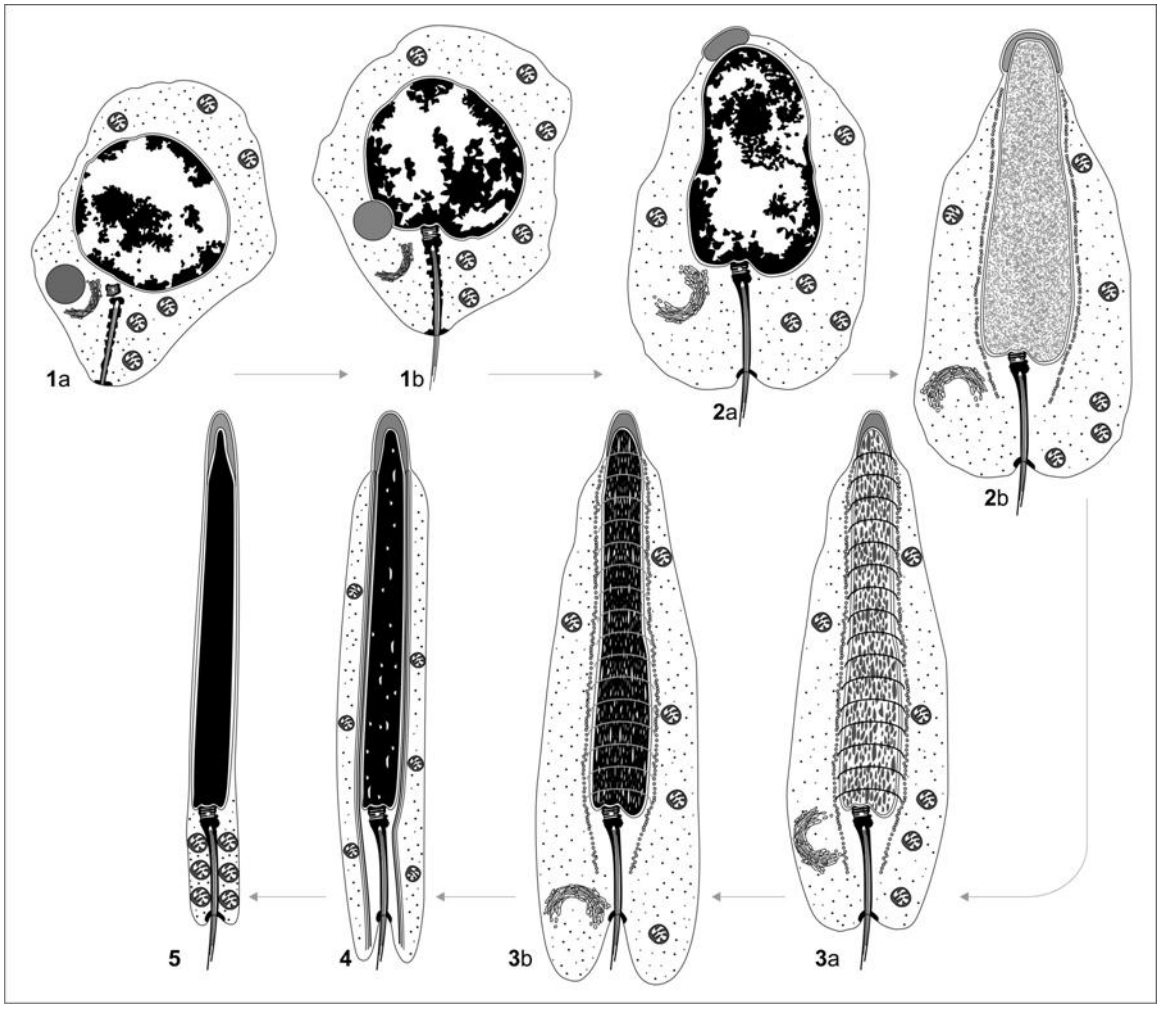

Figure 1. Schematic illustration of the various phases of spermatid development in the emu. **Phase 1** (1a & b): Round nucleus, peripheral aggregations of chromatin, attachment of round acrosomal vesicle. **Phase 2** (2a & b): Irregular (dumbbell)-shaped nucleus, fine granular chromatin, circular manchette evident. **Phase 3** (3a & b): Elongating nucleus, chromatin more condensed (filamentous) and circular manchette well developed. **Phase 4** (4): Elongated nucleus with dense compacted chromatin, longitudinal manchette present. (5) Fully formed sperm released into lumen of seminiferous tubule.

Phase 1: Spermatids with round nuclei

Early round spermatids displayed a prominent, centrally positioned, round nucleus, surrounded by a typical nuclear membrane. The nucleus contained scattered clumps of heterochromatin most of which was arranged peripherally against the nuclear membrane. The intervening clear areas contained fine flocculant material. A characteristic nucleolus was seldom observed although a

circumscribed unit of fine granular material was often present. The cytoplasm displayed numerous mitochondria, as well as smooth and granular endoplasmic reticulum, a Golgi apparatus, chromatoid bodies, the occasional lipid droplet and multivesicular bodies. No microtubules were obvious in the cytoplasm. Most of the organelles were concentrated around the diplosome in an organelle-rich region of the cytoplasm (Fig. 2).

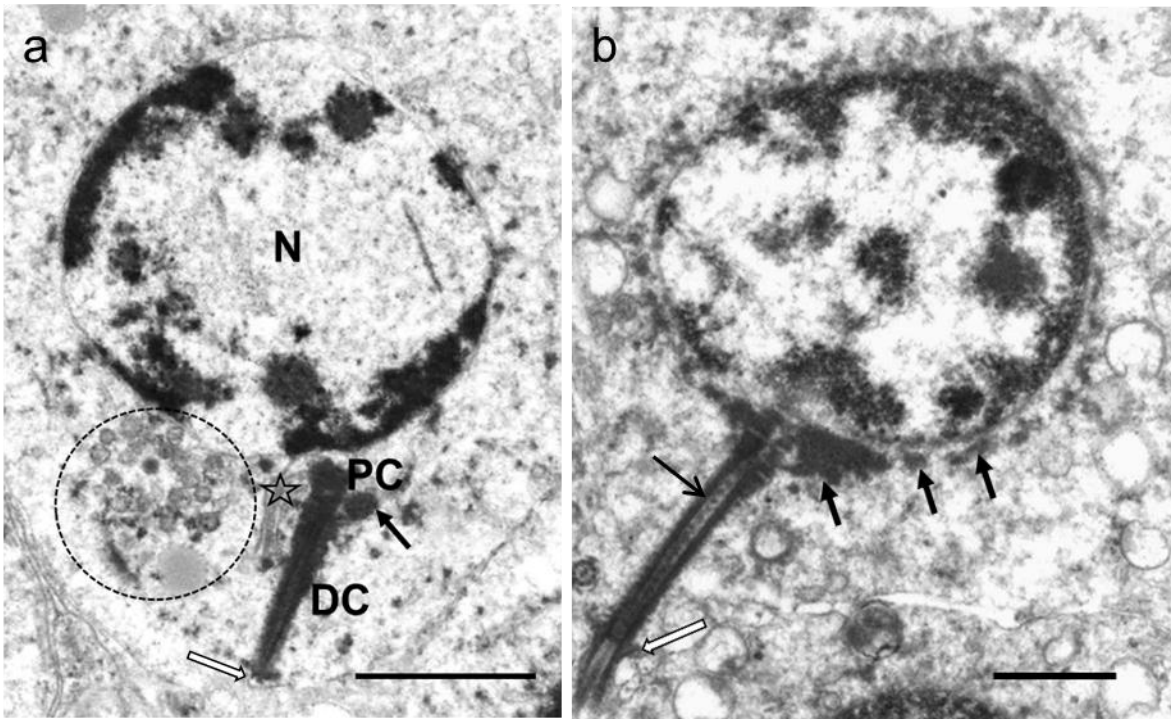

Figure 2. (a) A typical early phase 1 spermatid with a round nucleus showing peripheral arrangement of the chromatin. The proximal centriole (PC) has not yet attached to the nucleus (N) but the distal centriole (DC) is in contact with the plasmalemma (white arrow). Note also the organelle-rich region (dashed circle) in close proximity to the diplosome, Golgi apparatus (star) and chromatoid body (arrow). Fig. 2 (b) depicts a slightly later phase 1 cell. The nucleus is still round with peripheral chromatin but the diplosome has moved closer to the nuclear membrane. Note the abundance of dense material (chromatoid body) present in this area (thick black arrows). Blocks of electron dense material are visible within the lumen of the distal centriole (thick black arrow). Annulus (white arrow). Bar = 2µm.

During this stage, the first sign of acrosome formation was the appearance of a large, round acrosome vesicle close to the nuclear membrane which was filled with homogenous material of moderate electron density. This structure was generally, but not always, present in the vicinity of the Golgi apparatus (Figs. 4a-d). The typical proacrosomal vesicles described during spermiogenesis in the ostrich (Soley, 1996) were not observed in the material studied. The acrosomal vesicle was next seen to make contact with the nuclear membrane, nestling in a shallow concavity formed by the nucleolemma (Figs. 3a, 4a-d). At the point of attachment the

nuclear membrane narrowed and became more regular in appearance. As a result, this part of the nucleolemma appeared electron-dense. Patches of heterochromatin were always associated with the nuclear aspect of the concavity (Fig. 3a). The attached acrosome vesicle was observed to migrate towards the future cranial pole of the nucleus relative to the forming neck region of the spermatid but remained surrounded by ample cytoplasm.

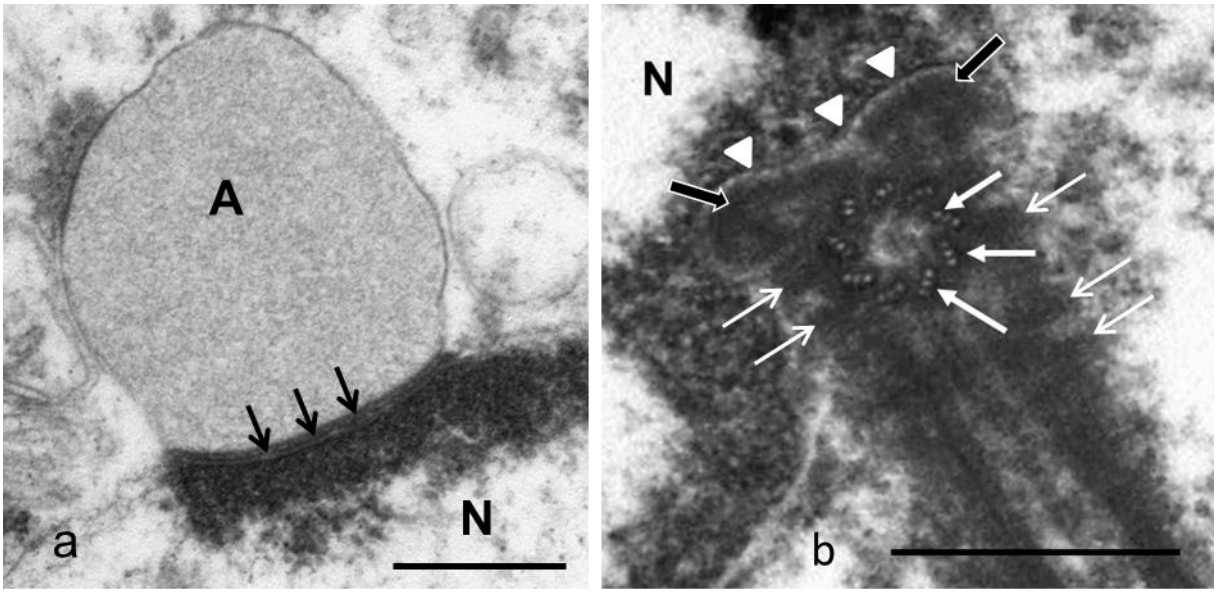

Figure 3. Phase I spermatids. (a) Point of contact between the acrosome vesicle (A) and the nucleus (N). Note the regular appearance of the nuclear membrane lining the nuclear depression (arrows) and the chromatin deposits on the nuclear aspect. (b) Transverse section showing implantation of the diplosome. The proximal centriole displays nine sets of triplet microtubules (white block arrows). Note the shallow implantation fossa (white triangles), the forming capitulum (black block arrows) and the ill-defined blocks of amorphous electron-dense material (thin white arrows) surrounding the centrioles. Bar = 0.5µm.

The diplosome was located in the vicinity of the forming acrosome and was intimately associated with the Golgi apparatus and chromatoid body (Figs. 2a, 5a). It consisted of a short proximal and long distal centriole which were positioned perpendicular to each other. The lumen of the distal centriole displayed centrally positioned small, evenly spaced blocks of electron-dense material (Figs. 2b, 5a). The proximal centriole was oriented towards, but not in contact with, the nucleus, whereas the free end of the distal centriole made contact with the plasmalemma. At its point of contact with the plasmalemma the axoneme, surrounded by the cell membrane, emerged from the free end of the distal centriole and projected into the intercellular space. There was an accumulation of electron dense material between the distal centriole and plasmalemma which represented the forming annulus. The developing flagellum was often found in the vicinity of a cytoplasmic bridge (Fig. 6b). The peripheral microtubules of the axoneme were continuous with the wall of the distal centriole. The diplosome was generally orientated perpendicularly, but

sometimes obliquely to the nucleus. In later stage phase 1 spermatids the diplosome made contact with the nuclear membrane via the proximal centriole. A shallow nuclear depression, often in the form of twin hollows, was formed at the point of contact (Figs. 3b, 5b,c). This

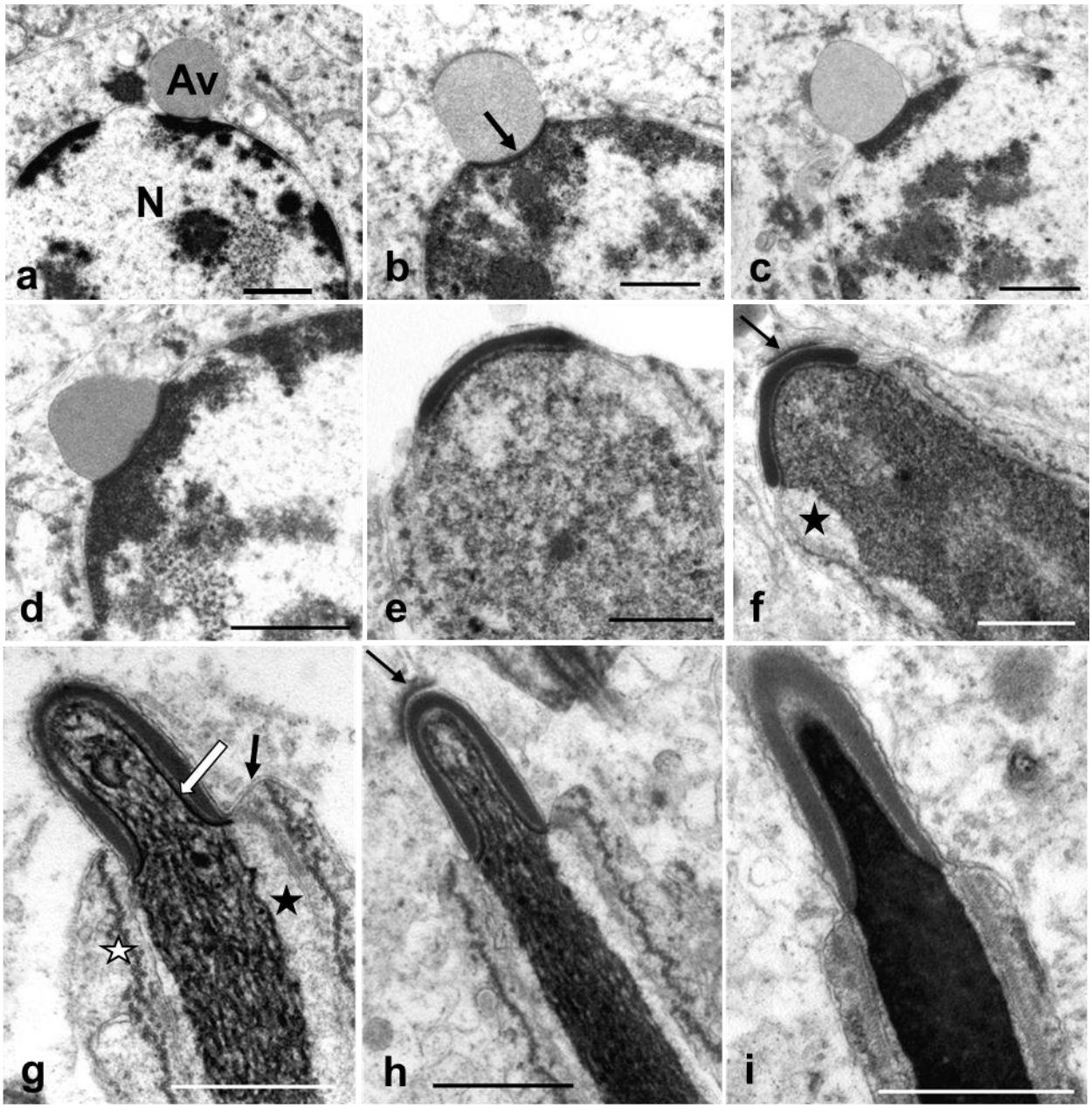

Figure 4. Progressive stages in the development of the acrosome. (a-d) Phase I spermatids showing the acrosome vesicle (AV) establishing contact with the future apical aspect of the nucleus (N). Note the fine homogenous contents of the vesicle and the shallow depression (arrow) in which it is housed. (e,f) Phase 2 spermatids illustrating the flattened, compact nature of the acrosome. Note the fine granular chromatin, more concentrated in (f) and the gap appearing between the condensing chromatin and the nucleolemma (star) in (f). (g, h) Typical phase 3 spermatids with the acrosome taking on a cone shape. The nucleus is composed of filamentous chromatin, which has pulled away from the nuclear membrane (black star). Note the dense nature of the nucleolemma (white arrow) beneath the forming acrosome, the positioning of the plasmalemma (black arrow) and the circular manchette (white star). (i) Phase 4 spermatid demonstrating the nuclear rostrum beneath the conical, tapered acrosome. The tip of the acrosome is characteristically rounded. In (f) and (h) a hemi-desmosome (arrow) connects a Sertoli cell to the tip of the spermatid. Bar = 1µm.

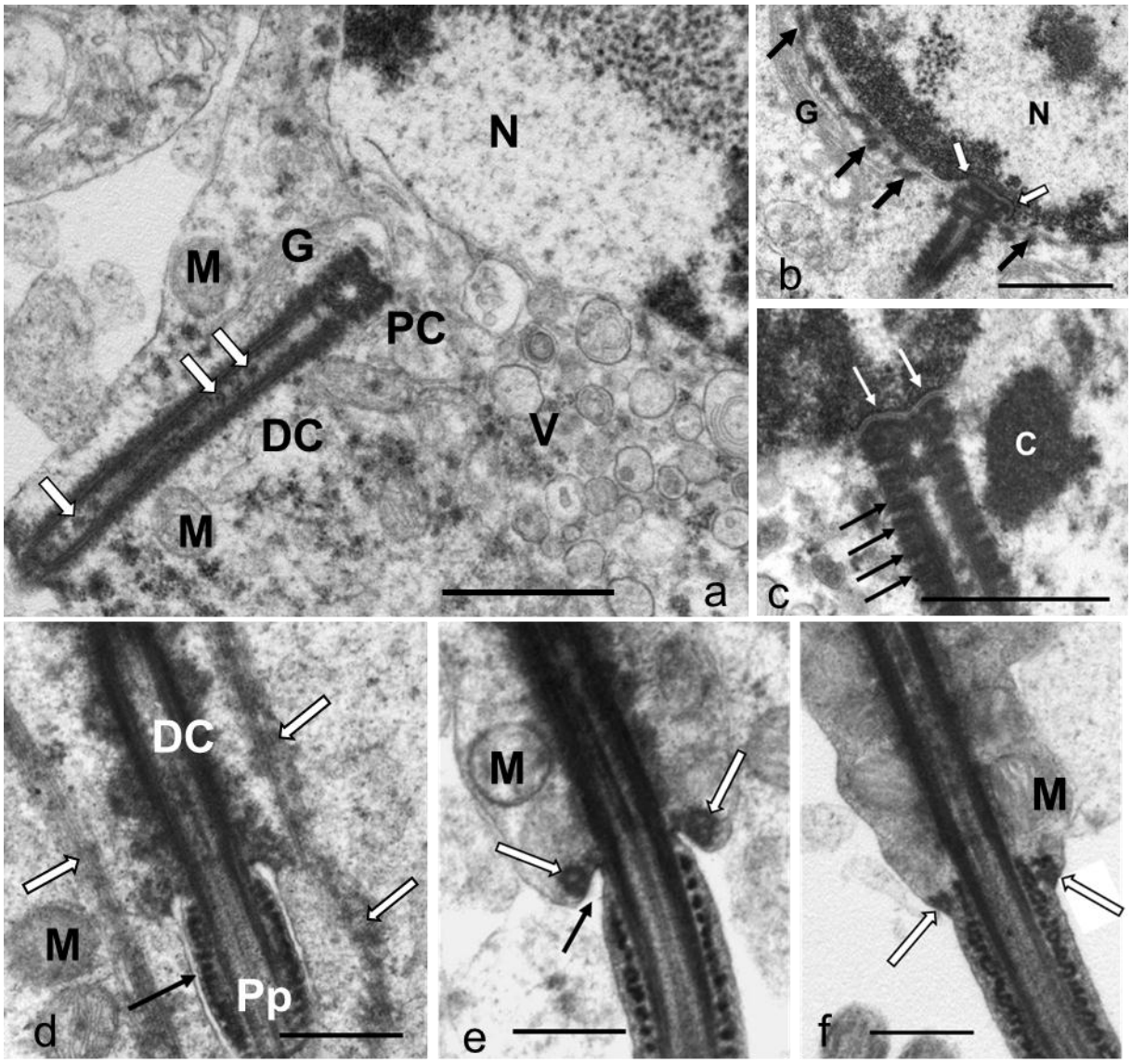

Figure 5. Progressive stages in the formation of the flagellum. (a-c) Phase 1 spermatids. Fig.5 (a) illustrates the organelle-rich region observed in the vicinity of the proximal (PC) and distal (DC) centrioles. Numerous vesicles (V), mitochondria (M) and elements of the Golgi-apparatus (G) can be seen. Blocks of dense material (white arrows) are visible within the lumen of the distal centriole. In (b) the centriolar complex nestles in a slight indentation (white arrows) in the nucleus. Note the nearby Golgi apparatus (G) and the patches of amorphous electron-dense material in the cytoplasm just beneath the nuclear membrane (black arrows). In (c) the forming segmented columns (black arrows) of the connecting piece are clearly visible, as well as the electron-dense appearance of the nuclear membrane lining the implantation fossa (white arrows). A chromatoid body (C) is closely associated with the centriolar complex. (d-f) Phase 4 spermatids. In (d) the principal piece (Pp) lies within the flagellar canal (arrow). The distal centriole (DC) and proximal region of the principal piece are surrounded by the longitudinal manchette (white arrows). In (e), a later stage 4 spermatid, the excess cytoplasm has been reduced and the flagellar canal is only represented by an annular recess (black arrow). The annulus (white arrows) is prominent at this stage, although it takes on a more inconspicuous form in late spermatids (f) just prior to spermiation. Mitochondria (M), nucleus (N). Bar (a-c) = 1µm; Bar (d-f) = 0.5µm.

depression showed similar features in respect of the nuclear membrane to the concavity housing the acrosomal vesicle. At this early stage of development, the structure of the centrioles and the forming elements of the connecting piece (segmented columns, capitulum) resembled the equivalent structures observed in the neck region of mature sperm (Fig. 3b) (see Chapter 2). The capitulum was separated from the nuclear depression by a thin layer of scanty amorphous material. A clearly defined basal plate was not observed. The modified diplosome now formed a centriolar complex (CC) which maintained a close association with the chromatoid body (Fig. 5c). The chromatoid body was an amorphous structure composed of electron-dense material and which was intimately associated with the walls of the proximal and distal (anterior part) centrioles. The chromatoid body appeared to represent the accumulation of deposits of similar material concentrated in the cytoplasm just beneath the nuclear membrane lining the future caudal pole of the nucleus (Fig. 5b).

Phase 2: Spermatids with irregular nuclei

The onset of this phase was characterized by a change in the shape of the nucleus (Fig. 6). Longitudinal sections of phase 2 spermatids revealed belt-like constrictions which, depending on their location, gave the nucleus a pear-, dumbbell-shaped or scalloped appearance. Associated with this change in nuclear profile was the appearance of microtubules in the cytoplasm close to the nuclear membrane, and which were present in greater numbers at the points of nuclear constriction (Fig. 7a). The nuclei of early phase 2 spermatids showed similar properties to phase 1 spermatids (Fig. 6a). During later stages the chromatin clumping became less obvious and the nucleus was filled with fine granular material (Fig. 8a). Changes in the appearance of the chromatin were accompanied by an increase in the number of microtubules which were now referred to as the circular manchette (CM). The CM ran the entire length of the nucleus, starting just below the acrosome-nuclear shoulder and ending in the proximal part of the midpiece (Fig. 1). In transverse sections of phase 2 spermatids the microtubules appeared as loosely arranged rings wrapped around the nucleus. In longitudinal sections they were visible as a single row of microtubules closely aligned to the nuclear membrane (Fig. 7b). During nuclear elongation and condensation the chromatin was observed to pull away from the nuclear membrane, leaving large gaps between the nuclear membrane and the karyoplasm. This was particularly evident in the proximal region of the nucleus just below the acrosome-nuclear shoulder (Figs. 4f, 8a). Later in phase 2, the manchette appeared more prominent, mainly through reinforcement of the single row of microtubules and the chromatin condensed further forming larger, coalesced electron-dense granules. At this stage small, isolated, finger-like projections of moderate electron density made their appearance in the narrow zone of cytoplasm between the CM and the nuclear membrane. These projections were closely associated with the nucleolemma (see Chapter 4).

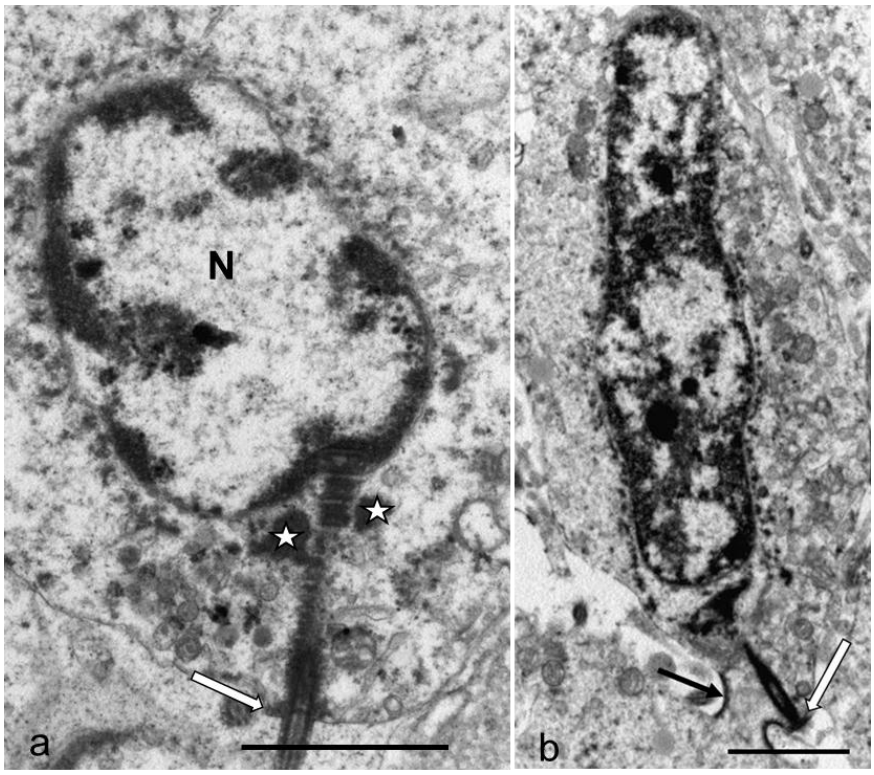

Figure 6. (a) Early phase 2 spermatid with irregularly-shaped nucleus (N) and peripherally arranged chromatin. Note the chromatoid bodies (stars) near the centriolar complex, as well as the concentration of organelles in this region. Annulus (white arrow). (b) Later phase 2 spermatid with multiple nuclear constrictions. The nucleus has elongated and the annulus (white arrow) is clearly visible near a cytoplasmic bridge (black arrow). Bar = 2µm.

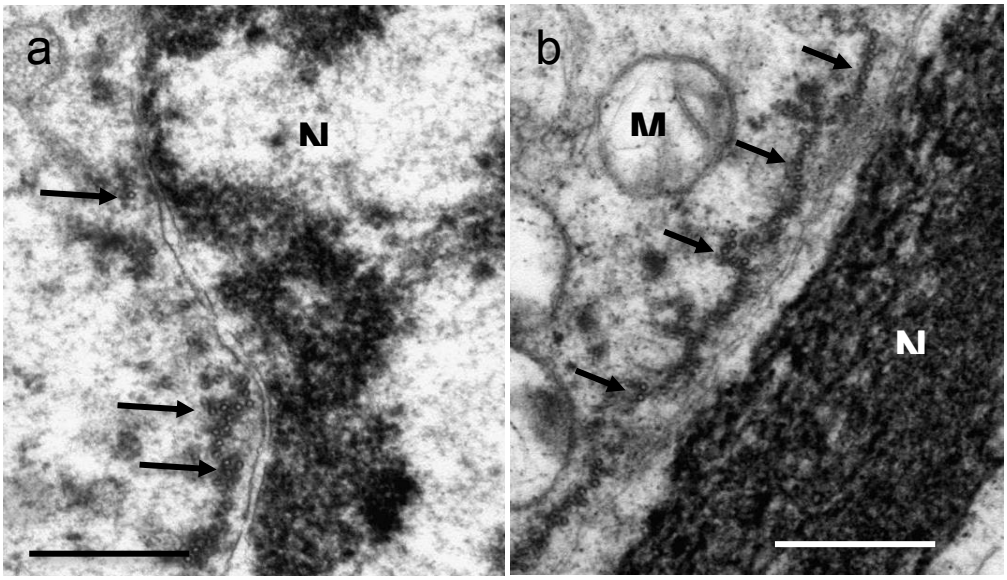

Figure 7. (a) Longitudinal section of an early phase 2 spermatid showing nuclear constrictions characterized by an accumulation of microtubules of the circular manchette in the adjacent cytoplasm (arrows). (b) Longitudinal section through a phase 3 spermatid. Note the filamentous chromatin and the single row of circular manchette microtubules (arrows) adjacent to the cytoplasmic surface of the nuclear membrane. Nucleus (N), mitochondria (M). Bar = 0.5µm.

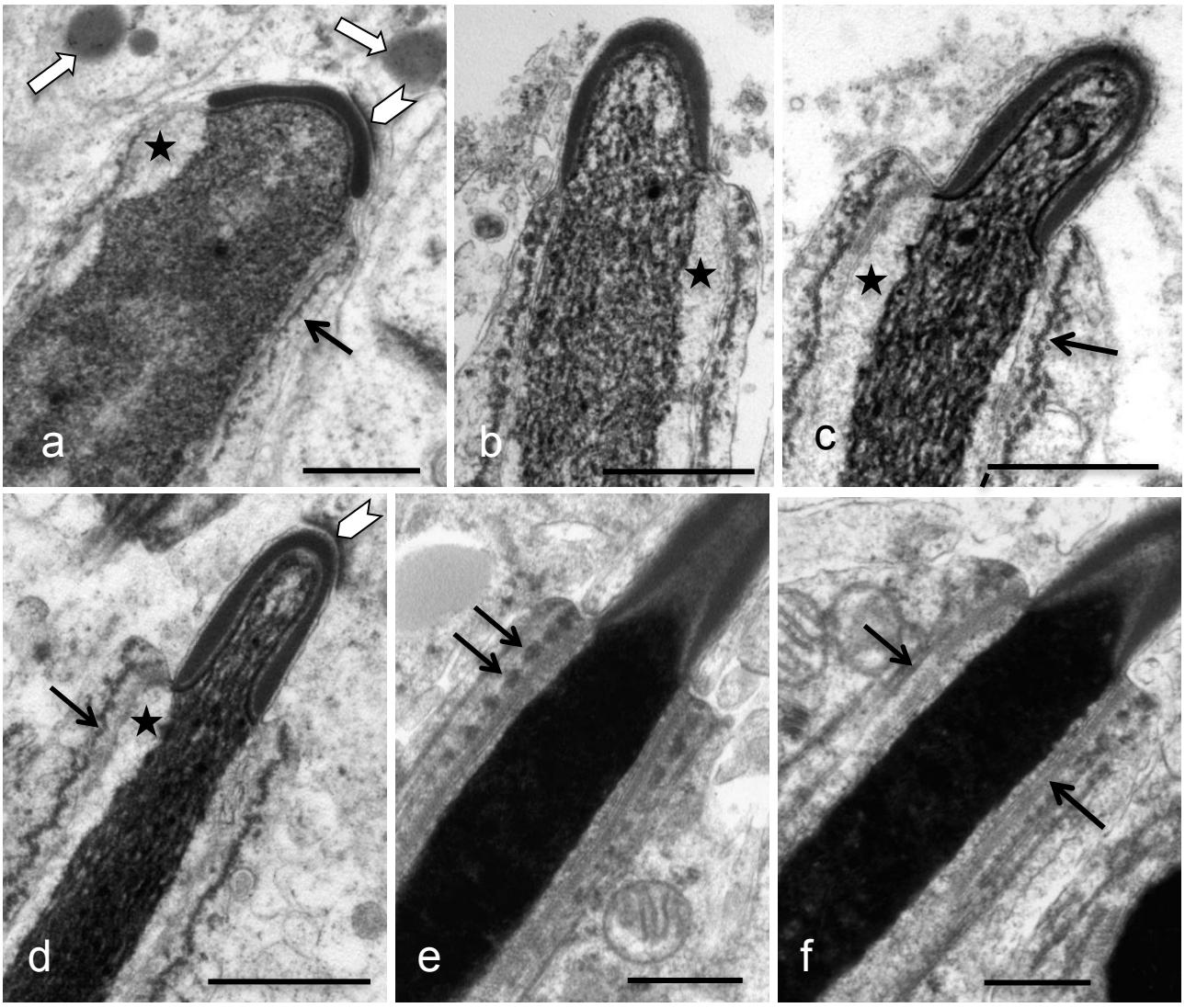

Figure 8. A series of longitudinal sections of spermatids illustrating chromatin condensation and manchette formation. (a) A typical phase 2 spermatid with fine granular chromatin. The acrosome is partly spread over the tip of the nucleus (white chevron) and the chromatin is contracting away from the nuclear membrane as it condenses (star). The circular manchette appears as a single row of transversely sectioned microtubules (black arrow). Note the lipid droplets (white block arrows) in the surrounding Sertoli cells. Fig. 8(b) shows a slightly later stage phase 2 spermatid with the chromatin appearing coarse granular. Figs. 8(c) and (d) represent successive stages of phase 3 spermatids. The chromatin is in the form of dense filaments and has contracted further away from the nucleolemma leaving a large gap (stars). The circular manchette is well developed (black arrows). (e) A late phase 3 / early phase 4 spermatid demonstrating electron-dense and homogenously condensed chromatin. The circular manchette has disappeared possibly indicating the transitional stage of manchette development and regularly spaced moderately electron-dense bodies are aligned along the length of the nucleus (black arrows). (f) A slightly later phase 4 spermatid clearly demonstrating the longitudinal manchette (black arrows) and an elongated electron-dense nucleus. The nucleolemma is closely applied to the nucleus. Note the junctional complex between the plasmalemma covering the acrosome and an adjacent Sertoli cell (chevron) in (a) and (d). Mitochondria (M) (For a series of cross sections indicating the sequence of chromatin condensation, see Chapter 4). Bar (a-d) = 1µm; Bar (e,f) = 0.5µm.

During phase 2 the acrosome vesicle, firmly attached to the nuclear membrane, had moved to the opposite pole of the nucleus from the CC and had started to change shape. It was seen to collapse onto the nucleus, flatten and spread over the nuclear surface, taking on an increasingly crescent shape. The original concave nuclear depression housing the acrosomal vesicle now formed a blunt convex projection pushing beneath the vesicle which appeared more electron-dense due to the compaction of its contents. The nuclear membrane in contact with the forming acrosome narrowed, making it appear electron-dense. A narrow electron-lucent layer was visible between the acrosome and the nucleus (Fig. 8a). The amount of cytoplasm at the acrosomal pole diminished markedly, concentrating more caudally towards the opposite pole of the nucleus. In later phase 2 spermatids (finely granular, homogenously spread chromatin), the plasmalemma was closely applied over the acrosome, with a conspicuous density being apparent beneath the plasmalemma of the adjacent Sertoli cell. This formed a hemi-desmosome-like junctional complex between the plasmalemma covering the acrosome and the surrounding arms of the Sertoli cell (Fig. 8a).

The positioning of the CC at the base of the nucleus was similar to that of phase 1 with the typical structures of the neck region becoming more defined. Immediately below the nuclear membrane a thin layer of electron-dense material, the basal plate, could be seen. Individual impressions (generally two), each housing one of the poorly defined segmented columns of the connecting piece, were discernible at the nuclear base (fossa). The proximal tips of the segmented columns merged, forming the capitulum. The basal plate and capitulum were separated by an electron-lucent layer. No specific arrangement of organelles was observed around the distal centriole at this stage of development.

The flagellum continued to develop from the caudal end of the distal centriole. With the cytoplasm concentrating in this region, the plasmalemma began to invaginate forming a flagellar canal. A thin layer of amorphous material lay between the microtubular doublets of the axoneme and the plasmalemma (Figs. 6a, 13 a inset), which, in later stage spermatids, transformed into the electron-dense elements of the fibrous sheath.

Phase 3: Spermatids with elongated nuclei containing coarse chromatin

The nucleus continued to elongate during this phase accompanied by further condensation and compaction of the nuclear chromatin. Further coalescing of the granules observed in phase 2 spermatids resulted in the formation of larger electron-dense granules (Fig. 8c) which in turn condensed further to form longitudinally disposed filaments separated by clear spaces (Fig. 8d). Concomitant with these changes, the gap between the chromatin and nuclear membrane observed during the preceding phase widened and was prominent along much of the length of

the nucleus (Figs. 8c,d). The CM was well-developed, consisting essentially of a single row of closely aligned microtubules supported periodically by additional groups of microtubules in longitudinal sections of spermatids (Fig. 10a). In transverse sections of the nucleus the manchette appeared in the form of a single, sometimes overlapping, microtubular coil (Fig. 10b). Neighbouring microtubules were connected by short filamentous linkers. The CM only extended as far as the proximal half of the distal centriole (Fig. 9b). The finger-like projections associated with the nuclear membrane observed during the previous phase of spermatid development increased in number and prominence, forming small scattered pockets throughout the surface of the nucleus (see Chapter 4). In later phase 3 spermatids, the manchette microtubules were seen to become disorganized, lose their concentric arrangement and to eventually disappear. During this transitional stage regularly spaced electron-densities appeared in the vicinity of the manchette microtubules (Fig. 8e). Towards the end of phase 3, a second set of microtubules, the longitudinal manchette (LM), orientated longitudinally and parallel to the nucleus, appeared. The LM extended from the acrosome-nuclear shoulder to well beyond the annulus. During this phase the chromatin was further compacted and there was a gradual and continual caudal migration and reduction of the cytoplasm. During the LM stage of spermatid development, the nuclear membrane-associated projections were well-developed, forming a uniformly and evenly-spaced array covering the entire surface of the nucleus (see Chapter 4).

The acrosomal contents appeared similar to that of phase 2 spermatids. The acrosome itself extended more caudally, adopting a cone / horse-shoe shape around the tip of the nucleus while tapering slightly towards its base. The plasmalemma fitted tightly over the extended acrosome. A thin zone filled with flocculant material was present between the acrosome and the nuclear membrane (Figs. 8c,d). A single hemi-desmosome-like junctional complex was again obvious between the plasmalemma covering the acrosome and the cytoplasmic processes of surrounding Sertoli cell (Fig. 8d).

Concurrently with the caudal displacement of the cytoplasm, the mitochondria migrated to the forming midpiece region. They were, however, prevented from forming a close association with the CC (as seen in mature sperm – see Chapter 2) by the presence of the CM or LM which was always interposed between the centrioles and the mitochondria. The principal piece, which was located in the flagellar canal, continued to elongate. The longitudinal columns and ribs of the fibrous sheath were formed from the amorphous material surrounding the axoneme of the principal piece. In longitudinal sections of spermatids the ribs appeared as small blocks of electron-dense material along the length of the flagellum. At this stage, both the ribs and the rudimentary longitudinal columns took on the typical features (including lamination of the two components) of the principal piece of phase 4 (Fig. 13a,b,c) spermatids and mature sperm.

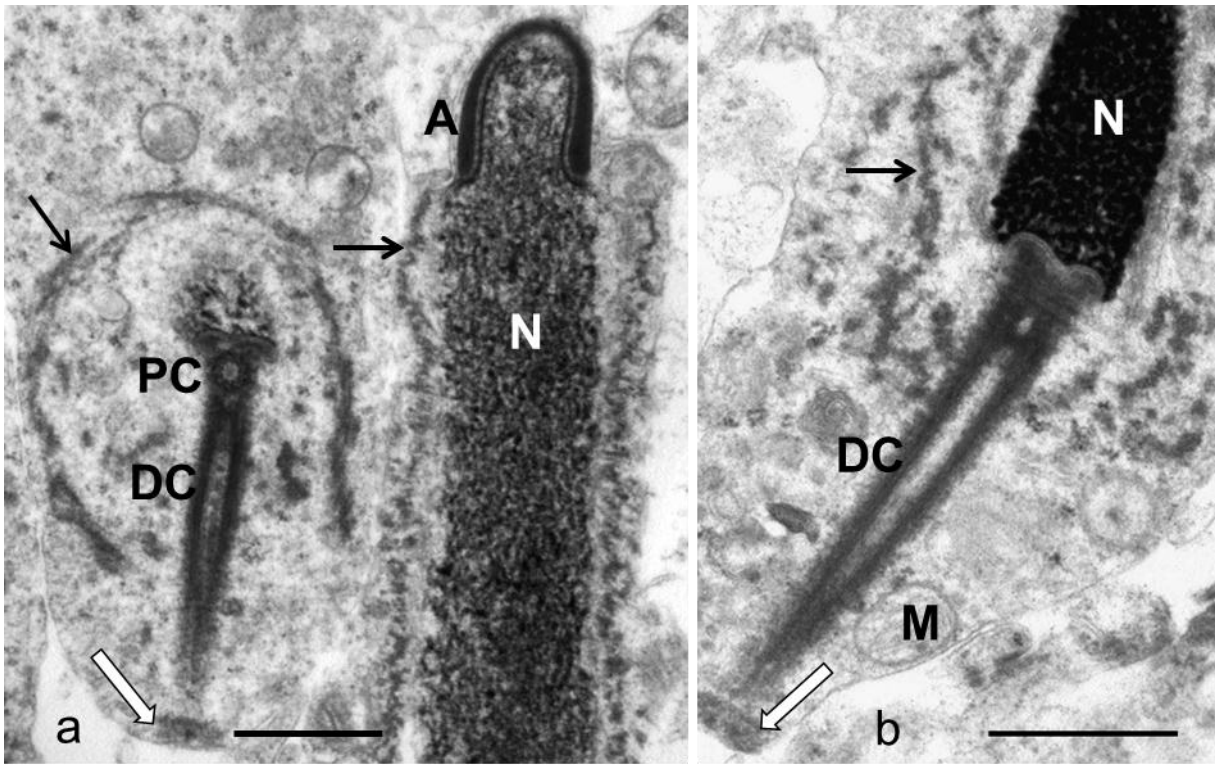

Figure 9. Longitudinal sections of early (a) and late (b) phase 3 spermatids. Note the difference in chromatin condensation between the two stages. The circular manchette (arrows) is clearly in evidence, while the annulus (white arrows) is prominent. Mitochondria (M) of the forming midpiece are present around the distal centriole (DC). Proximal centriole (PC); acrosome (A); nucleus (N). Bar = 1µm.

Phase 4: Spermatids with long nuclei and homogenous electron dense chromatin

Phase 4 spermatids displayed a long, narrow nucleus filled with homogeneous, electron-dense chromatin. Areas of incomplete chromatin condensation were occasionally observed, particularly towards the nuclear base. The gap between the condensing chromatin and the nuclear membrane had narrowed appreciably and in late stage phase 4 spermatids was seen to have disappeared leaving the nucleolemma tightly applied to the karyoplasm. The blunt, rounded tip of the nuclear rostrum seen during phase 3 was transformed into a tapering point. The now fully elongated acrosome completely covered the nuclear rostrum but displayed the same morphological features noted in phase 3 spermatids. The dense nature of the nuclear membrane covering the rostrum was no longer obvious due to the complete condensation of the chromatin. There was a marked reduction in the amount of cytoplasm surrounding the nucleus, with only the microtubules of the LM and the occasional mitochondrion being present in this region.

The LM was maximally developed during this phase and consisted of approximately three to four ill-defined rows of microtubules (Fig. 11a, b) interconnected by short filamentous linkers. When

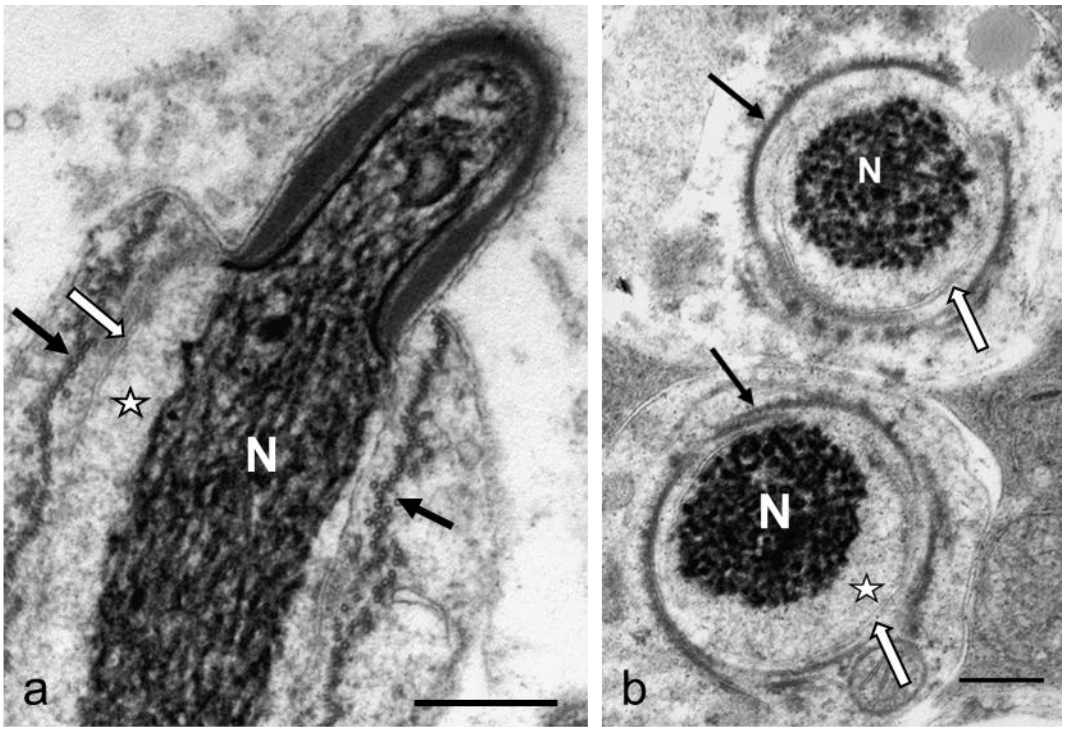

Figure 10. The circular manchette as seen in phase 3 spermatids. In longitudinal sections (a) the microtubules appear in transverse profile (arrows) while in transverse sections (b) they are seen in longitudinal profile forming circles (arrows) around the nucleolemma. Note the filamentous nature of the condensing chromatin in the nucleus (N) and the large gap (stars) between the nuclear membrane (white arrows) and the chromatin. Bar = 0.5µm.

viewed in transverse section, the inner row of microtubules was poorly represented, consisting of only a limited number of individual microtubules situated in close proximity to the nuclear membrane-associated projections that were prominent at this stage of development (see Chapter 4). The manchette microtubules and the nuclear membrane were not directly connected. In longitudinal section the manchette displayed two to four rows of longitudinally disposed microtubules (Figs. 8f, 11a). This difference in the number of rows was probably due to the small probability of sectioning the poorly represented inner row of microtubules. As previously noted in late stage phase 4 spermatids, the microtubules extended from the acrosome-nuclear shoulder to the caudal end of the midpiece and often beyond the annulus to within the cytoplasm forming the flagellar canal (Figs. 5d, 13b). No structure analogous to the nuclear ring described in mammalian spermatids was apparent in the emu (Figs. 8f, 12a). Towards the end of this phase and just prior to the mature sperm being released into the lumen of the seminiferous tubule, the manchette microtubules disappeared piecemeal (Fig. 13c).

During this phase the mitochondria were aligned in a single row around the distal centriole, forming the *pars spiralis* of the mitochondrial sheath. The mitochondria remained separated from

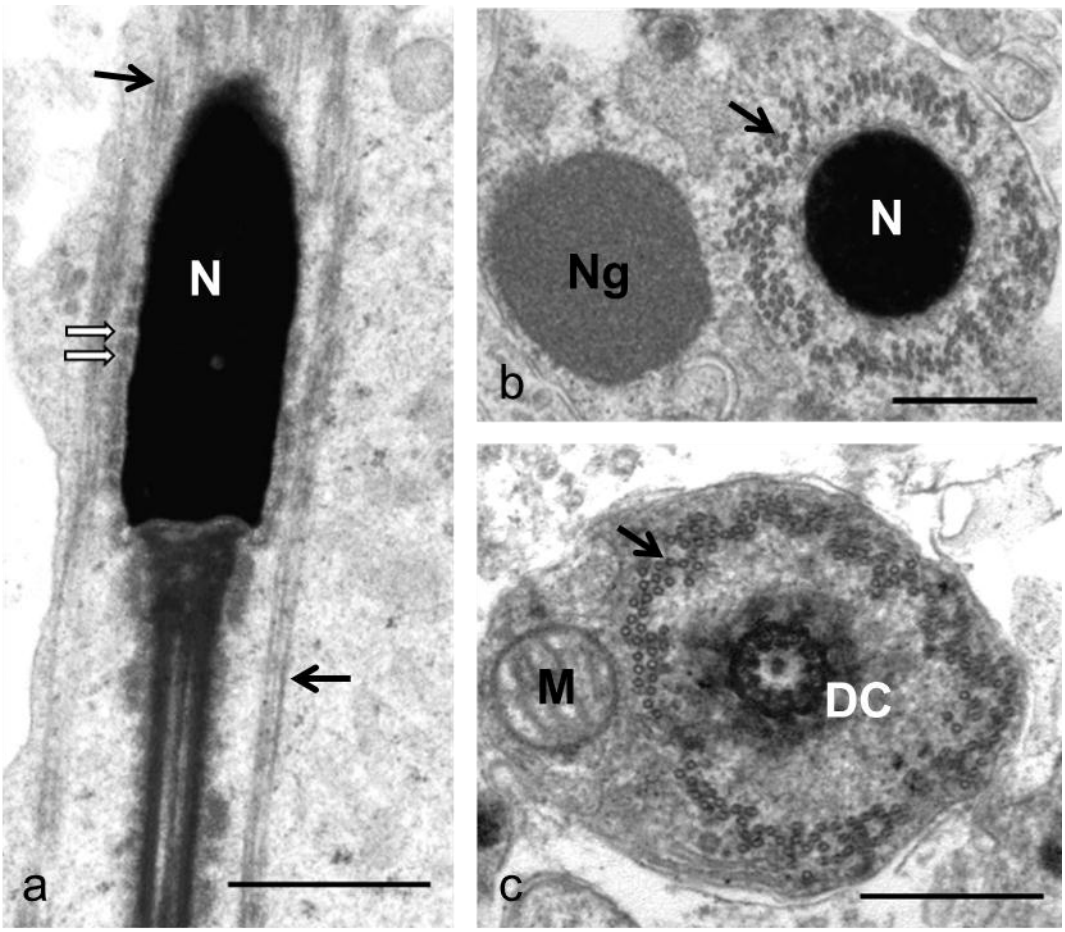

Figure 11. Phase 4 spermatids. (a) Longitudinal section through the nuclear base, neck and midpiece indicating the positioning of the longitudinal manchette (black arrows). Nuclear pores (white arrows) are concentrated at the nuclear base. (b) Transverse section through the nucleus (N) surrounded by the prominent and well-developed longitudinal manchette (arrow). A large unit of membrane-associated material (nuage) (Ng) lies in close proximity to the nucleus (N). (c) A transverse section through the midpiece. The longitudinal manchette (arrow) separates a mitochondrion (M) of the forming *pars spiralis* from the distal centriole (DC). Bar (a,b) = 0.5µm ; Bar (c) =1µm.

the CC by the intervening microtubules of the LM and only adopted their final position after its dissolution (Fig. 14a). The sheath stretched from the neck region and ended at the annulus. The numerous mitochondria forming the sheath were tightly packed against each other with no indication of mitochondrial cement being present between the individual organelles. A reduction in the excess cytoplasm surrounding the midpiece and proximal part of the flagellum resulted in the obliteration of the flagellar canal and the formation of a prominent annular recess (Fig. 5e). Continued retraction of the excess (residual) cytoplasm led to the complete disappearance of the retro-annular recess, representing the typical morphology observed in sperm from the *ductus deferens*. The finely granular residual cytoplasm, which contained redundant mitochondria and nuage, was often seen concentrated to one side of the spermatid prior to being pinched off by the surrounding Sertoli cells (Fig. 12).

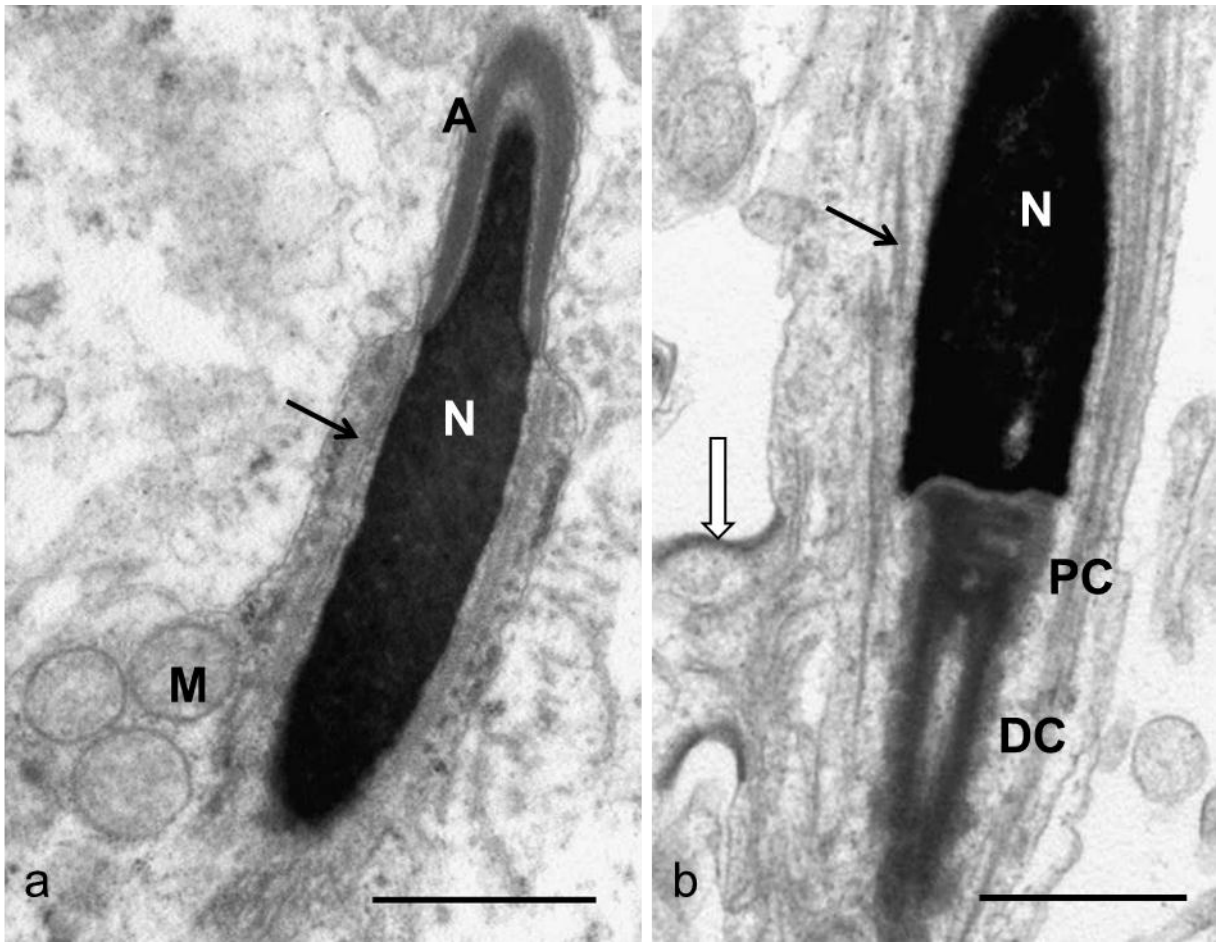

Figure 12. Phase 4 spermatids. (a) Longitudinal section of the apex of the nucleus (N) and the overlying acrosome (A). Note the longitudinal manchette (arrow) and mitochondria (M) moving towards the midpiece. The nuclear chromatin is highly condensed. (b) Longitudinal section of the nuclear base, neck and midpiece. A cytoplasmic bridge (white arrow) is situated near the neck region. Nucleus (N), proximal centriole (PC), distal centriole (DC), longitudinal manchette (arrow). Bar = 1µm.

In addition to redundant mitochondria, certain other cytoplasmic organelles and inclusions were infrequently observed during this late phase of sperm development. Although rarely present, annulate lamellae were seen in the vicinity of the nucleus (Fig. 14a,b). They were closely associated with what appeared to be swollen elements of the endoplasmic reticulum. A relatively large, moderately electron-dense structure filled with fine granular material similar to that referred to as “mitochondria associated material” in ostrich spermatids by Soley (1992), was sometimes observed during the duration of the LM (Fig. 11b). Another form of nuage infrequently observed was similar in structure to lipofuschin granules (Fig. 14a). A few myelinated bodies were also seen during the course of sperm development.

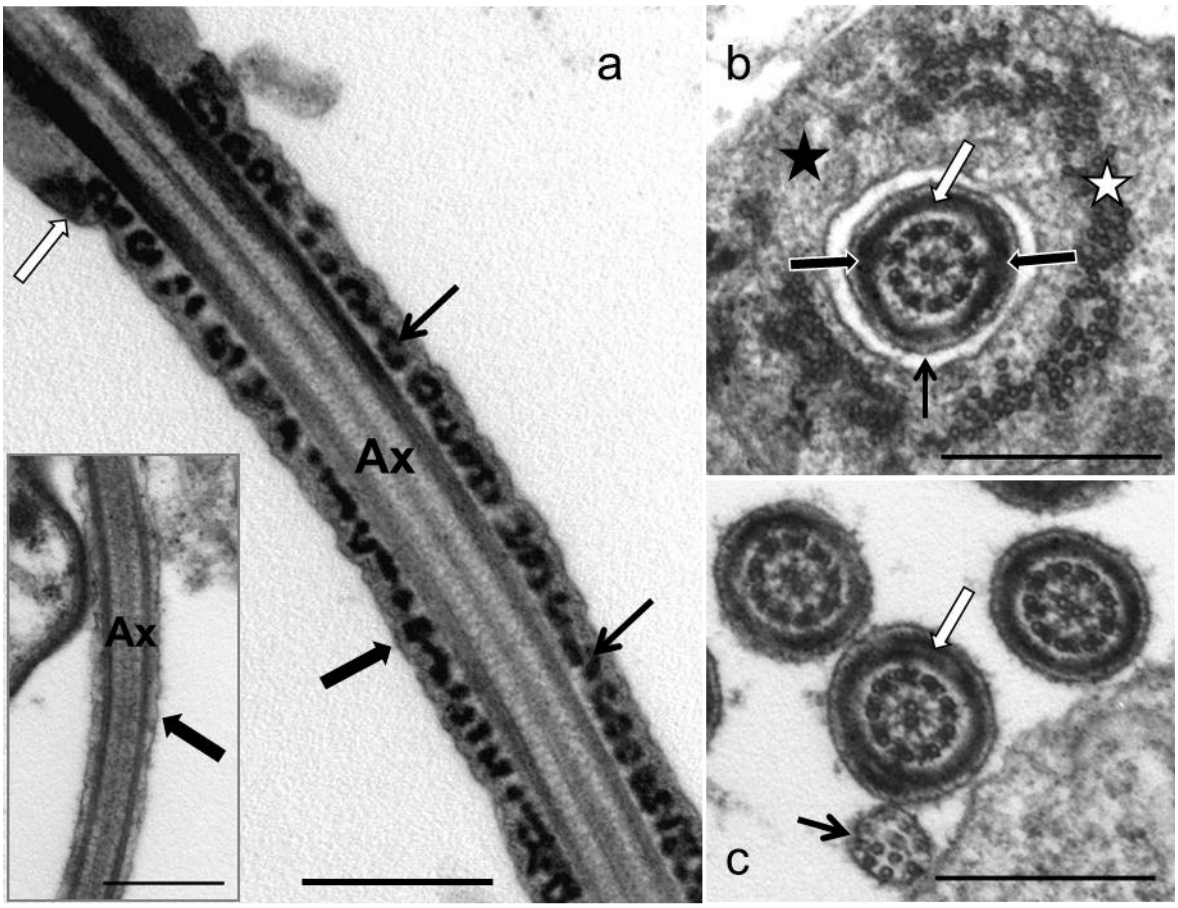

Figure 13. Longitudinal section of the midpiece and principal piece of a late stage spermatid lying in the intercellular space of the seminiferous epithelium. Note the annulus (white arrow), the ribs of the fibrous sheath in transverse section (black arrows) the plasmalemma (black block arrow) and the axoneme (Ax). The inset shows a similar section of the principal piece but at an earlier stage spermatid (phase 2). The ribs have not yet formed and only a layer of moderately electron-dense material lies between the plasmalemma (black block arrow) and the axoneme (Ax). (b) Transverse section of a late phase 4 spermatid showing the flagellar canal (black arrow) and the ribs (white arrow) and rudimentary longitudinal columns (black block arrows) of the principal piece. The longitudinal manchette (star) shows signs of dissolution (black star). (c) Transverse sections of the principal piece similar to that shown in Fig. 13 (b). The fibrous sheath appears laminated in the one section (white arrow). Note also the transverse section of the endpiece (black arrow). Bar = 0.5µm.

Discussion

Spermiogenesis in the emu followed the basic pattern previously described in other ratites (Phillips & Asa, 1989; Baccetti *et al*., 1991; Soley, 1994, 1996, 1997) and non-passerine birds in general (see review by Aire, 2007), but demonstrated certain species-specific differences. An interesting general observation was that certain structures that appeared to be well-developed during spermiogenesis were less obvious in mature sperm (see Chapter 2). These included the annulus and the segmented columns of the connecting piece. This phenomenon has also been noted in the ostrich in respect of the segmented columns (Soley, 1992) while in some pigeons

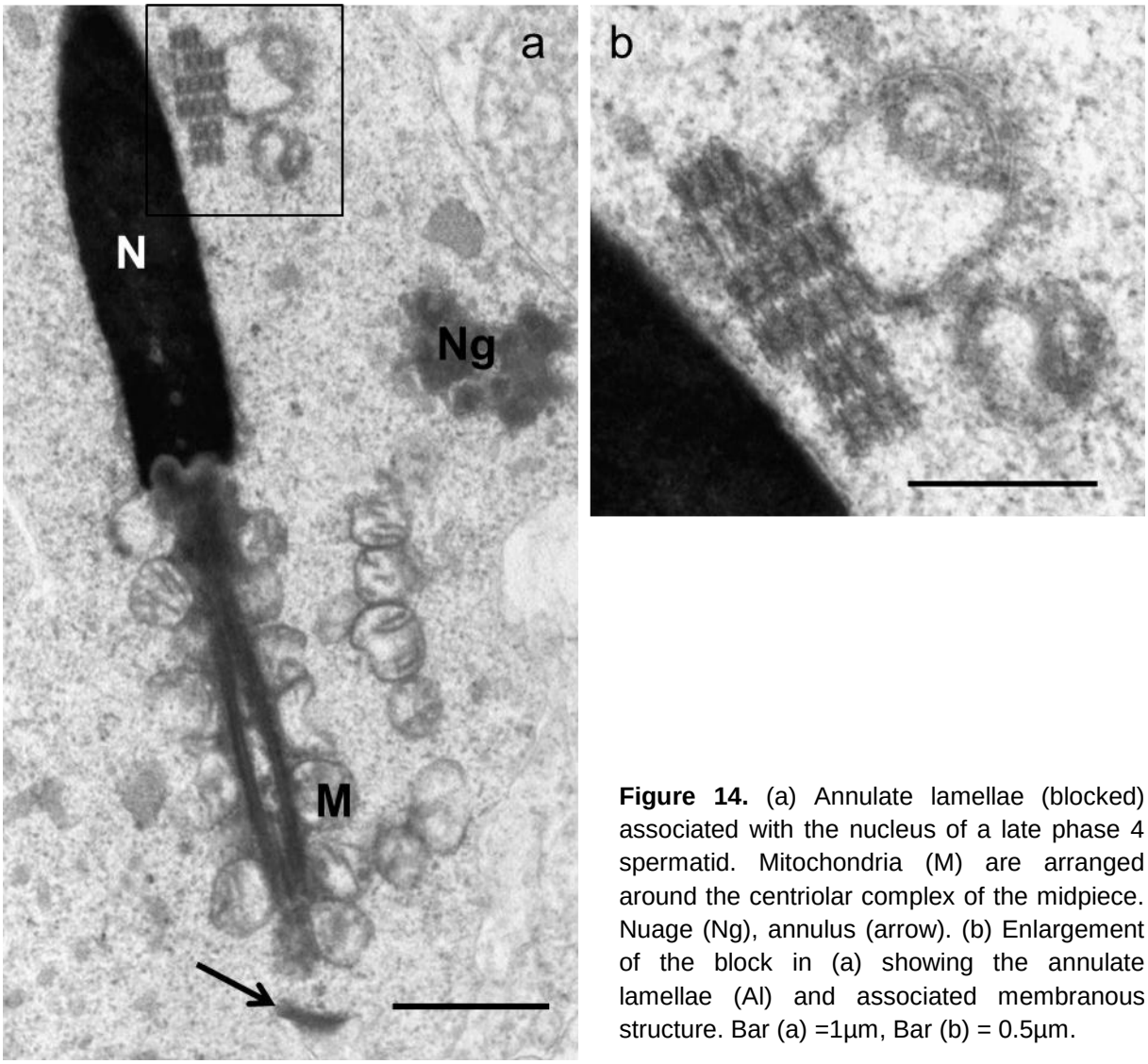

Figure 14. (a) Annulate lamellae (blocked) associated with the nucleus of a late phase 4 spermatid. Mitochondria (M) are arranged around the centriolar complex of the midpiece. Nuage (Ng), annulus (arrow). (b) Enlargement of the block in (a) showing the annulate lamellae (Al) and associated membranous structure. Bar (a) =1µm, Bar (b) = 0.5µm.

and doves (Mattei *et al*., 1972; Jamieson, 2007) the dense fibres of the tail are present in the spermatid, but are lost with maturation of the sperm.

Nuclear morphogenesis and formation of the manchette

In the emu, transformation in the shape of the nucleus and the process of chromatin condensation was similar to that described in other non-passerine birds, particularly the ostrich (Soley, 1992, 1997). The chromatin, at first finely granular in nature, systematically aggregated into coarse granules which compacted, turning into electron-dense filaments which ultimately coalesced, forming the homogenous and electron-dense nuclear material characteristic of mature emu sperm. A tendency for the chromatin filaments to spiral has been recorded in a number of bird species including the tinamou (Asa *et al*., 1986) and the ostrich (Soley, 1997). This phenomenon may be related to a reduction in nuclear length (Soley, 1997). However, no obvious morphological signs of spiralling were observed during chromatin condensation in emu

spermatids. The filamentous chromatin aggregates observed in ratites are also found in the lizard (Butler & Gabri, 1984) and alligator (Gribbins, 2011). The conspicuous gap between the condensing chromatin and the nuclear membrane that was evident throughout most of the condensation process has also been described in the ostrich (Soley, 1997). It may indicate that chromatin condensation occurs through processes inherent in the karyoplasm (Fawcett *et al*., 1971).

The change in nuclear shape and the process of chromatin condensation are intimately connected to the appearance of the manchette, a transient structure consisting of an array of microtubules. The arrangement, presence and formation of the manchette, however, differ between species. Mammalian spermatids typically only display a LM with its point of attachment at the nuclear ring which is a sub-plasmalemmal density situated just beneath the base of the acrosome (Ploën, 1971; Holstein & Roosen-Runge, 1981; Barth & Oko, 1989). In contrast, most non-passerine birds characteristically display both a CM and a LM. In some instances, a third, or transitional manchette being present, for instance in the ostrich (Soley, 1997) and rhea (Phillips & Asa, 1989). In the emu there was no convincing morphological evidence of a transitional manchette, but rather a regularly arranged collection of electron densities was seen in the vicinity of the CM microtubules prior to the emergence of the LM. Similar densities have been illustrated in the chicken (Nagano, 1962). Whether these densities represent the material required for the construction of the LM could not be determined. It should be noted that not all birds exhibit a CM. It is absent, for example, in the swift and nightjar (Jamieson & Tripepi, 2005). Short linkers connecting the microtubules of the manchette have been observed in both mammalian and avian species (MacKinnon *et al*., 1973, Russell *et al.,* 1991; Soley, 1997). These linkers were also present in the emu. The function of the linkers is uncertain, but it is speculated that they may be involved in the maintenance and functional integrity of the manchette (MacKinnon *et al*., 1973). Despite reports by Russell *et al*. (1991) and Soley (1997), indicating the presence of rod- or filament-like elements connecting the inner-most microtubules of the manchette to the outer nuclear leaflet in rat and ostrich spermatids, the projections observed in the emu (see Chapter 4) did not appear to constitute a link between the manchette microtubules and nuclear membrane.

Disagreement exists as to the point of origin of the CM. According to Okamura & Nishiyama (1976) in the chicken it starts rostrally at the acrosome-nuclear shoulder and proceeds caudally. Gunawardana and Scott (1977), in the same species, observed the reverse pattern with the microtubules first appearing at the centrioles. Lin and Jones (1993), in their study on quail spermiogenesis, reported that the microtubules were first seen around the spherical nucleus prior to nuclear elongation and that formation of the CM may start simultaneously at a number of regions. This would also appear to be the situation in the emu and in the ostrich (Soley, 1997) where the microtubules appear and concentrate at nuclear constrictions along the complete

length of the nucleus. The role of the CM in nuclear shaping in the emu is possibly supported by the observation that the CM ends around the proximal part of the distal centriole, whereas the LM (implicated in the translocation of spermatid cytoplasm) may reach well beyond the annulus.

The role of the manchette remains contentious. While most reports agree that it is associated with nuclear condensation, shaping of the nucleus and spermatid elongation (Nagano, 1962; McIntosh & Porter, 1967; Okamura & Nishiyama, 1976, Lin & Jones, 1993; Soley, 1997), Gunawardana and Scott (1977) reported that nuclear condensation preceded manchette formation in the domestic fowl. The present study, in agreement with observations on ostrich spermiogenesis (Soley, 1997), noted the appearance of the CM before any obvious signs of chromatin condensation could be detected. Only after the CM had been established in phase 2 spermatids were changes seen in the appearance of the nucleoplasm. In studies of spermiogenesis in the quail (Lin & Jones, 1993), duck (Maretta, 1995) and turkey (Aire, 2003) it was also reported that the CM typically appears in developing spermatids just prior to nuclear condensation. This observation would suggest that the CM is indeed involved in the initial change in shape of the spermatid nucleus. However, Fawcett *et al.* (1971) ruled out the possibility that the CM may play a role in determining nuclear shape. They argued that a single coil of microtubules could not possibly exert enough mechanical force on the nucleus to cause a change in shape. Contrasting reports (Myles & Hepler, 1982; Russell *et al*., 1991, 1994; Hermo *et al*., 2010) based on disruption of the microtubules during spermiogenesis, which resulted in the formation of abnormal sperm heads suggest that the manchette has indeed a profound effect on shaping of the sperm nucleus.

The current study agrees with the concept that the CM assists in the initial transformation of the nucleus, as well as compressing the nucleolemma as the chromatin condenses independently and pulls away from the nuclear membrane (Soley, 1997). In non-passerine birds the main function of the LM appears to involve the caudal translocation of the cytoplasm and associated organelles, slim-lining the spermatid into the typical filiform mature sperm. In mammals where only a LM is present, it plays a role in the assembly of the tail as well as in the shaping and condensation of the spermatid nucleus (Kierszenbaum *et al*., 2002; Kierszenbaum & Tres, 2004; Hermo *et al*., 2010).

Development of the acrosome

The sperm head of most non-passerine birds is capped by a cone-shaped acrosome. In some species the acrosome ends adjacent to the nucleus and does not overlap it (Humphreys, 1975, Samour *et al*., 1986; Phillips *et al*., 1987; Jamieson *et al*., 1995; Lovas *et al.*, 2012), whereas in others, including the emu, it covers the entire nuclear rostrum. Most reports on spermiogenesis in

birds state that the acrosome develops from pro-acrosomal vesicles arising from the Golgi apparatus and which fuse to form the acrosomal vesicle which in turn attaches to the nucleus (Nagano, 1962, Gunawardana & Scott, 1977; Soley, 1996; Aire, 2003, 2007). No such vesicles were observed in the emu where the first indication of acrosome development was the presence of a spherical membrane-bound structure composed of fine homogenous material. However, the presence of pro-acrosomal vesicles cannot be discounted and may have been missed by chance. As in other non-passerine birds, the next stage of acrosome formation was characterized by the acrosome vesicle collapsing over the tip of the nucleus, becoming electron-dense in the process. Contrary to the situation in other palaeognaths such as the ostrich (Baccetti *et al*., 1991; Soley, 1996), rhea (Phillips & Asa, 1989) and the tinamou (Asa *et al*., 1986), as well as the chicken (Nagano, 1962, Lake *et al*., 1968; Tingari, 1973; Xia *et al*., 1986; Thurston & Hess, 1987), turkey (Baccetti *et al*., 1980; Thurston and Hess, 1987; Aire, 2003), duck (Humphreys, 1972; Maretta, 1975a) and quail (Saita *et al*., 1980; Lin & Jones, 1993), at this stage of development, there was no perforatorium or endonuclear canal present in emu spermatids (see Chapter 2). The reason for this unexpected omission in the acrosome-nuclear morphology of the emu is not clear, especially as it appears to be present in birds both phylogenetically more “primitive” and more “advanced” than the emu (see review by Jamieson, 2007) (see Chapter 2 for further discussion on the phylogenetic implications of this morphological peculiarity). The only function that has been ascribed to the perforatorium in birds is as an inner support for the acrosome (Baccetti *et al*., 1980), but this function appears debatable (Soley, 1996).

Development of the centriolar complex and flagellum

Although some inaccurate reports (Simoĕs *et al*., 2005) have been published on the development and function of the CC in birds, most studies agree that the two centrioles align perpendicularly to each other before the proximal centriole attaches to the nucleus, and the distal centriole makes contact with the plasmalemma prior to forming the axonemal core of the flagellum (Lake *et al*., 1968; Thurston & Hess, 1987; Phillips & Asa, 1989; Soley, 1994; Simões *et al*., 2005; Tripepi *et al*., 2006; Lovas *et al*., 2012). The angle at which the CC makes contact with the round nucleus of early spermatids appears open to interpretation. The current study is in agreement with Maretta (1977) that the attachment is mainly perpendicular. However, numerous publications (Xia *et al*., 1986; Lin & Jones, 1993; Soley, 1994; Aire, 2003; Tripepi *et al*., 2006; Lovas *et al*., 2012) consistently illustrate an oblique attachment of the CC to the spermatid nucleus. It is plausible, particularly in ratites, that the length of the CC makes it inevitable that nuclear attachment will be at an oblique angle until such time as nuclear rotation and continued movement of the CC bring the two structures into perpendicular alignment. It is also a valid argument that should the attachment exceed a critical angle (which would still need to be determined), an anomalous situation would be reached resulting in defective spermiogenesis.

The complex structures in the neck region (segmented columns, capitulum and basal plate) associated with the anterior aspect of the CC are already in evidence in phase 1 spermatids in the emu, and contact with the nucleus via the implantation fossa is well established. The close connection observed between these structures and the chromatoid body (CB) has also been described in the ostrich (Soley, 1994) and rhea (Phillips & Asa, 1989) as well as in other non-passerine birds (Aire, 2003). The CB has been classified as “nuage”, a term used to describe various forms of dense material present in germ cells in a wide variety of species (Hermo *et al*., 2010; Onohara *et al*., 2010; Yokota, 2012) and which has been implicated, by virtue of its location, in the formation of the connecting piece and the annulus in mammals (Fawcett *et al*., 1970). A similar function in respect of the connecting piece has been proposed for the CB in birds (Soley, 1994) (see below).

The distal centriole varies in length between different vertebrate species and becomes redundant in mammals after forming the axoneme (Fawcett & Phillips, 1969). A long distal centriole appears to be typical of palaeognath sperm and extends the entire length of the midiece (Phillips, 1974; Asa & Phillips, 1986; Soley, 1994) while in other non-passerine birds, for example the chicken (Tingari, 1973), duck (Humphreys, 1972, Maretta, 1975b), budgerigar (Samour *et al*., 1986) and parrots (Jamieson *et al*., 1995), a much shorter distal centriole is restricted to the anterior aspect of the midpiece. In palaeognaths the nine triplet microtubules embedded in the wall of the distal centriole are continued, just beneath the annulus, as the 9 outer microtubular doublets of the axoneme that course through the principal piece and endpiece of the flagellum. A similar situation is evident in other non-passerine birds except that the microtubular doublets are also present in the posterior two thirds of the midpiece. A marked difference characterises the origin and positioning of the inner pair of axonemal microtubules between palaeognaths and other non-passerine birds. In the emu, as in the ostrich, rhea and tinamou, (Asa *et al*., 1986; Phillips & Asa, 1989; Soley 1994) (See Chapter 2, Normal sperm morphology), the two central microtubules are continuous with a pair of microtubules (in some species embedded in a rod of moderately electron-material) present in the lumen of the distal centriole. In other non-passerine birds these microtubules originate independently from the base of the distal centriole and extend, along with the other components of the axoneme, through the remainder of the midpiece and the rest of the flagellum (Maretta, 1977). Transformation of the blocks of dense material observed in the lumen of the distal centriole during the early phases of spermiogenesis in the emu appears to be the source of the intra-luminal microtubules. Similar material has been identified in the ostrich (Soley, 1994). and in the rooster (Maretta, 1977) although in the latter species no intraluminal microtubules are present in the distal centriole.

As previously noted in the ostrich (Soley, 1994) and rhea (Phillips & Asa, 1989), the caudal translocation of cytoplasm during the early stages of spermiogenesis in the emu moves the randomly scattered mitochondria of the round spermatid towards the CC of the midpiece. In ratites the mitochondria are confined to the region of cytoplasm between the manchette and the plasmalemma and are only arranged around the CC to form the mitochondrial sheath after the disappearance of the LM. A similar situation has been described in the turkey (Aire, 2003). In contrast, in the cockatiel (Lovas *et al*., 2012), chicken (Okamura & Nishiyama, 1976) and quail (Lin & Jones, 1993) mitochondria have been observed on either side of the LM during midpiece formation. It is also noteworthy that packing of the large number of mitochondria of the emu midpiece is achieved without the inter-mitochondrial cement reported in other ratites (Phillips and Asa, 1989; Soley, 1994), the tinamou (Asa *et al*., 1986) and non-passerine birds such as the budgerigar (Samour *et al*., 1986).

An interesting observation was that in most emu spermatids the inter-cellular bridges were situated in the vicinity of the CC and developing flagellum. This location closely coincides with the region in mature sperm where the thread-like cytoplasmic appendage emerges (see Chapter 2). An in-depth study of spermiation in the emu will be required to establish whether the cytoplasmic bridge represents the final point of sperm release from the residual cytoplasm in this species. The consistent location of the cytoplasmic appendage at the base of the sperm head would suggest that this is not the case.

Cytoplasmic organelles and inclusions

A number of unique organelles/inclusions were observed in the cytoplasm of developing emu spermatids of which the nuclear membrane-associated projections were the most significant. The presence and possible function of these structures is discussed fully in Chapter 4. Annulate lamellae were rarely observed in emu spermatids, but when encountered were situated close to the nucleus of the cell. This organelle has been implicated, together with the chromatoid body, in transporting ribonucleoproteins to the developing structures in the neck region of the spermatid in man (Paniagua *et al*., 1986). However, annulate lamellae were not found in close proximity to the neck region in the material studied. In the emu, densities commonly observed during spermiogenesis were the chromatoid body, the annulus and “mitochondria associated material” which, as indicated above, are classified as “nuage” (Onohara *et al*., 2010).

In mammals, the CB has been linked to the formation of the annulus (Yasuzumi *et al*., 1972; Phillips, 1974; Krstić, 1984) and, because of its close association with the CC, to the development of the connecting piece (Yasuzumi *et al*., 1972). The ring-like annulus is credited with partitioning the midpiece from the rest of the flagellum and is well-developed in the ostrich

(Baccetti *et al*., 1991; Soley, 1994) and rhea (Phillips & Asa, 1989). In contrast, it is often ill-defined in mature emu sperm although it forms a prominent structure during the earlier stages of flagellum formation. The annulus is reportedly absent in the cockatiel (Jamieson *et al*., 1995; Lovas *et al*., 2012), budgerigar and lovebird (Jamieson *et al*., 1995), all members of the Psittaciformes which form the third largest non-passerine avian order. Loss of the annulus appears to be indicative of the higher phylogenetic positioning of these birds, although the more "advanced" turtle dove also displays an annulus (Asa & Phillips, 1987; Jamieson, 2007). As pointed out in the ostrich (Soley, 1994), and observed in the emu, no association is apparent between the CB and the annulus, probably due to the distance between the two entities resulting from the length of the distal centriole in these species. Recent evidence based on the immunocytochemical localisation of nuage proteins would seem to support this assertion (Yokota, 2012). The role of the CB in the formation of elements of the connecting piece is also debatable, despite the close morphological association between the CB and the connecting piece. However, circumstantial evidence exists (patches of dense material beneath the nuclear membrane continuous with the CB) in both the emu (present study) and ostrich (Soley, 1992, 1994) to support the movement of ribonucleoproteins from the nucleus to the developing neck region of the spermatid via the CB as previously reported in man (Paniagua *et al*., 1986).

A density, similar in appearance to the "mitochondria associated material" reported by Soley (1991) in ostrich spermatids, was observed in late stage emu spermatids. In the ostrich this material was seen in close proximity to mitochondria. The similarity in composition between this material and the inter-mitochondrial cement of the forming midpiece was also noted (Soley, 1991, 1993, 1994). As no inter-mitochondrial cement was observed in emu spermatids, the presence of this nuage remains unexplained. It may represent redundant material not utilised during spermiogenesis and which is packaged for removal together with the residual body. The radial body, a collection of granular material and radiating cisternae reported in some avian spermatids (Soley, 1992; Lovas *et al*. 2012), was not observed in the emu. Other forms of nuage found in ostrich spermatids such as granulated bodies and reticulated bodies (Soley, 1994), were not obvious in emu spermatids.

References

Aire T.A. (2003) Ultrastructural study of spermiogenesis in the turkey, *Meleagris gallopavo*. *British Poultry Science* **44,** 674-682.

Aire T.A. (2007) Spermatogenesis and testicular cycles. In: Jamieson, B.M.G. (ed.) Reproductive Biology and Phylogeny of Birds Vol 6A. Science Publishers, Jersey, pp. 279-347.

Asa, C.S. & Phillips, D.M. (1987) Ultrastructure of avian spermatozoa. In: Mohari, H. (ed.) New Horizons in Sperm Cell Research. Japan Scientific Society Press, Tokyo, pp. 365-373.

Asa, C., Phillips, D.M. & Stover, J. (1986) Ultrastructure of spermatozoa of the crested tinamou. *Journal of Ultrastructure and Molecular Research* **94**, 170-175.

Baccetti, B., Bigliardi, E. & Burrini, A.G. (1980) The morphogenesis of vertebrate perforatorium. *Journal of Ultrastructure Research* **71**, 272-287.

Baccetti, B., Burrini, A.G. & Falchetti, E. (1991) Spermatozoa and relationships in Paleognath birds. *Biology of the Cell* **71,** 209-216.

Barth, A.D. & Oko, R.J. (1989) Abnormal morphology of bovine spermatozoa. Iowa State University Press, Ames.

Butler, R.D. & Gabri, M.S. (1984) Structure and development of the sperm head in the lizard *Podarcis* (=*Lacerta*) *taurica*. *Journal of Ultrastructure Research* **88**, 261-274.

Donoghue, A.M., Blanco, J.M., Gee, G.F., Kirby, Y.K. & Wildt, D.E. (2003) Reproductive technologies and challenges in avian conservation and management. In: Holt, W.V., Pickard, A.R., Rodger, J.C. & Wildt, D.E. (eds.). Conservation Biology and Reproductive Science and Integrated Conservation. Zoological Society of London, London, pp. 321-337.

Fawcett D.W. & Phillips D.M. (1969) The fine structure and development of the mammalian spermatozoon. *Anatomical Record* **165**, 153-184.

Fawcett DW, Eddy EM, Phillips DM (1970) Observations on the fine structure and relationships of the chromatoid body in mammalian spermatogenesis. *Biology of Reproduction* **2**,129-153.

Fawcett, D.W., Anderson, W.A. & Phillips, D.M. (1971) Morphognetic factors influencing the shape of the sperm head. *Developmental Biology* **26**, 220-251.

Gribbins, K.M. (2011) Reptilian spermatogenesis. A histological and ultrastructural perspective. *Spermatogenesis* **1**, 250-269.

Góes, R.M. & Dolder, H. (2002) Cytological steps during spermiogenesis in the house sparrow (*Passer domesticus*, Linnaeus). *Tissue and Cell* **34,** 273-282.

Gunawardana, V.K. (1976) Stages of spermatids in the domestic fowl – a light microscope study using Araldite sections. *Journal of Anatomy* **123**, 351-360.

Gunawardana, V.K. & Scott, M.G.A.D. (1977) Ultrastructural studies on the differentiation of spermatids in the domestic fowl. *Journal of Anatomy* **124**, 741-755.

Hermo, L., Pelletier, R-M., Cyr, D,G. & Smith C.E. (2010) Surfing the wave, cycle, life history, and genes/proteins expressed by testicular germ cells. Part 2: Changes in spermatid organelles associated with development of spermatozoa. *Microscopy Research and Technique* **73,** 279–319.

Holstein A.F. (1976) Ultrastructural observations on the differentiation of spermatids in man. *Andrologia* **8**, 157-165.

Holstein, A.F. & Roosen-Runge, E.C. (1981) Atlas of human spermatogenesis. Grosse Verlag, Berlin.

Humphreys, P.N. (1972) Brief observations on the semen and spermatozoa of certain passerine and non-passerine birds. *Journal of Reproduction and Fertility* **29**, 327-336.

Humphreys, P.N. (1975) The differentiation of the acrosome in the spermatid of the budgerigar (*Melopsittacus undulates*). *Cell and Tissue Research* **156**, 411-416.

Jamieson, B.G.M. (2007) Avian spermatozoa: structure and phylogeny. In: Jamieson, B.M.G. (ed.) Reproductive Biology and Phylogeny of Birds Vol. 6A. Science Publishers, Jersey, pp. 349-512.

Jamieson, B.G.M., Koehler, L. & Todd, B.J. (1995) Spermatozoal ultrastructure in three species of parrots (Aves, Psittaciformes) and its phylogenetic implications. *The Anatomical Record* **241**, 461-468.

Jamieson, B.M.G. & Tripepi, R. (2005) Ultrastructure of the spermatozoon of *Apus apus* (Linnaeus 1758), the common swift (Aves: Apodiformes; Appodidae), with phylogenetic implications. *Acta Zoologica* **86**, 239-244.

Kierszenbaum, A.L. & Tres, L.L. (2004) The acrosome-acroplaxome-manchette complex and the shaping of the spermatid head. *Archives of Histology and Cytology* **67**, 271–284.

Kierszenbaum, A.L., Gil, M., Rivkin, E. & Tres, L.L. (2002) Ran, a GTP- binding protein involved in nucleocytoplasmic transport and microtubule nucleation, relocates from the manchette to the centrosome region during rat spermiogenesis. *Molecular Reproduction and Development* **63**, 131–140.

Kristić, R.V. (1984) Illustrated encyclopedia of human histology. Springer-Verlag, New York.

Lake, P.E., Smith, W. & Young, D. (1968) The ultrastructure of the ejaculated fowl spermatozoan. *Quaterly Journal of Experimental Physiology* **53**, 356-366.

Leblond, C.P. & Clermont, Y. (1952a) Definition of the stages of the cycle of the seminiferous epithelium in the rat. *Annals of the New York Academy of Sciences* **55**, 548-573.

Leblond, C.P. & Clermont, Y. (1952b) Spermiogenesis of rat, mouse, hamster and guinea pig as revealed by the “Periodic acid-fuchsin sulfurous acid” technique. *American Journal of Anatomy* **90**,167-215.

Lin, M. & Jones, R.C. (1993) Spermiogenesis and spermiation in the Japanese quail (*Coturnix coturnix japonica*). *Jounal of Anatomy* **183,** 525-535.

Lin, M. & Jones, R.C. (2000) Spermiogenesis and spermiation in a monotreme mammal, the platypus, *Ornithorhynchus anatinus. Journal of Anatomy* **196**, 217-232.

Lin, M., Harman, A & Rodger, J.C. (1997) Spermiogenesis and spermiation in a marsupial, the tammar wallaby (*Macropus eugenii*). *Journal of Anatomy* **190**, 377-395,

Lovas, E.M., Filippich, L.J. & Johnston, S.D. (2012) Spermiogenesis in the Australian cockatiel *Nymphicus hollandicus*. *Journal of Morphology* in press.

MacKinnon, E.A., Abraham, P.J. & Svatek, A. (1973) Long link induction between the microtubules of the manchette in intermediate stages of spermiogenesis. *Zeitschrift fur Zellforschung und Mikroskopische Anatomie* **136**, 447-460.

Maretta, M. (1975a) The ultrastructure of the spermatozoon of the drake. I. Head. *Acta Veterinaria Academiae Scientiarum Hungaricae* **25**, 47-52.

Maretta, M. (1975b) The ultrastructure of the spermatozoon of the drake. II. Tail. *Acta Veterinaria Academiae Scientiarum Hungaricae* **25**, 53-60.

Maretta, M. (1977) The behavior of centrioles and the formation of the flagellum in rooster and drake spermatids. *Cell and Tissue Research* **176**, 265-273.

Maretta, M. (1995) Formation and role of the manchette microtubules in the poultry spermatids. *Acta Veterinaria, Brno* 64: 23-29.

Mattei, C., Mattei, X. & Manfredi, J-L. (1972) Electron microscopic study of the spermiogenesis of *Streptopelia roseogrisea*. *Journal of Submicroscopic Cytology* **4**, 57-73.

McIntosh, J.R. & Porter, K.R. (1967) Microtubules in the spermatids of the domestic fowl. *Journal of Cell Biology* **35,**153-173.

Myles, D.G. & Hepler, P.K. (1982) Shaping of the sperm nucleus in Marsilea: a distinction between factors responsible for shape generation and shape determination. *Developmental Biology* **90**, 238-252.

Nagano, T. (1962) Observations on the fine structure of the developing spermatid in the domestic chicken. *The Journal of Cell Biology* **14,** 193-205.

Okamura, F. & Nishiyama, H. (1976) The early development of the tail and the transformation of the shape of the nucleus of the spermatid of the domestic fowl, *Gallus gallus*. *Cell and Tissue Research* **169**, 345-359.

Onohara, Y., Fujiwara, T., Yasukochi, T., Himeno, M. & Yokota, S. (2010) Localization of mouse vasa homolog protein in chromatoid body and related nuage structures of mammalian spermatogenic cells during spermatogenesis. *Histochemistry and Cell Biology* **133**, 627–639.

Paniagua, R., Nistal, M., Amat, P. & Rodriguez, M.C. (1986) Ultrastructural observations on nucleoli and related structures during human spermatogenesis. *Anatomy and Embryology* **174**, 301-306.

Phillips, D.M. (1974) Spermiogenesis. Academic Press, New York.

Phillips, D.M., Asa, C. & Stover, J. (1987) Ultrastructure of spermatozoa of the white-naped crane. *Journal of Submicroscopic Cytology and Pathology* **19**, 489-494.

Phillips D.M. & Asa, C.S. (1989) Development of spermatozoa in the rhea. *The Anatomical Record* **223,** 276-282.

Ploën, L. (1971) Scheme of rabbit spermatelios based upon electron microscopic observations. *Zeitschrift fur Zellforschung und Mikroskopische Anatomie* **11**, 553-564.

Russell, L.D., Russell, J.A., MacGregor G.R. & Meistrich, M.L. (1991) Linkage of manchette microtubules to the nuclear envelope and observations of the role of the manchette in nuclear shaping during spermiogenesis in rodents. *American Journal of Anatomy* **192**, 97-120.

Russell, L.D., Ying, L. & Overbeek, P.A. (1994) Insertional mutation that causes acrosomal hypo-development: its relationship to sperm head shaping. *Anatomical Record* **238**, 437-455.

Saita, A., Longo, O.M., & Tripepe, S. (1983) Osservazioni comparative sulla spermiogenesi. III. Aspetti ultrastrutturali della spermiogenesis di *Jacana jacana* (Charariformes). *AccademiaNazionale Dei Lincei. (Rendiconti Della Classe Di Scienze Fisiche,Matematiche E Naturali)* **74,** 417–430.

Samour, J.H., Smith, C.A., Moore, H.D. & Markham, J.A. (1986) Semen collection and spermatozoa characteristics in budgerigars (*Melopsittacus undulates*). *Veterinary Record* **118**, 397-399.

Lloyd, S., Carrick, F. & Hall, L. (2008) Unique features of spermiogenesis in the Musky Rat-kangaroo: reflection of a basal lineage or a distinct fertilization process? *Journal of Anatomy* **212,** 257-274.

Sharma, R. K., Bhardwaj, J. K. & Ahlawat, N. (2009) Ultrastructural developments during spermiogenesis in goat (*Capra hircus*). *International Journal of Integrative Biology* **6**, 112-114.

Simões, K., Orsi, A.M. & Viegas, K.A.S. (2005) Ultrastructural characteristics of spermiogenesis in the domestic duck (*Anas platyrhynchos*). *Anatomica Histologica Embryologica* **34**,307-311.

Soley, J.T. (1991) Cytoplasmic densities in developing spermatids of the ostrich. *Proceedings of the Electron Microscopy Society of Southern Africa* (Cape Town) **21,** 245-246.

Soley, J.T. (1992) A histological study of spermatogenesis in the ostrich (*Struthio camelus*). Ph.D. Thesis, University of Pretoria, Pretoria.
Soley, J.T. (1993) Ultrastructure of ostrich (*Struthio camelus*) spermatozoa: I. Transmission electron microscopy. *Onderstepoort Journal of Veterinary Research* **60**, 119-130.

Soley, J.T. (1994) Centriole development and formation of the flagellum during spermiogenesis in the ostrich (*Struthio camelus*). *Journal of Anatomy* **185**, 301-313.

Soley, J.T. (1996) Differentiation of the acrosomal complex in the ostrich (*Struthio camelus*) spermatids. *Journal of Morphology* **227**, 101-111.

Soley, J.T. (1997) Nuclear morphogenesis and the role of the manchette during spermiogenesis in the ostrich (*Struthio camelus*). *Journal of Anatomy* **190**, 563-576.

Sprando R.L. & Russell L.D. (1988) Spermiogenesis in the red-ear turtle (*Pseudemys scripta*) and domestic fowl (*Gallus domesticus*): a study of cytoplasmic events including cell volume changes and cytoplasmic elimination. *Journal of Morphology* **198**, 95-118.

Thurston, R.J., Hess, R.A., Hughes, B.L. & Froman, D.P. (1982) Ultrastructure of the guinea fowl (*Numidia meleagris*) spermatozoan. *Poultry Science* **61**, 1738-1743.

Thurston, R.J. & Hess, R.A. (1987) Ultrastructure of spermatozoa from domesticated birds: Comparative study of turkey, chicken and guinea fowl. *Scanning Microscopy* **1**, 1829-1838.

Tingari, M.D. (1973) Observations on the fine structure of spermatozoa in the testis and excurrent ducts of the male fowl, *Gallus domesticus*. *Journal of Reproduction and Fertility* **34,** 255-265.

Tripepi, S., Jamieson, B.G.M. & Brunelli, E. (2006) Ultrastructure of the spermatid of *Caprimulgus europaeus* Linnaeus 1758, the European nightjar (Aves; Caprimulgidae), with phylogenetic implications. *Journal of Morphology* **267**, 1157-1164.

Xia, L., Clermont Y., Lalli, M. & Buckland, R.B. (1986) Evolution of the endoplasmic reticulum during spermiogenesis of the rooster: an electron microscopic study. *The American Journal of Anatomy* **177**, 301-312.

Yasuzumi, G., Shiraiwa, S. & Yamamoto, H. (1972) Spermatogenesis in animals as revealed by electron microscopy. *Zeitschrift fur Zellforschung und Mikroskopische Anatomie* **125**, 497-505.

Yokota, S. (2012) Nuage proteins: their localization in subcellular structures of spermatogenic cells as revealed by immunoelectron microscopy. *Histochemistry and Cell Biology* **138**, 1–11.

Chapter 4 A novel transient structure with phylogenetic implications associated with spermiogenesis

Introduction

Despite the application of a variety of techniques and the acquisition of volumes of morphological and molecular data, the phylogenetic relationships within the class Aves, and between birds and reptiles, remains a controversial topic.

Morphological and molecular studies support the concept that the avian phylogenetic tree consists of two major nodes, namely the Palaeognathae, which include the orders Struthioniformes (ostrich, rhea, emu, cassowary, kiwi) and Tinamiformes (tinamous) and the Neognathae to which all other bird species belong (Ericson, 2008; Hackett *et al*., 2008). Traditionally, the ratites and the tinamous are placed at the base of the avian phylogenetic tree and as such are considered to be the most primitive living birds (Cracraft 1988; Cracraft & Mindell, 1989). This "traditional" view has been supported by nuclear and mitochondrial DNA sequencing (Sibley & Ahlquist, 1981, 1995; Sibley *et al*., 1988; Paton *et al*., 2002; García-Moreno *et al*., 2003). However, using molecular techniques such as mitochondrial DNA and ribosomal sequencing contrasting evidence has been presented suggesting that the Passeriformes may in fact be the oldest lineage of modern birds, (Janke & Arnason, 1997; Mindell *et al*., 1999; Van Tuinen *et al*., 2000). This contradictory situation is further compounded by the observation that the method of data analysis can influence the allocation of phylogenetic relationships (Braun & Kimball, 2002).

Recently, the value of so-called non-traditional characters such as sperm ultrastructure and morphological aspects of spermiogenesis have been proposed as additional methods of indicating phylogenetic relationships (Koehler, 1995; Jamieson, 2007; Gribbins, 2011). Although spermiogenesis has been described in a number of non-passerine bird species such as the chicken (Nagano, 1962; Gunawardana & Scott, 1977; Xia *et al*., 1986; Sprando & Russell, 1988), duck (Maretta, 1995; Simões *et al*., 2005), quail (Yamamoto *et al*., 1967; Lin & Jones, 1993), turkey (Aire, 2003), house sparrow (Góes & Dolder, 2002), European nightjar (Tripepi *et al*., 2006), cockatiel (Lovas *et al.*, 2012), including ratites (Phillips & Asa, 1989; Baccetti *et al*, 1991; Soley, 1992, 1994, 1996, 1997), no morphological characters reflected during this process have, to date, been used as phylogenetic data.

This chapter describes in detail the morphology and composition of a transient structure that manifests during spermiogenesis in the emu and which may have value as a non-traditional phylogenetic character. The possible role of the structure during spermiogenesis is also discussed.

Materials & Methods

The testes of 15 sexually mature and active emus (*Dromaius novaehollandiae*) were collected during the breeding season following slaughter at commercial abattoirs. Small blocks of testicular tissue were prepared for conventional transmission electron microscopy (TEM) as described in Chapter 3 (Spermiogenesis).

Immunogold labelling

Additional blocks of the same material were collected and fixed in 1% glutaraldehyde in 0.13M Millonig's phosphate buffer, pH 7.4, for immunogold labelling. After fixation the samples were washed with Millonig's phosphate buffer, dehydrated and embedded in gelatin capsules in LR White acrylic resin. Thin sections were collected on nickel grids. The grids were pre-incubated for 30min with PBS-BSA-glycine (phosphate-buffered saline, pH7.2 containing 1.5% bovine serum albumin and 0.01M glycine) to quench free aldehyde groups before incubating for 60min with the primary antibody (diluted 1:50). The primary antibodies used were mouse monoclonal antibodies directed against chicken alpha-tubulin (ab80779), beta-tubulin (ab7287), gamma-tubulin (ab27074) and beta-actin (ab49846) (Abcam, Cambridge, United Kingdom). After incubation, the grids were rinsed in PBS-BSA (5 x 1min) and incubated for a further 60min with the secondary antibody (polyclonal goat anti-mouse antibody, ab27241, labeled with 10nm gold particles (Abcam, Cambridge, UK) diluted 1:20. The grids were again rinsed with PBS-BSA (5 x 1min) followed by rinsing in distilled water (5 x 1min). Grids were then stained with uranyl acetate and lead citrate and viewed under similar conditions as for conventional TEM.

Negative controls were performed by omitting the primary antibody and replacing it with PBS-BSA. Structural elements (manchette and axonemal microtubules, centrosome and actin filaments) of the developing spermatids, Sertoli cells and surrounding myofibroblasts known to display immunoreactivity when treated with the various primary antibodies (Aumüller & Seitz, 1988; Fouquet *et al*., 1989, 1998; Mancini *et al*., 2005) served as internal positive controls. Chicken testicular material (n = 4) fixed and processed (using the same antibody dilutions) as for the ratite material served as a further positive control.

Electron tomography

Appropriate thin sections clearly demonstrating the structure of interest were examined using a 200kV Tecnai-20 transmission electron microscope (FEI Company, Eindhoven). Data was collected automatically using the UCSF Tomo software (Zheng *et al*., 2007) which also controls the goniometer, the CCD camera and microscope optics. Single tilt axis images -55 to +55 with a 0.5 degree increment were collected and each tilt series was saved as a single stack image. The microscope magnification was x34000, corresponding to 6Å per pixel. Using the eTomo software package (Mastronarde, 1997) the data from the image stack was used to create a tomogram without using fiducial markers. The tomograms had dimensions of 2048 x 2048 x 400 pixels.

A total of seven tomograms of the projections were constructed, six showing transverse cuts through the nucleus designated as “side views” and one showing a glancing cut parallel to the nuclear membrane which was called a “top” view.

Individual, clearly defined structures were identified in the tomogram volumes the centres of which were marked using the clicker tool in the program Amira (www.amira.com). Volumes of 256x256x256 pixels centred on the points clicked were cut out of the tomograms. These are referred to as “sub-tomograms”. The sub-tomograms were reduced in resolution to 128x128x128 pixels by averaging adjacent pixels in three dimensions and were used in further alignment. A total of fifty “top” view sub-tomograms were extracted from the single “top” view tomogram and 117 “side” view sub-tomograms were extracted from the six “side” view tomograms. A diffraction pattern was created by computing the power spectrum of a section through the “top” view tomogram using the “V2” program within the EMAN suite (Ludthe *et al*., 1999).

The sub-tomograms were aligned by computing the optimum correlation between them with a six-dimensional search (three translations and three rotations) using the correlation function in the MATLAB package (http://www.MathWorks.com). Separate alignments of “side” and “top” views were made. The arrangement of the structures relative to the nuclear membrane made it possible to restrict the angular range required for the correlation search and thus economise on the computer time necessary to best align the sub-tomograms. The alignments were refined iteratively until convergence was achieved. The “top” view and “side” view averages were then aligned to one another and averaged to produce the final volume.

The tomograms were viewed using UCSF Chimera (Pettersen *et al*., 2004).

Results

Ultrastructural features

Late stage elongated spermatids (late phase 3 and phase 4 – see chapter 3) in the emu were characterised by the presence of a longitudinal collection of microtubules, the longitudinal manchette, surrounding the nucleus. The nucleus was composed of a dense mass of condensed chromatin closely enveloped by the nuclear membrane. The zone of cytoplasm between the manchette and the nuclear membrane was occupied by a continuous array of small, regularly-positioned, finger-like projections which appeared to emanate from the cytoplasmic surface of the nuclear membrane. In transverse sections of spermatids at this stage of spermiogenesis the uniform and symmetrical arrangement of the projections and their close association with the nuclear membrane gave the nucleus a cogwheel appearance (Figs. 1a, 2d,e). While individual microtubules of the manchette were frequently linked by short, filamentous connections (Fig. 1a), there were no obvious connections between the microtubules of the longitudinal manchette and the finger-like projections although the staggered arrangement of the manchette microtubules created the impression of a close association between the projections and some individual microtubules (Fig.1a). Projections situated at the base of the nucleus were orientated caudally and clearly not connected to the manchette (Fig. 3c). The morphology of the collective projections varied with the plane of section. In true transverse or longitudinal section the projections exhibited the typical finger-like structure. In oblique sections they appeared in the form of a hazy zone of moderately electron-dense material (Fig. 1a) or as a crystalline array with a distinct lattice pattern (Fig.1b). The morphological features of the projections were identical when viewed in transverse or longitudinal sections of developing spermatids. Based on the presence of the projections in all profiles at this stage of spermatid development, it was concluded that they were present throughout the entire surface of the nucleus. Using conventional TEM images the projections measured 29.75 ± 4.2nm in length and 14.36nm in width.

Origin, development and fate of the array

In early elongating spermatids the karyoplasm consisted of a homogeneous mass of fine chromatin granules enclosed by the nuclear membrane. Encircling the nucleus was an ill-defined band of microtubules, the circular manchette and positioned between the manchette and the nucleus was a thin layer of flocculant material (Fig. 2a). At a slightly later stage of development, characterised by the appearance of small chromatin granules within the karyoplasm, a variable number of discrete, isolated, finger-like projections, which appeared to emanate from the cytoplasmic surface of the nuclear membrane, became obvious within the thin zone of cytoplasm immediately surrounding the spermatid nucleus (Figs. 2b, 3a). In more mature elongating spermatids (typically displaying a contracted collection of relatively coarse, filamentous chromatin granules clearly separated from the nuclear membrane, and a more organised circular

manchette), the finger-like projections remained isolated or were arranged in small groups or pockets (Fig. 3b), arbitrarily situated at any point along the nuclear perimeter, including the nuclear base (Fig. 3c). They were particularly obvious around the nuclear shoulder abutting the base of the conical acrosome (Fig. 4a). During the subsequent transitional manchette stage of spermatid development (identified by signs of disassociation of the circular manchette and the

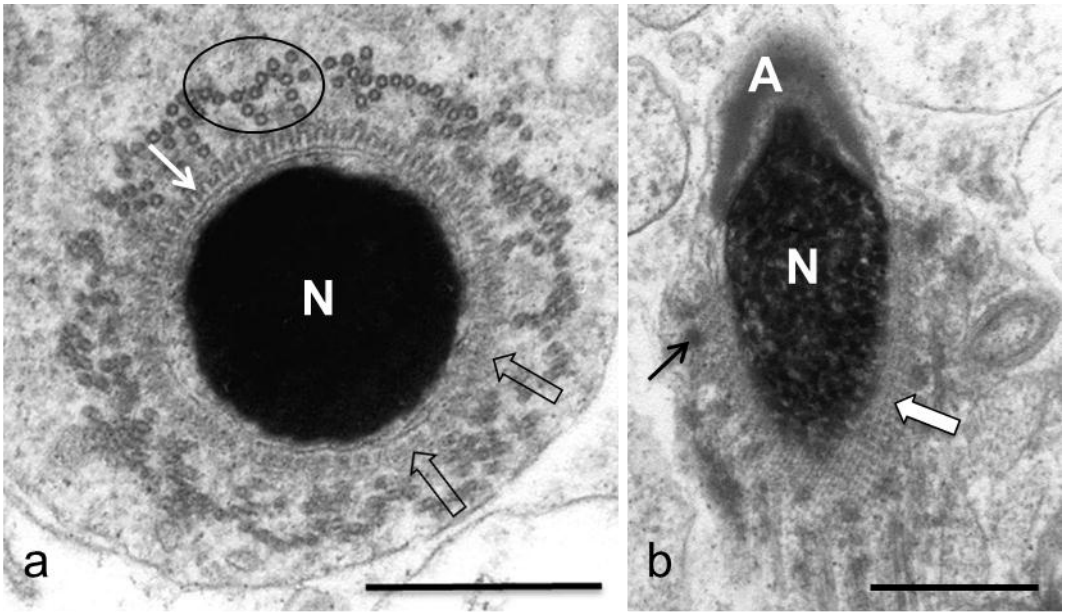

Figure 1. (a) Transverse section through a late stage elongated spermatid. Note the prominent longitudinal manchette microtubules (encircled), the finger-like projections (arrow) closely associated with the outer nuclear membrane and the condensed chromatin of the nucleus (N). Individual manchette microtubules are closely aligned with, but not attached to, the finger-like projections. Some of the projections (open block arrows) appear as a fuzzy layer due to the plane of section. (b) Oblique section of an elongated spermatid demonstrating the lattice pattern (block arrow) formed by the projections. The nuclear chromatin (N) is in the form of coarse granules, indicating an earlier stage of spermatid development. Note the cytoplasmic densities in the vicinity of the manchette (black arrow). Acrosome (A). Bar = 0.5µm.

karyoplasm appearing as a shrunken mass of dense, more compactly arranged chromatin granules) the projections showed little change in their arrangement or appearance (Fig. 2c). During this stage of development a number of equally-spaced, large, moderately electron-dense bodies appeared between the layer of finger-like projections and the disassociating circular manchette (Fig. 2c). However, during the longitudinal manchette stage of spermatid elongation (characterised by a well-developed array of longitudinally disposed microtubules arranged around the nucleus, and by the dense, shrunken appearance of the karyoplasm) the projections were observed to have increased markedly in number (Fig. 2d). The increase in number was again

particularly obvious towards the apical aspect of the nucleus where it abutted the cone-shaped acrosome (Fig. 4). This stage in the development of the array differed only in respect of the clear space between the condensed chromatin and the nuclear membrane when compared to the final stage outline above (Fig. 2e).

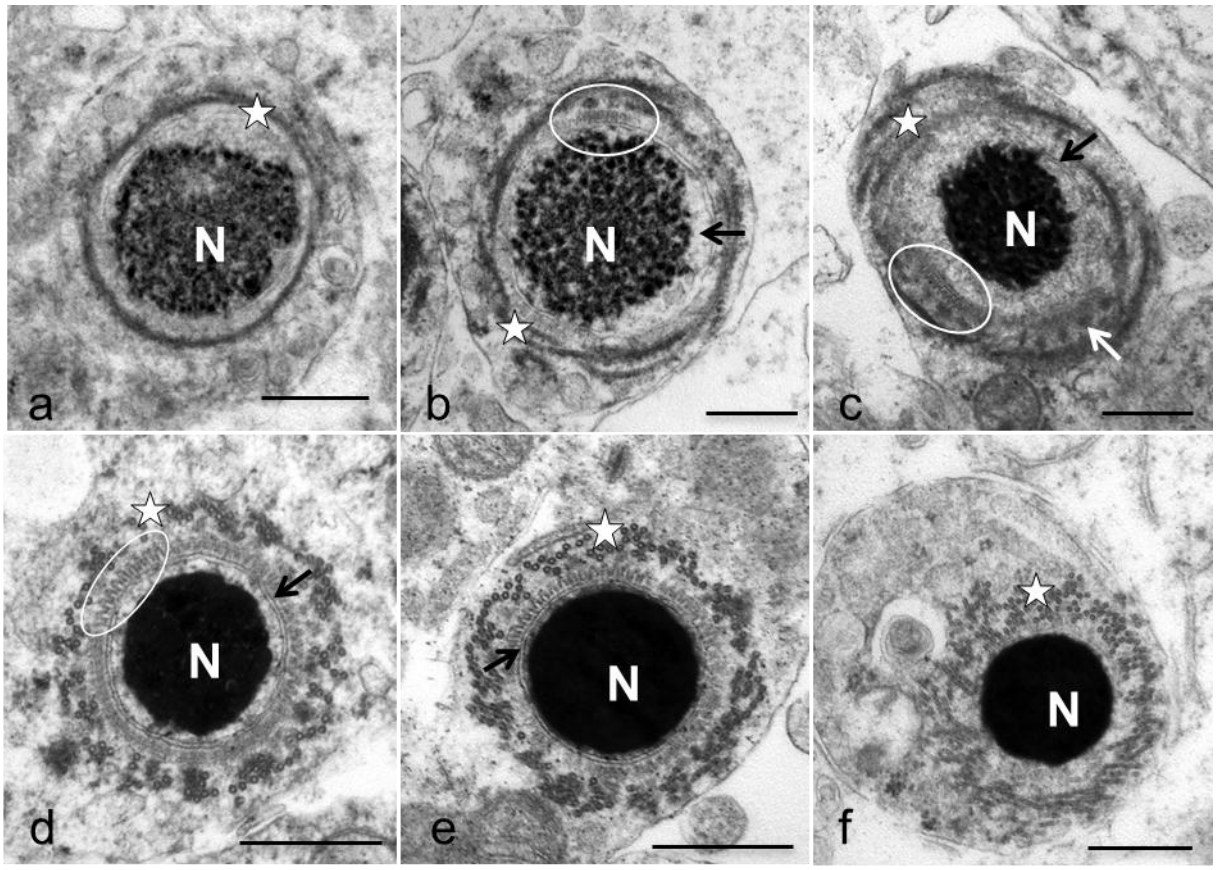

Figure 2. Transverse sections through the head of developing spermatids. (a) Early elongated spermatid with the forming circular manchette (star) Note the fine granular chromatin (N), the zone of flocculant material between the manchette and the nuclear membrane (arrow). No projections are visible. (b) Spermatid showing a slightly more advanced stage of nuclear condensation with an obvious gap between the chromatin and nuclear membrane (arrow). Projections (encircled) make their appearance. See enlargement in Fig 3a. (c) Transitional manchette stage spermatid. The chromatin appears more condensed, the circular manchette (star) starts to unravel and dense granules (white arrow) are present. The projections appear in pockets along the nuclear membrane (encircled). See enlargement in Fig 3b. (d) Longitudinal manchete (star) stage of spermatid development. The chromatin is highly condensed and the projections (encircled) appear to be associated with the cytoplasmic face of the nuclear membrane. Note the cog-wheel appearance of the nucleus; (e) Later stage spermatid with well-developed longitudinal manchette (star) and condensed chromatin. The projections are visible around the entire nuclear membrane which is closely applied to the condensed chromatin (arrow); (f) An advanced stage spermatid with the longitudinal manchette (star) still in evidence. The projections are no longer visible. Bar = 0.5µm.

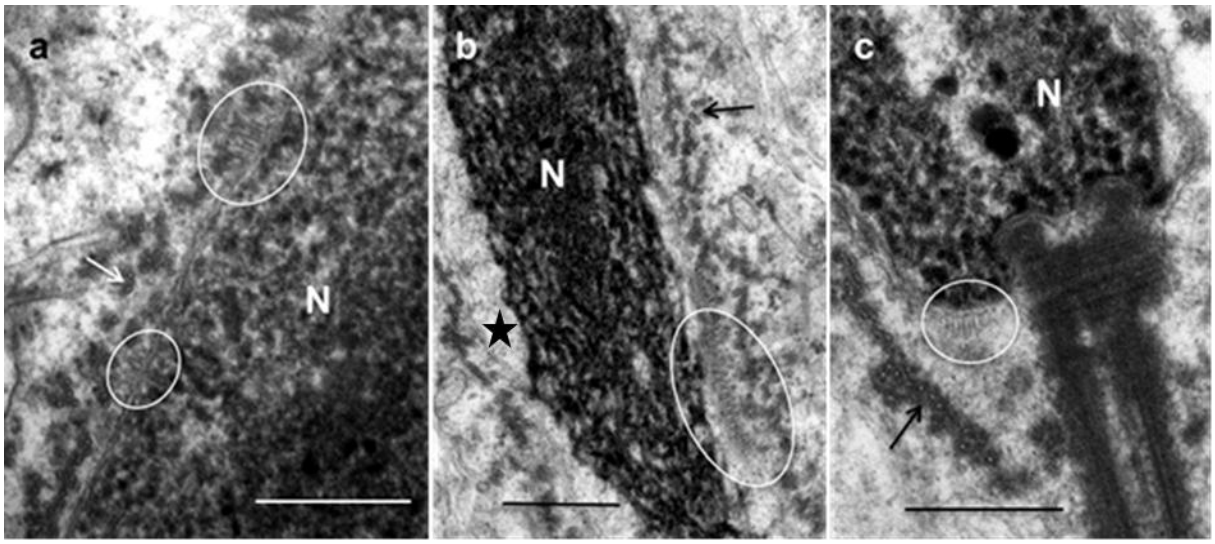

Figure 3. (a) Initial appearance of the projections (encircled) in a longitudinal section of an early elongated spermatid. The finely granular nuclear chromatin displays a degree of clumping. Note the developing circular manchette (arrow) and the double nuclear membrane. (b) A later stage of nuclear condensation with the chromatin in the form of electron-dense filaments. The projections are confined to an isolated pocket (oval) along the nuclear membrane. Note the obvious space between the condensing chromatin and the nucleolemma (star). (c) Similar stage spermatid to that in Fig.3b. A small collection of projections are visible at the nuclear base (oval). There is clearly no association between the projections and the manchette microtubules (arrow). Nucleus (N). Bar = 0.5µm.

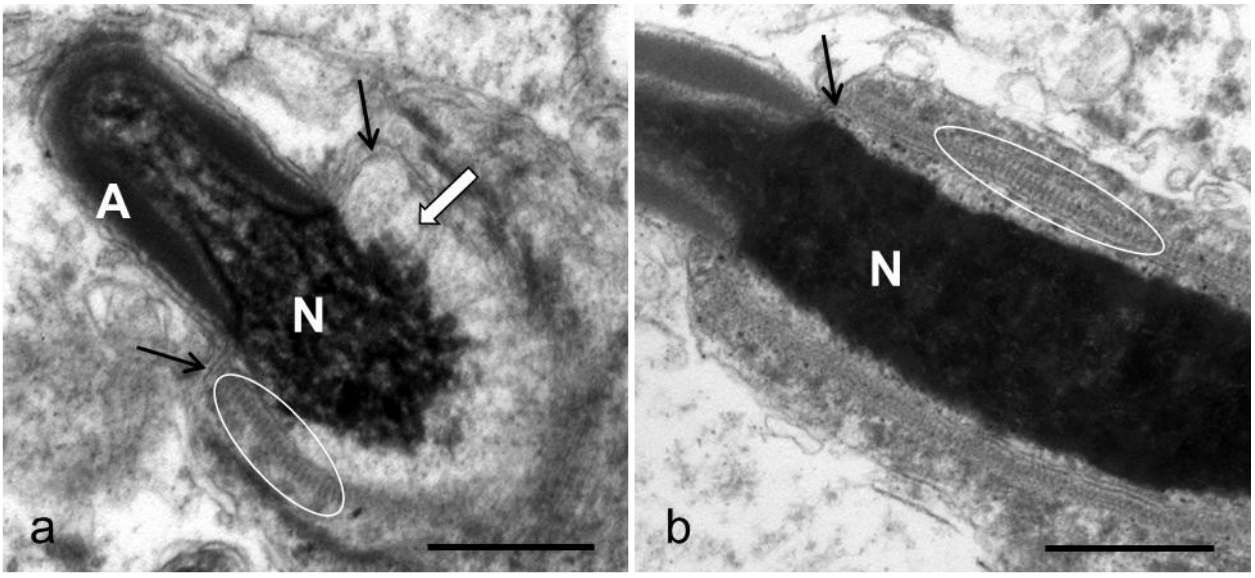

Figure 4. (a) Early stage of chromatin condensation. The projections (encircled) are concentrated just below the acrosome /nuclear shoulder (arrows). Note the filamentous chromatin granules and the wide space between the chromatin and the nuclear membrane (white arrow) (b) Late stage elongated spermatid with fully condensed chromatin. The projections (encircled) are arranged below the nuclear shoulder (arrow) and only a thin gap separates the condensed chromatin from the nuclear membrane. Bar = 0.5µm.

In a number of late longitudinal manchette stage spermatids the array of projections was seen to have completely disappeared leaving a zone of fine, moderately electron-dense particulate matter between the nuclear membrane and the manchette microtubules (Fig. 2f). This transition was abrupt and no intermediate stage was observed in the material studied.

Immunogold labelling

Although the immunogold labelling protocol was not optimal for the preservation of ultrastructural detail, the finger-like projections were clearly visible in thin sections indicating that they were extremely robust structures. No labelling of the projections with any of the tubulin antibodies or actin antibody was observed. The manchette microtubules, and to a lesser extent the axonemal microtubules, labeled positive for α-tubulin. Actin was detected in the interstitial tissue and peritubular tissue as evidenced by diffuse labeling of the myofibroblasts, but no labeling was obvious in the developing spermatids. The presence of β- and γ-tubulin could not be demonstrated in any of the emu testicular material.

Control sections of testicular material from chickens demonstrated intense labelling of the manchette, and to a lesser extent the axonemal microtubules by the monoclonal antibodies directed against α-tubulin while the centrioles of round spermatids labeled positive for the γ-tubulin antibody. In contrast, the β-tubulin antibody did not bind to any structures located within the testicular parenchyma. Actin was, however, detected within the peritubular and interstitial tissue. When the primary antibody was omitted, no labelling was found on the chicken sections. Negative controls showed no immunogold labelling.

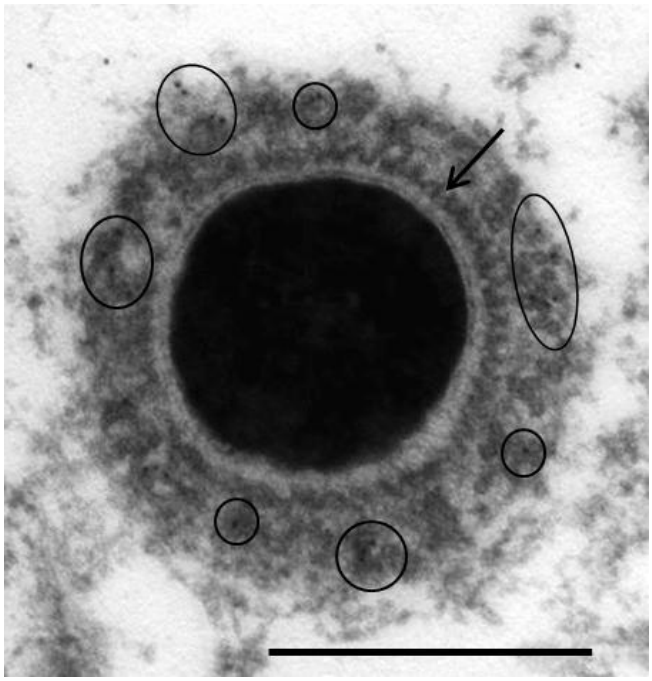

Figure 5. Immunogold labeling of a late emu spermatid for α-tubulin. Note the 10nm gold particles concentrated on the manchette microtubules (encircled). The projections (arrow) are devoid of any labeling. Bar = 0.5µm.

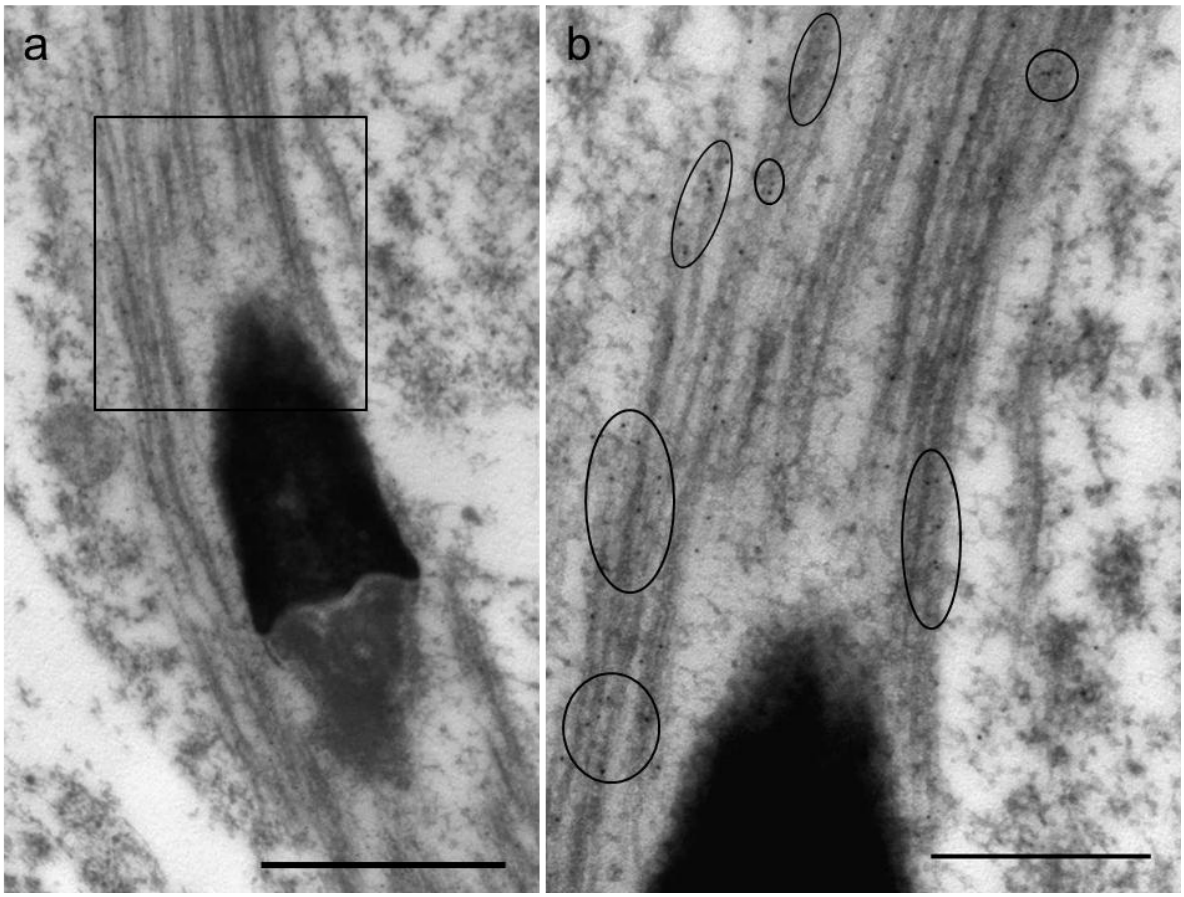

Figure 6. (a) Longitudinal manchette stage spermatid labelled for α-tubulin. The area within the square is enlarged in (b), showing the 10nm gold-particles (encircled) attached to the microtubules. Bar (a) = 1µm; Bar (b) = 0.5 µm.

Electron tomography

Electron tomography revealed the “structure” to be a continuous lattice which fully encapsulated the nucleus during the period of its existence. The individual elements of which the lattice was composed appear in the sub-tomogram average to be finger-like projections (Fig. 7) which are spaced 28nm apart (Fig. 8b). This contrasts with the slice through the tomogram parallel to the nuclear membrane which shows a regularly arranged lattice pattern with dimensions of a = 31nm, b= 23nm and γ = 78 degrees (Fig. 8c). These dimensions agree well with earlier estimates of their spacing. Sections through both the side (Fig.9a) and top view (Fig. 9b) of the tomogram, clearly show the regular arrangement and lattice pattern of the projections. Individual tomograms indicate that the “height” of the structure measured perpendicular to the surface of the nuclear membrane is variable as are the details of the structure distal from the nuclear membrane. This has resulted in a loss of detail in the sub-tomogram average. In general, the structure did not make contact with the nuclear membrane with the exception of isolated areas where a tenuous connection between the projections and nucleolemma could be seen (Fig. 9a).

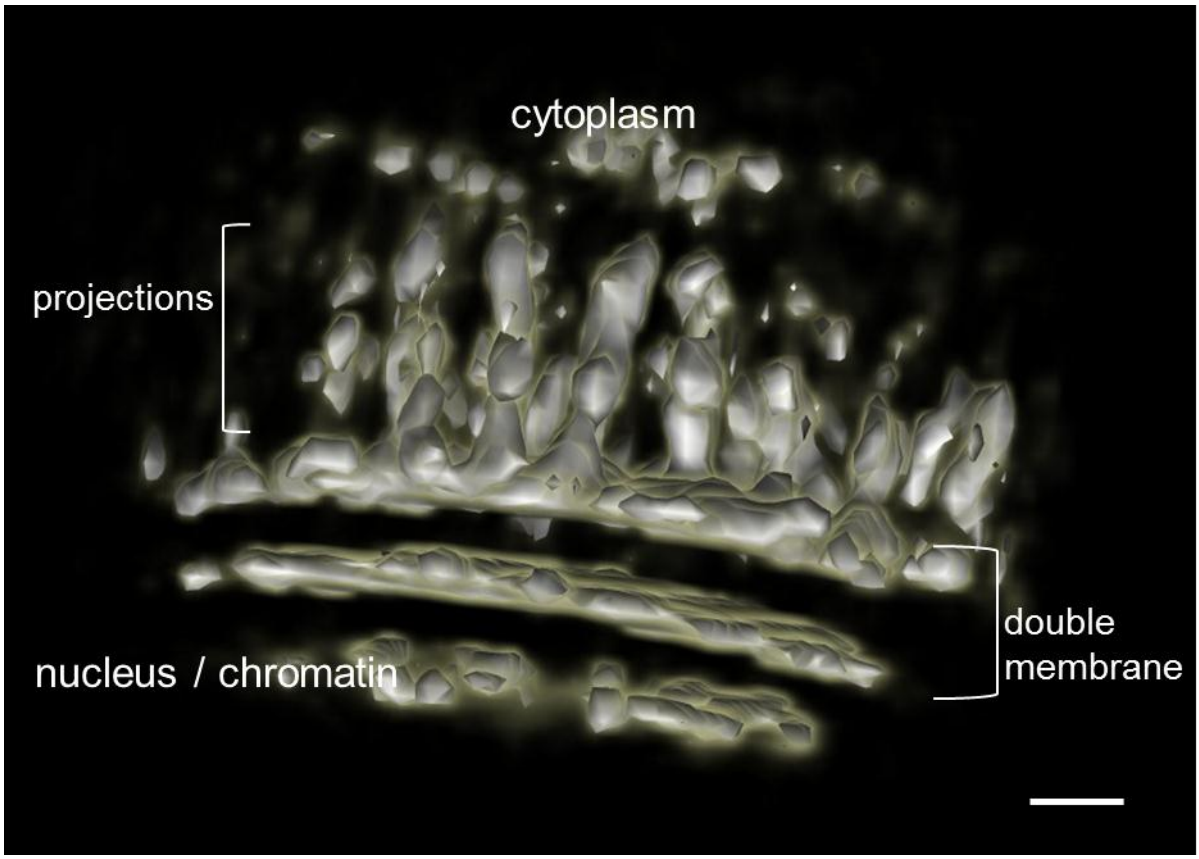

Figure 7. 3-D rendering of the average of 220 aligned sub-tomograms. Note the separate layers of the nuclear membrane with the projections closely associated with the outer leaflet. Bar = 100nm.

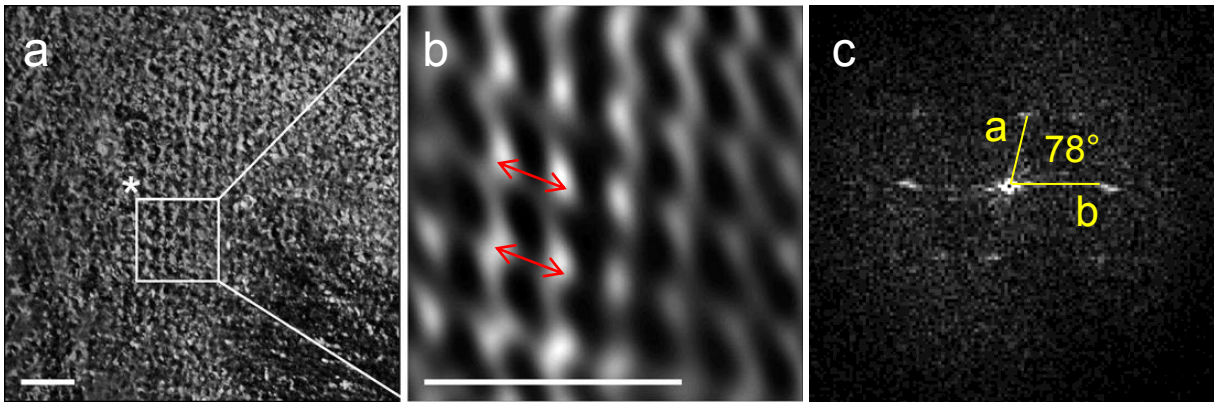

Figure 8. (a) Projection of the tomogram of the top view. Computation of the power spectrum (c) of this projection reveals the cell dimensions of the lattice to be a = 31.8nm, b = 23.4nm and γ = 78°. The square in (a) was filtered using these cell dimensions to emphasize the periodicity and the result is shown magnified in (b). The 28nm distance is indicated by the red lines. Bar = 100nm.

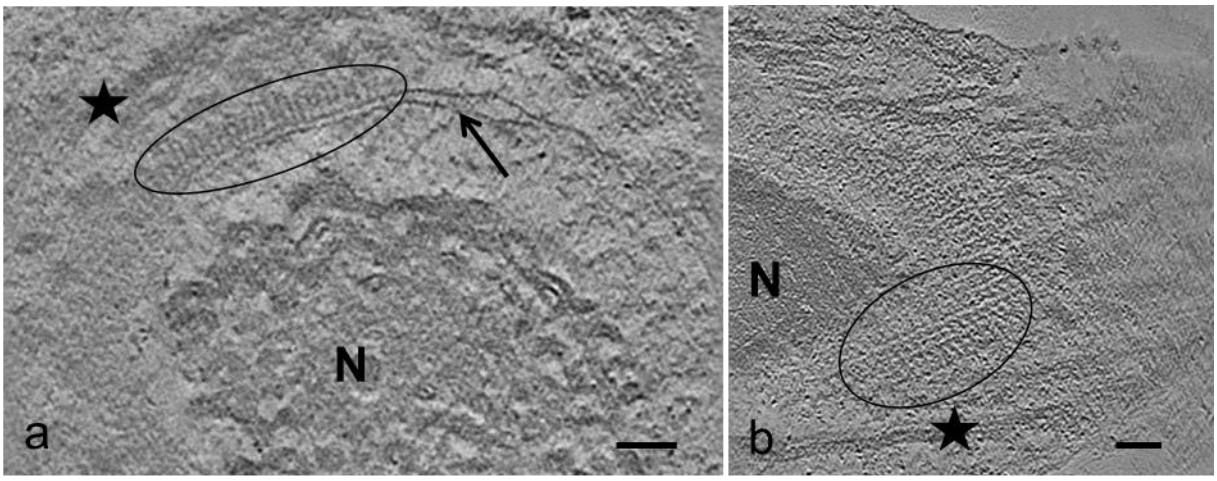

Figure 9. Sections (12Å thick) through the tomogram. (a) Side view. The structure (encircled) is visible at the cytoplasmic face of the nuclear membrane (arrow), with some projections appearing to make contact at the nuclear membrane. (b) Top view. The lattice-like pattern (encircled) of the structure in oblique section is easily recognisable. Nucleus (N), manchette microtubules (star). Bar = 100nm.

Discussion

Morphology

The transient nuclear membrane–associated projections observed during spermiogenesis in the emu have not previously been reported in birds. The zone of cytoplasm between the nuclear membrane and the manchette microtubules of all other non-passerine species remains conspicuously empty, composed only of fine flocculant material (Nagano, 1962; McIntosh & Porter, 1967; Tingari, 1973; Okamura & Nishiyama, 1976; Gunawardana & Scott, 1977; Sprando & Russell, 1988; Phillips & Asa, 1989; Baccetti *et al*., 1991; Lin & Jones, 1993; Maretta, 1995; Soley, 1997; Aire, 2003; Tripepi *et al*., 2006; Lovas *et al*., 2012). However, the projections bear a striking morphological resemblance to structures previously observed in various lizard species (Da Cruz-Landim & Da Cruz-Höfling, 1977; Da Cruz-Höfling & Da Cruz-Landim, 1978; Butler & Gabri, 1984; Al-Hajj *et al*., 1987; Vieira *et al*., 2001; Ferreira & Dolder, 2003) as well as in both the Caiman (*Caiman crocodiles*) (Saita *et al*., 1987) and Nile crocodile (*Crocodylus niloticus*) (personal observation, unpublished data). Although these structures have been illustrated, no morphological data, other than that the length of the “filaments” is 40nm in the Caiman crocodile (Saita *et al*., 1987), have been presented. A definitive description of the “structure” remains elusive. Based on TEM observations, the present study revealed that the projections were short, evenly spaced, peg- or finger-like extensions closely associated with the outer (cytoplasmic) face of the nuclear membrane. Electron tomography confirmed this observation (as previously noted in some lizards – see below) and additionally revealed the solid nature of the projections which on TEM gave the appearance of hollow cylinders. In the emu the projections were shorter than those

recorded for the Caiman (40nm) (Saita *et al*., 1987), measuring approximately 29nm in length using conventional TEM. This discrepancy may reflect differences in the calibration of equipment or the fact that the projections, despite being clearly defined near the nucleus, lost definition as they extended into the cytoplasm. This may be due to technical processing of the material, resin sectioning or even an inherited property of the structure.

In some lizard species (Butler & Gabri, 1984; Vieira *et al*., 2001) there is reportedly a connection between the microtubules of the manchette and the radial projections extending from the nuclear membrane. This phenomenon was particularly obvious in oblique sections of the "structure" which, due to the distortion resulting from the plane of section, places a question mark on the validity of the observations. Al-Haji *et al*. (1987) reported that the manchette microtubules are "anchored in" these projections. Although in ratites the staggered arrangement of the longitudinal manchette placed a few individual microtubules close to the finger-like projections, no obvious morphological connection was observed between the two structures. The structural properties of the projections outlined in the preceding paragraphs were also confirmed in ostrich and rhea spermatids (personal observation, unpublished data) using resin-embedded testicular material kindly supplied by Prof. J. T. Soley (ostrich) and Dr. D. M. Phillips (rhea).

Despite the lack of morphological data, various terms have been used to describe this transient structure, for example, short filaments forming a "hairy headband" (Saita *et al*., 1987), radial projections or trabeculae associated with the nuclear membrane (Da Cruz-Landim & Da Cruz-Höfling, 1977; Al-Hajj *et al*., 1987; Vieira *et al*., 2001; Ferreira & Dolder, 2003), bristles (Clark, 1967) and saturations originating from the nuclear envelope (Da Cruz-Höfling & Da Cruz-Landim, 1978). The use of these different and inconsistent terms further compounds the lack of morphological information available.

In lizards (Da Cruz-Landim & Da Cruz-Höfling, 1977; Da Cruz-Höfling & Da Cruz Landim, 1978; Butler & Gabri, 1984; Al-Hajj *et al*., 1987; Vieira *et al*., 2001; Ferreira & Dolder, 2003) and crocodiles (Saita *et al*., 1987), the projections appear to be restricted in location to the posterior aspect of the nucleus in the region just below the acrosome/nuclear shoulder, thus prompting the use of the term "hairy headband" (Saita *et al*., 1987). In contrast, at the height of its development in the emu, ostrich and rhea, the projections were observed to cover the entire surface of the elongating spermatid nucleus, although during earlier stages of its development in ratites, the "structure" was most prominent at the nuclear shoulder (see below).

Chronological development

It was clear from this study that in ratites the "structure" originated as a disorganised collection of projections during the circular manchette stage of development when nuclear elongation is initiated. The projections became progressively more obvious during the later stages of spermatid elongation, culminating, during the longitudinal manchette stage of development, in the formation of a continuous, uniform and symmetrical array around the entire surface of the nucleus. The extensive collection of projections disappeared abruptly in late stage elongated spermatids (identified by their densely compacted chromatin) while the microtubules of the longitudinal manchette were still clearly visible. It is difficult to gauge from the literature if a similar chronological development of the "structure" occurs in reptiles although it has been reported to be present at the beginning of cellular elongation (Ferreira & Dolder, 2003), the intermediate spermatid stage (Saita *et al*., 1987), and late stage of spermatid development (Clark, 1967). Additionally, little information is available on the duration of the structure in reptile spermatids, with Da Cruz-Landim & Da Cruz-Höfling (1977) simply reporting that in *Tropidurus torquatus* the spicular projections disappeared in the mature sperm. What does seem apparent from this study is that the development of the "structure" is closely linked to the formation of the manchette and, by association, with the change in shape of the spermatid nucleus.

Composition

None of the earlier reports on reptiles make any suggestions as to the possible composition of the "structure" other than to note the close connection of the projections with the cytoplasmic face of the nuclear membrane (Da Cruz-Landim & Da Cruz-Höfling, 1977; Da Cruz-Höfling & Da Cruz Landim, 1978; Butler & Gabri, 1984; Vieira *et al*., 2001; Ferreira & Dolder, 2003). The ICC results from the present study would indicate that it is neither a structural microtubule nor a contractile protein since it did not label with any of the anti-tubulin or anti-actin antibodies that were tested. The antibodies used were directed against chicken antigens and the possibility that they did not recognise / cross-react with the antigens of the emu due to species-specificity, cannot be ruled out. Preliminary electron tomography results appeared to indicate a structural protein with a tenuous connection to the nucleolemma, suggesting that the projections were not necessarily extensions of the outer face of the membrane *per se.*

Function

The function of the "structure" remains enigmatic and its role during spermiogenesis open to speculation. Ferreira and Dolder (2003) were of the opinion that it most likely connects the manchette microtubules to the nucleus, but failed to provide evidence or suggest a reason for such an association. Earlier reports noted a similar connection between the manchette microtubules and the "radial nuclear projections" (Butler & Gabri, 1984; Da Cruz-Landim & Da

Cruz-Höfling, 1977), leading to the suggestion that they functioned together to anchor this region of the developing spermatid so as to facilitate tapering of the nucleus and its embedding within the surrounding Sertoli cells (Butler & Gabri, 1984). Al-Haji *et al*. (1987) and Vieira *et al.* (2001) also speculated that the projections anchor the manchette microtubules. No function has been ascribed to this "structure" in crocodiles (Saita *et al*., 1987).

Based on the parallel development of the "structure" and the manchette microtubules observed during spermiogenesis in the emu (present study), ostrich and rhea (personal observations), the proposed microtubule anchoring role of the projections is a plausible hypothesis. Classically, in mammals a sub-plasmalemmal density, the nuclear ring, forms posterior to the base of the acrosome and from where the microtubules of the longitudinal manchette originate. The manchette has been widely implicated in mammals (Phillips, 1970, 1974; Myles & Hepler, 1982; Barth & Oko, 1989; Russell *et al*., 1991; Hermo *et al*., 2010) and birds (Nagano, 1962; McIntosh & Porter, 1967; Maretta, 1995; Okamura & Nishiyama, 1976; Lin & Jones, 1993; Soley, 1997; Aire, 2003) in nuclear shaping/elongation and the caudal displacement of excess spermatid cytoplasm. Besides being anchored by the nuclear ring, a number of studies have identified linkers between individual microtubules of the manchette *(*MacKinnon *et al*., 1973, Russell *et al.,* 1991; Soley, 1997) which presumably gives extra stability to the microtubular array. Russell *et al*. (1991) also reported on the existence of linkers between the manchette and the nucleus in rodents and speculated that they served to maintain a defined position of the manchette in relation to the nucleus. It is tempting to suggest that a similar situation occurs in ratites, particularly as a nuclear ring is not present, and that the projections serve as the link between the nucleus and the manchette. Although the projections appear to emanate from the outer face of the nuclear membrane in ratites, no obvious morphological connection between them and the manchette microtubules has been observed. This is clearly illustrated at the base of the nucleus where the projections point away from the manchette microtubules. In ratites the projections cover the entire surface of the nucleus whereas in lizards and crocodiles they are limited to the nuclear surface immediately beneath the acrosome. Should the observations in reptiles be accurate, and that there is indeed a link between the nucleus and manchette via the projections, it would appear as if the projections in these species fulfill a similar role to that of the nuclear ring in mammals.

The distribution of the projections throughout the spermatid nucleus in ratites and their lack of obvious contact with the manchette microtubules may indicate an alternative role, namely that of nuclear stabilization. Elongation of the nucleus in ratites is striking in comparison to the situation in mammals and in these avian species it may be necessary to support or stabilize the relatively long and thin developing nucleus. In this capacity the projections would act as a form of

scaffolding, particularly during the period of translocation of spermatid cytoplasm (longitudinal manchette stage) when they are maximally developed. The sudden disappearance of the projections at the height of nuclear elongation (head shaping and chromatin condensation completed) would support this proposed function. The scattered distribution of the projections in the form of small pockets during earlier stages of nuclear transformation may be necessary to ensure a degree of stability without sacrificing the flexibility required for morphological transformation.

It is not clear why ratite spermatids would require nuclear scaffolding when it is absent in other non-passerine birds which display equally long nuclei, for example the chicken (Gunawardana & Scott, 1977; personal observations), duck (Maretta, 1975; personal observations) and severely restricted in lizards (Ferreira & Dolder, 2003) and crocodiles (Saita *et al*., 1987). It could be argued that the nuclear membrane-associated projections seen in ratites and some reptilian species simply reflect an ancient, conserved character that is no longer of functional significance. An accurate determination of the composition of the projections would assist in answering this perplexing question. The finger-like projections which characterise this structure appear to be unique to the process of spemiogenesis in certain vertebrate / non-mammalian species. No homologous structures have been described elsewhere. It is therefore not possible to draw parallels with any other subcellular structure. As a consequence, its function must be sought by further investigations, possibly using cryo-electron microscopy for its superior sample preservation, combined with electron tomography. This may help to clarify the identity and molecular composition of the structure.

Phylogeny

The transient “structure” revealed in the present study appears to represent an important morphological character that can be applied for the resolution of phylogenetic questions. The observation that the only non-passerine birds with this unique structural adaptation appear to be the emu, ostrich and rhea, supports the traditional view that the extant ratites form a monophyletic group (Cracraft, 1974, 2001; Sibley & Ahlquist, 1995; Van Tuinen *et al*., 2000; Haddrath & Baker, 2001; Hackett *et al*., 2008; Johnston, 2011). This view is strengthened by the fact that studies on galliform birds such as the chicken (Nagano, 1962; Tingari, 1973; Gunawardana & Scott, 1977; personal observations), turkey (Aire, 2003), quail (Lin & Jones, 1993) and members of the anseriforms (Maretta, 1995; Simões *et al*., 2005; personal observations), two families closely linked phylogenetically to the ratites, have failed to reveal an equivalent structure. It would be interesting to determine whether the remaining members of the Ratidae (cassowaries and kiwis) also reflect the “structure” during spermiogenesis and indeed whether it is present in developing spermatids of the tinamous, as recent molecular studies have placed the tinamou together with

the ratites as a polyphyletic group (Hackett *et al*., 2008; Harshman *et al*., 2008; Smith *et al*., 2012).

The exclusive nature of the “structure” would also suggest that the ratites occupy a basal position in the avian phylogenetic tree as has been previously proposed (Stapel *et al*., 1984; Cracraft, 1988; Sibley & Ahlquist, 1995; Van Tuinen *et al*., 2000; García-Moreno *et al*., 2003). The only other vertebrates reported to display this “structure” are the crocodiles (Saita *et al*., 1987) and certain lizard species (Clark, 1967; Da Cruz-Landim & Da Cruz-Höfling, 1977; Da Cruz-Höfling & Da Cruz Landim, 1978; Butler & Gabri, 1984; Al-Hajj *et al*., 1987; Vieira *et al*., 2001; Ferreira & Dolder, 2003). This may be viewed as additional proof that reptiles and birds share a common ancestor (Walker, 1972; Whetstone & Martin, 1979; Sibley & Ahlquist, 1995; Janke & Arnason, 1997; Rest *et al*., 2003; Fraser & Parry, 2011). The birds, crocodiles and turtles are estimated to have branched from the Archosaurs approximately 272 million years ago (MYA), whereas lizards, together with snakes and the tuatara, derived from the Squamates approximately 230 MYA. As both the Archosaurs and Squamates evolved from early reptiles approximately 285 MYA (Rest *et al*., 2003), and as modern-day relatives of both groups share the transient structure, it is plausible that it represents an ancient character trait which has been conserved in certain extant species. Future studies on spermiogenesis in a wider variety of birds and reptiles may provide clarity in this respect.

There is further compelling evidence to support the basal positioning of the ratites outlined above. Comparative sequence analysis of the α-crystallin A chain, a major constituent of the vertebrate eye lens, suggested that the ratites represent the first offshoot of the avian line with the crocodiles, represented by the alligator, as the sister group of the birds (Stapel *et al*., 1984). Similarly, mitochondrial protein sequencing (Janke & Arnason, 1997), as well as amino acid sequencing and X-ray diffraction studies on the filament-matric of β-keratins in emu feathers and scales of a lizard claw (Fraser & Parry, 2011), supports the avian (ratite)/crocodile link. Various other anatomical / morphological studies have also reinforced the close relationship between reptiles and birds (Walker, 1972; Whetstone & Martin, 1979; Gower & Weber, 1998; 2003, including similarities in sperm structure (Jamieson, 2007).

In conclusion, it is proposed that the nuclear membrane-associated projections seen during spermiogenesis in ratites represent an ancient character trait linking birds and reptiles. Despite contrary reports on avian phylogeny proposing various other birds, notably the passerines, to be the oldest offshoot of the avian stem (Feduccia, 1995; Mindell *et al*., 1999; Härlid & Arnason, 1999; Johnson, 2001; Braun & Kimball, 2002), the existence of this unique structure in ratites

strengthens the argument that these birds form a monophyletic group with a basal position within the avian phylogenetic tree.

References

Aire T.A. (2003) Ultrastructural study of spermiogenesis in the turkey, *Meleagris gallopavo*. *British Poultry Science* **44,** 674-682.

Aire T.A. (2007) Spermatogenesis and testicular cycles. In: Jamieson, B.G.M. (ed.) Reproductive Biology and Phylogeny of Birds Vol 6A. Science Publishers, Jersey, pp. 279-347.

Al-Hajj, H., Janakat, S. & Mahmoud, F. (1987) Electron microscopic study of sperm head differentiation in the lizard *Agama stellio*. *Canadian Journal of Zoology* **65**, 2959-2968.

Aumüller, G. & Seitz, J. (1988) Immunocytochemical localization of actin and tubulin in rat testis and spermatozoa. *Histochemistry* **89**, 261-267.

Baccetti, B., Burrini, A.G. & Falchetti, E. (1991) Spermatozoa and relationships in Palaeognath birds. *Biology of the Cell* **71**, 209-216.

Barth, A.D. & Oko, R.J. (1989) Abnormal morphology of bovine spermatozoa. Iowa State University Press, Ames.

Braun, E.L. & Kimball, R.T. (2002) Examining basal avian divergences with mitochondrial sequences: model complexity, taxon sampling, and sequence length. *Systematic Biology* **51**, 614-625.

Butler, R.D. & Gabri, M.S. (1984) Structure and development of the sperm head in the lizard *Podarcis (=Lacerata) taurica*. *Journal of Ultrastructure Research* **88**, 261-274.

Clark, A.W. (1967) Some aspects of spermiogenesis in a lizard. *American Journal of Anatomy* **121**, 369-400.

Cracraft, J. (1974) Phylogeny and evolution of the Ratite birds. *Ibis* **116**, 494-521.

Cracraft, J. (1988) The major clades of birds. In: Benton, M.J. (ed.) The Phylogeny and Classification of Tetrapods. Clarendon Press, Oxford,pp. 339-361.

Cracraft, J. (2001) Avian evolution, Gondwana biogeography and the Cretaceous-Tertiary mass extinction event. *Proceedings of the Royal Society London B* **268**, 459-469.

Cracraft, J. & Mindell, D.P. (1989) The early history of modern birds: A comparison of molecular and morphological evidence. In: Fernholm, B., Bremer, K. & Jörnvall, H. (eds.) The hierarchy of life. Elsevier Science Publishers, Amsterdam, pp. 389-403.

Da Cruz-Höfling, M.A. & Da Cruz-Landim, C. (1978). The fine structure of nuclei during spermiogenesis in the lizard *Tropidurus torquatus* (Lacertilia). *Cytologia* **43**, 61-68.

Da Cruz-Landim, C. & Da Cruz-Höfling, M.A. (1977) Electron microscope study of lizard spermiogenesis in *Tropidurus torquatus* (Lacertilia).*Caryologia* **30**,151-162.

Ericson, P.G.P. (2008) Current perspectives on the evolution of birds. *Contributions to Zoology* **77**, 109-116.

Feduccia, A. (1995) Explosive evolution in tertiary birds and mammals. *Science* **267**, 637-638.

Ferreira, A. & Dolder, H. (2003) Sperm ultrastructure and spermiogenesis in the lizard, *Tropidurus itambere*. *Biology of the Cell* **27**, 353-362.

Fouquet, J-P., Kann, M.L. & Dadoune, J-P. (1989) Immunogold distribution of actin during spermiogenesis in the rat, hamster, monkey, and human. *The Anatomical Record* **223**, 35-42.

Fouquet, J-P., Kann, M.L., Combeau, C. & Melki, R. (1998) γ-tubulin during the differentiation of spermatozoa in various mammals and man. *Molecular Human Reproduction* **4**, 1122-1129.

Fraser, R.D.B. & Parry, D.A.D. (2011) The structural basis of the filament-matrix texture in the avian/reptilian group of hard β-keratins. *Journal of Structural Biology* **173**, 391-405

García-Moreno, J., Sorenson, M. & Mindell, D.P. (2003) Congruent avian phylogenies inferred from mitochondrial and nuclear DNA sequences. *Journal of Molecular Evolution* **57**, 27-37.

Góes, R.M.& Dolder, H. (2002) Cytological steps during spermiogenesisin the house sparrow (*Passer domesticus*, Linnaeus) *Tissue & Cell* **34**, 273-282.

Gower, D.J. & Weber, E. (1998) The braincase of Euparkeria, and the evolutionary relationships of birds and crocodilians. *Biological Reviews* **73**, 367-411.

Gribbins, K.M. (2011) Reptilian spermatogenesis: a histological and ultrastructural perspective. *Spermatogenesis* **1**, 250-269.

Gunawardana, V.K. & Scott, M.G.A.D. (1977) Ultrastructural studies on the differentiation of spermatids in the domestic fowl. *Journal of Anatomy* **124**, 741-755.

Hackett, S.J., Kimbali, R.T., Reddy, S., Bowie, R.C.K., Braun, E.L., Braun, M.J., Chojnowski, J.L., Cox, W.A., Han, K., Harshman, J., Huddleston, J., Huddleston, C.J., Marks, B.D., Miglia, K.J., Moore, W.S., Sheldon, F.H., Steadman, D.W. & Witt, C. (2008) A phylogenomic study of birds reveals their evolutionary history. *Science* **320**, 1763-1768.

Haddrath, O. & Baker, A.J. (2001) Complete mitochondrial DNA genome sequences of extinct birds: Ratite phylogenetics and the vicariance biogeography hypothesis. *Proceedings of the Royal Society of London Series B* **268**, 939-945.

Härlid, A. & Arnason, U. (1999) Analyses of mitochondrial DNA nest ratite birds within the Neognathae: supporting a neotenous origin of ratite morphological characters. *Proceedings of the Royal Society of London Series B* **266**, 305-309.

Harshman, J., Braun, E.L., Braun, M.J., Huddleston, C.J., Bowie, R.C.K., Chojnowski, J.L., Hackett, S.J., Han, K-L., Kimball, R.T., Marks, B.D., Miglia, K.J., Moore, W.S., Reddy, S., Sheldon, F.H., Steadman, D.W., Steppan, S.J., Witt, C.C. & Yuri, T. (2008) Phylogenetic evidence for multiple losses of flight in ratite birds. *Proceedings of the National Academy of Sciences of the United States of America (PNAS)* **105**, 13462-13467.

Hermo, L., Pelletier, R-M., Cyr, D.G. & Smith, C.E. (2010) Surfing the wave, cycle, life history, and genes/protein expressed by testicular germ cells. Part 2: Changes in spermatid organelles associated with

development of spermatozoa. *Microscopy Research and Techniques* **73**, 279-319.

Jamieson, B.M.G. (2007) Avian spermatozoa: structure and phylogeny. In: Jamieson, B.M.G. (ed.) Reproductive Biology and Phylogeny of Birds Part A, Science Publishers, Jersey, pp. 349-512.

Janke, A. & Arnason, U. (1997) the complete mitochondrial genome of Alligator mississippiensis and the separation between recent Archosauria (birds and crocodiles). *Molecular Biology and Evolution* **14**, 1266-1272.

Johnson, K.P. (2001) Taxon sampling and the phylogenetic position of Passeriformes: Evidence from 916 avian cytochrome b sequences. *Systematic Biology* **50**, 128-136.

Johnston, P. (2011) New morphological evidence supports congruent phylogenies and Gondwana vicariance for palaeognathous birds. *Zoological Journal of the Linnean Society* **163**, 959-982.

Koehler, L.D. (1995) Diversity of avian spermatozoa ultrastructure with emphasis on the members of the order Passeriformes. *Memoires du Museum National d'Histoire Naturelle* **166**, 437-444.

Lin, M. & Jones, R.C. (1993) Spermiogenesis and spermiation in the Japanese quail (*Coturnix coturnix japonica). Journal of Anatomy* **183**, 525–535.

Lovas, E.M., Filippich, L.J. & Johnston, S.D. (2012) Spermiogenesis in the Australian cockatiel *Nymphicus hollandicus. Journal of Morphology in press.*

Ludtke, S.J., Baldwin, P.R. & Chiu, W. (1999) EMAN: semiautomated software for high-resolution single particle reconstruction. *Journal of Structural Biology* **128**, 82-97.

MacKinnon, E.A., Abraham, P.J. & Svatek, A. (1973) Long link induction between the microtubules of the manchette in intermediate stages of spermiogenesis. *Zeitschrift fur Zellforschung und Mikroskopische Anatomie* **136**, 447-460.

Mancini, K., Báo, S.N., Fernandes, A.P. & Dolder, H. (2005) Immunocytochemical localization of tubulins in spermatids and spermatozoa of *Euptoieta hegesia* (Lepidoptera: Nymphalidae). *Tissue Cell* **37**, 81-89.

Maretta, M. (1975) The ultrastructure of the spermatozoon of the drake. *Acta Veterinaria* **25**, 47-52.

Maretta, M. (1995) Formation and role of the manchette microtubules in the poultry spermatids. *Acta Veterinaria* **64**, 23-29.

Mastronarde, D.N. (1997) Dual-axis tomography: an approach with alignment methods that preserve resolution. *Journal of Structural Biology* **120**, 343–352.

McIntosh, J.R. & Porter, K.R. (1967) Microtubules of the spermatids of the domestic fowl. *Journal of Cell Biology* **35**, 153-173.

Mindell, D.P., Sorenson, M.D., Dimcheff, D.E., Hasegawa, M., Ast, J.C. & Yuri, T. (1999) Interordinal relationships of birds and other reptiles based on whole mitochondrial genomes. *Systematic Biology* **48**, 138-152.

Myles, D.G. & Hepler, P.K. (1982) Shaping of the sperm nucleus in Marsilea: A distinction between factors responsible for shape generation and shape determination. *Developmental Biology* **90**, 238-252.

Nagano, T. (1962) Observations on the fine structure of the developing spermatid in the domestic chicken. *Journal of Cell Biology* **14**, 193-205.

Okamura, F. & Nishiyama, H. (1976) The early development of the tail and the transformation of the shape of the nucleus of the spermatid of the domestic fowl, *Gallus gallus*. *Cell and Tissue Research* **169**, 345-359.

Paton, T., Haddrath, O. & Baker, A.J. (2002) Complete mitochondrial DNA genome sequences show that modern birds are not descended from transitional shorebirds. *Proceedings of the Royal Society of London Series B* **269**, 839-846.

Pettersen, E.F., Goddard T.D., Huang, C.C., Couch, G.S., Greenblatt, D.M., Meng, E.C. & Ferrin, T.E. (2004) UCSF Chimera - a visualization system for exploratory research and analysis. *Journal of Computational Chemistry* **25**, 1605-1612.

Phillips, D.M. (1970) Development of the woolly opossum with special reference to the shaping of the sperm head. *Journal of Ultrastructure Research* **33**, 369-380.

Phillips, D.M. (1974) Spermiogenesis. Academic Press, New York.

Phillips, D.M. & Asa, C.S. (1989) Development of spermatozoa in the rhea. *Anatomical Record* **223**, 276-282.

Rest, J.S., Ast, J.C., Austin, C.C., Waddell, P.J., Tibbetts, E.A., Hay, J.M. & Mindell, D.P. (2003) Molecular systematics of primary reptilian lineages and the tuatara mitochondrial genome. *Molecular Phylogenetics and Evolution* **29**, 289-297.

Russell, L.D., Russell, J.A., MacGregor, G.R.& Meistrich, M.L. (1991) Linkage of manchette microtubules to the nuclear envelope and observations of the role of the manchette in nuclear shaping during spermiogenesis in rodents. *American Journal of Anatomy* **192**, 97-120.

Saita, A., Comazzi, M. & Perrotta, E. (1987) Electron microscope study of spermiogenesis in *Caiman crocodylus L*. *Italian Journal of Zoology* **4**, 307-318.

Sibley, C.G. & Ahlquist, J.E. (1981) The phylogeny and relationships of the ratite birds as indicated by DNA-DNA hybridization. In: Scudder, G.C.E. & Reveal, J.L. (eds.) Evolution Today. Proceedings of the Second International Congress of Systematic and Evolutionary Biology, University of British Columbia, Hunt Institute for Botanical Documentation, Carnegie-Mellon University, Pittsburgh, pp. 301-335.

Sibley, C.G. & Ahlquist, J.E. (1995) Phylogeny and classification of birds. Yale University Press, New Haven.

Sibley, C.G., Ahlquist, J.E. & Monroe, B.L. (1988) A classification of the living birds of the world based on DNA-DNA hybridization studies. *The Auk* **105**, 409-423.

Simões, *K*., Orsi, A.M. & Viegas, K.A.S. (2005) Ultrastructural characteristics of spermiogenesis in the domestic duck (*Anas platyrhynchos*). *Anatomia, Histologia, Embryologia* **34**, 307-311.

Smith, J.V., Braun, E.L. & Kimball, R.T. (2012) Ratite nonmonophyly: independent evidence from 50 novel loci. *Systematic Biology* in press.

Soley, J.T. (1992) A Histological study of spermatogenesis in the ostrich (*Struthio camelus*). Ph.D. Thesis. University of Pretoria, Pretoria.

Soley, J.T. (1994). Centriole development and formation of the flagellum during spermiogenesis in the ostrich (*Struthio camelus*). *Journal of Anatomy* **185**, 301-313.

Soley, J.T. (1996) Differentiation of the acrosomal complex in ostrich (*Struthio camelus*) spermatids. *Journal of Morphology* **227**,101-111.

Soley, J.T. (1997) Nuclear morphogenesis and the role of the manchette during spermiogenesis in the ostrich (*Struthio camelus*). *Journal of Anatomy* **190**, 563-576.

Sprando, R.L.& Russell, D. (1988) Spermiogenesis in the red-ear turtle (*Pseudemysscripta)* and the domestic fowl (*Gallus domesticus):* a study of cytoplasmic events including cell volume changes and cytoplasmic elimination. *Journal of Morphology* **198**, 95-118.

Stapel, S.O., Leunissen, J.A.M., Versteeg, M., Wattel, J. & de Jong, W.W. (1984) Ratites as oldest offshoot of avian stem – evidence from α-crystallin A sequences. *Nature* **311**, 257-259.

Tingari, M.D. (1973) Observations on the fine structure of spermatozoa in the testis and excurrent ducts of the male fowl, *Gallus domesticus*. *Journal of Reproduction and Fertility* **34**, 255-265.

Tripepi, S., Jamieson, B.G.M. & Brunelli, E. (2006) Ultrastructure of the spermatid of *Caprimulgus europaeus* Linnaeus 1758, the European nightjar (Aves; Caprimulgidae), with phylogenetic implications. *Journal of Morphology* **267**, 1157-1164.

Van Tuinen, M., Sibley, C.G. & Hedges, S.B. (2000) The early history of modern birds inferred from DNA sequences of nuclear and mitochondrial ribosomal genes. *Molecular Biology and Evolution* **17**, 451-457.

Vieira, G.H.C., Wiederhecker, H.C., Colli, G.R. & Báo, S.N. (2001) Spermiogenesis and testicular cycle of the lizard *Tropidurus torquatus* (Squamata, Tropiduridae) in the Cerrado of central Brazil. *Amphibia-Reptilia* **22**, 217-233.

Walker, A.D. (1972) New light on the origin of birds and crocodiles. *Nature* **237**, 257-266.

Whetstone, K.N. & Martin, L.D. (1979) New look at the origin of birds and crocodiles. *Nature* **279**, 234-235.

Xia, L., Clermont, Y., Lalli, M. & Buckland, R.B. (1986) Evolution of the endoplasmic reticulum during spermiogenesis of the rooster: an electron microscopic study. *American Journal of Anatomy* **177**, 301–312.

Yamamoto, S., Tamate, H. & Itikawa, O. (1967) Morphological studies on the sexual maturation in the male Japanese quail (*Coturnix coturnix japonica*). I. The germ cell types and cellular associations during spermatogenesis. *Tohoku Journal of Agricultural Research* **18**, 27-37.

Zheng, S.Q., Keszthelyi, B., Branlund, E., Lyle, J.M., Braunfeld, M.B., Sedat, J.W. & Agard, D.A. (2007) UCSF tomography: an integrated software suite for real-time electron microscopic tomographic data collection, alignment, and reconstruction. *Journal of Structural Biology* **157**, 138-147.

Chapter 5 Incidence and morphological classification of abnormal sperm

Introduction

In various parts of the world ratites such as ostriches, emus and rheas are farmed commercially for their skin, meat, fat and feathers. Although organised on a commercial basis, the industry is beset by a variety of production problems (Deeming & Ar, 1999; Soley & Groenewald, 1999; Malecki *et al*., 2008), particularly in respect of reproductive performance, which severely hamper the economic viability of the industry. The ratite industry currently relies on natural reproduction which is not always cost effective. In addition, the monogamous nature of ratites (Malecki *et al*., 2000, 2008) requires that a large number of males be kept for the sole purpose of breeding, adding an unnecessary financial burden to farming operations. Malecki *et al*. (2008) also point out that 'natural mating hampers rapid genetic improvement because the genes of an elite male can be offered to only a few females'. In order to address these constraints, it has been suggested that the ratite industry employ advanced reproductive technologies including the use of artificial insemination (AI) (Malecki *et al*., 2000, 2008).

Successful AI programmes require proven methods for the collection, handling, storage and cryopreservation of semen, as well as the accurate assessment of male fertility. Sperm morphology plays an important role in the assessment of semen quality (Malmgren, 1997) and has been considered by Bertschinger *et al*. (1992) to be the most important parameter in assessing male fertility in the ostrich. While considerable information has been collected on normal sperm morphology of ratites and closely related species (Asa *et al*., 1986; Phillips & Asa, 1989; Baccetti *et al*., 1991; Soley, 1993; Soley & Roberts, 1994), little is known regarding abnormal forms in this group of birds. Various types of sperm abnormalities which result in a decrease in fertility and can lead to infertility have been identified in mammals, including man, and detailed descriptions of the defects including their ultrastructure have been documented (Holstein *et al*., 1988; Oettlé & Soley, 1988; Barth & Oko, 1989; Feito, 1990; Menkveld *et al*., 1991). There are a number of reports on the incidence of sperm abnormalities in birds, particularly in domestic poultry such as the fowl (Łukaszewicz *et al*., 2008), turkey (Kamar & Rizik, 1972; Marquez & Ogasawara, 1975; Alkan *et al*., 2002), duck (Penfold *et al*., 2000) and goose (Ferdinand, 1992), as well as in ratites (Bertschinger *et al*., 1992; Malecki *et al*.,1998; Hemberger *et al*., 2001; Rozenboim *et al*., 2003) and exotic species

(Lindsay *et al*., 1999; Stelzer *et al*., 2005; Umapathy *et al*., 2005). However, the recording of the defects lacks conformity and the morphological description of the anomalies, confined mainly to light microscopic descriptions, suffers, with few exceptions (Marquez & Ogasawara, 1975; Bakst & Sexton, 1979; Bakst, 1980; Ferdinand, 1992; Soley & Els, 1993; Soley *et al*., 1996), from a lack of ultrastructural detail. Although the incidence of sperm defects has been described in some ratites (Malecki *et al*., 1998; Hemberger *et al*., 2001; Rozenboim *et al*., 2003), only Malecki *et al*. (1998) presented a description of the defects observed. In contrast, Bertschinger *et al*. (1992) recognised five major defects in a study of 65 ostriches but did not report on the incidence of the defects.

In this chapter light microscopy was employed to examine the incidence and morphology of abnormal forms of sperm in semen samples from 15 emus. Based on these findings, a system for the uniform recording of ratite sperm abnormalities is proposed.

Materials & Methods

Semen samples were collected mid-breeding season from 15 clinically healthy, sexually active emus following slaughter at a commercial abattoir. Droplets of semen were gently squeezed from the distal *ductus deferens* into tubes containing 2.5% glutaraldehyde in 0.13M Millonig's phosphate-buffer. Smears were made for light microscopy and stained with Rapidiff as previously described (see Chapter 2). Smears from each bird were examined using a 100x oil immersion objective and phase contrast illumination to evaluate sperm morphology and determine the incidence of sperm defects by counting the number of abnormal sperm present in a total of 300 cells. Abnormal sperm were expressed as a percentage of the total sperm count, while individual categories of abnormalities were expressed as a percentage of total sperm abnormalities (Table 1).

Results

Incidence

A mean value of 13.6% morphologically abnormal sperm was reflected in the samples examined. These defects were divided into four broad categories, namely, head defects (52.4%), tail defects (25.6%), multiple defects (11.5%) and cytoplasmic droplets (10.5%) (Table 1; Figs. 1, 2).

Table 1. Incidence of the various sperm defects expressed as a percentage of total sperm defects.

CATEGORY	*REGION*	*SPECIFIC DEFECT*
Head defects 52.4%	Nucleus 52.4%	Bent heads 27.8% Macrocephalic 11.1% Microcephalic 0.8% Acephalic: 9.9% Round heads 2.8%
Tail defects 25.6%	Neck/midpiece 15.7%	Disjointed sperm 15.1% Abaxial sperm 0.6%
	Principal piece 9.9%	Stump tails 3.8% Coiled tails 3.3% Multiple tails 2.8%
Cytoplasmic droplets 10.5%		
Multiple defects 11.5%		

Morphological classification

Head defects:

Most abnormalities occurred in the head region of which four forms, namely, bent heads, macrocephalic heads, round heads and acephalic sperm, were identified (Figs. 1,2). Various forms of head bending could be distinguished ranging from simple bending (gentle to acute bends) (Figs. 1a,c,e), to looping (Fig. 1b), kinking (which manifest as a single twist of the head, generally towards the base) (Fig. 1d), coiling (in most instances the formation of a single coil) and spiraling (Fig. 1f). Spiralled heads presented a corkscrew appearance and was the least frequent head defect noted. Bent heads were often associated with retained cytoplasmic droplets. The eccentric positioning of the droplets effectively determined the direction of the bend. Head bending was also frequently associated with defective or incomplete chromatin condensation, particularly towards the base of the nucleus. A detailed description of head-base bending is presented in Chapter 6.

Macrocephalic heads were markedly larger than normal heads (Fig. 1h). The giant heads were associated with either a single tail or multiple tails. Round-headed sperm (Fig. 1g inset) and pear-shaped heads (presumably microcephalic sperm) were occasionally noted. These heads were markedly smaller than those of normal sperm. In some instances they showed a projection that resembled the acrosome.

Acephalic sperm were easily identified by LM (Fig. 2f). The cell consisted of a complete flagellum (midpiece, principal piece and endpiece) of normal dimensions and morphology, but devoid of a head (See Chapter 9). No acrosome defects were observed in the material studied.

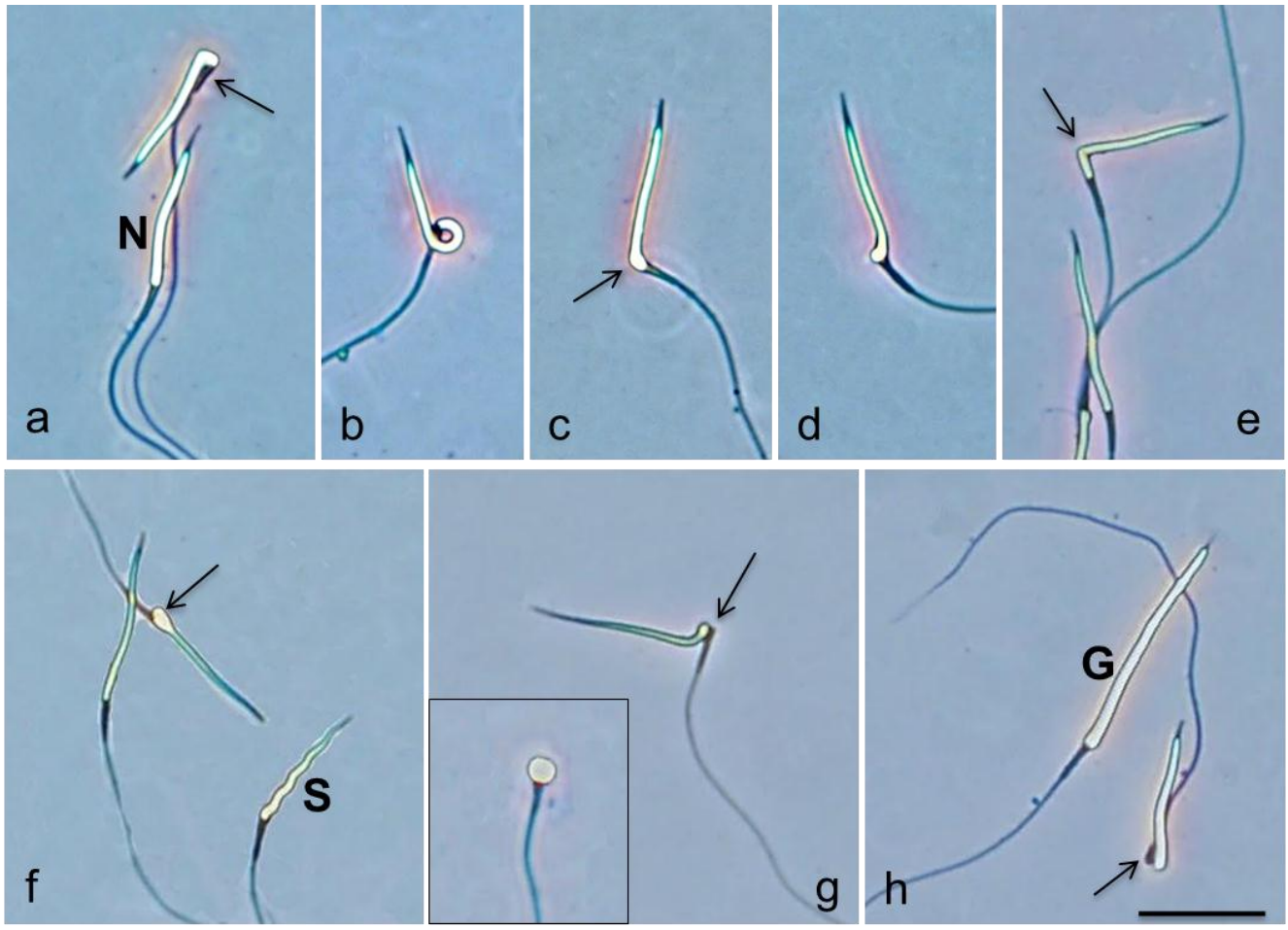

Figure 1. Light micrographs illustrating morphologically normal sperm (N) and various sperm defects. (a) Head base bend (arrow); (b) Looped sperm head; (c) 90º head bend with swelling (arrow); (d) Kinked head; (e) 90º head bend (arrow); (f) Abaxial sperm (arrow), and spiraled head (S); (g) Disjointed sperm with a bulge at the nuclear base (arrow), an example of a multiple defect; inset: small round-headed sperm; (h) Giant sperm head with a single tail (G) and a disjointed sperm (arrow). Bar = 10µm.

Tail defects:

Tail abnormalities were subdivided into neck/midpiece and principal piece defects. Defects observed in the neck/midpiece region included disjointed sperm and abaxial sperm. Disjointed sperm were characterized by the complete separation of the head and midpiece in the neck region but within the confines of the plasmalemma (Fig. 1g,h). The specific point of separation appeared to occur at the implantation fossa. On LM the defect appeared as a tight (complete) reflection of the head with the base of the head and the midpiece lying next to each other, the cell thus appearing disjointed (See Chapter 6 for details of disjointed sperm).

Abaxial tail implantation was characterized by the misalignment of the centriolar complex relative to the head base. Despite their low incidence defective sperm could readily be identified using light microscopy (Fig. 2c inset). Affected sperm displayed obvious misalignment of the head and flagellum with many cells additionally showing unilateral swelling and caudal extension of the nuclear base. This material overlapped the anterior aspect of the centriolar complex. More subtle forms of the defect which were not resolved by LM were revealed by TEM. For a detailed description of this defect, see Chapter 7.

Abnormalities of the principal piece were subdivided into stump (short) tails (Fig. 2c), coiled tails (Fig. 2b) and multiple tails (Fig. 2a). Short-tailed sperm displayed a range of under-length flagella, from an extremely shortened tail typical of the mammalian stump tail defect (Barth & Oko, 1989) to a flagellum approximately half the normal length. Coiled tails demonstrated one or more tight coils of the principal piece whereas multiple-tailed sperm exhibited two or more flagella.

Cytoplasmic droplets:

Cytoplasmic droplets (Figs. 2d,e) varied in size, appeared bulbous and were mostly eccentrically positioned. They were located either at the base of the head or covered both the head base and proximal section of the midpiece.

Multiple defects:

A small percentage of sperm displayed more than one abnormality simultaneously. Multiple defects included, for example, bent heads with multiple, short or coiled tails, multiple tailed sperm with droplets or macrocephalic heads with droplets and/or multiple tails (Figs. 2a,c).

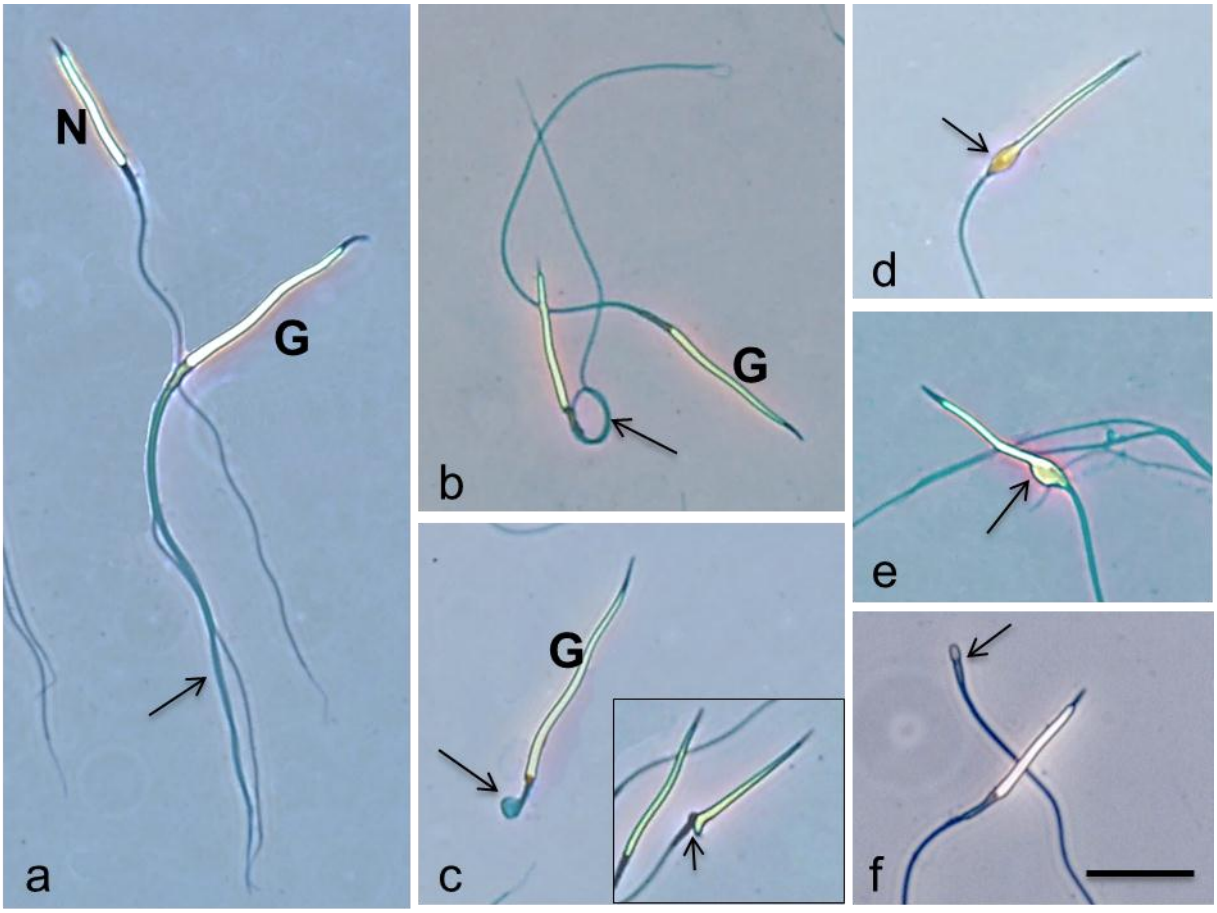

Figure 2. Light micrographs illustrating morphologically normal sperm (N) and various sperm defects. (a) Giant head sperm (G) with multiple tails (arrow); (b) Coiled sperm tail (arrow) and a macrocephalic sperm (G) with only one tail; (c) Macrocephalic sperm (G) with a short, curled tail; inset: abaxial tail implantation (arrow); (d) Cytoplasmic droplet covering the base of the nucleus and the midpiece (arrow); (e) Eccentrically positioned cytoplasmic droplet (arrow); (f) Acephalic sperm (arrow); Note the difference between this abnormality and the round-headed sperm in inset Fig. 1g. Bar = 10µm.

Discussion

Incidence of sperm defects

Conflicting information has been presented concerning the presence of abnormal sperm in avian semen. While Gee *et al*. (2004) noted that a variety of unusual sperm types are common in semen of some species, Blanco *et al*. (2009) reported that sperm pleomorphisms are uncommon in fresh semen samples. Abnormal sperm are commonly identified in ratite semen with the incidence ranging from approximately 5% (Rozenboim *et al*., 2003) to 17% (Hemberger *et al*., 2001) and 25% (Bertschinger *et al*., 1992) in the ostrich. A similar incidence of 13.6% abnormal sperm was observed in the emu (present study) although a much lower percentage of abnormalities (in the region of 2%) was reported by Malecki *et al*. (1998) in ejaculates of the same species. Alkan *et al*. (2002) recorded

a figure of 17% morphologically abnormal sperm in turkey semen. Rozenboim *et al*. (2003) and Bertschinger *et al*. (1992) both reported that more abnormal forms were detected in ostrich semen at the beginning of the breeding season with the least number of abnormalities being found mid-season. In the Northern pintail duck, the percentage normal sperm in semen samples collected mid-season is high (82.1%) (Penfold *et al*., 2000), which corresponds to the figure of 86% normal sperm obtained in the present study of emu samples collected in mid-season.

A more detailed discussion regarding the incidence and morphology of specific defects is presented in the relevant chapters.

Morphological classification of sperm defects

Various classification systems have been proposed for the morphological assessment of mammalian sperm (Blom, 1972; Barth & Oko, 1989; Menkveld et al., 1991; Saacke *et al*., 1994; Chenoweth, 2005; Mocé & Graham, 2008; Nöthling & Irons, 2008), and the importance of adopting a uniform (single) system for a specific species has been emphasised (Malmgren 1997; Card, 2005; Graham & Mocé 2005). Earlier classification systems identified primary and secondary sperm abnormalities (Blom, 1950) or divided anomalies into major or minor defects (Blom, 1972). A more modern concept is that of compensable or uncompensable sperm defects (Saacke *et al*., 1994). Further examples include the use of 'Tygerberg Strict Criteria' for assessing normal sperm morphology in humans (Menkveld *et al*., 1991), the identification of genetic sperm defects (Chenoweth, 2005) and the development of a multidimensional system for the recording and interpretation of sperm morphology in bulls (Nöthling & Irons, 2008).

Although criticism of some of the above classification systems has been expressed, each relies on the identification of specific sperm abnormalities and each presents a detailed list of observable anomalies, most of which have been thoroughly described by light microscopy supported by numerous ultrastructural studies. In contrast, the morphological classification of avian sperm abnormalities lacks uniformity and although the presence of abnormal sperm has been reported in a variety of bird species (Lindsay *et al*., 1999; Penfold *et al*., 2000; Klimowicz *et al*., 2005; Stelzer *et al*., 2005; Umapthy *et al*., 2005; Łukaszewicz *et al*., 2008; Siudzińska & Łukaszewicz, 2008; Tabatabaei *et al*., 2009), the anomalies are described in broad and variable terms which makes it difficult to draw meaningful comparisons. The lack of detailed descriptions of avian sperm abnormalities is compounded, with few exceptions (Marquez & Ogasawara, 1975; Bakst & Sexton 1979; Bakst, 1980; Ferdinand, 1992; Soley & Els, 1993; Soley *et al*., 1996), by a dearth of supportive ultrastructural data. This situation is clearly illustrated in ratites, where no uniform system for

classifying sperm abnormalities has been proposed. Bertschinger *et al*. (1992), for example, describe the most common major sperm defects in ostrich sperm as “mid-piece reflexes and coiled tails (‘Dag’ defects), partial or complete aplasia of the mitochondrial sheath, persistent cytoplasmic droplets and abnormally shaped heads”. Other studies on the ostrich simply note the incidence of abnormal sperm without providing descriptions of the defects (Hemberger *et al*., 2001; Rozenboim *et al*., 2003). Malecki *et al*. (1998) describe five types of sperm abnormalities in the emu, namely, bent, giant, broken, droplet and distorted, without defining the structural characteristics of the defects. It should be conceded that the adoption of a single uniform system for the classification of avian sperm defects or even ratite sperm defects is challenging. However, it would appear from the present study and a review of the relevant literature that a system based on the main morphologically identifiable segments of the sperm cell would be the most practical method. Based on observations from the present study, and information in the literature, it is tentatively proposed that the following morphological classification as set out in Table 2 be used to describe and categorise sperm defects in ratites.

As illustrated in Table 2, it is important to agree on a uniform terminology for the description of specific defects. For example, the specific form of head bending referred to as kinking (a single twist of the head) in the present study appears to be described as a ‘knotted’ head in studies of rooster sperm (Tabatabaei *et al*., 2009). More accurate descriptions of avian sperm abnormalities are required to definitively establish, for example, whether knotted heads and kinked heads are indeed synonymous. In the present study no acrosome defects were observed, neither are they mentioned in other studies of ratite sperm defects (Bertschinger *et al*., 1992; Malecki *et al*., 1998). However this should not invalidate the category of acrosome defects when studying ratite sperm as they may very well occur in

this group of birds. Likewise, the ‘Dag’ defect identified by Bertschinger *et al*. (1992) in ostrich semen is not specifically identified in other avian studies as a subdivision of either midpiece or tail abnormalities, although tail coiling has been described (Kamar & Rizik, 1972; Siudzińska & Łukaszewicz, 2008; Tabatabaei *et al*., 2009). Again, ultrastructural studies will be required to reveal the specific structural peculiarities that would define a particular form of tail coiling as the ‘Dag’ defect. There is little doubt that more defects will be added to each of the main categories in this list as further studies are conducted on ratite sperm.

Table 2. A proposed classification for ratite sperm abnormalities based on observations from the present study and documented information on ratites and other avian species.

CATEGORY	*REGION*	*SPECIFIC DEFECT*	*DESCRIPTION*
Head defects	**Acrosome**[1]	Detached	Acrosome missing[2,3]
		Deformed	Includes unusual shapes, such as small, knob-like, round or comma-shaped as well as swelling (also described as bulbous) of the acrosome[2,3,4]
	Nucleus	Bent	Any form or degree of bending of the nucleus, including looping, coiling, kinking and spiraling. Also referred to as knotted, twisted and hooked [2,3,5]
		Round head	Spherical-shaped nucleus, often reduced in size
		Macrocephalic	Head larger than the average; also described as giant, enlarged or large heads [5,6,7,8]
		Microcephalic	Head smaller than the average; also described as under-sized[8]
		Acephalic	Normal neck, midpiece and tail but no head. No detached heads observed in sample
		Detached head[1]	Total detachment of the head from the tail but associated with loose tails; also described as loose heads[2,3,9]
Tail defects	**Neck/midpiece**	Disjointed	The nucleus lies parallel to the midpiece but separated from the latter, with both components enclosed by the plasmalemma
		Abaxial	Misalignment of the centriolar complex relative to the head base
		Deformed[1]	Includes swelling, thickening, vacuolization and partial or complete aplasia of the mitochondrial sheath[2,3,4,9]
		Bent[1]	Includes varying degrees of bending, midpiece reflex or kinking in this region; also referred to as crooked- or broken-necked[2,3,9,10,11]
	Principal piece	Stump	Visibly shorter tail than normal[3]
		Multiflagellate	Two or more flagella present
		Coiled	Includes 'Dag' defect. Also referred to as curled, knotted, bent, rolled[4,8,9]
		Loose tail[1]	Total detachment of the tail from the head, in association with detached heads[2,3]
Cytoplasmic droplets			The presence of remnant cytoplasmic material; may cover the base of the nucleus, the midpiece or both regions
Multiple defects			Combination of two or more defects from different regions of the sperm

1. None observed in the present study, but described in other avian species; 2. Alkan *et al*., 2002; 3. Ferdinand, 1992; 4. Tabatabaei *et al*., 2009; 5. Kamar and Rizik, 1972; 6. Malecki *et al*., 1998; 7. Lindsay *et al*., 1999; 8. Stelzer *et al*., 2005; 9. Bertschinger *et al*., 1992; 10. Saeki, 1960; 11. Humphreys, 1972

This chapter attempts to consolidate the disparate descriptions and terminology used to describe abnormal sperm in birds into a uniform system for the recording of ratite sperm defects. The work also underlines the importance of detailed morphological descriptions of abnormal avian sperm as an essential prerequisite for the accurate placement of specific sperm defects in appropriate categories. This information may be of value in the application of reproduction techniques such as AI, both for

breeding and raising commercially important birds and for the conservation of rare species (Malecki *et al*., 2008; Lindsay *et al*., 1999; Blanco *et al*., 2009).

References

Alkan, S., Baran, A., Özdaş, Ö B. & Evecen, M. (2002) Morphological defects in turkey semen. *Turkish Journal of Veterinary and Animal Science* **26**, 1087-1092.

Asa, C., Phillips, D.M. & Stover, J. (1986) Ultrastructure of spermatozoa of the crested tinamou. *Journal of Ultrastructure and Molecular Structure Research* **94**, 170-175.

Baccetti, B., Burrini, A.G. & Falchetti, E. (1991) Spermatozoa and relationships in paleognath birds. *Biolology of the Cell* **71**, 209-216.

Bakst, M.R. (1980) Fertilizing capacity and ultrastructure of fowl and turkey spermatozoa in hypotonic extender. *Journal of Reproduction and Fertility* **60**, 121-127.

Bakst, M.R. & Sexton, T.J. (1979) Fertilizing capacity and ultrastructure of fowl and turkey spermatozoa before and after freezing. *Journal of Reproduction and Fertility* **55**, 1-7.

Barth, A.D. (1989) Abaxial tail attachment of bovine spermatozoa and its effect on fertility. *Canadian Veterinary Journal* **30**, 656-662.

Barth, A.D. & Oko, R.J. (1989) Abnormal Morphology of Bovine Spermatozoa. Iowa State University Press, Ames.

Bertschinger, H.J., Burger, W.P., Soley, J.T. & de Lange, J.H. (1992) Semen collection and evaluation of the male ostrich. *Proceedings of the Biennial Congress of the South African Veterinary Association,* pp. 154-158.

Blanco, J.M., Wildt, D.E., Höfle, U., Voelker, W. & Donoghue, A.M. (2009) Implementing artificial insemination as an effective tool for *ex situ* conservation of endangered avian species. *Theriogenology* **71**, 200-213.

Blom, E. (1950) A simple rapid staining method for the differentiation between live and dead sperm cells by means of eosin and nigrosin. *Nordisk Veterinaer Medicin* **2**, 58-61.

Blom, E. (1966) A new sterilizing and hereditary defect (the ‘Dag’ defect) located in the bull sperm tail. *Nature* **209**, 739-740.

Blom, E. (1972) The ultrastructure of some characteristic sperm defects and a proposal for a new classification of the bull spermiogram. *Atti del VII Simposia Internationale de Zootechnia*, pp. 125-139.

Blom, E. & Birch-Andersen, A. (1970) Ultrastructure of the decapitated sperm defect in Guernsey bulls. *Journal of Reproduction and Fertility* **23**, 67-72.

Card, C. (2005) Cellular associations and the differential spermiogram: Making sense of stallion spermatozoal morphology. *Theriogenology* **64**, 558-567.

Chemes, H.E., Puigdomenech, E.T., Carizza, C., Brugo Olmedo, S., Zanchetti, F. & Hermes, R. (1999) Acephalic spermatozoa and abnormal development of the head-neck attachment: a human syndrome of genetic origin. *Human Reproduction* **14**, 1811-1818.

Chenoweth, P.J. (2005) Genetic sperm defects. *Theriogenology* **64**, 457-468.

Deeming, D.C. & Ar, A. (1999) Factors affecting the success of commercial incubation. In: Deeming, D.C. (ed.) The Ostrich. Biology, Production and Health, CABI Publishing, Oxon, pp. 159-190.

Dowsett, K.F., Osborne, H.G. & Pattie, W.A. (1984) Morphological characteristics of stallion spermatozoa. *Theriogenology* **22**, 463-471.

Feito, R.J. (1990) Ultrastructural study of abnormal spermiogenesis in four hystricognate rodents. *Journal of Reproduction and Fertility* **88**, 411-418.

Ferdinand, A. (1992) Licht- und elektronenmikroskopische Untersuchungen zur Morphologie von Ganterspermatozoen. Ph.D Thesis, University of Veterinary Medicine, Hannover.

Gee, G.F., Bertschinger, H., Donoghue, A.M., Blanco, J. & Soley, J.T. (2004) Reproduction in nondomestic birds: Physiology, semen collection, artificial insemination and cryopreservation. *Avian and Poultry Biology Reviews* **15**, 47-101.

Graham, J.K. & Mocé, E. (2005) Fertility evaluation of frozen/thawed semen. *Theriogenology* **64**, 492–504.

Hemberger, M.Y., Hospes, R. & Bostedt, H. (2001) Semen collection, examination and spermiogram in ostriches. *Reproduction in Domestic Animals* **36**, 241-243.

Holstein , A.F., Roosen-Runge, E.C. & Schirren, C. (1988) Illustrated pathology of human spermatogenesis. Grosse Verlag, Berlin.

Humphreys, P.N. (1972) Brief observations on the semen and spermatozoa of certain passerine and non-passerine birds. *Journal of Reproduction and Fertility* **29**, 327–336.

Jainudeen, M.R., Bongso, T.A. & Dass, S. (1982) Semen characteristics of the swamp buffalo (*Bubalus bubalis*). *Animal Reproduction Science* **4**, 213-217.

Jamieson, B.G.M. (2007) Avian spermatozoa: Structure and Phylogeny. In: Jamieson, B.G.M. (ed.) Reproductive Biology and Phylogeny of Birds Part A, Science Publishers, Jersey, pp. 349-511.

Kamar, G.A.R. & Badreldin, A.L. (1959) Sperm morphology and viability. *Acta Anatomica* **39**, 81-83.

Kamar, G.A.R. & Rizik, M.A.A. (1972) Semen characteristics of two breeds of turkeys. *Journal of Reproduction and Fertility* **29**, 317-325.

Klimowicz, M., Łukaszewicz, E. & Dubiel, A. (2005) Effect of collection frequency on quantitative and qualitative characteristics of pigeon (*Columba livia*) semen. *British Poultry Science* **46**, 361-365.

Kopp, C., Sukura, A., Tuunainen, E., Gustavsson, I., Parvinen, M. & Anderson, M. (2007) Multinuclear-multiflagellar sperm defect in a bull – a new sterilizing sperm defect. *Reproduction in Domestic Animals* **42**, 208-213.

Lindsay, C., Staines, H.J., McCormick, P., McCullum, C., Choulani, F. & Wishart, G.J. (1999) Variability in the size of the nucleus in spermatozoa from the Houbara bustards, *Chlamydotis undulate undulate*. *Journal of Reproduction and Fertility* **117**, 307-313.

Łukaszewicz, E., Jerysz, A., Partyka, A. & Siudzińska, A. (2008) Efficacy of evaluation of rooster sperm morphology using different staining methods. *Research in Veterinary Science* **85**, 583-588.

Malecki, I.A., Cummins, J.M., Martin, G.B. & Lindsay, D.R. (1998) Effect of collection frequency on semen quality and the frequency of abnormal forms of spermatozoa in the emu. *Animal Production in Australia* **22**, 406.

Malecki, I.A., Beesley, J. & Martin, G.B. (2000) Changes in the characteristics of emu sperm with season. *British Poultry Science Supplement* **41,** S18.

Malecki, I.A., Rybnik, P.K. & Martin, G.B. (2008) Artificial insemination technology for ratites: a review. *Australian Journal of Experimental Agriculture* **48**, 1284-1292.

Malmgren, L. (1997) Assessing the quality of raw semen: a review. *Theriogenology* **48**, 523-530.

Maretta, M. (1975) Structural abnormalities in the middle piece of the drake's spermatozoon tail. *Acta Veterinaria Brno **25**, 245-250.*

Maretta, M. (1979) Ultrastructure of double and multiple sperm tails in drakes. *Veterinarni Medicina* **24**, 679-689.

Marquez, B.J. & Ogasawara, F.X. (1975) Scanning electron microscope studies of turkey semen. *Poultry Science* **54**, 1139-1143.

Marvan, F., Rob, O. & Janeckova, E. (1981) Classification of morphological abnormalities of gander sperm. *Zuchthygiene* **16**, 176-183.

Menkveld, R., Swanson, R.J., Oettlé, E.E., Acosta, A.A., Kruger, T.F. & Oehninger, S. (1991) Atlas of Human Sperm Morphology. Williams & Wilkins, Baltimore.

Mocé, E. & Graham, J.K. (2008) *In vitro* evaluation of sperm quality. *Animal Reproduction Science* **105**, 104-118.

Morton, D.B. & Bruce, S.G. (1989) Semen evaluation, cryopreservation and factors relevant to the use of frozen semen in dogs. *Journal of Reproduction and Fertility Supplement* **39**, 311-316.

Nöthling, J.O. & Irons, P.C. (2008) A simple multidimensional system for the recording and interpretation of sperm morphology in bulls. *Theriogenology* **69**, 603-611.

Oettlé, E.E. & Soley, J.T. (1988) Sperm abnormalities in the dog: a light and electron microscopic study. *Veterinary Medical Review* **59**, 28-70.

Pant, H.C., Mittal, A.K., Patel, S.H., Shukla, H.R., Kasiraj R., Prabhakar, J.H. & Barot, L.R. (2002) Abaxial sperm tails and fertility in the buffalo bull. *Indian Journal of Animal Science* **72**, 314-315.

Penfold, L.M., Wildt, D.E., Herzog, T.L., Lynch, W., Ware, L., Derrickson, S.E. & Monfort, S.L. (2000) Seasonal patterns of LH, testosterone and semen quality in the Northern pintail duck (*Anas acuta*). *Reproduction Fertility and Development* **12**, 229-235.

Phillips, D.M. & Asa, C.S. (1989) Development of spermatozoa in the rhea. *Anatomical Record* **223**, 276-282.

Rozenboim, I., Navot, A., Snapir, N., Rosenstrauch, A., El Halawani, M.E., Gvaryahu, G. & Degen, A. (2003) Method for collecting semen from the ostrich (*Struthio camelus*) and some of its quantitative and qualitative characteristics. *British Poultry Science* **44**, 607–611.

Saacke, R.G., Nadir, S. & Nebel, R.L. (1994) Relationship of semen quality to sperm transport, fertilization, and embryo quality in ruminants. *Theriogenology* **41**, 45-50.

Saeki, Y. (1960) Crooked-ncked spermatozoa in relation to low fertility in the artificial insemination of fowl. *Poultry Science* **39**, 1354-1360.

Sarlós, P., Wekerle, L. & Nagy, Z. (1990) Relationship of fertility with tail implantation in boar spermatozoa. *Reproduction in Domestic Animals* **25**, 87-89.

Siudzińska, A. & Łukaszewicz, E. (2008) Effect of semen extenders and storage time on sperm morphology of four chicken breeds. *Journal of Applied Poultry Research* **17**, 101-108.

Stelzer, G., Crosta, L., Bürkle, M. & Krautwald-Junghanns, M-E. (2005) Attempted semen collection using the massage technique and semen analysis in various psittacine species. *Journal of Avian Medicine and Surgery* **19**, 7-13.

Soley, J.T. (1993) Ultrastructure of ostrich (*Struthio camelus*) spermatozoa: I. Transmission electron microscopy. *Onderstepoort Journal of Veterinary Research* **60**, 119-130.

Soley, J.T. (1997) Nuclear morphogenesis and the role of the manchette during spermiogenesis in the ostrich (*Struthio camelus*). *Journal of Anatomy* **190**, 563-576.

Soley, J.T. & Els, H.J. (1993) The ultrastructure of retained cytoplasmic droplets in ostrich spermatozoa. *Proceedings of the Microscope Society of Southourn Africa* **23**, 58.

Soley, J.T., Bertschinger, H.J., Els, H.J. & Burger, W.P. (1996) The morphology and incidence of retained cytoplasmic droplets in ostrich spermatozoa. In: Deeming, D.C. (ed.) Improving our Understanding of Ratites in a Farming Environment, Ratite Conference, Manchester, pp. 16-18.

Soley, J.T. & Groenewald, H.B. Reproduction. (1999) In: Deeming, D.C. (ed.) The Ostrich. Biology, Production and Health, CABI Publishing, Oxon, pp. 129-158.

Soley, J.T. & Roberts, D.C. (1994) Ultrastructure of ostrich (*Struthio camelus*) spermatozoa: II. Scanning electron microscopy. *Onderstepoort Journal of Veterinary Research* **61**, 239-246.

Tabatabaei, S., Batavani, R.A. & Talebi, A.R. (2009) Comparison of semen quality in indigenous and ross broiler breeder roosters. *Journal of Animal and Veterinary Advances* **8**, 90-93.

Tabatabaei, S., Chaji, M. & Mohammadabadi, T. (2010) Correlation between age of rooster and semen quality in Iranian indigenous broiler chickens. *Journal of Animal and Veterinary Advances* **9**,195-198.

Umapathy, G., Sontakke, S., Reddy, A., Ahmed, S. & Shivaji, S. (2005) Semen characteristics of the captive Indian white-backed vulture. *Biology of Reproduction* **73**, 1039-1045.

Wakely W.J. & Kosin, I.L. (1951) A study of the morphology of the turkey spermatozoa–with special reference to the seasonal prevalence of abnormal types. *American Journal of Veterinary Research* **12**, 240-245.

Weissenberg, R., Aviram, A., Golan, R., Lewin, L.M., Levron, J., Madgar, I., Dor, J., Barkai, G. & Goldman, B. (1998) Concurrent use of flow cytometry and fluorescence in-situ hybridization techniques for detecting faulty meiosis in a human sperm sample. *Molecular Human Reproduction* **4**, 61-68.

Zini, A., Phillips, A., Courchesne, A., Boman, J.M., Baazeem, A., Bissonnette, F., Kadoch, I.J. & San Gabriel, M. (2009) Sperm head morphology is related to high deoxyribonucleic acid stainability assessed by sperm chromatin structure assay. *Fertility and Sterility* **91**, 2495-2500.

Zuleta, M., Koefoed-Johnsen, H.H. & Bresciani, J. (1978) The Dag defect of the tail of the bull spermatozoon. Observations with the scanning electron microscope. Yearbook of the Royal Veterinary and Agricultural University, Copenhagen, pp. 21-26.

Chapter 6 Morphology and origin of abnormal sperm I: Head-base bending and disjointed sperm

Introduction

Avian sperm defects, in particular those of poultry, have been extensively studied. Although some ultrastructural descriptions of abnormal avian sperm have been provided by scanning (Marquez & Ogasawara, 1975; Bakst & Sexton, 1979; Hess *et al.*, 1986; Maeda *et al*., 1986) and transmission electron microscopy (Bakst & Sexton, 1979; Maretta, 1979; Froman & Bernier, 1987; Ferdinand, 1992), most information on this topic stems from light microscopic observations. The paucity of corroborative ultrastructural data and the resultant lack of critical appraisal of avian sperm defects have led to the use of disparate and often confusing terminology for their classification.

Of the various defects identified in non-passerine birds, bending of the filiform avian spermatozoon appears to be a common anomaly and various terms have been used to describe and categorize this defect. Some authors have adopted a generalized approach and simply refer to head, midpiece and tail (flagellum) bends (Hess *et al.*, 1986; Ferdinand, 1992; Penfold *et al.*, 2000), while others qualify the degree of bending, recognizing 90° and 180° head and tail bends as well as midpiece bending (Alkan *et al.*, 2002; Tabatabaei *et al*., 2009, 2010). Other descriptions of bending are more specific and define the precise area where the bend occurs. Bakst and Sexton (1979), for example, use the term “bent spermatozoa” to describe “those in which the head was reflexed at the neck, midpiece or distal aspect of the nucleus”. This description was later extended to include the proximal part of the principal piece and further defined as an acute flexion of the tail bringing it adjacent and parallel to the head (Bakst, 1980). This anomaly was particularly evident in sperm subjected to adverse osmotic conditions, temperature variations and different storage times (Saeki, 1960; Van Wambeke, 1972; Yamane, 1972; Bakst & Sexton, 1979; Bakst 1980; Maeda *et al.*, 1984, 1986; Bozkurt *et al*., 1998; Siudzińska & Łukaszewicz, 2008). Earlier literature referred specifically to bent necks where the head was typically observed to lie back along the tail. This anomaly was originally described by Saeki (1960) as crooked–necked sperm, the term being defined by Maeda *et al.* (1984) as an acute bend in the neck region or anywhere along the length of the midpiece. Various terms such as “broken-necked”, “bent-neck” and “neck-bending” have also been used and this defect has been described, but not always defined, in a number of avian species including the fowl, duck, goose,

turkey, partridge, Japanese quail and parrots (Humphreys, 1972; Van Wambeke, 1972; Bozkurt *et al*., 1998; Steltzer *et al*., 2005; Patryka *et al*., 2007; Chelmońska *et al*., 2008; Łukaszewicz *et al*., 2008).

Although little attention has been given in the literature to the description of sperm anomalies in ratites, bending also appears to be a common defect in this commercially important group of birds. Reporting on the incidence of abnormal sperm in the emu, Malecki *et al*. (1998) provide a category for "bent sperm" without defining the term whereas Góes *et al*. (2010) simply report that bent heads, folded tails and strongly folded tails are observed in the rhea. Midpiece reflexes have been described in the ostrich (Bertschinger *et al*., 1992; Irons *et al*., 1996) and Soley *et al.* (1996) reported an association between cytoplasmic droplets and bent tails in the same species. In a recent study of abnormal sperm in the emu it was noted that the majority of defects occurred at the base of the head and in the neck region. The head-base defects exclusively involved varying degrees of bending as well as looping and kinking of the nucleus, whereas in the neck region a defect referred to as "disjointed sperm" and which superficially resembled a form of "bending" was displayed (Du Plessis & Soley, 2011).

In order to fully understand the distinction between head-base bending and "bending" in the neck region (disjointed sperm) in the emu, this chapter provides a comprehensive, comparative morphological description of the two defects utilizing both light and electron microscopy. The incidence of the two defects is presented but as this study focused on establishing a morphological basis for the accurate assessment of the defects using abattoir material, functional data detailing the possible effects of the anomalies on fertility, although speculated on, are not provided. The results are compared with relevant information in the literature on avian sperm defects and definitive terminology is suggested for the two abnormalities in order to eliminate the confusing terminology currently in use. This study also provides previously unreported ultrastructural data relevant for future descriptions and comparisons of sperm defects in non-passerine birds.

Materials & Methods

Semen samples were collected from 15 sexually mature and active emus within 30 min of slaughter at a commercial abattoir. The birds ranged in age from 2 to 4 years. Droplets of semen were gently squeezed from the distal *ductus deferens* directly into 2.5% glutaraldehyde in 0.13M Millonig's

phosphate buffer, pH 7.4 at room temperature. Thin smears for light microscopy were made from the fixed semen samples and stained with Wright's stain (Rapidiff®, Clinical Sciences Diagnostics, Johannesburg, South Africa) before viewing with a 100x oil immersion lens using both bright field and phase contrast microscopy (see Chapter 2). Smears were also stained with the Feulgen stain and acidic aniline blue according to the methods described by Vieytes *et al.* (2008) to evaluate the degree of chromatin condensation. The incidence of the two defects was determined by examining the smears using a 100x oil immersion objective and counting the number of abnormal spermatozoa present in a total of 300 cells for each bird. The incidence is expressed as a percentage of the total cell count. Due to unforeseen circumstances, the incidence was only calculated in 14 birds.

Semen samples were prepared for scanning and transmission electron microscopy as previously described (see Chapter 2), while small blocks of testicular material were also collected and processed for transmission electron microscopy as described in Chapter 3.

Results

Light Microscopy (LM)

Head-base bends and disjointed sperm were observed in all samples and could be readily distinguished using both bright field (Figs. 1a,c) and phase contrast (Figs. 1b,d) microscopy. However, phase contrast microscopy resolved the differences between the two defects more clearly. A total of 13.6% abnormal sperm were detected in the animals studied of which head-base bending and disjointed sperm represented 3.8% and 1.9% of the total cell count, respectively. The incidence of the defects in individual birds is shown in Figure 2.

Head-base bending typically involved a 180° bend at the base of the nucleus which placed the head and midpiece (and in some instances part of the principal-piece) into close apposition and parallel to each other. A few intermediate forms were observed. No part of the neck or midpiece was involved and bending was restricted exclusively to the base of the nucleus (Figs. 1a,b). The free aspect of the bend (essentially the anterior aspect of the defective sperm) presented a typically rounded profile with nuclear material clearly visible at both ends of the bend (Figs. 1a,b). The principal-piece was often angled across the sperm head (Fig. 1a).

Disjointed sperm displayed some of the characteristics of head-base bending, notably, an apparently 180° reflex of the tail, parallel alignment of the head and midpiece, and angling of the principal-piece

across the sperm head (Figs. 1c,d). The most striking difference, however, was the obvious disconnection of the head and tail at the head/tail interface resulting in the neck and base of the nucleus lying next to and level with each other. This arrangement produced a straight profile (Fig. 1c) in contrast to the rounded profile typical of head-base bending. The neck was occasionally positioned posterior to the nuclear base creating a staggered appearance or the impression that both components were completely separated (Fig. 1e). However, SEM and TEM confirmed that in both defects the parallel-aligned head and neck/midpiece remained firmly attached (see below).

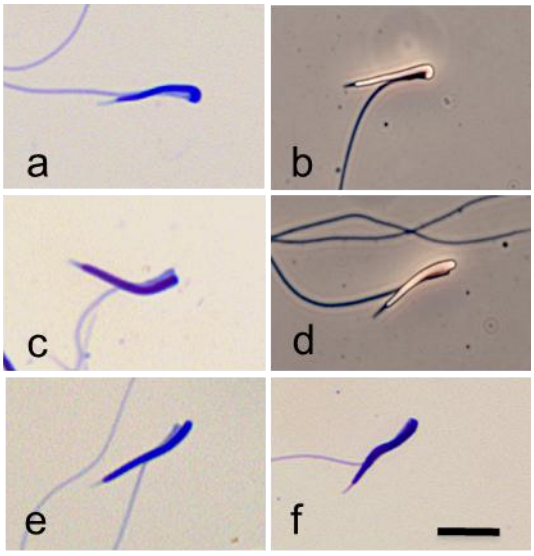

Figure 1. Light microscopy of Wright's-stained smears. Head-base bending illustrated by bright field microscopy (a) and phase contrast microscopy (b). Note the rounded profile of the bend, the presence of nuclear material on both sides of the bend and the lack of involvement of the neck or midpiece. Disjointed heads revealed by bright field microscopy (c) and phase contrast microscopy (d). Note the straight profile of the parallel-aligned neck and nuclear base in (c) and the staggered appearance in (d). (e) A disjointed sperm showing a staggered orientation of the head and neck/midpiece, creating the erroneous impression of complete separation of the head and tail. (f) A presumptive disjointed sperm. As the nucleus lies on top of the midpiece obscuring their relationship, it is difficult to accurately classify the defect. (e) and (f) bright field microscopy. Bar = 10µm.

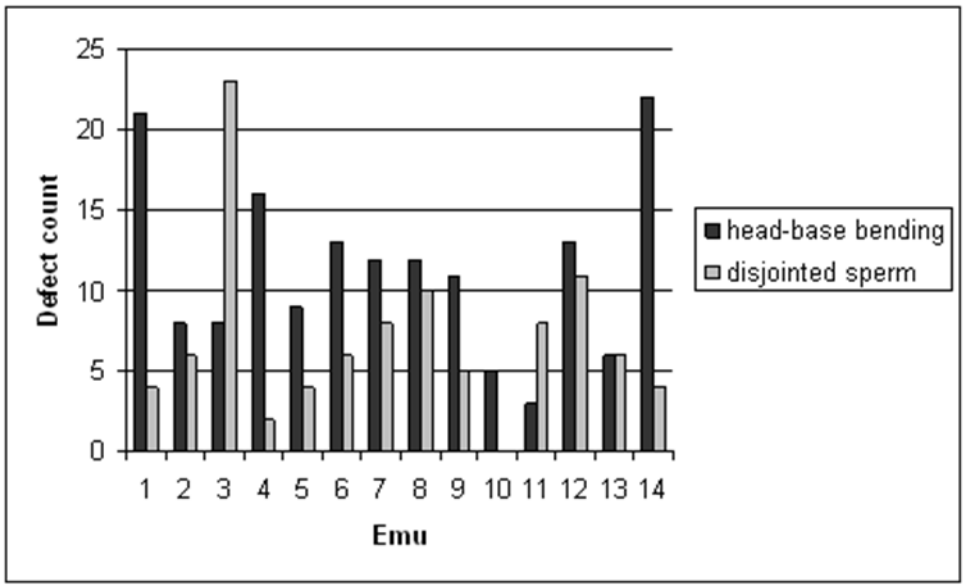

Figure 2. Histogram showing the incidence of head-base bending and disjointed sperm in each of the 14 birds studied. Each bar represents the number of defective cells observed in a total of 300 cells counted. Cell counts were obtained from smears stained with Wright's stain.

No loose heads or tails were observed in the smears. Occasionally the orientation of the sperm head relative to the neck/midpiece made it difficult to accurately distinguish between the two defects (Fig. 1f). In such instances scoring of the defect depended on the experience of the observer although this involved a degree of subjectivity.

The use of specialized stains (Feulgen and acid aniline blue) to indicate the possible role of defective chromatin condensation in the formation of the defects produced inconclusive results. Feulgen staining of the emu sperm was weak and the nuclei exhibited a uniform light pink staining reaction with no indication of localized loss of the dye. Acid aniline blue staining produced more graphic, yet inconsistent results. Most cells (normal morphology) appeared pale indicating no uptake of the dye (i.e. normal chromatin condensation). However, some spermatozoa with head-base bending showed localized accumulation of the dye indicating a lack of chromatin condensation, while others remained unstained.

Scanning Electron Microscopy (SEM)

SEM confirmed the basic structural features of the two defects seen on LM. It was also clear using this technique that only the base of the nucleus was involved in the formation of head-base bending, and that the neck and midpiece remained unaffected (Fig. 3a). Disjointed sperm again revealed complete separation of the neck and head-base, with both structures lying parallel and level with each other (Figs. 3b,d) or staggered (Fig. 3c). It was sometimes possible to observe a shallow concavity at the base of the head indicating the implantation fossa, thus suggesting that separation of the neck from the head occurred at the connecting piece (Fig. 3d). In both defects the midpiece and head appeared to be attached to each other by a membrane and the principal piece of the tail was often seen to lie at an angle across the sperm head (Figs. 3a-d).

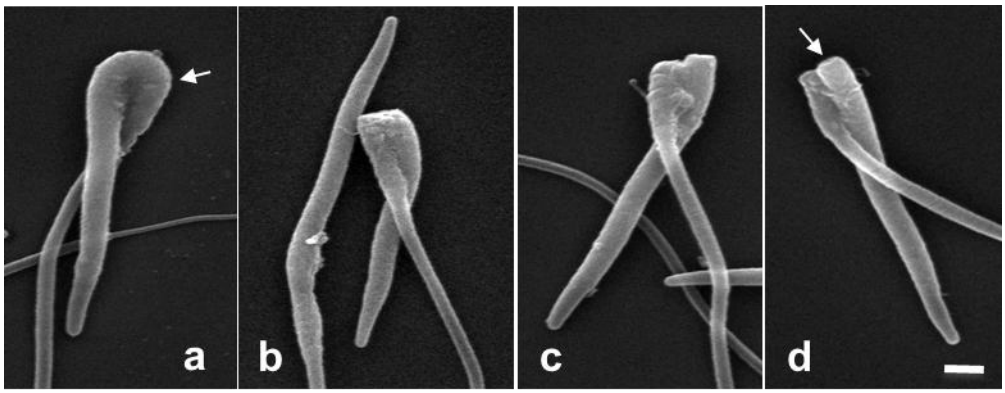

Figure 3. Scanning electron micrographs of defective sperm showing head-base bending (a) and disjointed heads (b-d). In (a) the position of the nuclear/midpiece junction is indicated by an arrow. The midpiece and head appear to be attached by a membrane. Note the hollow (arrow) indicating the implantation fossa in (d). The disjointed sperm illustrated in Figs. 3b, d and in Fig. 3c are similar to those shown in Fig. 1c and Fig. 1e, respectively. Bar = 1µm.

Transmission Electron Microscopy (TEM)

In addition to the obvious morphological characteristics of the defects defined by LM and SEM, TEM revealed a number of significant structural peculiarities which further differentiated head-base bending (Fig. 4) from disjointed sperm (Fig. 5). In heads bent at the base, TEM clearly demonstrated the presence of nuclear material on both sides of the bend. The nuclear chromatin in the vicinity of the bend was generally incompletely condensed, with variably-sized gaps filled with flocculent or granular material and occasional thread-like strands occurring in the karyoplasm. These gaps were generally positioned at the convex surface of the bend (Figs. 4a-d) and in most instances extended into both legs of the bend. Despite the acute bending of the nuclear base, the nucleus always remained firmly attached to the basal plate lining the implantation fossa. In some defective cells a lack of karyoplasm at the base of the nucleus created the erroneous impression of nuclear detachment. Although such cells superficially resembled disjointed sperm, they technically represented a form of head-base bending as the nuclear membrane was still firmly attached to the connecting piece (Figs. 4e,f). The region of contact between the head (nucleus) and the neck/midpiece resulting from the bend was enclosed as a unit by the plasmalemma (Figs. 4a-e, 6). Except for the absence of the plasmalemma on the surface apposed to the head, the structural elements of the neck and midpiece appeared normal. The nucleus and centriolar complex were always separated by the *pars spiralis* mitochondria of the midpiece.

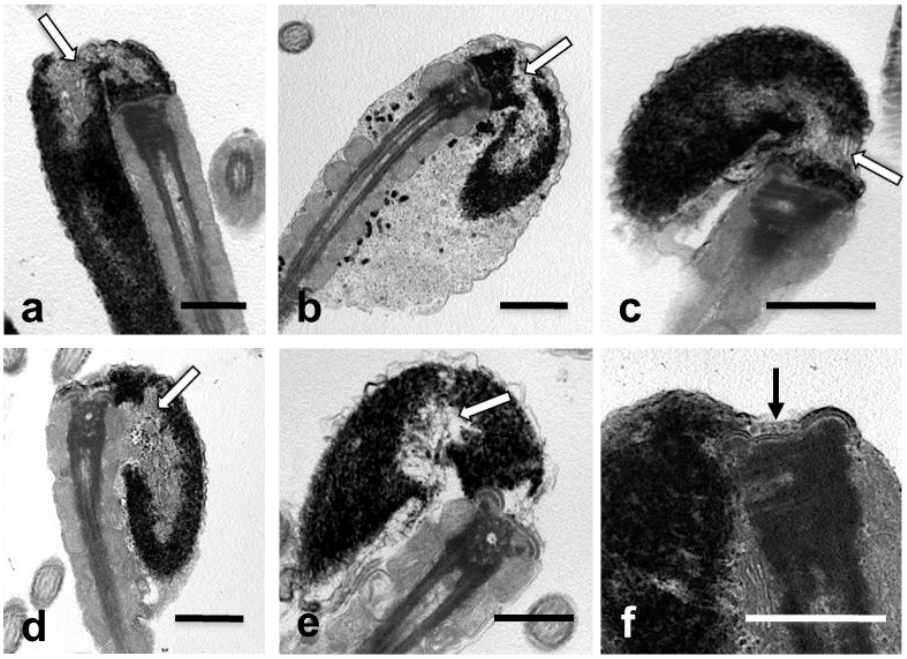

Figure 4. Transmission electron micrographs showing various forms of nuclear base bending. (a-e) Regions of incompletely condensed chromatin (white arrows) are present in the vicinity of the bend. (f) One leg of the nuclear bend (arrow) is represented only by the nucleolemma enclosing a few chromatin granules. Bar = 0.5um.

As indicated by SEM, longitudinal sections of disjointed sperm (Fig. 5) showed complete separation of the neck from the head-base at the level of the connecting piece. A thin layer of moderately electron-dense material representing the basal plate and possibly elements of the capitellum remained associated with the implantation fossa (Fig. 5a). The segmented columns (poorly developed in non-passerine birds) of the connecting piece and the enclosed proximal centriole remained associated with the proximal aspect of the midpiece. The structure of the connecting piece and the proximal centriole appeared normal. In most instances the disjointed nucleus appeared fully condensed (Fig. 5b), but occasional defective cells displaying zones of incomplete chromatin condensation were observed (Fig. 5a). As with head-base bending, the region of contact between the disjointed nucleus and the midpiece was contained as a unit within the plasmalemma even in sperm displaying a staggered arrangement of the head and neck/midpiece (Fig. 5c). This phenomenon was particularly obvious in transverse sections of this region, although it was not possible to determine whether such sections represented head-base bending or disjointed sperm (Fig. 6). TEM also revealed intermediate stages in the development of disjointed sperm with some cells displaying a tenuous, mal-aligned connection between the rim of the implantation fossa and the connecting piece (Fig. 5d).

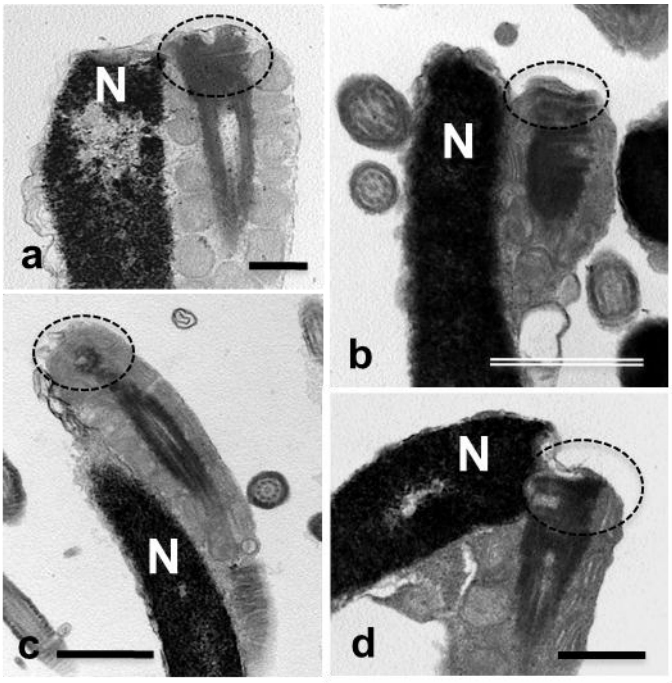

Figure 5. Disjointed sperm. (a,b) Typical forms of the defect. Note the complete separation of the connecting piece (encircled) from the nuclear base (N). (c) Staggered form. (d) Intermediate form of the defect. Bar = 0.5µm.

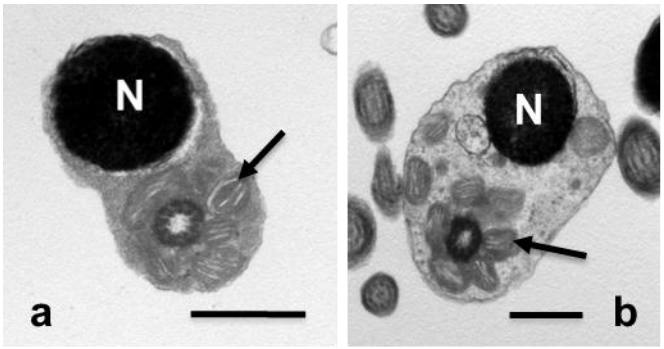

Figure 6. (a,b) Transverse sections of head-base bending or disjointed sperm. Note the parallel arrangement of the nucleus (N) and midpiece (arrows). The plasmalemma collectively surrounds both structures. Bar = 0.5µm.

Both defects were observed by TEM in the testicular material. Isolated sperm demonstrating head-base bending were randomly scattered in the testis parenchyma (Fig. 7a). These cells showed the typical characteristics described in defective sperm from the *ductus deferens*. In all instances a lack of chromatin condensation was again observed in the region of the bend (Fig. 7b). Intermediate forms of disjointed sperm were also seen in the testis (Fig. 8), clearly indicating the misalignment of the head and neck region (compare with Fig. 5d).

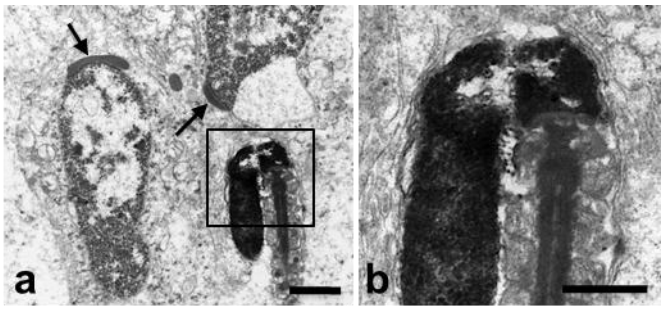

Figure 7. (a) Section of the testis parenchyma revealing a cell with head-base bending (square) positioned near two early elongating spermatids (arrows). Bar = 1µm. The area within the square is enlarged in (b). Note the similarity to the cells illustrated in Fig. 4. Bar = 0.5µm.

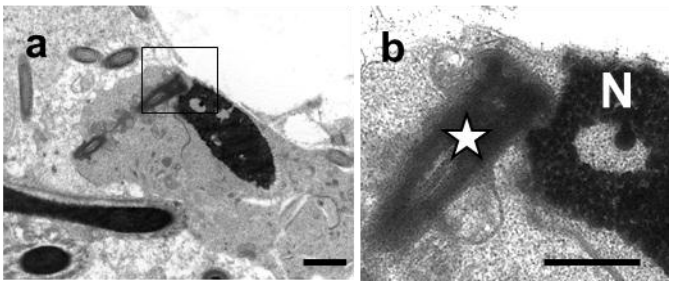

Figure 8. (a) An intermediate form of a disjointed sperm in the testis. The area within the square is enlarged in (b) and shows misalignment of the nucleus (N) and flagellum (star). Bar (a) =1µm; Bar (b) = 0.5µm.

Discussion

The present study indicated that when assessing emu sperm morphology a clear distinction should be made between head-base bending, which represents a true form of bending, and disjointed sperm which, although resembling bending, represents a separate sperm anomaly. The available literature on avian sperm abnormalities does not differentiate between the two defects despite the fact that micrographs and illustrations in a number of papers appear to portray disjointed sperm as well as sperm bent at the head-base. These defects are generally grouped using generic terminology such as “crooked-necked sperm” and “bent sperm”. For example, Bakst and Sexton (1979) illustrate a typical example of head-base bending as well as what appears to be a disjointed sperm, describing both as “bent spermatozoa”. Maeda *et al.* (1986) demonstrate sperm acutely bent at the neck region, at any point along the midpiece, and at the head-base, referring to them collectively as crooked-necked sperm. The sketches by Saeki (1960) of crooked-necked sperm can in fact be interpreted as head-base bending and disjointed sperm, respectively. Failure to recognize specific sperm defects can be attributed to the continuing use of established, inappropriate descriptive terminology coupled with a lack of accurate descriptions of avian sperm anomalies. The situation is further complicated by a dearth of supporting ultrastructural information on avian sperm defects.

Avian sperm appear prone to bending, especially in the region encompassing the base of the head, neck, midpiece and the adjacent segment of the principal piece (Bakst, 1980). A number of studies have reported on the fragility of the neck region of poultry sperm, which makes this region susceptible to damage (Lake, 1954; Saeki, 1960; Van Wambeke, 1972; Yamane, 1972; Bakst & Sexton, 1979; Bakst, 1980; Maeda *et al*., 1986; Alkan *et al*., 2002), particularly when the cells are exposed to adverse physiological influences. Various external factors such as osmolarity, storage time and temperature have been implicated in sperm bending (Saeki, 1960; Yamane, 1972). However, the present study utilized semen from the *ductus deferens* which, barring the possible effects of glutaraldehyde fixation, would not have been influenced by potentially damaging external factors. Possible temporal and temperature effects inherent in the sampling procedure, should possibly also be considered.

Head bending in the emu was, with few exceptions, confined to the base of the head (Du Plessis & Soley, 2011) and was associated with apparent incomplete chromatin condensation in the vicinity of the bend. The areas of incomplete condensation were generally positioned towards the outside of the bend and displayed coarse granules and intervening spaces, similar to regions of uncondensed chromatin described in mammalian sperm (Zamboni, 1992; Dadoune, 1995; Chemes & Rawe, 2003).

This phenomenon is considered to be a morphological manifestation of chemical or molecular abnormalities in the condensation process (Zamboni, 1992; Dadoune, 1995; D'Occhio *et al*., 2007) resulting in single stranded DNA being formed as opposed to the more stable double stranded form. The nucleus is therefore more fragile (Chemes & Rawe, 2003) and as these results suggest, would make it more prone to bending. Attempts to consistently demonstrate incomplete chromatin condensation at the LM level with acid aniline blue and Feulgen stains were unsuccessful. Santiago-Moreno *et al*. (2009) similarly reported inconclusive results with the aniline blue stain when used to predict fertility in roosters.

Disjointed sperm clearly represent a separate anomaly which is characterized by the distinct separation of the nuclear base and connecting piece within the confines of the plasmalemma. An anomaly referred to as "dislocated" sperm and displaying similar morphological features to those reported in the present study, has been reported in epididymal sperm in mice (Mochida *et al*., 1999). It was speculated that this defect resulted from structural deficiencies and/or deficiencies in the assembly of peri-axonemal proteins, causing the dislocation of the segmented columns of the connecting piece from the nuclear attachment sites. A number of other mammalian sperm defects, such as acephalic sperm, decapitated sperm and the flexed head defect, are believed to originate from eccentric implantation of the head and neck, or structural deficiencies of the neck region (Zamboni, 1992). Similarly Chemes and Rawe (2003, 2010) reported on sperm with misaligned head-midpiece junctions, stating that different degrees of incorrect alignment results in either acephalic sperm (the most severe form of the defect) or sperm where the head is misaligned. They further ascribed the misalignment to the lack or abnormal implantation of the centrioles during the early stages of spermiogenesis. In the emu, all structural elements in the neck region appeared to be present and morphologically normal, although the connecting piece was not correctly related to the implantation fossa. This would appear to indicate failure of the connecting piece to establish proper contact with the head-base during spermiogenesis. The extremely shallow implantation fossa in this species may further compound this problem. Based on the above observations (Zamboni, 1992; Mochida *et al*., 1999; Chemes & Rawe, 2010), it is proposed that disjointed sperm are closely related to dislocated, flexed, decapitated and acephalic sperm as described in mammals.

Although the two defects can generally be distinguished by LM, a small proportion of abnormal cells are difficult to categorize. As revealed by TEM, some defective cells which technically would be defined as "head-base bending" appear to be disjointed sperm. Such cells would be impossible to differentiate by LM. The orientation of some cells would also preclude their accurate classification. A slight degree of overlap between the two defects could therefore be expected when assessing

semen samples. It was clear from this study that the two sperm defects made up only a small proportion of the total sperm count. An interesting observation was that the incidence of head-base bending (3.8%) was double that of disjointed sperm (1.9%). Additionally, only two birds showed a higher proportion of disjointed perm compared to head-base bending (See Fig. 2). Although the present study was not designed to test functional parameters, it is doubtful whether the low incidence of the two defects would have had a marked influence on fertility.

The presence in the testis parenchyma of developing spermatids displaying head-base bending and misalignment of the head and flagellum points to a testicular origin for both defects in the emu. This is the first morphological evidence of any form of head (head-base bending) or neck (disjointed sperm) “bending” taking place in the avian testis. Despite numerous publications on “bent” or “crooked-necked” sperm (Saeki, 1960; Humphreys, 1972; Van Wambeke, 1972; Yamane, 1972; Bakst & Sexton, 1979; Bakst 1980; Maeda *et al*., 1984,1986; Bertschinger *et al*., 1992; Bozkurt *et al*., 1998; Alkan *et al*., 2002; Łukaszewicz *et al*., 2008; Siudzińska & Łukaszewicz, 2008; Tabatabaei *et al*., 2009, 2010) in birds, no information on the origin of this defect has been presented. Both defects could conceivably also develop in the *ductus deferens* due to a combination of inherent and external factors. The most probable inherent factors appear to be defective chromatin condensation (for head-base bending) coupled with early misalignment of the flagellum (both defects) during the round spermatid stage of development (personal observations). Therefore, inherent deficiencies in the process of spermiogenesis may be responsible for the eventual manifestation of the defect in the excurrent duct system. The most likely external factors are those proposed by Yamane (1972) where flagellar movement coupled with intrinsic weaknesses in the head-base (defective chromatin condensation) and neck (misalignment and/or missing elements of the connecting piece) could adversely affect sperm structure during their progress along the deferent duct.

In summary, terms such as “bent sperm” and “crooked-necked sperm” should be avoided when assessing emu sperm morphology as they are non-specific and do not reflect the existence of two separate and distinct abnormalities, namely head-base bending and disjointed sperm. Head-base bending is a true form of bending and as it involves only the head is classified as a head defect. In contrast, while disjointed sperm superficially appear bent, they actually reflect dislocation of the head and tail in the neck region, thus representing a tail defect. The lack of supportive morphological data for the accurate identification of avian sperm defects and the perpetuation of loosely used terminology for their classification requires critical reappraisal.

References

Alkan, S., Baran, A., Özdas, Ö.B. & Evecen, M. (2002) Morphological defects in turkey semen. *Turkish Journal of Veterinary and Animal Science* **26**, 1087-1092.

Bakst, M.R. (1980) Fertilizing capacity and morphology of fowl and turkey spermatozoa in hypotonic extender. *Journal of Reproduction and Fertility* **60**, 121-127.

Bakst, M.R. & Sexton, T.J. (1979) Fertilizing capacity and ultrastructure of fowl and turkey spermatozoa before and after freezing. *Journal of Reproduction and Fertility* **55**, 1-7.

Bertschinger, H.J., Burger, W.P., Soley, J.T. & de Lange, J.H. (1992) Semen collection and evaluation of the male ostrich. *Proceedings of the Biennial Congress of the South African Veterinary Association*, Grahamstown, pp.154-158.

Bozkurt, H.H., Alkan, S., Arda, O., Dağlioğlu, S. & Ileri I.K. (1998) The effect of BPSE (Beltsville poultry semen extender) and PBS (phosphate buffered saline) semen extender on ultrastructure of turkey spermatozoa kept in the cold. *Veteriner Fakültesi Dergisi (Istanbul)* **24**, 343-354.

Chelmońska, B., Jerysz, A., Łukaszewicz, E., Kowalczyk, A. & Malecki, I. (2008) Semen collection from Japanese Quail (*Coturnix japonica*) using a teaser female. *Turkish Journal of Veterinary and Animal Science* **32**, 19-24.

Chemes, H.E. & Rawe, V.Y. (2003) Sperm pathology: a step beyond descriptive morphology. Origin, characterization and fertility potential of abnormal sperm phenotypes in infertile men. *Human Reproduction Update* **9**, 405-428.

Chemes, H.E. & Rawe, V.Y. (2010) The making of abnormal spermatozoa: cellular and molecular mechanisms underlying pathological spermiogenesis. *Cell and Tissue Research* **341**, 349-357.

Dadoune, J-P. (1995) The nuclear status of human sperm cells. *Micron* **26**, 323-345.

D'Occhio, M.J., Hengstberger, K.J. & Johnston, S.D. (2007) Biology of sperm chromatin structure and relationship to male fertility and embryonic survival. *Animal Reproduction Science* **101**, 1-17.

Du Plessis, L. & Soley, J.T. (2011) Incidence, structure and morphological classification of abnormal sperm in the emu (*Dromaius novaehollandiae*). *Theriogenology* **75**, 589-601.

Ferdinand, A. (1992) Licht- und elektronenmikroskopische Untersuchungen zur Morphologie von Ganterspermatozoen. Ph.D Thesis, University of Veterinary Medicine, Hannover.

Froman, D.P. & Bernier, P.E. (1987) Identification of heritable spermatozoal degeneration within the ductus deferens of the chicken (*Gallus domesticus*). *Biology of Reproduction* **37**, 969-977.

Góes, P.A.A., Cavalcante, A.K. da S., Nichi, M., Perez, E.G. de A., Barnabe, R.C. & Barnabe, V.H. (2010) Reproductive characteristics of captive greater rhea (*Rhea americana*) males reared in the state of São Paulo, Brazil. *Brazilian Journal of Poultry Science* **12**, 57-62.

Hess, R.A., Hughes, B.L. & Thurston, R.J. (1986) Frequency and structure of macrophages and abnormal sperm cells in guinea fowl semen. *Reproduction, Nutrition and Development* **26**, 39-51.

Humphreys, P.N. (1972) Brief observations on the semen and spermatozoa of certain passerine and non-passerine birds. *Journal of Reproduction and Fertility* **29**, 327-336.

Irons, P.C., Bertschinger, H.J., Soley, J.T. & Burger, W.P. (1996) Semen collection and evaluation in the ostrich. In*:* Deeming, D.C. (ed.) Improving our Understanding of Ratites in a Farming Environment, Ratite Conference, Manchester, pp. 157-159.

Lake, P.E. (1954) The relationship between morphology and function of fowl spermatozoa. *Proceedings of the Xth World's Poultry Congress*, Edinburgh, pp. 79-85.

Łukaszewicz, E., Jerysz, A., Partyka, A. & Siudzińska, A. (2008) Efficacy of evaluation of rooster sperm morphology using different staining methods. *Research in Veterinary Science* **85**, 583-588.

Maeda, T., Terada, T. & Tsutsumi, Y. (1984) Comparative study of the effects of various cryoprotectants in preserving the morphology of frozen and thawed fowl spermatozoa. *British Poultry Science* **25**, 547-553.

Maeda, T., Terada, T. & Tsutsumi, Y. (1986) Studies of the factors causing abnormal acrosomes and crooked-necks in fowl spermatozoa during freezing and thawing. *British Poultry Science* **27**, 695-702.

Malecki, I.A., Cummins, J.M., Martin, G.B. & Lindsay, D.R. (1998) Effect of collection frequency on semen quality and the frequency of abnormal forms of spermatozoa in the emu. *Animal Production in Australia* **22**, 406.

Maretta, M. (1979) Ultrastructure of double and multiple sperm tails in drake. *Veterinarni Medicina* **24**, 679-689

Marquez, B.J. & Ogasawara, F.X. (1975) Scanning electron microscope studies of turkey semen. *Poultry Science* **54**, 1139-1143.

Mochida, K., Tres, L.L. & Kierszenbaum, A.L. (1999) Structural and biochemical features of fractionated spermatid manchettes and sperm axonemes of the *Azh/Azh* mutant mouse. *Molecular Reproduction and Development* **52**, 434-444.

Patryka, A., Jerysz, A. & Pokorny, P. (2007) Lipid peroxidation in fresh and stored semen of green-legged partridge. *Electronic Journal of Polish Agricultural Universities* **10**, 8.

Penfold, L.M., Wildt, D.E., Herzog, T.L., Lynch, W., Ware, L., Derrickson, S.E. & Monfort, S.L. (2000) Seasonal patterns of LH, testosterone and semen quality in the Northern pintail duck (*Anas acuta*). *Reproduction, Fertility and Development* **12**, 229-235.

Saeki, Y. (1960) Crooked-necked spermatozoa in relation to low fertility in the artificial insemination of fowl. *Poultry Science* **39**, 1354-1361.

Santiago-Moreno, J., López-Sebastián, A., Castaño, C., Coloma, M.A., Gómez-Brunet, A., Toledano-Díaz, A. Prieto, M.T. & Campo, J.L. (2009) Sperm variables as predictors of fertility in Black castellana roosters; use in the selection of sperm donors for genome resource banking purposes. *Spanish Journal of Agricultural Research* **7**, 555-562.

Siudzińska, A. & Łukaszewicz, E. (2008) Effect of semen extenders and storage time on sperm morphology of four chicken breeds. *Journal of Applied Poultry Research* **17**, 101-108.

Soley, J.T., Bertschinger, H.J., Els, H.J. & Burger, W.P. (1996) The morphology and incidence of retained cytoplasmic droplets in ostrich spermatozoa. In: Deeming, D.C. (ed.) Improving our Understanding of Ratites in a Farming Environment. Ratite Conference, Manchester, pp.16-18.

Steltzer, G., Crosta, L., Bűrkle, M. & Krautwald-Junghanns, M-E. (2005) Attempted semen collection using the massasge technique and semen analysis in various psittacine species. *Journal of Avian Medicine and Surgery* **19**, 7-13.

Tabatabaei, S., Batavani, R.A. & Talebi, A.R. (2009) Comparison of semen quality in indigenous and Ross broiler breeder roosters. *Journal of Animal and Veterinary Advances* **8**, 90-93.

Tabatabaei, S., Chaji, M. & Mohammadabadi, T. (2010) Correlation between age of rooster and semen quality in Iranian indigenous broiler chickens. *Journal of Animal and Veterinary Advances* **9**, 195-198.

Van Wambeke F. (1972) The effect of tonicity of storage media for fowl semen on the occurrence of neck-bending spermatozoa, fertility and hatchability. *British Poultry Science* **18**, 163-168.

Vieytes, A.L., Cisale, H.O. & Ferrari, M.R. (2008) Relationship between the nuclear morphology of the sperm of 10 bulls and their fertility. *Veterinary Record* **163**, 625-629.

Yamane, J. (1972) Neck-bending of cock sperm and its causal genesis. In: *Riproduzione animale e fecondazione artificiale: scritti in onore di Telesforo Bonadonna.* Societa Italiana per il Progresso della Zootecnica. Edizioni Agricole, Bologna, pp. 327-331.

Zamboni, Z. (1992) Sperm ultrastructure and its relevance to infertility. *Archives of Pathology and Laboratory Medicine* **116**, 325-344.

Chapter 7 Morphology and origin of abnormal sperm II: Abaxial tail implantation

Introduction

Abaxial tail implantation is an anomaly occurring in the neck region of sperm involving the eccentric positioning of the centriolar complex relative to the head base (Afzelius, 1996). It has been described in a number of mammalian species including the bull (Barth, 1989; Barth & Oko, 1989), buffalo (Jainudee *et al*., 1982; Pant *et al*., 2002), boar (Thilander *et al*., 1985a; Pinart *et al*., 1998), dog (Oettlé & Soley, 1988; Morton & Bruce, 1989), stallion (Dowsett *et al*., 1984) and man (Menkveld *et al*., 1991). In general, it is not an uncommon defect in mammalian sperm, although the incidence of the anomaly is low (Barth, 1989). However, a few cases with a high incidence have been reported in the bull (Onstad, 1963; Fischerleitner *et al*., 1981; Barth, 1989) and boar (Thilander *et al*., 1985a). The defect originates in the testis (Thilander *et al*., 1985a,b; Pinart *et al*., 1998), but its influence on fertility has not been unequivocally established (Onstad, 1963; Dowsett *et al*., 1984; Morton & Bruce, 1989; Sarlós *et al*., 1990; Pant *et al*., 2002; Nöthling & Irons, 2008).

With the exception of an incidental reference to this defect in the turkey (Wakely & Kosin, 1951), a light micrograph of 'paraxial' sperm in the goose (Ferdinand, 1992), and the presentation of a transmission electron micrograph illustrating abnormal articulation between the sperm head and tail in the duck (Maretta, 1975), abaxial sperm tails have not, as far as could be ascertained, been described in any other avian species. This would suggest that this defect is rarely observed in non-passerine birds. Considering the apparent paucity of this defect in birds and the total lack of descriptive data, this chapter details the morphological features of abaxial tails observed in emu (*Dromaius novaehollandiae)* spermatozoa. Information on the development of this defect during spermiogenesis is also presented.

Materials & Methods

Semen samples were collected from the distal deferent duct of 15 sexually mature emus slaughtered at commercial abattoirs. The age of the birds ranged between 22 months and four years. The samples were immediately fixed in 2.5% glutaraldehyde in 0.13M Millonig's phosphate buffer, pH 7.4. Smears for light microscopy (LM) were prepared as described in Chapter 2.

Semen samples were prepared for transmission electron microscopy (TEM) as previously described in Chapter 2. Small blocks of testicular tissue were also collected from each of the birds in 4% glutaraldehyde in 0.13M Millonig's phosphate buffer, pH 7.4 and prepared as described in Chapter 3. Thin sections of both the semen samples and testicular blocks were stained with lead citrate and uranyl acetate and viewed in a Philips CM10 transmission electron microscope (Philips Electron Optical Division, Eindhoven, The Netherlands) operated at 80kV. Relevant features of the anomaly and stages of its development in the testis were described and digitally recorded.

Results

Incidence

The incidence of the defect was low and was scored in only one of the 15 birds examined during the random count of 300 cells (see Chapter 5 on incidence of defects). This bird was one of the younger emus, i.e. one of those that were 22 months old. In this instance the defect formed 0.6% of the total cells counted. However, when examining the entire semen smear, occasional abaxial tails were noted in a further five birds.

Light microscopy (LM)

Abaxial sperm were observed on LM using both bright field and phase contrast microscopy, despite the relative scarcity of the defect. The defect was more easily resolved with phase contrast microscopy. In contrast to the normal axial alignment of the head and neck/midpiece (Figs. 1a-c), abnormal sperm demonstrated an abaxial relationship between the head and tail resulting in a non-linear or staggered arrangement of the two components (Fig. 1). The base of the head appeared gently swollen and in some cells was observed to unilaterally overlap the neck region. The degree of overlapping varied from a subtle expansion of the nuclear base (Figs. 1c,d) to prominent bulging of the karyoplasm that extended along an appreciable part of the midpiece (Figs. 1a,b,e).

Transmission electron microscopy (TEM)

Despite the low incidence of the anomaly observed by LM, defective sperm were readily identified by TEM in affected birds. Using this technique, normal sperm revealed the typical ultrastructural features previously described for the head-base/neck interface in the emu (Du Plessis, & Soley, 2011) (Fig. 2a). Defective sperm displayed two basic forms of the defect, those with a flat nuclear (head) base and those demonstrating a caudally directed nuclear projection. In defective sperm with a flat nuclear base the centriolar complex (proximal and distal centrioles) and attendant

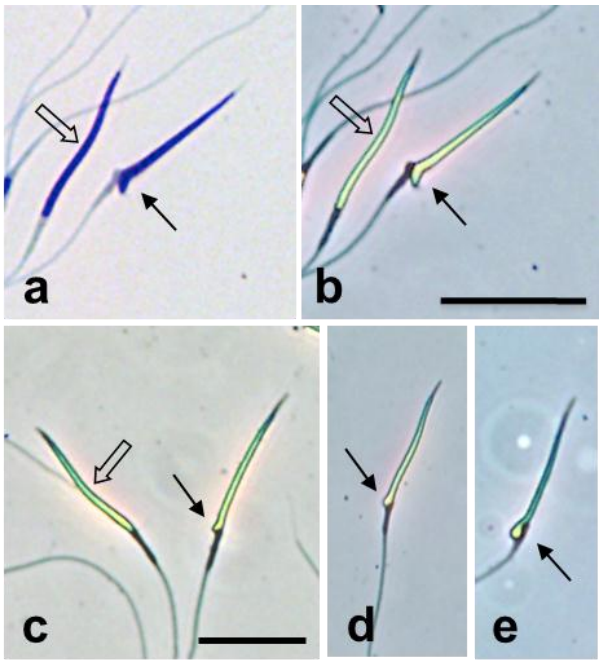

Figure 1. Light micrographs of normal (block arrows) and defective sperm (arrows) as revealed by bright field microscopy (Wright's stain) (a) and phase contrast microscopy (b). Note the improved detail revealed by the latter technique. Figs. 1c-e illustrate varying forms of the defect as observed by phase contrast microscopy. Compare the axial implantation of the tail in normal sperm (block arrows) with the abaxial connection in defective sperm. Note the prominent unilateral projection of the nucleus in Fig. 1e covering the proximal midpiece. Bar (a, b) = 10µm; Bar (c-e) = 10µm.

connecting piece were grossly misaligned in respect of the nuclear base. In these cells the nuclear base appeared to accommodate the abaxial centriolar complex by widening or by laterally extending a thin, horizontal sliver of karypolasm covered by the nucleolemma (Fig. 2b). In the other form of the defect the centriolar complex was more broadly yet abaxially attached to the nuclear base. In such instances the part of the nuclear base overlapping the misaligned centriolar complex extended caudally as a variably sized nuclear projection (Figs. 2c,d). In addition to the nuclear projection, that part of the nuclear base above the misaligned centriolar complex sometimes formed a thin lateral extension similar to that observed in grossly misaligned cells (Fig. 2d). In both forms of the defect the various components of the neck region (basal plate, capitellum, arms of the connecting piece) appeared normal. However, the shallow implantation fossa typical of emu sperm (Du Plessis & Soley, 2011) was not always discernable in defective cells. An association between the connecting piece/centriolar complex and the base of the nucleus, no matter how tenuous, was always apparent in sperm with abaxial tails.

In some defective cells the nuclear projection was associated with a rudimentary, moderately electron-dense structure resembling components of the connecting piece (Fig. 3). These structures were associated with either the base or medial wall of the nuclear projection and were generally related to a narrow implantation fossa structurally similar to that of the adjacent fossa housing the abaxial tail. The structures were contained within the cytoplasm of the neck region and were not associated with an attendant centriolar complex or mitochondria.

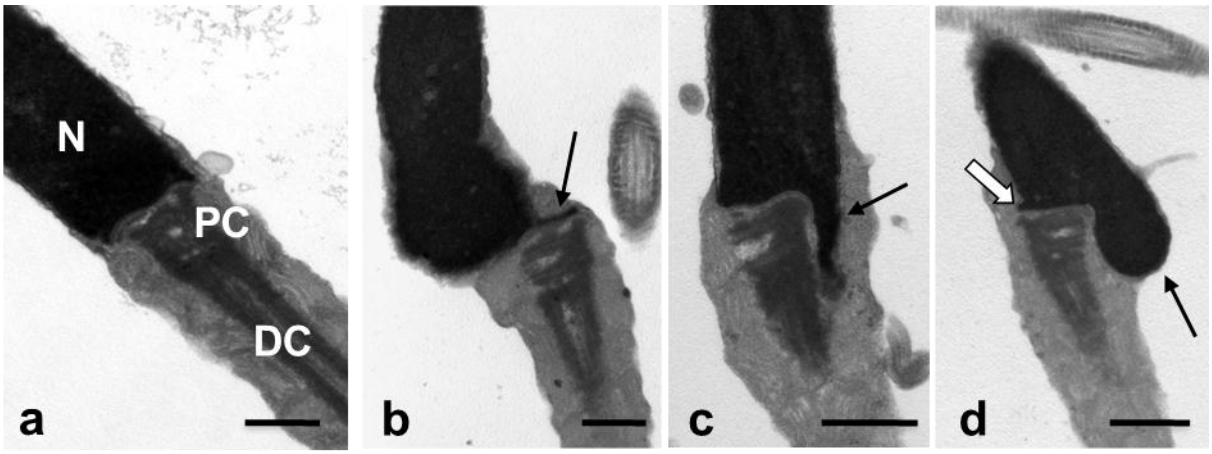

Figure 2. Mid-saggital sections of normal (a) and defective (b-d) sperm demonstrating the ultrastructural features of the head-neck/midpiece region. In normal cells (a) the nuclear base and neck/midpiece are similar in width and the connecting piece of the centriolar complex attaches axially to the base of the nucleus via a shallow implantation fossa. In defective cells the centriolar complex is abaxially positioned in respect of the head (nuclear) base. In Fig. 2b the nuclear base displays a thin nuclear extension (arrow) to accommodate the grossly misaligned centriolar complex whereas in Figs. 2c,d the broadly connected yet abaxially positioned centriolar complex is unilaterally flanked by a bulbous projection (arrow) of nuclear material (compare to Figs. 1d,e). Note the short, lateral nuclear extension (block arrow) in Fig. 2d. Nucleus (N); proximal centriole (PC); distal centriole (DC). Bar = 0.5µm.

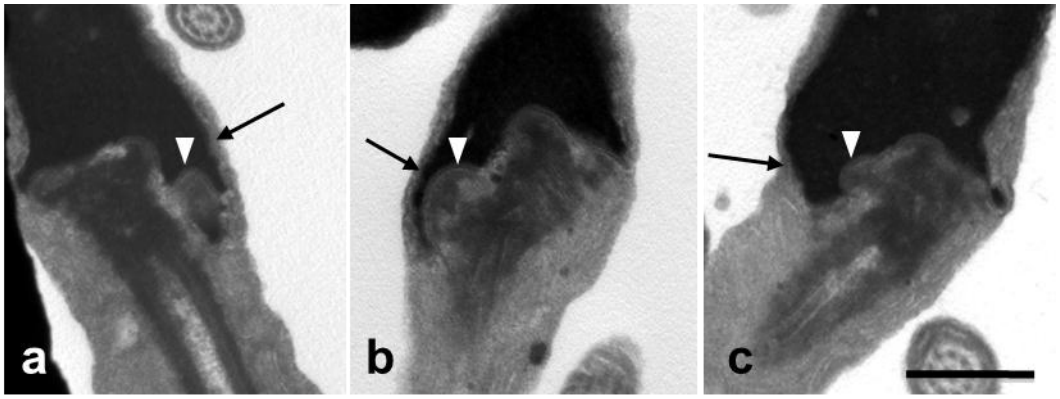

Figure 3. Transmission electron micrographs of defective sperm illustrating attachment of presumptive elements of the connecting piece to the base (Fig. 3a) or medial surface (Figs. 3b,c) of the caudal nuclear projection (arrow). In each instance the nuclear membrane in contact with the centriole-associated structures forms a rudimentary implantation fossa (arrowheads). Note the thin lateral extension of the nuclear base in (a) and (c) which partially accommodates the abaxially positioned centriolar complex. Bar = 0.5µm.

Origin of the defect

Stages in the formation of abaxial sperm were observed in the testicular material from the six affected birds. The defect could be identified in early elongated spermatids which were characterized by lengthened nuclei containing moderately electron-dense, finely granular chromatin, and by the presence of the circular manchette (Fig. 4). The centriolar complex was

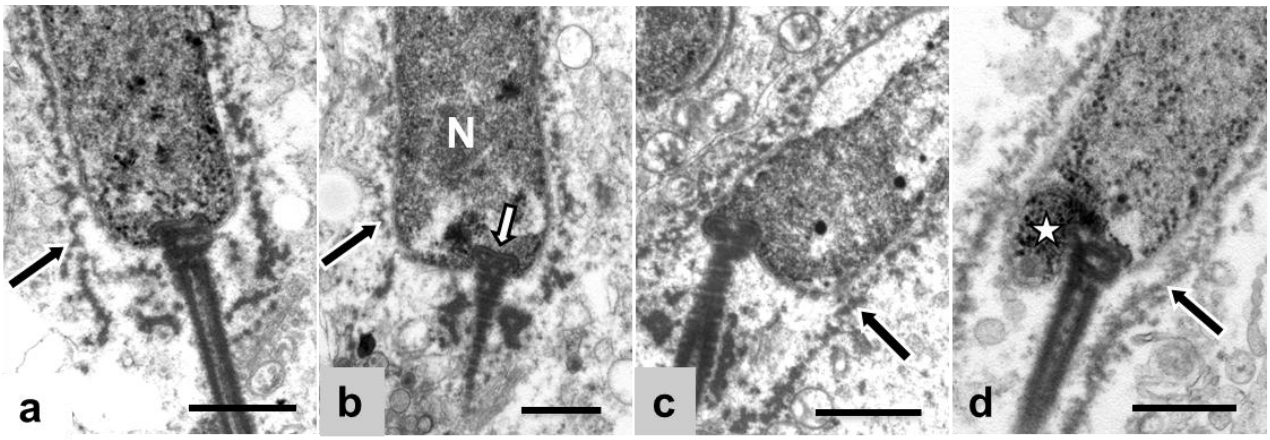

Figure 4. Transmission electron micrographs of early stage elongated spermatids showing normal (a) and abaxially implanted flagella (b-d). In (b) the centriolar complex is abaxially attached to the base of the nucleus (N) via a clearly defined implantation fossa (white arrow). Fig. 4c shows a similar stage in the development of the defect to that shown in b except that the centriolar complex is obliquely attached to the base of the nucleus. In Fig. 4d the abaxially positioned centriolar complex is unilaterally flanked by a projection of the nuclear base (star)(compare to Figs. 1e, 2d and 5c.). Note the circular manchette (black arrow) associated with both the normal and defective cells. Bar = 1µm.

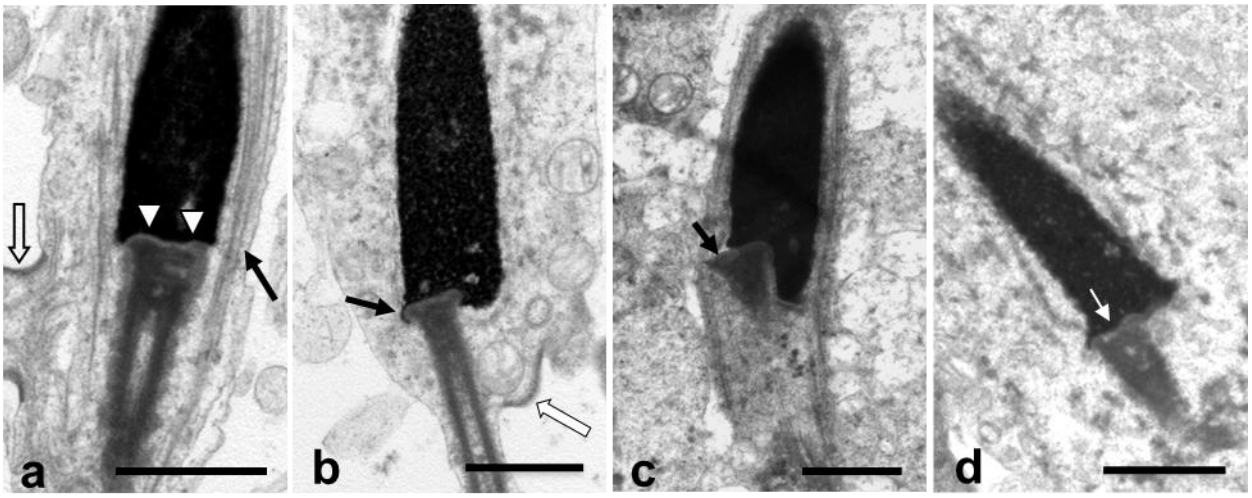

Figure 5. Transmission electron micrographs of late stage elongated spermatids. Fig. 5a demonstrates a normally aligned head and tail. Note the shallow yet distinct implantation fossa (arrowheads), the prominent longitudinal manchette (arrow) and the cytoplasmic bridge (block arrow) connecting neighboring cells. In Fig. 5b the centriolar complex attaches abaxially to one half of the nuclear base. A thin strip of karyoplasm (arrow) completes the implantation fossa. In Fig. 5c the connecting piece (arrow) markedly overlaps the nuclear base which unilaterally extends a nuclear projection (compare with Figs. 1d,e; Figs. 2c,d and Fig. 4d). In Fig. 5d a widened nuclear base accommodates the abaxially positioned centriolar complex. Only a single implantation fossa (arrow) is obvious. Bar = 1µm.

clearly misaligned in respect of the longitudinal axis of the cell at this stage of spermiogenesis and both forms of the defect could be detected (Figs. 4b-d). The implantation fossa and structural features of the centriolar complex (Figs. 4b-d) were similar to those of normal spermatids (Fig. 4a) at the same stage of development. No lateral extension of the nuclear base was observed at this stage of development. Late elongated spermatids typically displayed a condensed mass of chromatin and the late circular, transitional or longitudinal manchette (Figs. 5b-d). At this stage of development the two forms of the defect adopted the more definitive characteristics typical of mature sperm, including, where present, the formation of lateral extensions from the base of the nucleus (Figs. 5b,d). The structure of the components in the neck region of defective spermatids were again similar to those seen in normal cells at the same stage of development (Fig. 5a).

Discussion

Abaxial tail implantation in birds is rare and has only previously been reported in the turkey (Wakely & Kosin, 1951), goose (Ferdinand, 1992) and duck (Maretta, 1975). No category for this defect is reflected in the numerous classification systems for sperm defects in poultry (Wakely & Kosin, 1951; Kamar & Badreldin 1959; Marvan *et al*., 1981; Alkan *et al*., 2001; Łukaszewicz *et al*., 2008; Tabatabaei *et al*., 2009, 2010) and was not included in a recently proposed classification for ratite sperm abnormalities (Du Plessis & Soley, 2011). In the present study the defect was scored in only one of the 15 birds sampled, although careful examination of entire semen smears (all cells scanned) identified isolated examples of the defect in a further five birds. This observation is in agreement with studies on mammalian sperm where the incidence of the defect is reported to be low (Barth, 1989; Oettlé, 1993). It has been pointed out that abaxial tails in birds (Ferdinand, 1992) and in the bull (Barth & Oko, 1989) may easily be overlooked on routine semen smears, particularly if the smears are poorly prepared or the resolution of the microscope inadequate. In the emu, this situation is further complicated by the cylindrical conformation of non-passerine bird sperm as incorrect orientation of the cell on the smear may mask the existence of the defect. It was clear from the present study that LM only revealed gross forms of the anomaly and that more subtle forms of the defect could only be identified by TEM. This may partially explain why abaxial tails were readily seen on TEM despite the low incidence of the defect revealed by LM. It has been noted that abaxial tails appear to increase in number in older bulls (Mandal *et al*., 2010) and that certain sperm defects (larger heads, smaller heads, 180° bent heads) in the rooster also increase with age (Tabatabaei *et al*., 2010). As the birds used in the present study were young (not older than 4 years), this may also explain the low incidence of the defect observed.

Some reports have suggested that abaxial tail implantation can have an adverse affect on fertility. Thilander *et al.* (1985a) and Malmgren (1997), in studies of boar and stallion sperm respectively, concluded that this anomaly negatively affects fertility due to its influence on sperm motility. Onstad (1963) linked sterility in an 18 month-old bull to a 60% incidence of abaxial tail attachment in the ejaculate.

In contrast, this anomaly has been classified as a minor defect in the dog (Oettlé & Soley, 1988) and in man (Menkveld *et al*., 1991). Semen evaluation studies in the dog (Morton & Bruce, 1989), buffalo (Jainudeen *et al*., 1982; Pant *et al*., 2002) and bull (Barth, 1989) have also indicated that abaxial tails have no influence on fertility, even when the incidence is greater than 50% (Barth, 1989). Some authors even consider the anomaly to be a normal variation of sperm morphology (Pant *et al*., 2002; Morton & Bruce, 1989; Dowsett *et al*., 1984; Nöthling & Irons, 2008). However, Sarlós *et al.* (1990) reported improved fertility in the boar with an increase in the incidence of abaxial tail implantation. The low incidence of the abnormality in the emu, coupled with the evidence from studies on mammalian sperm defects, would suggest that abaxial tail implantation has no affect on fertility in this bird.

Little is known about the morphological features of abaxial tail implantation in avian sperm. No descriptions of this defect have been provided and some doubt exists that the illustration by Wakely and Kosin (1951) represents a true abaxially implanted tail, as the head/midpiece connection demonstrates normal alignment and it is only the principal piece of the flagellum that appears to be abaxially positioned. The electron micrograph of a defective sperm in the drake appears to represent an abaxially implanted tail although it is simply described as an “abnormality in the articulation between tail and head” (Maretta, 1975).

This study revealed that abaxial tail implantation occurs in emu sperm. However, certain morphological peculiarities are obvious in defective emu sperm when compared to, for example, that of the bull (Barth & Oko, 1989) and boar (Thilander *et al*., 1985a). In mammals the broad head base allows for abaxial attachment of the flagellum without the connecting piece overlapping the nuclear base (Oettlé & Soley, 1988; Menkveld *et al*., 1991). In the emu, and presumably in other non-passerine birds, the similarity in width between the connecting piece and head base (Asa *et al*., 1986; Phillips & Asa, 1989; Baccetti *et al*., 1991; Soley, 1993, 1994; Jamieson, 2007; Du Plessis & Soley, 2011) results in a staggered alignment of the head and tail in defective sperm, with the connecting piece being positioned at a variable distance from the head base axis. In addition, the nuclear base of defective mammalian sperm remains morphologically unaltered in comparison to the situation in the emu where a thin lateral extension of the karyoplasm often covers the misaligned portion of the connecting piece, and a variably

sized nuclear projection extends caudally in some cells from the nuclear base overlapping the centriolar complex. An additional implantation fossa has been reported in abaxial sperm in the bull, and which is sometimes associated with an accessory tail (Barth, 1989; Barth & Oko, 1989). However, the free nature of the accessory tail in bull sperm and its association with a centriolar complex, connecting piece and attendant mitochondria (Barth, 1989; Barth & Oko, 1989), differs markedly from the rudimentary structures observed in emu sperm. The association between abaxial tails and multiple tails suggested for the bull appears unlikely in the emu although some defective cells displayed a widened nuclear base typical of the multiflagellate sperm reported for this species (See Chapter 8). Despite the structural differences outlined above, it is clear that abaxial tail attachment in the emu parallels that described for mammalian sperm thus further emphasizing the point that basic sperm anomalies can occur across a wide spectrum of vertebrate species (Soley, & Els, 1996).

In the emu the defect is clearly visible at the early elongated spermatid stage of spermiogenesis although there are indications that earlier predisposing factors concerning the movement of the centriolar complex precipitate the subsequent misalignment of the nucleus and flagellum. In human sperm abnormal head-tail alignment (abaxial sperm) occurs when the sperm centrioles “are unable to migrate and attach normally to the caudal pole of the spermatid nucleus” (Chemes & Rawe, 2010). A similar mechanism may be involved during spermiogenesis in the emu.

References

Afzelius, B.A. (1996) The sperm cytoskeleton and its defects. *Cytoskeleton* **3**, 325-357.

Alkan, S., Baran, A., Özdas¸ B.O. & Evecen, M. (2001) Morphological defects in turkey semen. *Turkish Journal of Veterinary and Animal Science* **26**, 1087-1092.

Asa, C., Phillips, D.M. & Stover, J. (1986) Ultrastructure of spermatozoa of the crested tinamou. *Journal of Ultrastructure and Molecular Structure Research* **94**, 170-175.

Baccetti, B., Burrini, A.G. & Falchetti, E. (1991) Spermatozoa and relationships in Palaeognath birds. *Biology of the Cell* **71**, 209-216.

Barth, A.D. (1989) Abaxial tail attachment of bovine spermatozoa and its effect on fertility. *Canadian Veterinary Journal* **30**, 656-662.

Barth, A.D. & Oko, R.J. (1989) Abnormal morphology of bovine spermatozoa. Iowa State University Press, Ames.

Chemes, H.E. & Rawe, V.Y. (2010) The making of abnormal spermatozoa: Cellular and molecular mechanisms underlying pathological spermiogenesis. *Cell and Tissue Research* **341**, 349-357.

Dowsett, K.F., Osborne, H.G. & Pattie, W.A. (1984) Morphological characteristics of stallion spermatozoa. *Theriogenology* **22**, 463-471.

Du Plessis, L. & Soley, J.T. (2011) Incidence, structure and morphological classification of abnormal sperm in the emu (*Dromaius novaehollandiae*). *Theriogenology* **75**, 589-601.

Ferdinand, A. (1992) Licht- und elektronenmikroskopische Untersuchungen zur Morphologie von Ganterspermatozoen. Ph.D Thesis, University of Veterinary Medicine, Hannover.

Fischerleitner, F., Sinowatz, F., Mayr, B. & Mostl, E. (1981) Paraxial tails in bull semen. *Zuchthygiene* **16**,116-126.

Jainudeen, M.R., Bongso, T.A. & Dass, S. (1982) Semen characteristics of the swamp buffalo (*Bubalus bubalis*). *Animal Reproduction Science* **4**, 213-217.

Jamieson, B.G.M. (2007) Avian spermatozoa: Structure and Phylogeny. In: Jamieson B.G.M. (ed.) Reproductive Biology and Phylogeny of Birds Part A. Science Publishers, Jersey, pp. 349-511.

Kamar, G.A.R. & Badreldin, A.L. (1959) Sperm morphology and viability. *Acta Anatomica* **39**, 81-83.

Łukaszewicz, E., Jerysz, A., Partyka, A. & Siudzińska, A. (2008) Efficacy of evaluation of rooster sperm morphology using different staining methods. *Research in Veterinary Science* **85**, 583-588.

Maretta, M. (1975) Structural abnormalities in the middle piece of the drake's spermatozoon tail. *Acta Veterinaria Brno* **25**, 245-250.

Malmgren L. (1997) Assessing the quality of raw semen: A review. *Theriogenology* **48**, 523-530.

Mandal, D.K., Kumar, M. & Tyagi, S. (2010) Effect of age on spermiogram of Holstein Friesian x Sahiwal crossbred bulls. *Animals* **4**, 595-603.

Marvan, F., Rob, O. & Janeckova, E. (1981) Classification of morphological abnormalities of gander sperm. *Zuchthygiene* **16**, 176-183.

Menkveld, R., Oettlé, E.E., Kruger, T.F., Swanson, R.J., Acosta, A.A. & Oehninger. S. (1991) Atlas of human sperm morphology. Williams & Wilkins, Baltimore.

Morton, D.B. & Bruce, S.G. (1989) Semen evaluation, cryopreservation and factors relevant to the use of frozen semen in dogs. *Journal of Reproduction and Fertility Supplement* **39**, 311-316.

Nöthling, J.O. & Irons P.C. (2008) A simple multidimensional system for the recording and interpretation of sperm morphology in bulls. *Theriogenology* **69**, 603-611.

Oettlé, E.E. (1993) Sperm morphology and fertility in the dog. *Journal of Reproduction and Fertility Supplement* **47**, 257–260.

Oettlé, E.E. & Soley, J.T. (1988) Sperm abnormalities in the dog: A light and electron microscopic study. *Veterinary Medical Review* **59**, 28-70.

Onstad, O. (1963) Abaxial attachment of the middle piece of the spermia in connection with sterility in a bull. *Nordisk Veterinaer Medicin* **15**, 92-96.

Pant, H.C., Mittal, A.K., Patel, S.H., Shukla, H.R., Kasiraj, R., Prabhakar J.H., Barot, L.R. (2002) Abaxial sperm tails and fertility in the buffalo bull. *Indian Journal of Animal Science* **72**, 314-315.

Phillips, D.M. & Asa, C.S. (1989) Development of spermatozoa in the rhea. *Anatomical Record* **223**, 276-282.

Pinart, E., Camps, R., Briz, M.D., Bonet, S. & Egozcue, J. (1998) Unilateral spontaneous abdominal cryptorchidism: Structural and ultrastructural study of sperm morphology. *Animal Reproduction Science* **49**, 247-268.

Sarlós, P., Wekerle, L. & Nagy, Z. (1990) Relationship of fertility with tail implantation in boar spermatozoa. *Reproduction in Domestic Animals* **25**, 87-89.

Soley, J.T. (1993) Ultrastructure of ostrich (*Struthio camelus*) spermatozoa: I. Transmission electron microscopy. *Onderstepoort Journal of Veterinary Research* **60**, 119-130.

Soley, J.T. (1994) Centriole development and formation of the flagellum during spermiogenesis in the ostrich (*Struthio camelus*). *Journal of Anatomy* **185**, 301-313.

Soley, J.T. & Els, H.J. (1996) Sperm defects in vertebrates: Variations on a theme? *Proceedings of the Electron Microscopy Society of Southern Africa* **26**, 102.

Tabatabaei, S., Batavani, R.A. & Talebi, A.R. (2009) Comparison of semen quality in indigenous and Ross broiler breeder roosters. *Journal of Animal and Veterinary Advances* **8**, 90-93.

Tabatabaei, S., Chaji, M. & Mohammadabadi, T. (2010) Correlation between age of rooster and semen quality in Iranian indigenous broiler chickens. *Journal of Animal and Veterinary Advances* **9**, 195-198.

Thilander, G., Settergren, I. & Plöen, L. (1985a) Abaxial implantation of the middle piece in spermatozoa and spermatids in related sterile boars. *Acta Veterinaria Scandinavica* **26**, 513-520.

Thilander, G., Settergren, I. & Plöen, L. (1985b) Abnormalities of testicular origin in the neck region of bull spermatozoa. *Animal Reproduction Science* **8**, 151-157.

Wakely, W.J. & Kosin, I.L. (1951) A study of the morphology of the turkey spermatozoa with special reference to the seasonal prevalence of abnormal types. *American Journal of Veterinary Research* **12**, 240-245.

Chapter 8 Morphology of abnormal sperm III: Multiflagellate sperm

Introduction

Significant advances have recently been made in gathering data relevant to the application of artificial insemination (AI) technology in the ratite industry (Malecki *et al*., 2008; Ciereszko *et al*., 2010; Bonato *et al*., 2011; Sood *et al*., 2011). However, considering the primary importance of semen evaluation in establishing AI programmes, relatively little information is currently available on the morphology of sperm defects in this commercially important group of birds, particularly at the ultrastructural level. Whereas various abnormal forms of spermatozoa have been named in the ostrich (Bertschinger *et al*., 1992) and emu (Malecki *et al*., 1998) but not described, and some morphological data provided on cytoplasmic droplets in ostrich sperm (Soley & Els, 1993; Soley *et al*., 1996), the only comprehensive accounts of abnormal sperm structure in ratites are those on the emu (Du Plessis & Soley, 2011a,b, 2012). The evaluation of sperm motility, sperm concentration and sperm morphology form the three most important parameters in semen analysis (Hotchkiss *et al*., 1938; MacLeod & Gold, 1951; Zamboni, 1992; Jørgensen *et al*., 1997; Cooper *et al*., 2002). The importance of sperm morphology in the assessment of semen quality in ratites has been recognised by Bertschinger *et al*. (1992) who note that in the ostrich “sperm morphology is the single most important factor in predicting fertility”.

The occurrence of multiflagellate sperm has been reported in a number of mammalian species including the stallion (Arns *et al*., 1988; Brito, 2007), bull (Barth & Oko, 1989; Kopp *et al*., 2007), boar (Bonet & Briz, 1991; Briz *et al*., 1996; Pinart *et al*., 1998) and dog (Oettlé & Soley, 1988), as well as in man (Holstein, 1975; Nistal *et al*., 1977; Escalier, 1983; Holstein *et al*., 1988; Weissenberg *et al*., 1998; Perrin *et al*., 2008). This anomaly is characterised by the presence of two or more flagella and is considered a rare condition which adversely influences sperm motility and therefore fertility (Nistal *et al*., 1977; Escalier, 1983; Barth & Oko, 1989). It has also been reported that a high proportion of macrocephalic sperm often, but not always (Bonet & Briz, 1991), display multiple flagella (Nistal *et al*., 1977; Escalier, 1983; Weissenberg *et al*., 1998; Lewis-Jones *et al*., 2003; Kopp *et al*., 2007). The ultrastructural features of this defect have been thoroughly described, demonstrating the uniformity of

the anomaly across different mammalian species (Nistal *et al*., 1977; Escalier, 1983; Barth & Oko, 1989).

In contrast, little information has been presented on the occurrence, incidence and structure of multiflagellate sperm in birds. Most classification systems on avian sperm defects fail to reflect multi- or biflagellate sperm (Wakely & Kosin, 1951; Kamar & Rizik, 1972; Alkan *et al*., 2002; Umapathy *et al*., 2005; Tabatabaei *et al*., 2009). However, this anomaly has been mentioned (Gee & Temple, 1978; Gee *et al*., 2004; Stelzer *et al*., 2005), briefly described, and/or illustrated in some avian species such as the Houbara bustard (Lindsay *et al*., 1999), goose (Marvan *et al*., 1981; Gee & Sexton, 1990; Ferdinand, 1992), duck (Maretta, 1979), guinea fowl (Nwakalor *et al*., 1988) and, more recently, in the emu (Du Plessis & Soley, 2011a). With the exception of a detailed study on the ultrastructure of multiple sperm tails in the drake (Maretta, 1979), the morphological features of this defect are poorly understood in birds. This chapter presents a comprehensive description of multiflagellate sperm in the emu utilising both light and electron microscopy and provides supporting information on the origin of the defect.

Materials & Methods

Semen and testes samples were collected during the breeding season from 15 sexually mature and active emus, *Dromaius novaehollandiae,* following slaughter at a commercial abattoir. Semen samples were gently expressed from the distal *ductus deferens* and immediately fixed in 2.5% glutaraldehyde in 0.13M Millonig's phosphate buffer, pH 7.4. Smears for light microscopy (LM) were prepared from the fixed semen samples and stained with Rapiddiff® (Clinical Sciences Diagnostics, Johannesburg, South Africa). The smears were examined with a Leica DM6000-B light microscope (Leica Microsystems, Wetzlar, Germany) using a 100x oil immersion objective and phase contrast illumination to evaluate sperm morphology. The incidence of multiflagellate sperm defects was determined by counting for each bird the number of multiple tailed sperm present in a total of 300 cells.

Semen samples were routinely prepared for scanning (SEM) and transmission electron microscopy (TEM) (see Chapter 2). Small blocks of testicular material were fixed in 4% glutaraldehyde in 0.13M Millonig's phosphate buffer, pH 7.4 and routinely prepared for TEM (see Chapter 3).

Thin sections of both sperm and testicular material were stained with lead citrate and uranyl acetate and viewed in a Philips CM10 transmission electron microscope (Philips Electron Optical Division, Eindhoven, The Netherlands) operated at 80kV. Samples for SEM were viewed in a JEOL Model 6010LA scanning electron microscope (JEOL Electron Optics Instrumentation, Tokyo, Japan) operated at 5kV.

To distinguish between sperm of normal dimensions and macrocephalic sperm, linear measurements of head (nuclear) length and tail length (n = 30) were taken on light micrographs, and nuclear base width measurements (n = 25) on transmission electron micrographs. Measurements were processed using the Soft Imaging System iTEM software (Olympus, Münster, Germany) and expressed as the average ± SD.

Results

Light microscopy (LM)

Multiflagellate sperm were readily identified by LM (Fig. 1) and were present in all the samples, albeit in low numbers. Sperm displaying multiple tails formed only 1% of the total cell count, although the anomaly accounted for 7% of total sperm defects. Multiple-tailed sperm were often, but not always, associated with macrocephalic sperm. Abnormal cells displaying this association formed 0.6% of the total cell count while sperm with normal sized heads and multiple tails comprised 0.4% of the total cell count. The ratio of macrocephalic sperm with multiple flagella to normal heads with multiple flagella was 3:2. Macrocephalic sperm with a single flagellum were also observed and constituted 1.5% of the total cell count. The heads of macrocephalic sperm measured approximately 1.5 times the length of normal sperm heads and exhibited a wider head base (Fig. 1b). The difference in head base width was also 1.5 times as determined from transmission electron micrographs. The individual tails (midpiece, principal piece and endpiece) of multiflagellate sperm were of similar length (52.7 ± 3.09µm; n = 15), irrespective of head size and conformed to the tail length of normal sperm (53.11 ± 3.0µm; n = 15). On LM a maximum of five tails were observed on individual spermatozoa, although the biflagellate form of the defect was most commonly encountered. Sperm displaying this anomaly exhibited a single midpiece. The proximal aspect of the multiple principal pieces appeared fused or intimately spiralled with the greater portion of the duplicate tails lying free (Figs. 1a,b).

Figure 1. Light micrographs showing (a) a normal sized sperm head (black arrow) with a double tail (white arrow) and (b) a macrocephalic sperm (black arrow) with a double tail (white arrow). Note the single midpiece and apparently fused proximal principal pieces of both biflagellate sperm. Bar = 10µm.

Electron microscopy

Scanning electron microscopy generally confirmed the light microscopic features of the anomaly. In most multiflagellate sperm a single but widened midpiece was evident (Fig. 2), although in some instances biflagellate sperm appeared to possess a double (split) midpiece. The proximal part of the individual principal pieces of the multiflagellate tails were either spiralled around each other (Figs. 2a,b) or lay closely aligned.

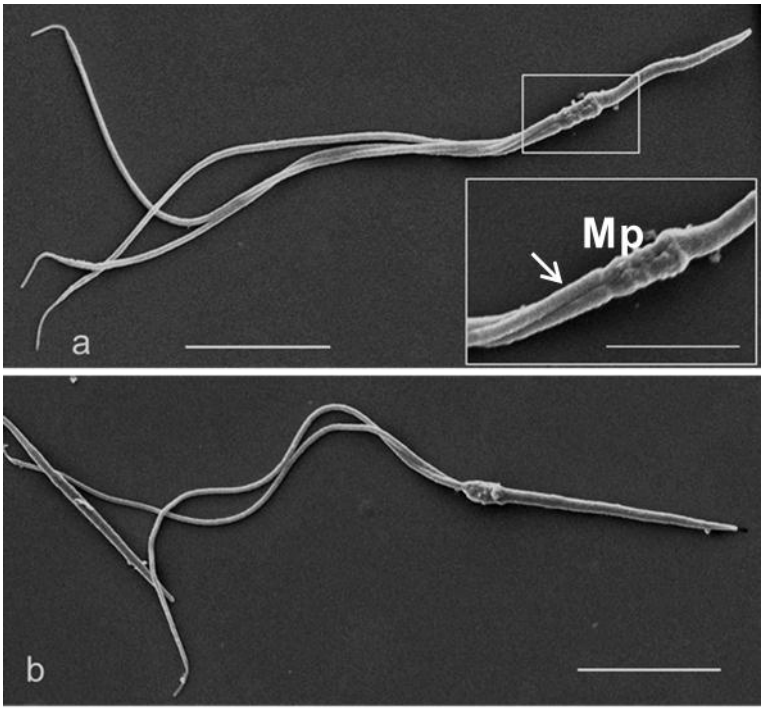

Figure 2. Scanning electron micrographs showing (a) a normal-sized sperm with three tails and (b) a macrocephalic sperm with two tails. Note the spiralling of the proximal aspect of the principal piece in both defective cells. Inset: Magnification of the rectangle in Fig. 2a showing the 'common' midpiece (Mp) studded with mitochondria and the free emergence of the 3 principal pieces (arrow). Bar = 10µm; inset Bar = 5µm.

When viewed by TEM, longitudinal sections of the neck and midpiece of affected sperm revealed the presence of two or more centriolar complexes (Fig. 3). In biflagellate sperm with normal head dimensions the proximal aspect of the twin centriolar complexes was associated with duplicated elements of the connecting piece and, due to the limited space available at the base of the head, each attached abaxially to the nucleus via shallow, twin implantation fossae (Figs. 3a-c). In some cells the nuclear base was abnormally attenuated at the periphery, artificially widening the base to accommodate the multiple tails (Figs. 3a,b), while in others the nuclear base was stepped (Fig. 3d). In favourable sections, each implantation fossa resembled that of normal sperm, being composed of two shallow impressions in the nuclear base, each housing part of the capitellum and one of the poorly defined segmented columns that formed the connecting piece (Du Plessis & Soley, 2011b). In some defective cells the fossae appeared shallow and the elements of the connecting piece appeared incomplete. Whether this was a true reflection of structural deficiencies or due to the plane of section could not be determined. The twin fossae were separated from each other by a conspicuous medial spine of karyoplasm (Fig. 3a). The two proximal centrioles were generally similarly oriented in respect of the nuclear base (Fig. 3a) although in some cells the orientation alternated, one centriole being observed in longitudinal profile and the other in transverse profile (Fig. 3b). In rare instances a single proximal centriole and two distal centrioles were observed (Fig. 3f). A distinct gap was generally present between the proximal centrioles and which was filled by homogeneous, moderately electron-dense material or in some instances by a mitochondrion emanating from the midpiece. The proximal and distal centrioles were generally linearly arranged but were occasionally misaligned, particularly when more than two centriolar complexes were present (Fig. 3e).

In macrocephalic multiflagellate sperm the head (nuclear) base was distinctly wider (average width 1.02 ± 0.13µm) than that of multiflagellate sperm of normal dimensions (average width 0.66 ± 0.05µm) and did not display the degree of peripheral attenuation typical of these cells. The larger heads comfortably accommodated the supernumerary centriolar complexes within the confines of the nuclear base. In instances where more than two proximal centrioles were present, the base of the nucleus presented a series of shallow depressions and the centrioles were compacted, with little space between them (Fig. 3e). All other structural features were similar to those described for normal-sized multiflagellar sperm. When three or more centriolar complexes were present they were circularly arranged beneath the nuclear base (Figs. 4a,b).

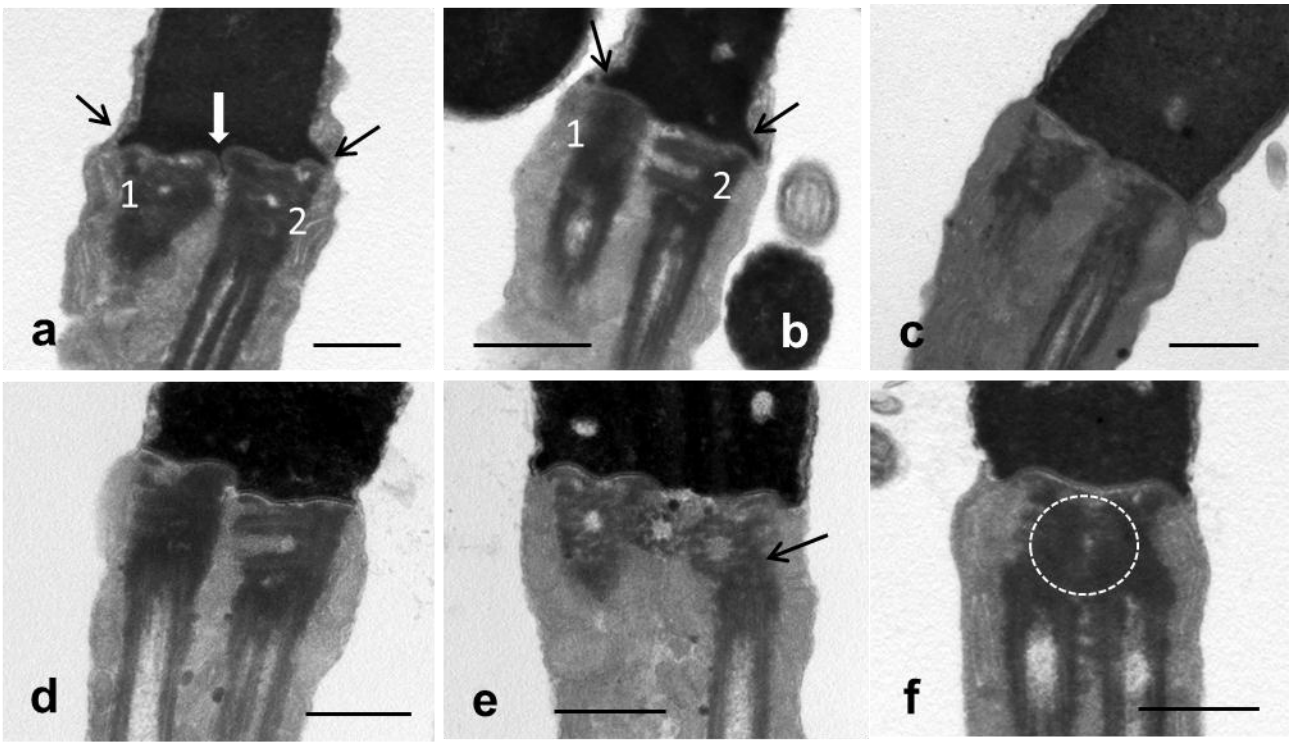

Figure 3. Transmission electron micrographs of the head-base, neck and proximal midpiece of multiflagellate sperm. Figs. 3(a) and (b) illustrate sperm of normal head dimensions. Note the widened but peripherally attenuated nuclear base (black arrows) and the medial spine of karyoplasm (white arrow). The proximal centriolar pair (1 and 2) is similarly oriented in (a) but alternately oriented in (b) (see also Fig. 3d). Figs. 3 (c) to (f) represent macrocephalic multiflagellate sperm. The nuclear base appears flat (c), stepped (d) or scalloped (e) and does not display the lateral flaring observed in (a) and (b). In (e) note the close apposition of the triple proximal centrioles and the misalignment of the one set of proximal and distal centrioles (black arrow). In Fig. 3(f) only one proximal centriole (outlined) is obvious and shares contact with the two distal centrioles. Bar = 0.5µm.

In all multiflagellate sperm the duplicated distal centrioles were arranged in parallel and extended the full length of the midpiece (from the neck region to the annulus). Each centriole was closely invested by its respective mitochondrial sheath although only a single row of mitochondria was present between adjacent centriolar complexes. This phenomenon was obvious in both longitudinal (Fig. 5) and transverse sections (Figs. 4a,b) of the midpiece. The impression on SEM that a double midpiece was present in some biflagellate sperm was not confirmed by TEM. The transition between the midpiece and principal piece was marked by a poorly developed but distinct annulus. The individual principal pieces of multiple flagella emerged freely from the collective midpiece, although in some cells the proximal part of the respective principal pieces was bound together by the plasmalemma (Fig. 4c). The structural components of the midpiece and principal piece (axoneme, mitochondrial sheath, annulus and ribbed sheath) appeared normal.

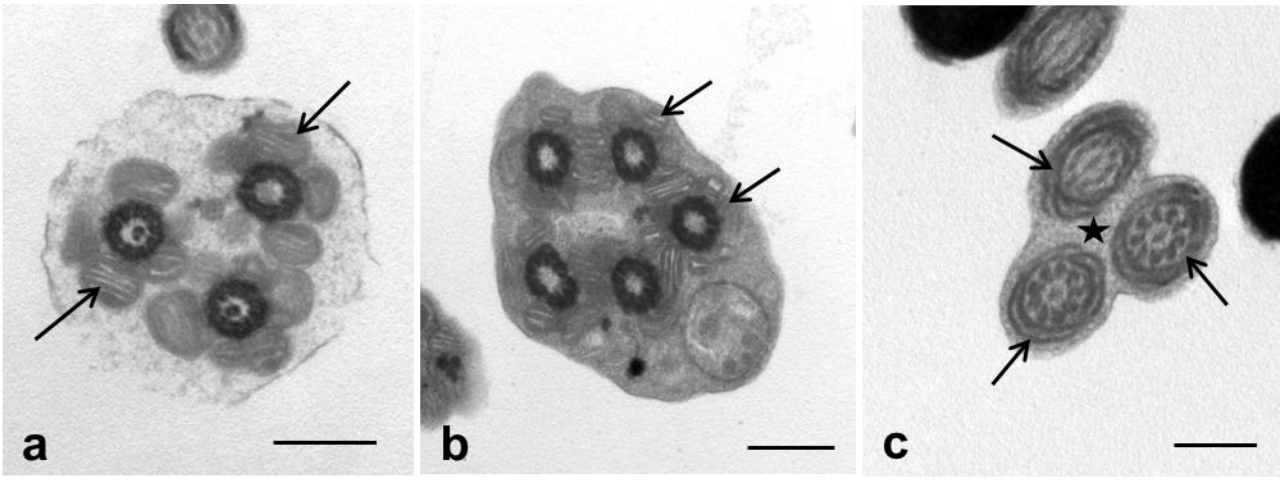

Figure 4. Transverse sections of the midpiece of multiflagellate sperm displaying three (a) and five (b) distal centrioles respectively. The centrioles are circularly arranged and are surrounded by their respective mitochondrial sheaths (arrows). Fig. 4(c) represents a transverse section through the proximal principal piece of a cell with triple tails bound together by the plasmalemma. Each tail demonstrates the typical fibrous sheath (arrows) and axoneme characteristic of this region. Flocculant material (star) occupies the space between the supernumerary tails. Bar = 0.5µm.

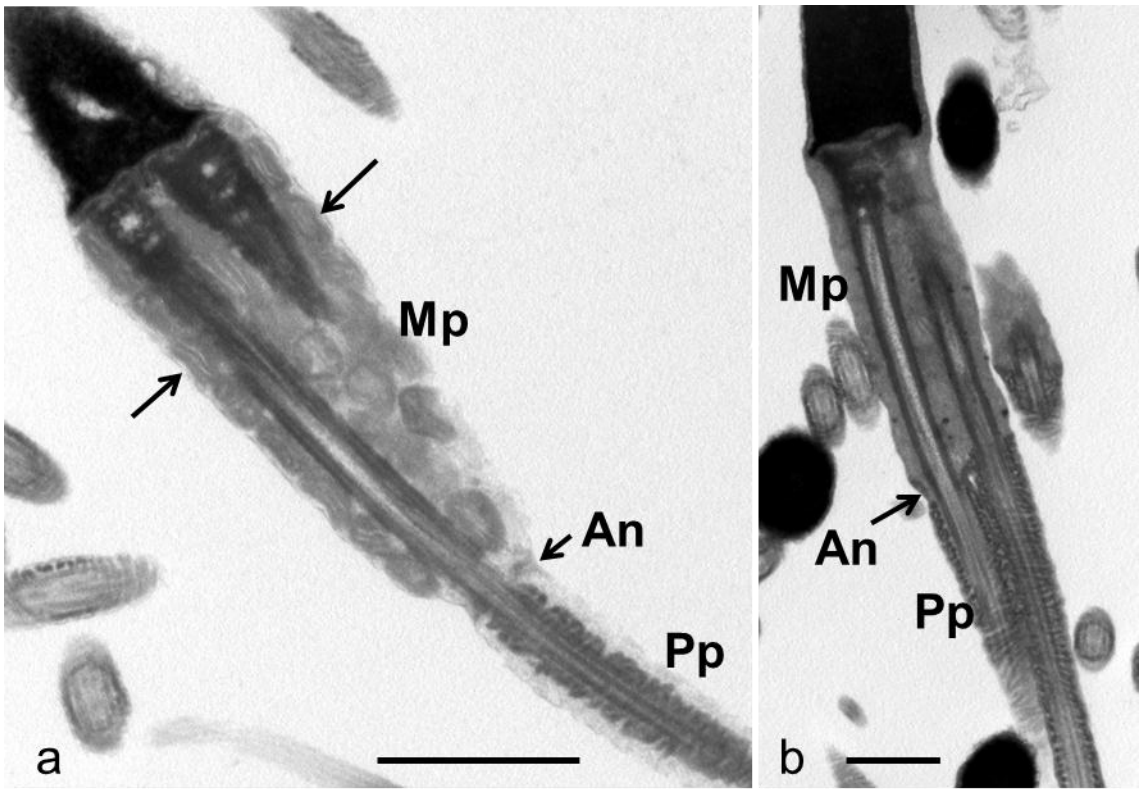

Figure 5. Longitudinal sections of biflagellate sperm showing the unitary midpiece (Mp) containing the twin centriolar complexes surrounded by their respective mitochondrial sheaths (arrows). In (a), due to the plane of section, only a single principal piece (Pp) appears to be present. The annulus (An) is indistinct. In (b) the twin principal pieces (Pp) emerge independently from the midpiece although they are closely apposed. Bar = 1µm.

Due to the paucity of the defect and the difficulty in obtaining favourable sections, coupled with the similarity in morphological features between secondary spermatocytes and round spermatids, it was not possible to determine at what stage of spermatogenesis centriolar duplication was initiated. In the

testis, the biflagellate form of the defect was again most obvious and was characterised by the appearance of twin centriolar complexes close to the nuclear membrane in round spermatids (Fig. 6a). Contact between the proximal centrioles and the nucleolemma occurred during this stage of spermiogenesis but was more obvious in spermatids displaying irregular-shaped nuclei (Fig. 6b). At this stage the twin implantation fossae and attendant structures around the proximal centriole (basal plate, forming capitellum, segmented columns) displayed the characteristic features of mature sperm. The irregular-shaped nucleus was surrounded by elements of the circular manchette and the chromatoid body was often closely associated with the centriolar complexes. The posterior aspect of the distal centriole was surrounded by a distinct annulus at its point of attachment to the plasmalemma (Fig. 6b). From this point the flagellar axoneme emerged and extended freely between the elements of the seminiferous epithelium. Early elongated spermatids (displaying coarse chromatin granules and the circular manchette) (Fig. 6c) and late elongated spermatids (with homogeneous, electron-dense chromatin and exhibiting the longitudinal manchette) displayed the morphological features typical of mature biflagellate sperm.

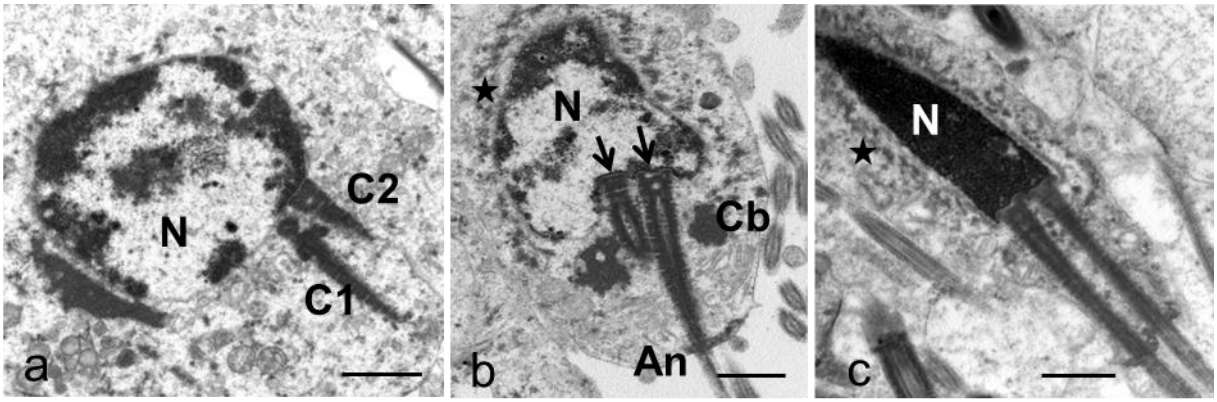

Figure 6. Various stages in the formation of biflagellate sperm in the testis. (a) A round spermatid demonstrating the close proximity of twin centriolar complexes (C1 and C2) to the nuclear membrane but without obvious attachment. (b) Spermatid with an irregular shaped nucleus showing attachment of the twin centriolar complexes (arrows). Note the presence of the circular manchette (star). (c) An elongated spermatid illustrating the typical positioning of the twin flagella relative to the nucleus. The nucleus contains coarse chromatin granules and the circular manchette (star) is still evident. Nucleus (N), chromatoid body (Cb), annulus (An). Bar = 1µm.

Discussion

Although multiflagellate sperm have been identified in a range of mammalian species, contrasting information has been presented on the occurrence (Barth & Oko, 1989; Brito, 2007) and incidence of this defect. Some reports suggest that, when present, the incidence of this anomaly is high (Nistal *et al*., 1977; Escalier, 1983; Kopp *et al*., 2007), while Pinart *et al*. (1998) regard it as a rare defect with a 1% incidence being considered normal. The literature on avian sperm defects is relatively silent on the occurrence, let alone incidence, of multiflagellate sperm in birds, probably due to the scarcity of the defect in this vertebrate group. The finding in the present study that multiflagellate sperm comprised on average only 1% of the total cell count reinforces this position.

In humans, multiple tails occur most frequently in association with macrocephalic sperm (Revay *et al*., 2010), with Escalier (1983) reporting an average of 3.6 flagella originating from each sperm head. A link between macrocephalic sperm and multiple flagella was also apparent in the emus studied where 0.6% of cells with multiple tails were associated with giant heads. In the Houbara bustard macrocephalic sperm are reported to occasionally be associated with multiple tails (Lindsay *et al*., 1999). Although macrocephalic sperm have been reported in other avian species (Wakely & Kosin, 1951; Malecki *et al*., 1998; Penfold *et al*., 2000; Klimowicz *et al*., 2005; Chelmońska *et al*., 2008), no mention is made of multiple tails or other defects associated with this anomaly. A more careful assessment of avian sperm defects may clarify this situation.

The structural features of multiflagellate sperm in the emu, particularly of the biflagellate form, were similar to those described in the drake (Maretta, 1979). The main features identified in both species were the duplicated (and apparently structurally normal) centriolar complexes occupying a common midpiece, peripheral widening of the nuclear base, duplicated shallow implantation fossae and sharing of mitochondria between adjacent centriolar complexes. The presence of a single proximal centriole associated with two distal centrioles was occasionally observed in both bird species. In common with defective drake sperm, the proximal part of the supernumerary principal pieces in the emu was sometimes contained within a common plasmalemma. However, the structurally deformed mitochondria of the midpiece and defective annulus reported in biflagellate drake sperm (Maretta, 1979), were not observed in the emu. The poorly developed annulus of emu sperm may account for this discrepancy.

Multiflagellate sperm in birds appear to share the basic structural features described in multiflagellate mammalian sperm (Nistal *et al*., 1977; Escalier, 1983; Barth & Oko, 1989). However, certain

disparities are apparent. The most obvious difference involves the accommodation of the supernumerary centriolar complexes beneath the nuclear base. In mammalian sperm the broad nuclear base provides enough space for the implantation of multiple tails, albeit abaxially (Barth & Oko, 1989). In emu and drake (Maretta, 1979) sperm of normal dimensions the narrow, cylindrical head base displays tenuous peripheral widening in order to accommodate the additional tails. This observation points to the pliability of the nuclear membrane and nuclear base during spermiogenesis in birds. This observation would clearly need to be tested in further studies. Another noticeable difference is the deep implantation fossae associated with mammalian sperm in contrast to the shallow fossae typical of the emu and drake. In multiple tailed human sperm, the axonemal complexes often appear to be defective (Nistal *et al*., 1977; Escalier, 1983). However, this was not observed in the emu.

Consensus of opinion would seem to suggest that multiflagellate sperm have a dual origin in mammals. On the one hand, disruption of meiotic division during spermatogenesis and the resultant production of diploid and polyploid cells (essentially the fusion of two or more potential sperm) would account for the high proportion of macrocephalic sperm with multiple tails reported in various animals and man (Barth & Oko, 1989; Weissenberg *et al*., 1998; Lewis-Jones *et al*., 2003; Kopp *et al*., 2007; Perrin *et al*., 2008; Revay *et al*., 2010). On the other hand, as suggested by several authors (Bartoov *et al*., 1980; Escalier, 1983; Lewis-Jones *et al*., 2003), abnormal cycles of centriole formation would similarly result in multiflagellate sperm. A similar situation is apparent in the emu as reflected in the proportion of macrocephalic multiflagellate sperm (0.6%) to multiflagellate sperm of normal dimensions (0.4%). Examination of testicular material suggests that multiflagellate sperm (particularly the biflagellate form) of normal dimensions are the result of duplication of the centriolar complex in the emu. However, convincing structural evidence of incomplete or disrupted meiotic division leading to large cells with multiple flagella was not observed. In birds, therefore, a distinction should be made between sperm of normal dimensions with multiple tails (classified as a tail defect) resulting from abnormal centriolar duplication and macrocephalic sperm with multiple tails (classified as a multiple defect – macrocephalic and multiflagellate) formed through incomplete cytokinesis (Du Plessis & Soley, 2011a).

A high percentage of multiple tails in man and bulls has been reported to adversely affect motility and fertility (Nistal *et al*., 1977; Escalier, 1983; Barth & Oko, 1989; Kopp *et al*., 2007). However the low incidence of this defect in mammals would suggest that it has little influence on fertility. Multiflagellate sperm constituted only 1% of the total cell count in the emus studied and consequently would have

had little effect on semen quality and fertility in this species. However, the occurrence of this defect indicates a serious disturbance of normal spermiogenesis which, in instances where the incidence is high, could have a marked influence on fertility in avian species

References

Alkan, S., Baran, A., Özdas, Ö.B. & Evecen, M. (2002) Morphological defects in turkey semen. *Turkish Journal of Veterinary and Animal Science* **26**, 1087-1092.

Arns, M.J., Neck, K.F., Evans, J.W. & Caceci, T. (1988) Ultrastructural abnormalities in equine spermatozoa from a cryptorchid stallion. *Journal of Equine Veterinary Science* **8**, 122-124.

Barth, A.D. & Oko, R.J. (1989) Abnormal Morphology of Bovine Spermatozoa. Iowa State University Press, Ames.

Bartoov, B., Eltes, F., Weissenberg, R. & Lunenfeld, B. (1980) Morphological characteristics of abnormal human spermatozoa using transmission electron microscopy. *Archives of Andrology* **5**, 305-322.

Bertschinger, H.J., Burger, W.P., Soley, J.T. & de Lange, J.H. (1992) Semen collection and evaluation of the male ostrich. *Proceedings of the Biennial Congress of the South African Veterinary Association*, Grahamstown, pp. 154-158.

Bonato, M., Rybnik, P.K., Malecki, I.A., Cornwallis, C.K. & Cloete, S.W.P. (2011) Twice daily collection yields greater semen output and does not affect male libido in the ostrich. *Animal Reproduction Science* **123**, 258-264.

Bonet, S. & Briz, M. (1991) New data on aberrant spermatozoa in the ejaculate of *Sus domesticus*. *Theriogenology* **35**, 725-730.

Brito, L.F.C. (2007) Evaluation of stallion sperm morphology. *Clinical Techniques in Equine Practice* **6**, 249-264.

Briz, M.D., Bonet, S., Pinart, E. & Camps, R. (1996) Sperm malformations throughout the boar epididymal duct. *Animal Reproduction Science* **43**, 221-239.

Chelmońska, B., Jerysz, A., Łukaszewicz, E., Kowalczyk, A. & Malecki, I. (2008) Semen collection from Japanese quail (*Coturnix japonica*) using a teaser female. *Turkish Journal of Veterinary and Animal Science* **32**, 19-24.

Ciereszko, A., Rybnik, P.K., Horbańczuk, J.O., Dietrich, G.J., Deas, A. & Słowińska, M. (2010) Biochemical characterization and sperm motility parameters of ostrich (*Struthio camelus*) semen. *Animal Reproduction Science* **122**, 222-228.

Cooper, T.G., Björndahl, L., Vreeburg, J. & Nieschlag, E. (2002) Semen analysis and external quality control schemes for semen analysis need global standardization. International *Journal of Andrology* **25**, 306-311.

Du Plessis, L. & Soley, J.T. (2011a) Incidence, structure and morphological classification of abnormal sperm in the emu (*Dromaius novaehollandiae*). *Theriogenology* **75**, 589-601.

Du Plessis, L. & Soley, J.T. (2011b) Head-base bending and disjointed spermatozoa in the emu (*Dromaius novaehollandiae*): a morphological comparison of two closely related defects. *Theriogenology* **76**, 1258-1265.

Du Plessis, L. & Soley, J.T. (2012) Abaxial tail implantation in the emu, *Dromaius novaehollandiae*: morphological characteristics and origin of a rare avian sperm defect. *Theriogenology* **77**, 1137-1143.

Escalier, D. (1983) Human spermatozoa with large heads and multiple flagella: a quantitative ultrastructural study of 6 cases. *Biology of the Cell* **48**, 65-74.

Ferdinand, A. (1992) Licht- und elektronenmikroskopische Untersuchungen zur Morphologie von Ganterspermatozoen. Dissertation zur erlangung des grades eines Doctor Medicinae Veterinariae. Hannover.

Gee, G.F. & Temple, S.A. (1978) Artificial insemination for breeding non-domestic birds. *Symposium Zoological Society, London* **43**, 51-72.

Gee, G.F. & Sexton, T.J. (1990) Cryogenic preservation of semen from the Aleutian Canada goose (*Branta Canadensis leucopareia*). *Zoo Biology* **9**, 361-371.

Gee, G.F., Bertschinger, H., Donoghue, A.M., Blanco, J. & Soley, J.T. (2004) Reproduction in nondomestic birds: Physiology, semen collection, artificial insemination and cryopreservation. *Avian and Poultry Biology Reviews* **15**, 47-101.

Holstein, A.F., Roosen-Runge, E.C. & Schirren, C. (1988) Illustrated Pathology of Human Spermatogenesis. Grosse Verlag, Berlin.

Holstein, A.F. (1975) Morphologische studien an abnormen spermatiden und spermatozoon des menschen. *Virchows Archiv A – Pathological Anatomy and Histopathology* **367**, 93-112.

Hotchkiss, R.S., Brunner, E.K. & Grenley, P. (1938) Semen analysis of two hundred fertile men. *American Journal of Medical Science* **196,** 362-384.

Jørgensen, N., Auger, J., Giwercman, A., Irvine, D.S., Jensen, T.K., Jouannet, P., Keiding, N., Le Bon, C., Macdonald, E., Pekuri, A-M., Scheike, T., Simonsen, M., Suominen, J. & Skakkebœk, N.E. (1997) Semen analysis performed by different laboratory teams: an intervariation study. *International Journal of Andrology* **20**, 201-208.

Kamar, G.A.R. & Rizik, M.A.A. (1972) Semen characteristics of two breeds of turkeys. *Journal of Reproduction and Fertility* **29**, 317-325.

Klimowicz, M., Łukaszewicz, E. & Dubiel, A. (2005) Effect of collection frequency on quantitative and qualitative characteristics of pigeon (*Columba livia*) semen. *British Poultry Science* **46**, 361-365.

Kopp, C., Sukura, A., Tuunainen, E., Gustavsson, I., Parvinen, M. & Anderson, M. (2007) Multinuclear-multiflagellar sperm defect in a bull – a new sterilizing sperm defect. *Reproduction in Domestic Animals* **42**, 208-213.

Lewis-Jones, I., Aziz, N., Seshadri, S., Douglas, A. & Howard, P. (2003) Sperm chromosomal abnormalities are linked to sperm morphologic deformities. *Fertility and Sterility* **79**, 212-215.

Lindsay, C., Staines, H.J., McCormick, P., McCullum, C., Choulani, F. & Wishart, G.J. (1999) Variability in the size of the nucleus in spermatozoa from the Houbara bustards, *Chlamydotis undulate undulate*. *Journal of Reproduction and Fertility* **117**, 307-313.

MacLeod, J. & Gold, R.Z. (1951) The male factor in fertility and infertility, IV: sperm morphology in fertile and infertile marriage. *Fertility and Sterility* **2**, 394-414.

Malecki, I.A., Cummins, J.M., Martin, G.B. & Lindsay, D.R. (1998) Effect of collection frequency on semen quality and the frequency of abnormal forms of spermatozoa in the emu. *Animal Production in Australia* **22**, 406.

Malecki, I.A., Rybnik, P.K. & Martin, G.B. (2008) Artificial insemination technology for ratites: a review. *Australian Journal of Experimental Agriculture* **48**, 1284-1292.

Maretta, M. (1979) Ultrastructure of double and multiple sperm tails in drakes. *Veterinarni Medicina* **24**, 679-689.

Marvan, F., Rob, O. & Janeckova, E. (1981) Classification of morphological abnormalities of gander sperm. *Zuchthygiene* **16**, 176-183.

Nistal, M., Paniagua, R. & Herruzo, A. (1977) Multi-tailed spermatozoa in a case with asthenospermia and teratospermia. *Virchow Archiv B. Cell Pathology* **26**, 111-218.

Nwakalor, L.N., Okeke, G.C. & Njoku, D.C. (1988) Semen characteristics of the guinea fowl *Numida meleagris meleagris*. *Theriogenology* **29**, 545-554.

Oettlé, E.E. & Soley, J.T. (1988) Sperm abnormalities in the dog: a light and electron microscopic study. *Veterinary Medical Review* **59**, 28-70.

Penfold, L.M., Wildt, D.E., Herzog, T.L., Lynch, W., Ware, L., Derrickson, S.E. & Monfort, S.L. (2000) Seasonal patterns of LH, testosterone and semen quality in the Northern pintail duck (*Anas acuta*). *Reproduction, Fertility and Development* **12**, 229-235.

Perrin, A., Morel, F., Moy, L., Colleu, D., Amice, V. & De Braekeleer, M. (2008) Study of aneuploidy in large-headed, multiple-tailed spermatozoa: case report and review of the literature. *Fertility and Sterility* **90**, 13-17.

Pinart, E., Camps, R., Briz, M.D., Bonet, S. & Egozcue, J. (1998) Unilateral spontaneous abdominal cryptorchidism: structural and ultrastructural study of sperm morphology. *Animal Reproduction Science* **49**, 247-268.

Revay, T., Kopp, C., Flyckt, A., Taponen, J., Ijäs, R., Nagy, S., Kovacs, A., Rens, W., Rath, D., Hidas, A., Taylor, J.F. & Andersson, M. (2010) Diploid spermatozoa caused by failure of the second meiotic division in a bull. *Theriogenology* **73**, 421-428.

Soley, J.T. & Els, H.J. (1993) The ultrastructure of retained cytoplasmic droplets in ostrich spermatozoa. *Proceedings of the Microscopy Society of Southern Africa* **23**, 58.

Soley, J.T., Bertschinger, H.J., Els, H.J. & Burger, W.P. (1996) The morphology and incidence of retained cytoplasmic droplets in ostrich spermatozoa. In: Deeming, D.C. (ed.) Improving our Understanding of Ratites in a Farming Environment. Ratite Conference, Manchester, pp. 16-18.

Sood, S., Malecki, I.A., Tawang, A. & Martin, G.B. (2011) Response of spermatozoa from the emu (*Dromaius novaehollandiae*) to rapid cooling, hyperosmotic conditions and dimethylacetamide (DMA). *Animimal Reproduction Science* **129**, 89-95.

Stelzer, G., Crosta, L., Bürkle, M. & Krautwald-Junghanns, M-E. (2005) Attempted semen collection using the massage technique and semen analysis in various psittacine species. *Journal of Avian Medicine and Surgery* **19**, 7-13.

Tabatabaei, S., Batavani, R.A. & Talebi, A.R. (2009) Comparison of semen quality in Indigenous and Ross broiler breeder roosters. *Journal of Animal and Veterinary Advances* **8**, 90-93.

Wakely, W.J. & Kosin, I.L. (1951) A study of the morphology of the turkey spermatozoa with special reference to the seasonal prevalence of abnormal types. *American Journal of Veterinary Research* **12**, 240-245.

Umapathy, G., Sontakke, S., Reddy, A., Ahmed, S. & Shivaji, S. (2005) Semen characteristics of the captive Indian white-backed vulture. *Biology of Reproduction* **73**, 1039-1045.

Weissenberg, R., Aviram, A., Golan, R., Lewin, L.M., Levron, J., Madgar, I., Dor, J., Barkai, G. & Goldman, B. (1998) Concurrent use of flow cytometry and fluorescence in-situ hybridization techniques for detecting faulty meiosis in a human sperm sample. *Molecular Human Reproduction* **4**, 61-68.

Zamboni, Z. (1992) Sperm structure and its relevance to infertility: an electron microscopic study. *Archives of Pathology and Laboratory Medicine* **116**, 325-344.

Chapter 9 Morphology and origin of abnormal sperm IV: Miscellaneous defects

Introduction

Besides the anomalies described in the previous chapters, a number of additional defects affecting various regions of the sperm were observed in the emu samples studied. These defects were generally present in small numbers and, by virtue of their morphological peculiarities and scarcity, were difficult to view ultrastructurally. Individual birds with a high incidence of defects will be required to provide a more accurate account of the anomalies and their ontogeny. The term "miscellaneous" is used here in the chapter title to describe those defects presented in the classification of emu sperm defects (see Chapter 5) that have not been specifically described in the preceding chapters and does not indicate a set of defects for which specific categories could not be chosen.

The fragility of the head and neck regions of sperm has been well established and various reports have highlighted this weakness in both mammalian and avian sperm (Lake, 1954; Saeki, 1960; Afzelius, 1996; Chemes & Rawe, 2003). This was also the case in the emu (see Chapter 5) with most of the sperm defects observed occurring in the head region (52% of total defects). Various forms of bent heads were the most prevalent defect in the emu samples, representing approximately 28% of the total number of aberrations observed. Other forms of defective heads, such as macrocephalic, microcephalic, round-headed and acephalic sperm were also present, albeit less frequently. The presence of these particular defects has repeatedly been observed in mammals, for example in man (Dadoune, 1988; Zamboni, 1992; Afzelius, 1996; Chemes & Rawe, 2003, 2010), bulls (Barth & Oko, 1989), red wolf (Koehler *et al*., 1998); stallions (Kavak *et al.,* 2004), black bears (Brito *et al*., 2010), as well as a number of birds (Wakely & Kosin, 1951; Kamar & Rizik, 1972; Marvan *et al*., 1981; Nwakalor *et al*., 1988; Ferdinand, 1992; Malecki *et al*., 1998; Lindsay *et al*., 1999; Penfold *et al*., 2000; Alkan *et al*., 2002; Sontakke *et al*., 2004; Umapathy *et al*., 2005; Tabatabaei *et al*., 2010) and detailed descriptions of their morphology presented.

In contrast to the prevalence of head defects, anomalies of the tail were less frequently observed in the emu. Various tail defects, including those seen in the emu, have been reported in mammals (Barth & Oko, 1989; Briz *et al*., 1996; Koehler *et al*., 1998; Chemes *et al*., 1999; Kavak *et al*., 2004; Chemes & Sedo, 2012) and birds (Wakely & Kosin, 1951; Kamar & Rizik, 1972; Marvan *et*

al., 1981; Nwakalor *et al*., 1988; Ferdinand, 1992; Malecki *et al*., 1998; Lindsay *et al*., 1999; Penfold *et al*., 2000; Alkan *et al*., 2002; Sontakke *et al*., 2004; Umapathy *et al*., 2005; Tabatabaei *et al*., 2010). Most of these defects were found in the neck/midpiece region of the tail, either as abaxial tail implantation or disjointed sperm (see Chapters 6 and 7), representing 16% of total defects. Defects of the principal piece were less prominent (10% of total defects) and included tail coiling, stump tails and multiflagellate tails (see Chapter 8).

The morphology and positioning of the mammalian cytoplasmic droplet has been well described (Barth & Oko, 1989; Brito *et al*., 2010). Despite the fact that some reports question the existence of the avian cytoplasmic droplet, this structure has been noted in birds (Penfold *et al*., 2000; Sontakke *et al*., 2004; Umapathy *et al*., 2005). It appears to be a common defect in ratites. Bertschinger *et al*. (1992) considered the presence of cytoplasmic droplets to be common in ostriches, while Soley and Els (1993) gave a detailed description on the ultrastructure of droplets in the same species. Similarly, Malecki *et al*. (1998) found a high percentage of cytoplasmic droplets present in emu ejaculates.

This chapter examines the morphology of these additional forms of sperm defects in the emu using light and electron microscopy and provides a comprehensive description of the morphological characteristics of the defects. In addition, where feasible, the origin and development of the defects are also presented.

Materials & Methods

Semen and testicular tissue samples were collected during mid-breeding season from 15 clinically healthy, sexually active emus following slaughter at commercial abattoirs. The semen samples were immediately fixed in 2.5% glutaraldehyde in 0.13M Millonig's phosphate buffer, pH 7.4 and prepared for light microscopy (LM) as well as transmission (TEM) and scanning electron microscopy (SEM) as described in Chapter 2. Small blocks of testicular tissue were fixed in 4% glutaraldehyde in 0.13M Millonig's phosphate buffer, pH 7.4 and prepared for TEM as described in Chapter 3. Thin sections of both the pelleted sperm samples and testicular tissue were stained with lead citrate and uranyl acetate and viewed in a Philips CM10 transmission electron microscope (Philips Electron Optical Division, Eindhoven, The Netherlands) operated at 80kV. Relevant features of the anomalies and stages of their development in the testis, where feasible, were described and digitally recorded.

Linear measurements comparing the head lengths of normal (n = 370) and apparently diploid sperm (macrocephalic heads; n = 46) were obtained using light micrographs. Measurements

were processed using the Soft Imaging System iTEM software (Olympus, Műnster, Germany) and expressed as the mean ± SD.

Results

Head defects

In addition to the more prevalent head-base bending described in Chapter 6, various other forms of head bending could be distinguished. Bending varied from simple 90° bends in the body of the nucleus (see Chapter 5, Figure 1e) to more acute bends. Other forms of head bending observed included spiralling (a corkscrew appearance of the head), kinking (a single twist of the head, generally towards the base) or looping of the nucleus (the formation of a single coil of the head) (Fig. 1). These forms of head defects were only rarely observed on LM and SEM, and due to their scarcity, difficult to observe on TEM. For the same reasons it was also not possible to identify the defects during spermiogenesis in the testis.

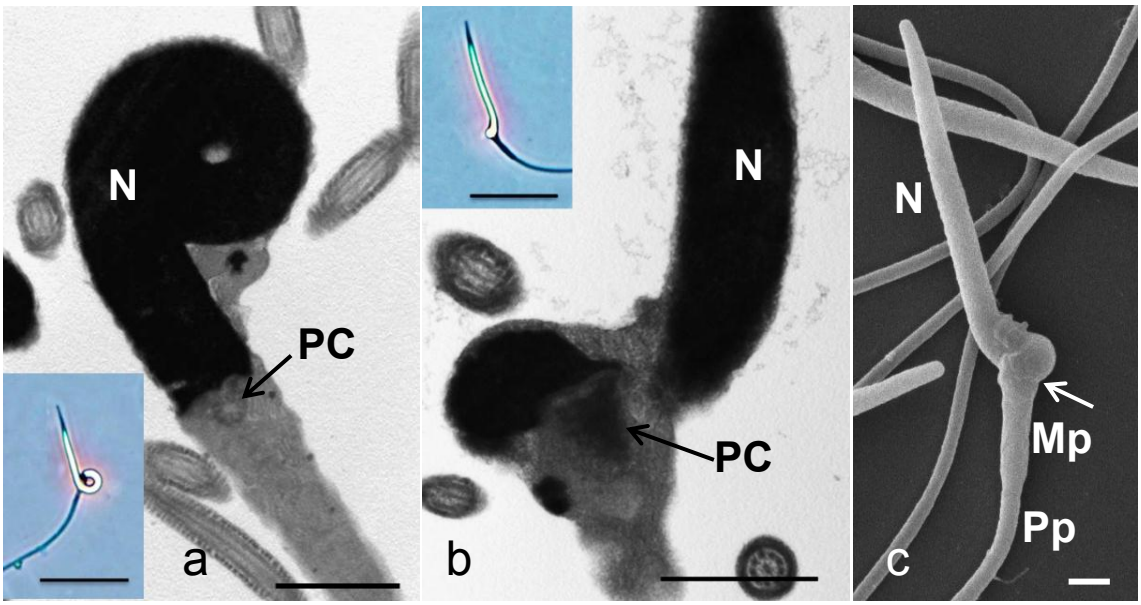

Figure 1. Head defects. (a) Looped sperm heads revealed by transmission electron microscopy and light microscopy (inset). (b,c) Sperm head kinking as seen in longitudinal section and scanning electron microscopy respectively. The arrow in (c) indicates the head-base/midpiece junction. The inset in (b) is a typical view of a kinked sperm head as observed on a semen smear. Nucleus (N); proximal centriole (PC), midpiece (Mp), principal piece (Pp). Bar (a-c) = 1µm, insets Bar = 10µm.

Macrocephalic heads were markedly longer (approximately 50%) than normal heads (Fig. 2), measuring 17.86 ± 1.87µm while the average length of normal heads was 11.02 ± 0.78µm. Macrocephalic heads were associated with either a single tail or multiple tails and were readily identified in semen samples using both light and electron microscopy (See Chapter 8 on

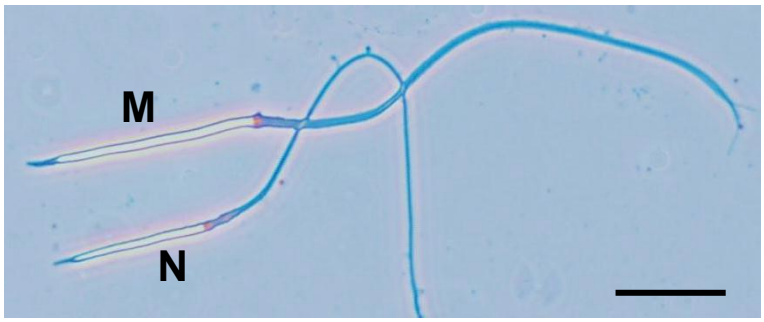

Figure 2. Light micrograph illustrating a sperm of normal dimensions (N) and a sperm with a macrocephalic head (M). The difference in head lengths can clearly be seen. The macrocephalic cell also displays a double tail. Bar = 10µm.

multiflagellate sperm). Structurally, the larger heads of macrocephalic sperm were similar to those of normal sized sperm. Based on their larger dimensions, macrocephalic sperm could be discerned during the later stages of their development in the seminiferous epithelium. No structural differences in the formation of the macrocephalic sperm could be observed.

Microcephalic sperm were sporadically noted on LM and SEM (Fig. 3a, b). The small heads were spherical (Fig. 3a and inset) to pear-shaped (Fig. 3b and inset) and in most instances revealed a projection resembling the acrosome. The nucleus was much reduced in size, and on phase contrast LM appeared as an obvious, illuminated structure producing the same glowing effect as normal nuclei when using this form of microscopy. TEM sections of microcephalic sperm demonstrated a small round nucleus with condensed chromatin surrounded by a thin layer of cytoplasm (Fig. 3c). In some instances (Figs. 3b,c) the defective cells displayed an abnormally formed midpiece.

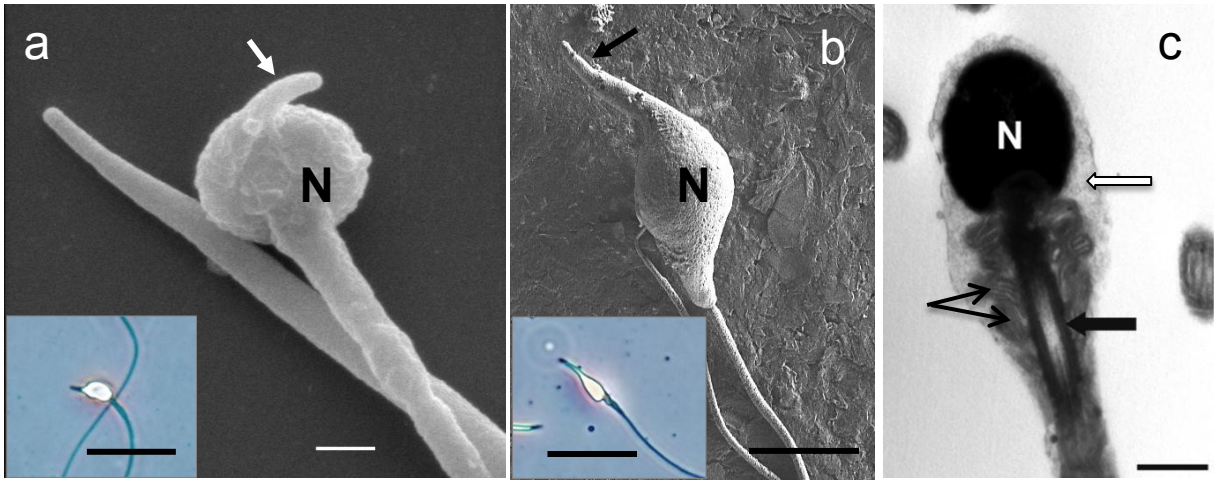

Figure 3. Scanning electron micrographs showing (a) a round-headed form and (b) a pear-shaped form of microcephalic sperm. Note the typical acrosome (arrows) projecting from the tip of the nucleus. The respective insets illustrate the typical appearance of the defect as seen by phase contrast microscopy. Note the glowing nature of the nuclear material. (c) Longitudinal section through a round-headed sperm. Note the homogenous electron-dense nucleus (N), the mitochondrial sheath (black arrows) surrounding the proximal and distal centrioles (black block arrow) of the aberrant midpiece and the surrounding thin layer of cytoplasm (white block arrow). Bar (light micrographs) = 10µm; Bar (electron microscope images) = 1µm.

Acephalic sperm were easily recognized on LM and SEM (Fig. 4). On LM the cell consisted of a complete flagellum (midpiece, principal piece and endpiece) of normal dimensions and morphology but devoid of a head. The apical tip of such cells often appeared as a small swelling. The swelling presumably represented retained residual cytoplasm and elements of the midpiece because phase contrast microscopy revealed a total absence of nuclear material (lack of illumination), thus eliminating the possibility that these cells were microcephalic sperm. At the ultrastructural level the tip of the cell either appeared as a small bulbous swelling (Fig. 4) or as a typical midpiece (Fig. 4 inset a). Acephalic cells were difficult to recognize on TEM due to the difficulty in obtaining the correct plane of section. In cells with a bulbous tip the excess cytoplasm (enclosed by the plasmalemma) was clearly visible (Figs. 5a, b) surrounding the randomly distributed mitochondria. In some defective cells the mitochondria were more systematically organized and arranged around the centriolar complex as in normal sperm, except that the organelles also surrounded the proximal centriole anteriorly (Fig. 5c). There were no tailless heads observed in any of the samples studied.

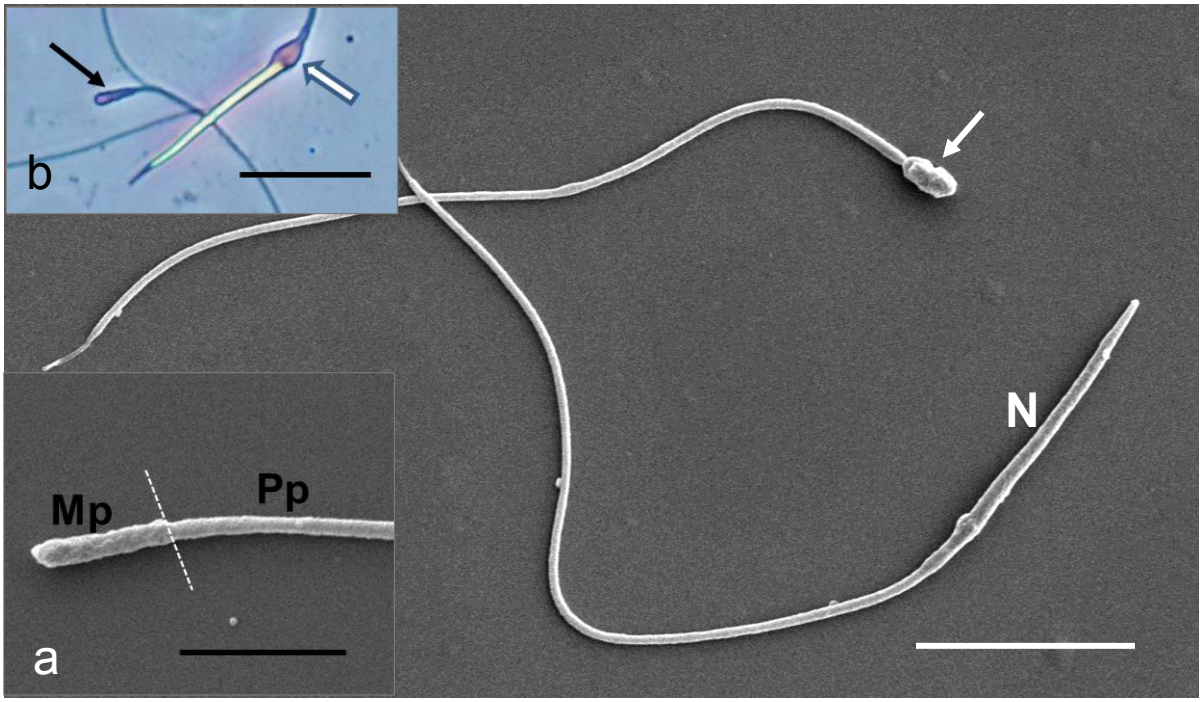

Figure 4. Scanning electron micrograph of a normal (N) and an acephalic sperm (arrow). Note the obvious absence of a head. The neck/midpiece appears swollen, while in inset (a) this region appears normal with the mitochondrial profiles visible. Inset (b) represents the swollen form of an acephalic sperm (arrow) as shown by phase contrast light microscopy. The white arrow illustrates the visual similarities between an acephalic sperm and the midpiece of a normal sperm as seen by light microscopy. Note the obvious difference between this cell and the microcephalic sperm illustrated in Fig. 3a & b insets. Midpiece (Mp), principal piece (Pp). Bar = 10µm; Bar inset (a) = 5µm; Bar inset (b) = 10µm.

Examination of thin sections of the seminiferous epithelium revealed two ways in which the defect could be formed. In the first instance, already discernible in phase 1 spermatids, the centriolar complex was completely misaligned in respect of the nuclear implantation fossa although normal contact with the plasmalemma was established via the annulus (Fig. 6). Although morphological evidence was not obtained, this arrangement clearly separated the two components (head and tail) of the cell, the tail presumably being freed during spermiation and the head being internalized by the Sertoli cells.

In the second instance, the centriolar complex showed normal alignment in respect of the implantation fossa but without contact being made between the two components. In some defective cells the proximal centriole was seen positioned within the implantation fossa but separated from the distal centriole by a wide cytoplasmic space (Fig. 7). Both centrioles appeared morphologically normal but with no connection between the two. In this instance the tail would again be freed during sperm release, but the head retained.

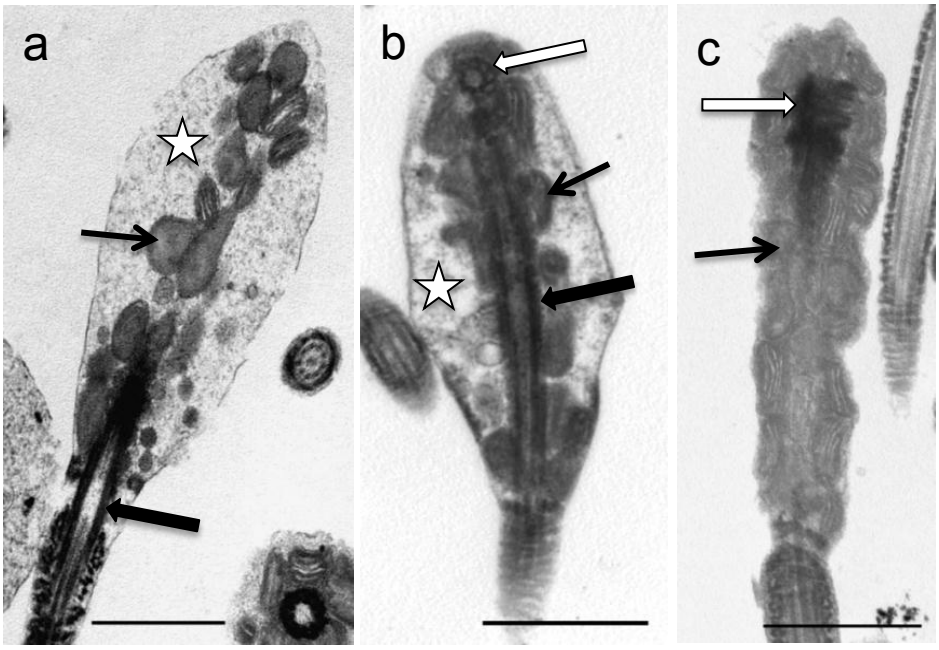

Figure 5. Transmission electron micrographs of acephalic sperm. Note in (a) and (b) the excess cytoplasm (star) surrounding the mitochondria (black arrow), giving the midpiece a bulbous appearance. In (b) and (c) the proximal (white block arrow) and distal centrioles (black block arrow) are visible, indicating true sections of the acephalic sperm. In (c) the mitochondria (black arrow) are more evenly arranged along the distal centriole and completely surround the proximal centriole (white arrow). No excess cytoplasm surrounds the midpiece. Bar = 1µm.

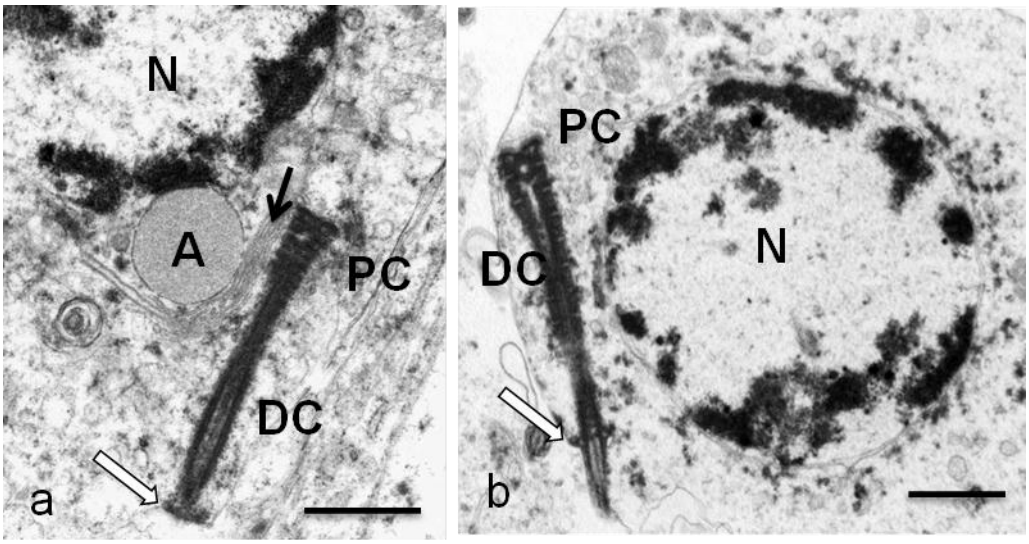

Figure 6. In (a) the acrosomal vesicle (A) is attached to the nucleus (N) and separated from the grossly misaligned proximal (PC) and distal (DC) centrioles by elements of the Golgi apparatus (arrow). The distal centriole is attached to the plasmalemma by the annulus (white block arrow). A similar situation is apparent in (b) where the proximal centriole (PC) is far removed from the nuclear membrane. Note the flagellum emerging from the annulus (white block arrow) at the base of the distal centriole (DC).Nucleus (N). Bar = 1µm.

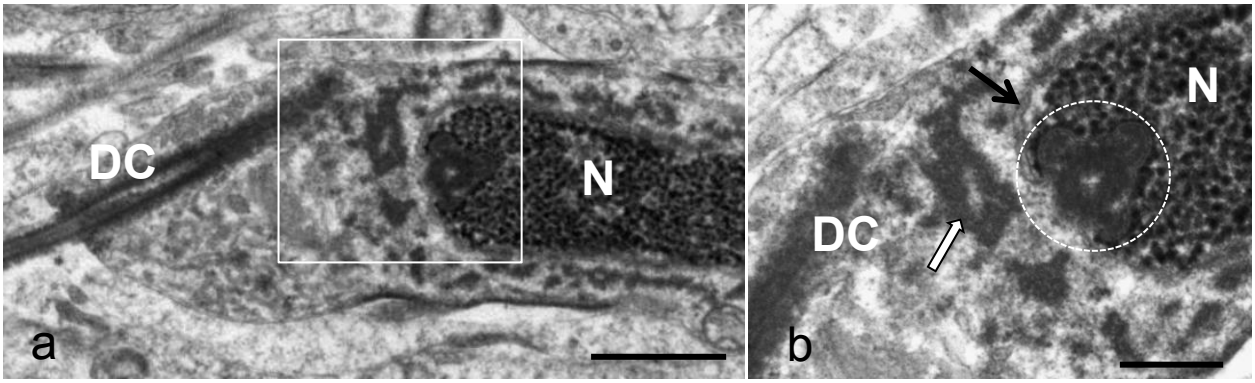

Figure 7. An early phase 3 spermatid displaying the formation of an acephalic cell. In (a) note the slightly angled orientation of the distal centriole (DC) which is misaligned in respect of the nuclear (N) base. The flagellum emerges from the free end of the centriole. The square in (a) is enlarged in (b). (b) Note the position of the proximal centriole (encircled) within the base of the nucleus (N) and clearly unconnected with the distal centriol (DC). Note the electron-dense material (white arrow) representing the chromatoid body, associated with the circular manchette. This material effectively separates the two centrioles. Nuclear membrane (black arrow). Bar (a) = 1µm; Bar (b) = 0.5µm.

Tail defects

Miscellaneous tail defects manifested as stump (short) tails and coiled tails, with both defects involving the principal piece of the flagellum. Stump tails were rarely observed (3.8% of total sperm defects). On light microscopy stump-tailed sperm revealed an apparently normal head from which a short tail, composed of the midpiece and a short segment of the principal piece, emerged. This defect was not observed at the ultrastructural level in either semen samples or testicular samples probably due to its scarcity. Some forms of tail coiling in which a shortened principal piece was observed tightly coiled beneath the midpiece (Figs. 8c, 10b) may in fact also represent the stump tail defect.

Despite a low incidence of 3.3% of total defects, various forms of coiled tails were noted. Coiling was generally restricted to the region of the principal piece lying just distal to the midpiece. The coils, easily noticeably on LM and SEM, displayed either a figure of eight configuration (Fig. 8a), randomly distributed coils (Fig. 8b) or tightly and concentrically distributed coils (Figs. 8d,e). In some instances the coils appeared to be enclosed within the plasmalemma (Fig. 8c), but, again due to the limited number of cells with coiled tails in the material studied (both semen samples and testicular samples), missing or translocated elements of the axoneme, indicative of the 'Dag' defect, were not observed on TEM.

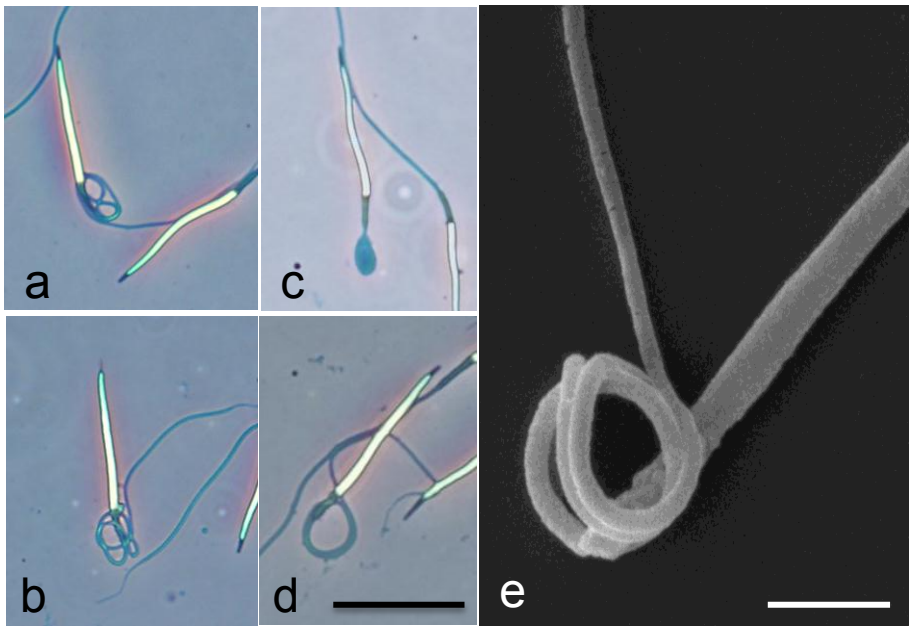

Figure 8. Various forms of tail coiling as observed by light and scanning electron microscopy. Note the location of the coils just beneath the head base but not involving the midpiece. (a) figure of eight coil; (b) randomly distributed coils; (c) coils confined within the plasmalemma; (d & e) concentric coils. Bar (a-d) = 10µm; Bar (e) = 2 µm.

Cytoplasmic droplets

Cytoplasmic droplets formed 10.5% of the total sperm defects observed in the emu samples. The droplets, which varied in size, were generally positioned around the base of the head and proximal part of the midpiece (Figs. 9a,d). Occasionally, droplets were eccentrically positioned to one side of the head, appearing to bend the head in the direction of the droplet (Figs. 9 b,c,d). The droplets were contained within the plasmalemma and consisted of a homogeneous, finely granular cytoplasmic matrix (Fig. 9d). There were rarely any organelles or vesicles seen within the droplets.

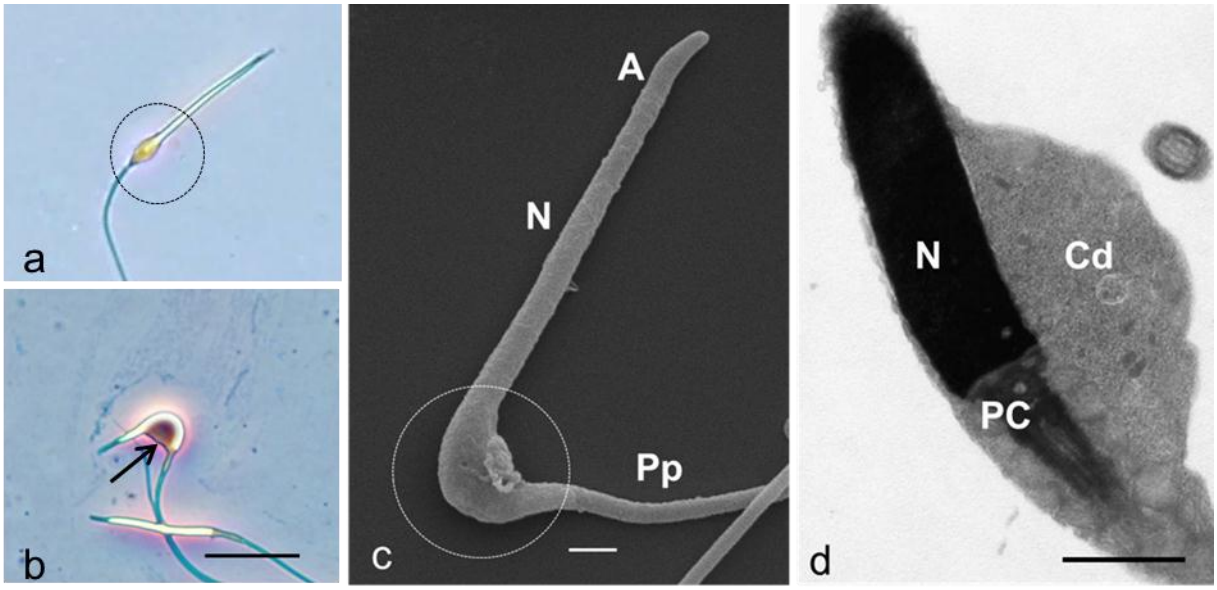

Figure 9. Cytoplasmic droplets. In the light micrograph (a) the droplet is seen positioned around the base of the head and part of the midpiece (circled), while in (b) it is associated exclusively with the head (arrow), causing it to bend acutely. (c) A droplet situated at the base of the head as seen by scanning electron microscopy, resulting in a 90° bend. (d) A longitudinal section through the head and midpiece displaying an eccentrically positioned droplet (Cd). Note the homogenous contents of the droplet. Acrosome (A), nucleus (N), principal piece (Pp), proximal centriole (PC). (a,b) Bar = 10µm; (c,d) Bar = 1µm.

Multiple defects

A number of sperm (11.5% of total sperm defects) displayed more than one abnormality simultaneously (Fig. 10). Multiple defects included for example, bent heads with multiple, short or coiled tails, macrocephalic sperm with multiple tails or cytoplasmic droplets, acephalic sperm with multiple tails or multiple-tailed sperm with droplets. Despite the limited numbers of these defects, they could readibly be seen by LM and SEM, but again, due to the low incidence it was difficult to detect their presence in thin sections with TEM.

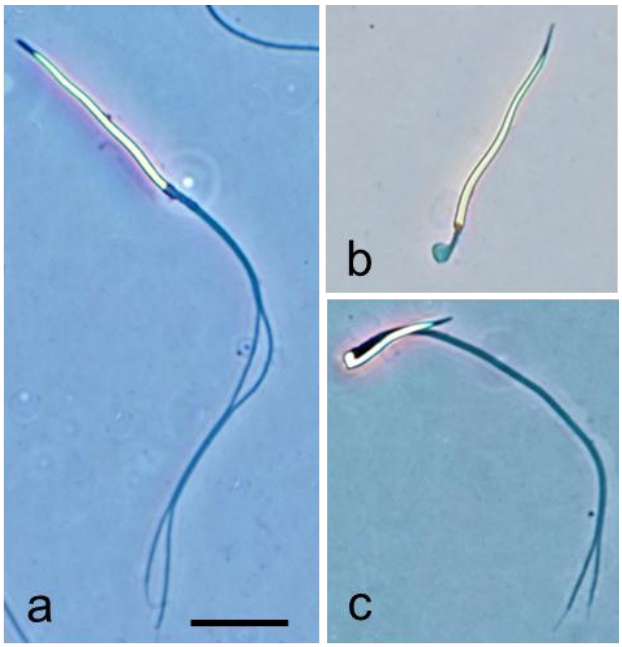

Figure 10. Examples of multiple defects as observed with the light microscope. (a) Macrocephalic sperm with two tails. (b) Macrocephalic sperm with a short, coiled tail. (c) Sperm of normal dimensions demonstrating head-base bending coupled with twin tails. Bar = 10µm.

Discussion

Sperm morphology is widely accepted as one of the three most important parameters for the accurate evaluation of semen quality (Guzick *et al*., 2001; Mortimer, 2002; Brito, 2007), yet for any given species there are no absolute values for what is considered 'normal'. For example, in stallions, 50% morphologically normal sperm is considered acceptable (Brito, 2007), while in humans, a fertile man may have only 12% sperm with normal morphology (Guzick *et al*., 2001). In birds the percentages of normal sperm are as varied. For example, Stelzer *et al*. (2005) reported a range of 42-92% morphologically normal sperm in a study on 40 individual birds (various parrot species).

The influence of breeding season on sperm morphology in ostriches was determined by Bertschinger *et al.* (1992). They reported an average of 77.5% normal sperm during mid-season, with the most common defects being midpiece reflexes, coiled tails (specifically the "Dag" defect), cytoplasmic droplets and abnormally shaped heads. Similarly, Rozenboim *et al*. (2003) and Irons *et al*. (1996) found the season to influence the quality of sperm in ostriches, while in geese (Marvan *et al*., 1981), an incidence of up to 30% morphologically abnormal sperm were noted at the beginning and end of the breeding season, with head defects forming up to 80% of the abnormalities observed. This seasonal trend was also observed in turkey semen (Wakely &

Kosin, 1951; Kamar & Rizik, 1972). Interestingly, in the present study performed on semen samples collected during the middle of the breeding season, most defects observed were also found in the head region.

Brito (2007) also reported on the influence of age in his review on sperm morphology in stallions. According to the review, abnormalities decreased after puberty (ineffective spermiogenesis prior to puberty) and increased again in animals with advancing age (testicular degeneration). Similar results were obtained by Tabatabaei *et al*. (2010) in their study on the correlation between age and semen quality in chickens which revealed that macrocephalic and microcephalic heads as well as 180° head bends increased with age, while tail defects decreased. As all the birds in this study were of normal breeding age, no indication of the effects of age on the incidence of sperm abnormalities could be determined.

Head defects

As noted above, head defects were the most prevalent sperm abnormality present in emu semen samples and constituted 52% of the total sperm defects. Similarly, Kamar and Badreldin (1959) found that most defects in chicken sperm were present in the head region. The shape of the sperm head is dictated by the shape of the nucleus, which in turn is determined by forces exerted on the developing spermatid by the surrounding Sertoli cells as well as by the influence of the manchette microtubules and chromatin condensation (Dadoune, 1995). The various manifestations of bent heads in emu sperm would probably have resulted from one or a combination of the above factors. The location of some of the forms of bending towards the nuclear base would also suggest involvement of the centriolar complex in these anomalies (see Chapter 6).

Micro- and macrocephalic heads are most likely to result from an uneven distribution of chromatin following abnormal cell division (Brito, 2007). Macrocephalic sperm have been noted in a number of avian species, including the chicken (Tabatabaei *et al*., 2009), turkey (Wakely & Kosin, 1951), goose (Ferdinand, 1992), Houbara bustard (Lindsay *et al*., 1999), guinea fowl (Nwakolor *et al*., 1988; Barna & Wishart, 2003), quail (Chelmońska *et al*., 2008), pigeon (Sontakke *et al*., 2004; Klimowicz *et al*., 2005) and golden eagle (Wishart *et al*., 1999). The presence of these giant cells has also been reported in the emu (Malecki *et al*., 1998). The incidence of macrocephalic sperm in pigeon semen is reported to decrease with increased frequency of collection (Klimowicz *et al*., 2005) although this could not be confirmed in a similar study in the emu (Malecki *et al*., 1998).

Macrocephalic sperm formed 11% of total sperm defects in the present study, and were often, but not always, associated with multiple tails. Malecki *et al*. (1998), however, reported a larger percentage of this abnormality (almost 40%) in the same species. Macrocephalic sperm have been observed in large numbers in Houbara bustard semen, ranging from 5 to 40% in individual birds, with the nucleus measuring up to twice the mean length of the nucleus of normal sperm (Lindsay *et al*., 1999). Based on this obvious size differential and on the intense diamidino-phenylindole (DAPI) staining seen throughout the nucleus, it was suggested that "these spermatozoa contained more than the haploid content of genetic material and that some were actually diploid" (Lindsay *et al*., 1999). The same reasoning seems to apply to mammals regarding the origin of giant heads (Mortimer, 2002; Pesh & Bergman, 2006; Sun *et al*., 2006). A similar situation is indicated in the present study where the giant heads identified by LM measured approximately 1.5 times the length of normal sized sperm heads.

The combined incidence of round-headed sperm and microcephalic sperm as classified in the present study (see Chapter 5) was low. However, these defects have also been observed in various other avian species (Nwakalor *et al*., 1988; Ferdinand, 1992; Penfold *et al*., 2000; Alkan *et al*., 2002). Ferdinand (1992) made a distinction between microcephalic sperm and round-headed sperm in the goose, although the illustrations in this regard are not entirely convincing. Subsequent ultrastructural examination of "microcephalic" and "round-headed" sperm in the emu revealed numerous morphological similarities between the two anomalies, questioning their classification as separate defects. In the emu, therefore, it is proposed that two forms of microcephalic sperm appear to be present; those with round heads and those with pear-shaped heads. The nucleus in both instances was greatly reduced in size and displayed an apparently normal acrosome. The presence of an acrosome in avian species seems to be a deviation from the typical mammalian round-headed sperm, which characteristically has no acrosome and often displays incompletely condensed chromatin (Zamboni, 1987; Afzelius, 1996; Chemes & Sedo, 2012).

This observation is challenged by a recent report in which two subtypes of round-headed sperm were observed in man; type 1 typically demonstrating an abnormal, spherical-shaped collection of chromatin with no acrocome present, and type 2, similar in structure but with an acrosome present (Carrell *et al*., 1999). Round-headed sperm reportedly have a genetic origin (Chenoweth, 2005). This was confirmed by Dam *et al*. (2007) who also noted that when present, most of the sperm will appear as round-headed cells. Zamboni (1987) stated that the anomaly develops because of an abnormal topographical relationship between a defective Golgi complex and the nucleus prior to formation of the acrosome and to the absence of the manchette microtubules. Ultrastructural features would seem to indicate that microcephalic sperm in the emu are the

product of defective spermiogenesis, specifically involving the failure of nuclear elongation. It would be interesting to determine whether this defect is the product of defective formation of the circular manchette which has been credited with initiating and maintaining nuclear elongation in a number of avian species, including the ostrich (Soley, 1997).

Neck/midpiece defects

A significant finding was the presence of acephalic sperm in all the emu samples studied. This abnormality has not previously been reported in ratite semen. Łukaszewicz *et al*. (2008) and Ferdinand (1992) both illustrate an abnormal sperm in fowl and goose semen respectively which appears remarkably similar to the acephalic sperm observed in the present study, but which is referred to as a spermatid (fowl) and a small round-headed sperm (goose). The absence of loose sperm heads in the emu semen smears or SEM samples would further indicate that the acephalic sperm observed did not result from sample preparation or mechanical damage. Zamboni (1987) reported that the defect with the greatest implications for fertility in mammals is separation of the sperm head from the flagellum. This defect has generally been referred to as the decapitated sperm defect and is particularly common in bulls (Blom & Birch-Anderson, 1970). The headless tails are ultrastructurally normal and display a typical axoneme which, at the anterior aspect of the defective cell, is surrounded by displaced mitochondria and excess cytoplasm (Toyama & Itoh, 1996). Due to the small size of the droplet thus formed, the cells are often incorrectly classified as pin-heads or microcephalic sperm (Holstein *et al*., 1988; Zamboni, 1992; Afzelius, 1996; Chemes *et al*., 1999; Chemes, 2000; Chemes & Rawe, 2003). The present study confirmed the essential difference between the two types of defect, namely, that the absence of nuclear material, easily seen at the light microscopic level using phase contrast illumination, was characteristic for acephalic sperm. LM and EM preparations confirmed the knoblike anterior aspect of emu sperm displaying this defect, where the knob is formed by an excessive amount of cytoplasm surrounding the distal centriole. Another form of the defect was also observed in the emu samples. In this instance the midpiece retained its usual slender shape, and exhibited the normal orderly arrangement of mitochondria around the distal and proximal centrioles. No excess cytoplasm was present.

In mammals, acephalic sperm are known to originate during spermiogenesis as a result of a faulty head-midpiece connection, through the abnormal positioning of the centriolar complex (CC) relative to the nucleus, or as a result of a fracture between the two centrioles (Blom & Birch-Anderson, 1970; Holstein *et al*., 1988; Zamboni, 1992; Afzelius, 1996; Chemes *et al*., 1999; Chemes, 2000; Rawe *et al*., 2002). According to Baccetti *et al*. (1984), biopsy material of human testes showed that decapitation was significantly correlated with the overproduction of membranous vesicles near the centrioles during spermiogenesis. In a later study they related the

defect to a testicular origin, but with head detachment only occurring in the epididymis (Baccetti *et al*., 1989). Evidence of a lack of connection between the two centrioles resulting in acephalic sperm formation as described by Afzelius (1996) was observed in the emu material studied.

During the early round spermatid stage of spermiogenesis of ratite sperm the long CC was often observed to orientate itself obliquely with respect to the nucleus. In some instances the CC failed to make contact with the nucleus resulting in the formation of disjointed sperm (see Chapter 6). A similar, but more pronounced situation, would suggest the origin of acephalic sperm in these birds. The fact that detached heads (morphologically normal heads without a tail attached) were absent in smears and SEM preparations studied would confirm, as the literature implies (Chemes *et al*., 1999), that acephalic sperm originate during spermiogenesis and are not the product of separation of the head and tail following spermiation or the result of sample processing.

Tail defects

The incidence of principal piece defects in emu sperm was low and restricted to stump, coiled and multiflagellate tails. Both Wakely and Kosin (1951) and Alkan *et al.* (2002) gave detailed accounts of defects observed in turkey semen, yet neither mentioned the presence of stump (short) or multiple tails, although various forms of coiled tails were noted. Kamar and Rizik (1972) also reported on the presence of coiled tails in the turkey. 'Bent' and 'curled' tails have also been noted in various other bird species, including the chicken (Tabatabaei *et al*., 2010), goose (Marvan *et al*., 1981; Ferdinand, 1992), duck (Penfold *et al*., 2000), guinea fowl (Nwakalor *et al*., 1988) and pigeon (Sontakke *et al*., 2004). Coiling of the sperm tail generally involves the proximal part of the principal piece and it appears to be a common defect, with coiled sperm often being seen in ejaculates of fertile men (Yeung *et al*., 2009). Again, the possible reason for this anomaly is not understood although it may be associated with a hostile endogenous milieu (Yeung *et al*., 2009).

In a study of the stump tail defect in boars (Fischman *et al*., 2009), ultrastructural examination revealed that the organized structure of the axonemal microtubules and mitochondrial helix was lost but offered no explanation for the origin of the defect. In a case report of a sterile bull with a 78% incidence of stump tails, the defect was again characterized by disruption of the mitochondrial sheath and the "fibrils" of the midpiece (Peet and Mullins, 1991). The authors were of the opinion that the defect originated during spermatogenesis and not during passage through the epididymis or due to technical errors while handling the samples. Whether the stump-tail sperm identified in the emu samples represent the true form of the defect as observed in various mammals, or merely reflect a modified form of tail coiling, remains to be determined. The low incidence of this defect in the emu will make this a challenging task.

Cytoplasmic droplets

Cytoplasmic droplets are generally considered to represent excess cytoplasm which was not removed from the spermatid as a residual body during spermiogenesis. In mammals both proximal and distal cytoplasmic droplets are recognised with the former being considered as a sign of sperm immaturity and therefore as a major defect (Blom, 1972). Cytoplasmic droplets appear to be rare in birds, although their presence has been noted in the duck (Penfold *et al*., 2000), pigeon (Sontakke *et al*., 2004), vulture (Umapathy *et al*., 2005), ostrich (Bertschinger *et al*., 1992; Soley & Els, 1993) and emu (Malecki *et al*., 1998). The location and eccentric positioning of retained cytoplasmic droplets in the emu samples were similar to that described in ostrich sperm (Soley & Els, 1993) although the composition of the droplets differed markedly between the two species. In ostriches (Soley & Els, 1993) the droplets were exclusively restricted to the neck region of the sperm, overlapping and eccentrically positioned over both the base of the nucleus and proximal part of the midpiece. In this species the droplets displayed various vesicular elements and the occasional mitochondrion within the cytoplasmic matrix (Soley *et al*., 1996), but in the emu, using similar techniques, only a fine homogenous ground-substance was generally present. Although the location of the avian cytoplasmic droplet is similar to that described for the proximal droplet in mammals (Barth & Oko, 1989), there is presently no evidence to suggest that the avian cytoplasmic droplet shifts significantly from its point of origin (proximal droplet) to a more distal location (distal droplet). It remains to be determined whether the detrimental effect of the avian cytoplasmic droplet is purely mechanical in nature, or may reflect a deficiency in sperm maturation. A detailed study of the process of spermiation will be required to fully appreciate the importance of the avian cytoplasmic droplet. It appears in the emu that the removal of residual cytoplasm by the Sertoli cells is almost complete, leaving only a slim cytoplasmic projection (as described in Chapter 2). Failure to remove the residual cytoplasm results in the formation of a cytoplasmic droplet.

Multiple defects

A small percentage of sperm (6.3% of total sperm defects) displayed multiple abnormalities. A common multiple defect that occurs in many species, including the emu, is that of macrocephalic sperm associated with multiple tails (Brito, 2007; Kopp *et al*., 2007) (see Chapter 8). Sperm with this defect are considered to be the product of defective meiosis (Escalier, 1983). The scoring of multiple defects remains a challenge as a decision has to be made regarding which defect carries the greater weight. A multiple recording system has recently been proposed to alleviate this problem (Nöthling and Irons, 2008).

References

Afzelius, B.A. (1996) The sperm cytoskeleton and its defects. *The Cytoskeleton* **3**, 325-357.

Alkan, S., Baran, A., Özdaş, Ö.B. & Evecen, M. (2002) Morphological defects in turkey semen. *Turkish Journal of Veterinary and Animal Science* **26**, 1087-1092.

Baccetti, B., Biglardi, E., Burrini, A.G., Gabbiani, G., Jockusch, B.M. & Leoncini, P. (1984) Microfilaments and intermediate sized filaments in sperm tails. *Journal of Submicroscopic Cytology and Pathology*, **16**, 79-84.

Baccetti, B., Burrini, A.G., Collodel, G., Magnamo, A.R., Piomboni, P., Renieri, T. & Sensini, C. (1989) Morphogenesis of the decapitated and decaudated sperm defect in two brothers. *Gamete Research* **23**, 181-188.

Baccetti, B., Burrini, A.G. & Falchetti, E. (1991) Spermatozoa and relationships in Paleognath birds. *Biology of the Cell* **71**, 209-216.

Barna, J. & Wishart, G.J. (2003) Excess nuclear DNA in spermatozoa of guinea fowl. *Theriogenology* **59**, 1685-1691.

Barth, A.D. & Oko, R.J. (1989) Abnormal morphology of bovine spermatozoa. Iowa State University Press, Ames.

Bertschinger, H.J., Burger, W.P., Soley, J.T. & de Lange, J.H. (1992) Semen collection and evaluation of the male ostrich. Proceedings of the Biennial Congress of the South African Veterinary Association, Grahamstown, pp.154-158.

Blom, E. (1972) The ultrastructure of some characteristic sperm defects and a proposal for a new classification of the bull spermiogram. *Atti del VII Simposia Internationale de Zootechnia*, pp. 125-139.

Blom, E. & Birch-Andersen, A. (1970) Ultrastructure of the decapitated sperm defect in Guernsey bulls. *Journal of Reproduction and Fertility* **23**, 67-72.

Brito, L.F.C. (2007) Evaluation of stallion sperm morphology. *Clinical Techniques in Equine Practice* **6**, 249-264.

Brito, L.F.C., Sertich, P.L., Stull, G.B., Rives, W. & Knobbe, M. (2010) Sperm ultrastructure, morphometry, and abnormal morphology in American black bears (*Ursus americanus*). *Theriogenology* **74**, 1403-1413.

Briz, M.D., Bonet, S., Pinart, B. & Camps, R. (1996) Sperm malformations throughout the boar epididymal duct. *Animal Reproduction Science* **43**, 221-239.

Carrell, D.T., Emery, B.R. & Liu, L. (1999) Characterization of aneuploidy rates, protamine levels, ultrastructure, and functional ability of round-headed sperm from two siblings and implications for intracytoplasmic sperm injection. *Fertility and Sterility* **71**, 511-516.

Chelmońska, B., Jerysz, A., Łukaszewicz, E., Kowalczyk, A. & Malecki, I. (2008) Semen collection from Japanese Quail (*Coturnix japonica*) using a teaser female. *Turkish Journal of Veterinary and Animal Sciences* **32**, 19-24.

Chemes, H.E. (2000) Phenotypes of sperm pathology: Genetic and acquired forms in infertile men. *Journal of Andrology* **21**, 799-808.

Chemes, H.E. & Rawe, V.Y. (2003) Sperm pathology: a step beyond descriptive morphology. Origin, characterization and fertility potential of abnormal sperm phenotypes in infertile men. *Human Reproduction Update* **9**, 405-428.

Chemes, H.E. & Rawe, V.Y. (2010) The making of abnormal spermatozoa: cellular and molecular mechanisms underlying pathological spermiogenesis. *Cell and Tissue Research* **341**, 349-357.

Chemes, H.E., Puigdomenech, E.T., Carizza, C., Brugo Olmedo, S., Zanchetti, F. & Hermes, R. (1999) Acephalic spermatozoa and abnormal development of the head-neck attachment: a human syndrome of genetic origin. *Human Reproduction* **14**, 1811-1818.

Chemes, H.E. & Sedo, C.A. (2012) Tales of the tail and sperm head aches. Changing concepts on the prognostic significance of sperm pathologies affecting the head, neck and tail. *Asian Journal of Andrology* **14**, 14-23.

Chenoweth, P.J. (2005) Genetic sperm defect. *Theriogenology* **64**, 457-468.

Dadoune, J-P. (1988) Ultrastructural abnormalities of human spermatozoa. *Human Reproduction* **3**, 311-318.

Dadoune, J-P. (1995) The nuclear status of human sperm cells. *Micron* **26**, 323-345.

Dam, A.H.D.M., Feenstra, I., Westphal, J.R., Ramos, L., Van Golde, R.J.T. & Kremer, J.A.M. (2007) Globozoospermia revisited. *Human Reproduction Update* **13**, 63-75.

Escalier, D. (1983) Human spermatozoa with large heads and multiple flagella. A quantitative ultrastructural study of 6 cases. *Biology of the Cell* **48**, 65-74.

Ferdinand, A. (1992) Licht- und elektronenmikroskopische Untersuchungen zur Morphologie von Ganterspermatozoen. Ph.D Thesis, University of Veterinary Medicine, Hannover.

Fischman, M.L., Bolondi, A. & Cisale, H. (2009) Ultrastructure of sperm tail stump defect in wild boar. *Andrologia* **41**, 35-38.

Gunawardana, V.K. & Scott, M.G.A.D. (1977) Ultrastructural studies on the differentiation of spermatids in the domestic fowl. *Journal of Anatomy* **124**, 741-755.

Guzick, D.S., Overstreet, J.W., Factor-Litvak, P., Brazil, C.K., Nakajima, S.T., Coutifaris, C., Carson, S.A., Cisneros, P., Steinkampf, M.P., Hill, J.A., Xu, D. & Vogel, D.L. (2001) Sperm morphology, motility, and concentration in fertile and infertile men. *New England Journal of Medicine* **345**, 1388-1393.

Holstein, A.F., Roosen-Runge, E.C. & Schirren, C. (1988) Illustrated Pathology of Human Spermatogenesis. Grosse Verlag, Berlin.

Irons, P.C., Bertschinger, H.J., Soley, J.T. & Burger, W.P. (1996) Semen collection and evaluation in the ostrich. In: Deeming, D.C. (ed.) Improving our understanding of ratites in a farming environment. Ratite Conference, Manchester, pp. 157-159.

Jamieson, B.G.M. (2007) Avian spermatozoa: Structure and Phylogeny. In: Jamieson, B.G.M. (ed.) Reproductive Biology and Phylogeny of Birds Part A. Science Publishers, Jersey, pp. 349-511.

Kamar, G.A. & Badreldin, A.L. (1959) Sperm morphology and viability. *Acta Anatomica* **39**, 81-83.

Kamar, G.A.R. & Rizik, M.A.A. (1972) Semen characteristics of two breeds of turkeys. *Journal of Reproduction and Fertility* **29**, 317-325.

Kavak, A., Lundeheim, N., Aidnik, M. & Einarsson, S. (2004) Sperm morphology in Estonian and Tori breed stallions. Acta Veterinaria Scandinavica 45, 11-18.

Klimowicz, M., Łukaszewicz, E. & Dubiel, A. (2005) Effect of collection frequency on quantitative and qualitative characteristics of pigeon (*Columba livia*) semen. *British Poultry Science* **46**, 361–365.

Koehler, J.K., Platz, C.C., Waddell, W., Jones, M.H. & Behrns, S. (1998) Semen parameters and electron microscope observations of spermatozoa of the red wolf, *Canis rufus*. *Journal of Reproduction and Fertility* **114**, 95-101.

Kopp, C., Sukura, A., Tuunainen, E., Gustavsson, I., Parvinen, M. & Anderson, M. (2007) Multinuclear-multiflagellar sperm defect in a bull – a new sterilizing sperm defect. *Reproduction in Domestic Animals* **42**, 208-213.

Lake, P.E. (1954) The relationship between morphology and function of fowl spermatozoa. *Proceedings of the Xth World's Poultry Congress*, Edinburgh, pp. 79-85.

Lindsay, C., Staines, H.J., McCormick, P., McCullum, C., Choulani, F. & Wishart, G.J. (1999) Variability in the size of the nucleus in spermatozoa from the Houbara bustards, *Chlamydotis undulate undulate*. *Journal of Reproduction and Fertility* **117**, 307-313.

Łukaszewicz, E., Jerysz, A., Partyka, A. & Siudzińska, A. (2008) Efficacy of evaluation of rooster sperm morphology using different staining methods. *Research in Veterinary Science* **85**, 583-588.

Malecki, I.A., Cummins, J.M., Martin, G.B. & Lindsay, D.R. (1998) Effect of collection frequency on semen quality and the frequency of abnormal forms of spermatozoa in the emu. *Animal Production in Australia* **22**, 406.

Marvan, F., Rob, O. & Janeckova, E. (1981) Classification of morphological abnormalities of gander sperm. *Zuchthygiene* **16**, 176-183.

Mortimer, D. (2002) Sperm form and function: beauty is in the eye of the beholder. 9th International Symposium on Spermatology, Cape Town, pp. 257-262.

Nöthling, J.O. & Irons, P.C. (2008) A simple multidimensional system for the recording and interpretation of sperm morphology in bulls. *Theriogenology* **69**, 603–611.

Nwakalor, L.N., Okeke, G.C. & Njoku, D.C. (1988) Semen characteristics of the guinea fowl Numida melagris melagris. *Theriogenology* **29**, 545-554.

Peet, R.L. & Mullins, K.R. (1991) Sterility in a poll Hereford bull associated with the 'tail stump' sperm defect. *Australian Veterinary Journal* **68**, 245.

Penfold, L.M., Wildt, D.E., Herzog, T.L., Lynch, W., Ware, L., Derrickson, S.E. & Monfort, S.L. (2000) Seasonal patterns of LH, testosterone and semen quality in the Northern pintail duck (*Anas acuta*). *Reproduction, Fertility and Development* **12**, 229-235.

Pesh, S. & Bergman, M. (2006) Structure of mammalian spermatozoa in respect to viability, fertility and cryopreservation. *Micron* **37**, 597-612.

Rawe, V.Y., Terada, Y., Nakamura, S., Chillik, C.F., Brugo Olmedo, S. & Chemes, H.E. (2002) A pathology of the sperm centriole responsible for defective sperm aster formation, syngamy and cleavage. *Human Reproduction* **17**, 2344-2349.

Rozenboim, I., Navot, A., Snapir, N., Rosenstrauch, A., El Halawani, M.E., Gvaryahu, G. & Degen, A. (2003) Method for collecting semen from the ostrich (*Struthio camelus)* and some of its quantitative and qualitative characteristics. *British Poultry Science* **44**, 607-611.

Saeki, Y. (1960) Crooked-necked spermatozoa in relationship to low fertility in the artificial insemination of fowl. *Poultry Science* **39**, 1354-1361.

Soley, J.T. (1997) Nuclear morphogenesis and the role of the manchette during spermiogenesis in the ostrich (Struthio *camelus). Journal of Anatomy* **190**, 563-576.

Soley, J.T. & Els, H.J. (1993) The ultrastructure of retained cytoplasmic droplets in ostrich spermatozoa. *Proceedings of the Microscope Society of Southourn Africa* **23**, 58.

Soley, J.T., Bertschinger, H.J., Els, H.J. & Burger, W.P. (1996) The morphology and incidence of retained cytoplasmic droplets in ostrich spermatozoa. In: Deeming, D.C. (ed.) Improving our Understanding of Ratites in a Farming Environment. Ratite Conference, Manchester, pp. 16-18.

Sontakke, S.D., Umapathy, G., Sivaram, V., Kholkute, S.D. & Shivaji, S. (2004) Semen characteristics, cryopreservation, and successful artificial insemination in the Blue rock pigeon (*Columba livia*). *Theriogenology* **62**, 139-153.

Stelzer, G., Crosta, L., Bürkle, M. & Krautwald-Junghanns, M-E. (2005) Attempted semen collection using the massage technique and semen analysis in various psittacine species*. Journal of Avian Medicine and Surgery* **19**,7–13.

Tabatabaei, R.A., Batavani, R.A. & Talebi, A.R. (2009) Comparison of semen in indigenous and Ross broiler breeder roosters. *Journal of Animal and Veterinary Advances* **8**, 90-93.

Tabatabaei, S., Chaji, M. & Mohammadabadi, T. (2010) Correlation between age of rooster and semen quality in Iranian indigenous broiler breeder chickens. *Journal of Animal and Veterinary Advances* **9**, 195-198.

Toyama, Y. & Itoh, Y. (1996) Ultrastructural features and pathogenesis of decapitated spermatozoa in a boar. *Andrologia* **28**, 109-115

Umapathy, G., Sontakke, S., Reddy, A., Ahmed, S. & Shivaji, S. (2005) Semen characteristics of the captive Indian white-backed vulture. *Biology of Reproduction* **73**,1039-1045.

Wakely, W.J. & Kosin, I.L. (1951) A study of the morphology of the turkey spermatozoa – with special reference to the seasonal prevalence of abnormal forms. *American Journal of Veterinary Research* **12**, 240-245.

Wishart, G.J., Lindsay, M. & Knowles-Brown, A. (1999) Sperm quality in a captive-bred golden eagle. *Journal of Reproduction and Fertility Abstract Series* **24**, 6.

Yeung, C.H., Tüttelmann, F., Bergmann, M., Nordhoff, V., Vorona, E. & Cooper, T.G. (2009) Coiled sperm from infertile patients: characteristics, associated factors and biological implication. Human Reproduction 24, 1288-1295.

Zamboni, L. (1987) The ultrastructural pathology of the spermatozoon as a cause of infertility: the role of electron microscopy in the evaluation of semen quality. *Fertility and Sterility* **48**, 711-734.

Zamboni, L. (1992) Sperm structure and its relevance to infertility. *Archives of Pathology and Laboratory Medicine* **116**, 325-344.

Chapter 10 General conclusions

A comprehensive morphological description of emu sperm at the light microscopic level, an essential prerequisite for the evaluation of semen quality in this species, is not currently available. In this study, the method for the visualization of sperm structure, using light microscopy, by making conventional semen smears from samples collected from the distal *ductus deferens* and fixed in 2.5% glutaraldehyde, followed by air-drying the smears and staining with a Romanowsky type stain such as Wright's stain, gave consistently good results. Examination of the smears using phase contrast illumination and a 100x oil immersion lens readily resolved the various components of the cell, namely, the acrosome, nucleus, midpiece, principal piece and endpiece. This technique was simple to use and produced reproducible results. It could also be used to examine ejaculated semen samples although this was not applied in the current investigation. Normal emu sperm were typically filiform (threadlike) in appearance and closely resembled sperm of the ostrich and other non-passerine species, particularly poultry.

Sperm dimensions in the emu were similar to those of other ratites. This was reflected by a head:tail ratio of 1:4 which is in accordance with the value reported for the ostrich (see Chapter 2). The head:tail ratio of other non-passerine birds, for example the chicken and pigeon, is much higher indicating longer tails in these species. An explanation for this difference is that sperm competition in these birds is more intense due to their promiscuous nature, and as such the longer tail would lead to faster swimming sperm. Ratites are monogamous and as sperm competition may not play a role in their reproductive strategy would therefore not require sperm with longer tails. However, this hypothesis remains controversial.

Whereas the standard light microscope is irreplaceable as a diagnostic tool, its limited resolution cannot give insights into the causes of sperm defects or detect subtle structural abnormalities. The application of scanning and transmission electron microscopy in this study allowed for a detailed ultrastructural description of the subcellular components of both normal and defective emu sperm. Electron microscopy revealed that, in common with sperm of other ratites, the nuclear rostrum is covered by a conical acrosome, an elongated distal centriole runs the length of the midpiece and a fibrous sheath surrounds the principal piece of the flagellum. Additionally, only rudimentary outer dense fibres surround the axonemal doublets in the anterior part of the principal piece. Most of these features are unique to ratites and the tinamou and group these birds together phylogenetically. Within this group, however, distinct morphological differences are

found. Unlike in other ratite sperm, there was no endonuclear canal or perforatorium in emu sperm. Based on the degree of development of the perforatorium in palaeognathous birds, the tinamou is considered to be the most “primitive” member of this group due to the extension of the endonuclear canal and perforatorium throughout the entire length of the nucleus, followed by the ostrich and rhea where these structures extend only partly into the nucleus. This would imply that the emu, bereft of an endonuclear canal or perforatorium, represents the most phylogenetically advanced bird within the palaeognaths. Another distinguishing feature of emu sperm was the presence of a large number of mitochondria in the midpiece. The mitochondria were closely juxtaposed with no discernible evidence of the inter-mitochondrial cement reported in other ratites and the tinamou. Although these results confirmed the previously published data on emu sperm, additional information was revealed in the present study. A cytoplasmic appendage was located near the base of the nucleus, possibly representing the point of release of the cells during spermiation. This appendage has not previously been described in avian sperm.

The emergence of niche farming enterprises based on raising ratites such as the emu, ostrich and rhea has focussed attention on the lack of knowledge of the reproductive biology of these birds, particularly regarding semen parameters in the male. This study led to the compilation of the first comprehensive classification of sperm defects in any ratite, paving the way for similar studies in other commercially important ratites such as the ostrich and rhea. Head defects were the most prevalent and represented 52.4% of total sperm defects observed in the emu. The most common form of head defect was head bending (27.8%) which ranged from simple bending (gentle to acute bends) to looping, kinking, coiling and spiralling. Incomplete condensation or decondensation of the nuclear material was implicated in the formation of bent heads although misalignment of the centriolar complex during the early stages of spermiogenesis may in some instances play a role. Acephalic sperm (9.9%) were observed in all the samples, but were not associated with loose heads. The complete absence of detached heads reflects release of the tails but retention of the heads, possibly due to faulty alignment of the two components during spermiogenesis. Misalignment of the centriolar complex was again implicated in the formation of this defect. Acephalic sperm can potentially be confused with microcephalic sperm (0.8%) although the presence of nuclear material in the latter defect was readily detected by light microscopy. Macrocephalic sperm (11.1%) were commonly observed and appeared to be the product of incomplete meiosis resulting in the formation of diploid nuclei. Round heads formed 2.8% of head defects. Tail abnormalities were subdivided into neck/midpiece and principal piece defects. Defects observed in the neck/midpiece region included disjointed sperm (15.1%) and abaxial sperm (0.6%). Disjointed sperm were characterized by the complete separation of the head and midpiece in the neck region but within the confines of the plasmalemma and abaxial tail implantation by the misalignment of the centriolar complex relative to the head base.

Abnormalities of the principal piece were subdivided into stump tails (3.8%), coiled tails (3.3%) and multiple tails (2.8%). Cytoplasmic droplets (10.5%) and multiple defects (11.5%) were also observed. Examination of testicular material ascribed the occurrence of the anomalies to defective spermiogenesis rather than to damage of the cells in the excurrent duct system or as the result of sample processing. However, further studies will be required to ascertain the role of genetic and environmental factors, as well as the effects of feed, toxins and diseases on spermiogenesis in the emu.

Although the process of spermiogenesis in the emu was similar to that described in other non-passerine birds, the presence of a novel, transient structure observed during the formation of the manchette, was unexpected. This structure had not previously been described in any non-passerine species, yet on re-examination of resin-embedded testicular material, was found to be present in at least two other ratites, the ostrich and rhea. A similar structure has been described in the region just below the acrosome-nuclear shoulder in some lizard species and in the Caiman crocodile. Given the reported close association between birds and reptiles this structure possibly represents an ancient character trait that links the birds and reptiles as sister groups. Further morphological studies on other birds and reptiles are needed to confirm this specific characteristic as a reliable phylogenetic marker. Studies on the testes of the cassowary, kiwi and tinamou will assist in determining whether the ratites form a monophyletic group at the base of the avian phylogenetic tree or whether they form a polyphyletic assemblage together with the tinamous.

This study aimed to provide information of a practical nature that would improve the economic viability of niche farming enterprises such as emu farming. The investigation led to a suggested uniform terminology for describing sperm defects in the emu and proposed a classification system appropriate for ratite, and possibly other avian sperm. While recognising the value of other techniques such as Computer-Aided Sperm Analysis and flow cytometry in semen evaluation, this study further optimised the methodology for the rapid and accurate light microscopic examination of semen smears. The morphological information gathered by this study will be useful as baseline data for identifying male birds with potential fertility problems and would contribute towards the accurate morphological assessment of semen to be used in artificial insemination programmes. This work also provided interesting data of academic value. The transient structure observed during spermiogenesis in the emu is unique and can potentially be used as a non-traditional character to provide insight into, and help resolve, the debate surrounding the phylogenetic relationships within the ratites and between birds in general. The identification of this character will also allow further exploration of the link between birds and reptiles.